# Bioinspired Model Complexes For Vanadium Haloperoxidases

DISSERTATION

zur Erlangung des akademischen Grades doctor rerum naturalium

(Dr. rer. nat.)

vorgelegt dem Rat der Chemisch-Geowissenschaftlichen Fakultät

der Friedrich-Schiller-Universität Jena

von M. Sc. Simona Filofteia Nica

geborem am 19.12.1976

in Curtea de Argeş, Romania

Gutachter

1. Winfried Plass

2. Matthias Westerhausen

Tag der öffentlichen Verteidigung: September $22^{nd}$ 2005

"Most zealously I've studied matters great and small;
Though I know much, I should like to know all." Goethe

Din sînul veciniculuiieri
Trăieşte azi ce moare,
Un soare de s-ar stinge-n ceri
S-aprinde iaraşi soare.
Mihai Eminescu

*In memory of the most beloved father and to the memory of an extraordinary Professor,*
*Dr. Ovidiu Maior.*

# Acknowledgements

I would like to thank my supervisor, Prof. Dr. Winfried Plass, for giving me the opportunity to work in this interesting field and for support with new ideas and advises during my research.

Special thanks to my partner, colleague and best friend, Adrian Ion, for moral support, patience and especially for helping me in having new ideas through our multitude of scientific conversations.

I also thank to my colleague, Dr. Axel Pohlmann, who helped a romanian student lost in the german bureaucracy. Thanks also for bringing me from Siegen to Jena and taking care of the new employment procedures. Without you, most likely, I would have been deported three years ago. Of course, I thank to him, more importantly, for helping me find the way through the german world of computers and teaching me how to use special programs.

Lots of thanks to Dr. Andrew Hall for nice friendship and for language support. Only with your support my thesis reassembles now the English language. And because we are here, I say millions of thanks to Dr. Ioana Pera, my best romanian friend. Thank you very much for helping me to find my house in Siegen, for accompanying me shopping and for the very nice time spent together.

Thanks to Masroor, my Pakistani colleague for nice and enjoyable evenings spent together and also for the nice talks about the structure of the enzyme and for correcting my English in the manuscripts. I also thank to my colleague Arne Roth for his patience in explaining me how the LaTeXworks and especially for his help in the arrangement of the thesis.

Many thanks to Ines Seidel for helping me with catalytic tests and some experiments in the last months while writing my manuscripts and my thesis. Also, lots of thanks to my

student, Björn Kusebauch for bringing me so many results during his "Forschungspraktikum".

I would like to thank to Dr. Manfred Rudolph, who measured the cyclic voltammetry experiments of my complexes and also for helping me to interpret the spectrophotometric titration data.

I would like to thank to the NMR team, who measured my tons of samples and also for trying to understand my very bad german language. Many thanks to Lotte Neupert for the HPLC measurements.

Lots of thanks to a special person, Dr. Helmar Görls for measuring my X-ray crystal structures and for his high sense of humor. He knew how to bring the smile on my face even when the measured structures were the by-products. Thank you very much.

I also thank to my romanian friend, now Dr. Maria-Magadalena Titirici for her help and understanding me.

Last but not least, I would like to thank to all my family for financial and moral support during all my studies. Thanks to my brother, Dr. Dorel-Daniel Nica for his kindness and financial support and also many thanks for the nice political and literature talks. Thanks to my parents for understanding and supporting me in all my life decisions. Unique thoughts of gratitude go to my wonderful father. I wish I would had the opportunity to share all this achievements with you. I miss you and I wish you were still here with me.

# Summary

Vanadium haloperoxidases represent a class of non-heme peroxidases with a high stability to organic solvents and high temperatures. These enzymes proved also to be very stable in presence of excess of their product (HOCl) which will readily inactivate the heme-haloperoxidases. The active group of the enzymatic system consists in a vanadate moiety, solely covalently bonded to a histidine residue and embedded in the protein shell via a strong hydrogen bonding network. Structural similarities between the hydrogen bonding site of vanadium haloperoxidases and some acid phosphatases are evident. An important role for the haloperoxidase activity has been attributed to the hydrogen bonding interactions which besides the fixation of the prosthetic group in the protein environment are also activating the peroxide-intermediate.

The goal of this work was the synthesis of vanadium(V) complexes which model the active site and the catalytic function of these enzymes. Vanadium in the highest oxidation state proved to be a compulsory characteristic of model complexes, since the reduced form of vanadium haloperoxidase showed no activity. Therefore, vanadium(V) complexes with versatile N-salicylidene carbonic acid hydrazide were prepared. Both oxo and dioxovanadium complexes will be described in Chapter 2 and Chapter 3, with both types of vanadium coordination compounds regarded as model complexes for the natural system. Besides the crystallographic description of these complexes, reactivity in solution will be also discussed.

Starting from a non-substituted aliphatic side chain of the N-salicylidene hydrazide ligand, new functionalities were introduced stepwise. This achievement had the role to probe the importance of the amino acid residues which are in hydrogen bonding interaction with the equatorial oxygen atoms of the prosthetic group in vanadium containing haloperoxidases. The modification of the aliphatic side chain will be discussed in separate chapters, therefore additional groups such as hydroxyl, amine and guanidine afforded vanadium(V) complexes with relevant functionalized side chain for the vanadium haloperoxidases, namely regarding the serine, lysine and arginine residues.

The mechanism of the catalytic reaction performed by vanadium haloperoxidases was proposed to take place by addition first of the hydrogen peroxide at the vanadate

center to form a peroxo-intermediate which is subsequently able to oxidize the halides in slightly acidic media. In Chapter 2, the characterization and reactivity of an oxo-monoperoxovanadium(V) complex is presented. Further on, the cyclization on vanadium coordination of a short amino-functionalized aliphatic side chain of N-salicylidene hydrazide ligand as well as the first example of guanilation reaction of a vanadium coordination compound will be described in Chapter 4 and 5, respectively.

The *cis*-dioxovanadium(V) complexes obtained with N-salicylidene carbonic acid hydrazides proved also to catalyze the biomimetic reaction. The bromide oxidation reaction by hydrogen peroxide was monitored by bromination of 1,3,5-trimetoxybenezene in acidified DMF solution. Apart from this specific enzymatic reaction, the model complexes were also able to catalyze the peroxide-mediated oxidation of phenyl methyl sulfide to the corresponding sulfoxide.

The replacement of vanadate from vanadium haloperoxidase with molybdate or tungstate yielded an inactive enzyme. Therefore, *cis*-dioxomolybdenum(VI) complexes based on N-salicylidene amino-functionalized aliphatic acid hydrazide were also obtained in order to address the question whether a synthetic molybdenum complex can catalyze the bromoperoxidase reaction. This was also based on the reported high bromoperoxidase activity of the inorganic $MoO_3$ (aq.) compound. But, however the *cis*-dioxomolybdenum complex based on N-salicylidene dihydropyrrole hydrazide showed no bromoperoxidase activity, but instead the complex was capable of catalyzing efficiently the oxidation of sulfide to sulfoxide.

In the last chapter, bis-N-salicylidene hydrazide ligands were prepared by the condensation of salicylaldehyde with bis-aliphatic hydrazides. The ligand $H_4Ln$ may be considered as two N-salicylidene hydrazide cavities linked via a methylene chain of variable length. The ligand is able to bind two metal ions in a hexacoordinate fashion yielding binuclear *cis*-dioxovanadium(V) and *cis*-dioxomolybdenum(VI) complexes. The complexes showed a high efficient capacity in catalyzing the oxidation of sulfide when $H_2O_2$ was used as oxidant. Moreover, a chiral binuclear *cis*-dioxomolybdenum(VI) complex was isolated and used as catalyst of the sulfoxidation reaction. The complex proved to be an efficient catalyst of the reaction, but only 4% *ee* was obtained when the catalytic reaction was performed in dichlormethane.

# Zusammenfassung

Vanadium-Haloperoxidasen stellen eine Klasse von nicht-Häm-Peroxidasen mit hoher Beständigkeitgegenüber organischen Lösungsmitteln und hohen Temperaturen dar. Diese Enzyme sind außerdem in Gegenwart von Überschuss ihres Produktes (HOCl), was häm-Haloperoxidasen leicht inaktivieren würde, sehr stabil. Das aktive Zentrum des enzymatischen Systems besteht aus einer Vanadatumgebung, welche kovalent an nur einen Histidinrest gebunden und im Proteinrumpf mittels eines starken Wasserstoffbrückennetzwerks verankert ist. Strukturelle Ähnlichkeiten zwischen der Wasserstoffbrückenumgebung von Vanadium-Haloperoxidasen und einigen sauren Phophatasen sind bewiesen. Eine wichtige Rolle für die Haloperoxidaseaktivität wird den Wasserstoffbrückenwechselwirkungen einerseits bei der Fixierung der prosthetischen Gruppe in der Proteinumgebung und andererseits bei der Aktivierung des Peroxid-Intermediates zugeordnet.

Das Ziel dieser Arbeit war die Synthese von Vanadium(V)-Komplexen welche das aktive Zentrum und die katalytischen Eigenschaften dieser Enzyme nachbilden. Die höchste Oxidationsstufe für das Vanadium wird als zwingende Eigenschaft solcher Modellkomplexe angesehen, da die reduzierte Form der Vanadium-Haloperoxidase keine Aktivität zeigte. Folglich wurden Vanadium(V)-komplexe mit vielseitigen N-Salicylidensäurehydraziden hergestellt. Die Oxo- und Dioxo-Vanadium-Komplexe werden in Kapitel 2 und 3 beschrieben. Sie stellen die zwei Arten von Vanadium-Koordinationsverbindungen dar, welche als Modell-Komplexe für das natürliche System angesehen werden. Neben der kristallographischen Beschreibung dieser Komplexe wird auch ihre Reaktivität in Lösung diskutiert werden.

Ausgehend von den unsubstituierten aliphatischen Seitenketten der N-Salicylidenhydrazid-Liganden werden schrittweise neue Funktionalitäten eingeführt. Dies hat zum Ziel die Bedeutung der Aminosäurereste, welche über Wasserstoffbrückenbindungen mit den equatorialen Sauerstoffatomen der prosthetischen Gruppe in vanadium haltigen Haloperoxidasen wechselwirken, zu erkunden. Die Modifizierung der aliphatischen Seitenkette wird in eigenen Kapiteln diskutiert werden. Dabei dienen zusätzliche Gruppen, wie Hydroxyl, Amin und Guanidin und die davon abgeleiteten Vanadium(V)-Komplexe mit wichtigen funktionalisierten Seitenketten als Vanadium-Haloperoxidase-Modelle, die spe-

ziell die Serin-, Lysin- und Argininreste betrachten.

Im postulierten Mechanismus der durch Vanadium-Haloperoxidasen katalysierten Reaktion findet erst die Addition des Wasserstoffperoxids am Vanadat-Zentrum unter Bildung eines Peroxo-Intermediates statt, welches dann in leicht saurem Medium die Halogene oxidieren kann. In Kapitel 2 ist die Charakterisierung und Reaktivität eines Oxomonoperoxo-Vanadium(V)-Komplexes beschrieben. Weiterhin werden, in Kapitel 4 und 5, die Zyklisierung einer an Vanadium-koordinierten kurzen mit Amino-Funktion versehenen aliphatischen Seitenkette des N-Salicylidenhydrazid-Liganden sowie das erste Beispiel einer Guanilierungsreaktion einer vanadium-koordinierten Verbindung beschrieben.

Die *cis*-Dioxovanadium(V)-Komplexe der N-Salicylidencarbonsäurehydrazid-Liganden katalysieren die biomimetische Reaktion. Die Oxidation von Bromid mit Wasserstoffperoxid wurde durch die Bromierung von 1,3,5-Trimethoxybenzen in saurer DMF-Lösung beobachtet. Unabhängig von dieser spezifischen enzymatischen Reaktion waren die Modellkomplexe in der Lage die peroxidvermittelte Oxidation von Phenylmethylsulfid zum korrespondierenden Sulfoxid zu katalysieren.

Der Austausch von Vanadat in Vanadium-Haloperoxidasen gegen Molybdat oder Wolframat führte zu inaktiven Enzymen. Es wurden *cis*-Dioxomolybdän(VI)-Komplexe der N-salicyliden-amnino-funktionalisierten aliphatischen Hydrazide dargestellt um die Frage zu beantworten, ob ein synthetischer Molybdänkomplex die Bromoperoxidasereaktion katalysieren kann. Für die anorganische $MoO_3$(aq.)-Verbindung konnte Bromoperoxidaseaktivität nachgewiesen werden. Die auf N-Salicylidenhydrazid basierenden *cis*-Dioxomolybdän(VI)-Komplexe zeigten leider keine Bromoperoxidaseaktivität, statt dessen war der Komplex in der Lage die Oxidation von Sulfid zu Sulfoxid effizient zu katalysieren.

Im letzten Kapitel wurden *bis*-N-Salicylidenhydrazid-Liganden durch Kondensation von Salicylaldehyd mit *bis*-aliphatischen Dihydraziden dargestellt. Die Verbindung $H_4Ln$ kann als ligand mit zwei N-Salicylidenhydrazid-Taschen, welche über eine Methylenkette variabler Länge verbunden sind, angesehen werden. Der Ligand kann zwei Metallionen in Sechsfachkoordination binden, was zu binuklearen *cis*-Dioxovanadium(V)- und *cis*-Dioxomolybdän(VI)-Komplexen führt. Die Komplexe zeigten eine sehr effiziente Fähigkeit die Oxidation von Sulfid mittels $H_2O_2$ zu katalysieren. Ferner wurde ein chiraler

binuklearer *cis*-Dioxomolybdän(VI)-Komplex isoliert und als Katalysator für die Sulfoxidation eingesetzt. Der Komplex stellte sich als effizienter Katalysator für die Reaktion heraus, es wurden aber nur 4% *ee* bei Durchführung in Dichlormethan gefunden.

# Contents


**1 Theoretical Background** **11**

1.1 History and occurrence of vanadium . . . . . 11

1.2 Vanadium in biological systems . . . . . 13

1.3 Vanadium-containing haloperoxidase enzymes . . . . . 20

1.4 From vanadium haloperoxidases to acid phosphatases . . . . . 31

1.5 Model complexes for vanadium haloperoxidases . . . . . 33

1.6 Design of vanadium(V) complexes with N-salicylidene hydrazides . . . . . 40

**2 Vanadium(V) complexes based on N-salicylidene aliphatic acid hydrazides** **43**

2.1 *cis*-Dioxovanadium(V) complexes derived from N-salicylidene aliphatic acid hydrazides . . . . . 45

2.1.1 Structural characterization . . . . . 45

2.1.2 Spectroscopic data . . . . . 51

2.1.3 Oxidative bromination . . . . . 53

2.2 Mono-oxovanadium(V) complexes based on N-salicylidene aliphatic acid hydrazides . . . . . 55

2.2.1 Structural characterization . . . . . 56

2.2.2 Spectroscopic studies . . . . . 59

2.2.3 Electrochemical investigations . . . . . 62

2.2.4 Peroxidative bromination reaction of 1,3,5-trimethoxybenzene catalyzed by mono-oxovanadium(V) complexes . . . . . 66

2.3 Conclusions . . . . . 67

2.4 Experimental Part . . . . . 69

2.4.1 Materials . . . . . 69
2.4.2 Synthesis of N-salicylidene $\omega$-carbonic acid hydrazides . . . . . 70
2.4.3 Synthesis of the ammonium salts of *cis*-dioxovanadium complexes 71
2.4.4 Synthesis of the neutral *cis*-dioxovanadium complexes . . . . . 72
2.4.5 Synthesis of the mono-oxovanadium(V) complexes . . . . . 73
2.4.6 Catalytic oxidative bromination of TMB . . . . . 76

**3 Vanadium complexes based on N-salicylidene hydrazides with hydroxyl substituted aliphatic side chains 77**

3.1 *cis*-Dioxovanadium(V) complexes derived from N-salicylidene 4-hydroxy-butanoic acid hydrazide . . . . . 82
3.1.1 Structural characterization . . . . . 82
3.1.2 Spectroscopic data . . . . . 88
3.1.3 Oxidative bromination of 1,3,5-trimethoxybenzene . . . . . 89
3.1.4 Reactivity of the complexes towards HCl . . . . . 90
3.1.5 Reactivity of the complexes towards $H_2O_2$ . . . . . 93
3.2 Reactivity of the oxo-monoperoxovandium(V) complex . . . . . 103
3.3 Mono-oxovanadium(V) complexes based on N-salicylidene hydrazides that contain an hydroxyl-substituted aliphatic side-chain . . . . . 104
3.3.1 Structural characterization . . . . . 105
3.3.2 Spectroscopic studies . . . . . 108
3.3.3 Electrochemical investigations . . . . . 110
3.4 Conclusions . . . . . 113
3.5 Experimental Part . . . . . 114
3.5.1 Synthesis of $\omega$-hydroxy aliphatic acid hydrazide . . . . . 114
3.5.2 Synthesis of N-salicylidene $\omega$-hydroxyl aliphatic hydrazides . . . . 115
3.5.3 Synthesis of ammonium salts of *cis*-dioxovanadium(V) complexes 117
3.5.4 Synthesis of neutral *cis*-dioxovanadium(V) complexes . . . . . 118
3.5.5 Synthesis of neutral oxo-monoperoxovanadium(V) complexes . . . 119
3.5.6 Reactivity of the oxo-monoperoxovanadium(V) complex . . . . . 121

3.5.7 Synthesis of mono-oxovanadium(V) complexes . . . . . 122
3.5.8 Catalytic oxidative bromination of TMB . . . . . 124

**4 Vanadium(V) complexes based on N-salicylidene hydrazides that contain an amino-functionalized aliphatic side-chain 125**

4.1 *cis*-Dioxovanadium(V) complexes based on N-salicylidene 4-amino butanoic acid hydrazide hydrochloride . . . . . 127
4.1.1 Spectroscopic characterization . . . . . 132
4.1.2 Peroxidative bromination of TMB . . . . . 134
4.2 *cis*-Dioxovanadium(V) complexes derived from N-salicylidene 6-amino hexanoic acid hydrazides . . . . . 140
4.2.1 Spectroscopic studies . . . . . 144
4.2.2 Reactivity of the complex . . . . . 145
4.3 Oxidation of sulfides catalyzed by *cis*-dioxovanadium(V) complexes . . . 151
4.4 Conclusions . . . . . 152
4.5 *cis*-Dioxomolybdenum(VI) complexes based on N-salicylidene hydrazides that contain an amino-functionalized aliphatic side-chain . . . . . 153
4.5.1 Spectroscopic characterization . . . . . 156
4.5.2 Catalytic tests . . . . . 157
4.6 Experimental Section . . . . . 159
4.6.1 Synthesis of amino-aliphatic hydrazide as hydrochloride salts . . . 159
4.6.2 Synthesis of Schiff base ligands as hydrochloride salts . . . . . 160
4.6.3 Synthesis of *cis*-dioxovanadium(V) complexes . . . . . 161
4.6.4 Synthesis of *cis*-dioxomolybdenum(VI) complexes . . . . . 163
4.6.5 Reactivity of the *cis*-dioxovanadium(V) complexes . . . . . 165
4.6.6 Catalytic oxidative bromination of TMB . . . . . 166
4.6.7 Catalytic oxidation of methyl phenyl sulfide . . . . . 166

**5 Vanadium(V) complexes based on N-salicylidene hydrazides that contain an guanidino-functionalized aliphatic side-chain 167**

5.1 *cis*-Dioxovanadium(V) complex based on N-salicylidene guanidino acetic acid hydrazide hydrochloride ligand . . . . . 169

5.1.1 Spectroscopic studies . . . 173
5.2 *cis*-Dioxovanadium(V) complex based on N-salicylidene 6-guanidino hexanoic acid hydrazide . . . 174
5.2.1 Spectroscopic studies . . . 179
5.3 Oxidative bromination of 1,3,5-trimethoxybenzene . . . 179
5.4 Oxidation of sulfides catalyzed by *cis*-dioxovanadium(V) complexes based on guanidine functionalized N-salicylidene hydrazides . . . 180
5.5 Conclusions . . . 181
5.6 Experimental Section . . . 182

**6 Binuclear vanadium(V) and molybdenum(VI) complexes as catalysts for sulfoxidation reaction 187**

6.1 Binuclear *cis*-dioxovanadium(V) complexes with *bis*-N-salicylidene hydrazides . . . 190
6.1.1 Sulfoxidation catalytic reaction . . . 193
6.2 Binuclear *cis*-dioxomolybdenum(VI) complexes based on *bis*-N-salicylidene hydrazide ligands . . . 196
6.2.1 Spectroscopic characterization . . . 198
6.2.2 Sulfoxidation reaction . . . 200
6.3 Conclusions . . . 202
6.4 Experimental Part . . . 203
6.4.1 Synthesis of *bis*-aliphatic acid hydrazides . . . 203
6.4.2 Synthesis of Schiff base ligands . . . 205
6.4.3 Synthesis of *cis*-dioxovanadium(V) complexes . . . 207
6.4.4 Synthesis of binuclear *cis*-dioxomolybdenum(VI) complexes . . . 209

**7 Conclusions and Future Projects 213**

**8 Characterization techniques and crystallographical data 218**

# Chapter 1

# Theoretical Background

## 1.1 History and occurrence of vanadium

Vanadium was first discovered in Mexico in 1802 by the mineralogist A. M. del Rio, who named the new element "panchromium" due to its various colors when it changes oxidation state.

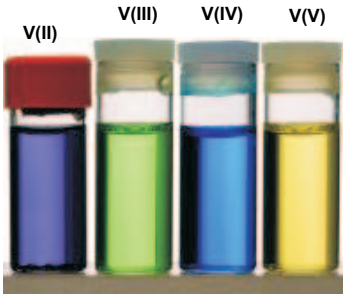


Later he renamed it "erythronium" due to the the red colored salts of the new metal obtained when it was treated with acids. However shortly thereafter he withdrew his discovery, being convinced that he had discovered only a new source of chromium. In 1831, the element was rediscovered in remnants of iron ore from southern Sweden by the Swedish chemist N. G. Sefström, who named it "vanadin" (vanadium) in honor of the goddess of beauty, love and youth, "Vanadis", commonly known as the goddess Freya by the Northern Germanic tribes. In the same year, "erythronium" was reanalyzed by Wöhler who establish its identity with vanadium.[1]

Vanadium can be found in earth's crust in 0.014% abundance, as well as in aquasphere in concentrations ranging between 20-35 nM. In ores, vanadium is quite rare, but nevertheless few examples are known, such as patronite (a mixture of $VS_4$ with $SiO_2$ and $Al_2O_3$), vanadinite ($Pb_5[(VO_4)_3Cl]$) and carnotite ($K[VO_2{\cdot}UO_2]$, a mineral which after preparation affords concomitantly both uranium and vanadium). Vanadium is instead more often found in iron ores, clays and basalts, as well as in fossilized organic materials and crude oil. In seawater, vanadium is the second most abundant transition metal, existing mainly in the ionic form as $H_2VO_4^-$. It is contained in red and brown algae[2,3] and in tunicates, which accumulate vanadium in their blood cells.[4,5] However the accumulation of vanadium by living organisms is not restricted to marine organisms and vanadium-containing enzymes have been also isolated from terrestrial fungi *Curvularia Inaequalis*,[6] as well as from the toadstool *Amanita muscaria* where a low molecular weight vanadium compound has been found.[7,8]

Vanadium compounds have a large variety of applications, ranging from the semiconductoring properties of the $V_2O_5$-$GeO_2$ system to the industrial use of $V_2O_5$ as catalyst in the production of sulfuric acid. Moreover, a few vanadium complexes have been reported to posses therapeutic effects, ranging from the insulin-like mimetic peroxovanadates[9] to the antitumor effect shown by vanadocene dichloride.[10]

The oxidation state of vanadium varies between -1 and +5, with the exception of +1, but only the higher oxidation states +3, +4 and +5 are of biological importance. Vanadium forms stable compounds in the +4 and +5 oxidation states under normal conditions. Vanadium(IV) chemistry is dominated by vanadyl complexes, which contain a $VO^{2+}$ unit. Due to the $d^1$ configuration, vanadium(IV) species can be identified by EPR spectroscopy when an eight-hyperfine line signal is observed as a consequence of electron-nuclei (I=7/2) interaction. Vanadium(V) compounds are diamagnetic species and $^{51}V$ NMR is a useful tool to characterize them, since the resonances are sensitive to the coordination sphere of the vanadium center.[11] Thus, vanadium in complexes that contain O and N donor atoms resonate between -400 and -600 ppm. Resonances far downfield have been reported for vanadium complexes that contain a catecholate and hydroxymate entity,[12] while resonances upfield of -600 ppm have been found in bidentate ligands, such as peroxide ligands.[13] Early $^{51}V$ NMR spectroscopy studies on vanadium(V)-containing

enzyme reported a very broad -1200 ppm resonance.[14] The association of the quadrupolar vanadium nuclei (Q=-0.052·$10^{-28}$m$^2$) with the protein can be responsible for broadening of the signal width, but no synthetic vanadium models have been reported to give similar $^{51}$V resonances.

## 1.2 Vanadium in biological systems

Vanadium in the oxidation state +3 has been found in the blood cells of ascidians such as *Ascidia gemmata*, and the fan worm *Pseudopotamilla occelata*.[4,15] Ascidians (tunicates or sea squirts) constitute a class of invertebrate marine organisms that accumulate vanadium(III). Investigations on these organisms have been made and suggest a redox conversion of V(V) species from seawater to V(IV) and V(III), respectively. Isolation and characterization of such organisms showed that considerable amounts of sulfate coexist with vanadium(III).[16–18] Vanadium in the lower oxidation state has been reported to be accumulated especially in morula cells, a class of vacuolated cells of ascidians that are strongly yellow fluorescent due to the tunichrome content. Tunichromes are polyphenolic tripeptides (see Figure 1) capable of binding V(III) and maintaining it in its +3 oxidation state at physiological pH.[19,20] Hypothesis of the implications of these tunichromes in the redox process of vanadium have been proposed, but the mechanism remains unclear.

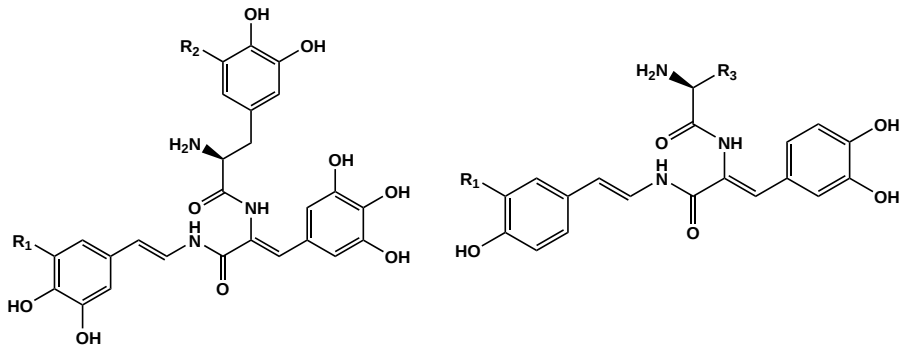


Figure 1: Selected examples of tunichrome ligands, $R_1$=$R_2$=OH, $R_1$=H $R_2$=OH, $R_1$=OH $R_2$=H, $R_3$=H and/or iso-butyl.

The accumulation of vanadium(III) in ascidian blood cells was correlated to the existence of the anionic transporter and a vanadium transporter has been suggested.[21] Vanabis is a vanadium-associated protein complex that has been proposed to facilitate the transport and accumulation of vanadium in the vacuoles of these organisms.[21,22] The fact that vanabis binds V(IV) preferentially suggests that the reduction takes place before the vanadium ion binds to the protein. Spectroscopic studies showed that vanadium(V) persists in blood plasma and that it is trapped by the blood cells, thus facilitating the reduction to vanadium(IV) and vanadium(III).[22] However, the accumulation and storage of vanadium(III) ions by ascidians is still a subject left unsolved and the role of vanadium(III) is both a controversial issue and big challenge for inorganic chemists. The aqua ion $[V(H_2O)_6]^{3+}$ can be obtained from $V_2O_5$ by reaction with acids or by electrolytic or chemical reductions of vanadium(IV) and (V) under stringent anaerobic conditions. Vanadium(III) can be maintained in solution only under acidic conditions or in the presence of potent chelate systems, otherwise the aqua vanadium(III) blue-green ion is rapidly oxidized by air to vanadium(IV) (standard reduction potential vs. normal hydrogen electrode is 0.337 V for vanadium(III)).

Vanadium in the oxidation state +4 has been found in vanadium nitrogenases isolated from the nitrogen fixing bacteria *Azotobacter*[23] and as amavadin isolated from the mushroom *Amanita muscaria*.[24]

The bacterial enzyme nitrogenase is able to catalyze the reduction of atmospheric $N_2$ to $NH_3$ and is responsible for cycling about $10^8$ tons of nitrogen per year from the atmosphere to the soil.[23,25] The industrial fixation of $N_2$ to form $NH_3$ requires temperatures between 300 and 500°C, pressure over 300 atmospheres and the presence of Fe-based catalyst, whereas the nature paradoxically solved the process with relatively small number of microorganisms called diazotrophs and nitrogenase enzyme systems.[23] Nitrogenases are a class of enzymes that contain two metalloprotein components: the Fe-protein and the MoFe-protein and/or VFe-protein as cofactors.[26] Conventional nitrogenase with the molybdenum cofactor has been well studied and it has been reported to function by substrate reduction, a process that involves three basic types of electron transfer reactions: 1) the Fe-protein component can be reduced *in vivo* by electron carriers such as dithionite; 2) transfer of single electrons from the Fe-protein to the MoFe-protein component

in a MgATP-dependent process with a minimum two MgATPs hydrolyzed per electron transferred; and 3) electron transfer to the substrate which is bound to the active site within the FeMo-protein. The overall reaction of dinitrogen reduction by nitrogenases involves 16 molecules of MgATP under optimal conditions.[27]

$$N_2 + 8e^- + 8H^+ + 16MgATP \longrightarrow 2NH_3 + H_2 + 16MgADP + 16P_i$$

X-ray crystal structure determination of Mo-nitrogenase showed that the Fe-protein component is formed by a $[Fe_4S_4]$ cluster, while the MoFe-protein component consists of a $[Fe_8S_7]$ unit known as P-cluster and a FeMo-cofactor (FeMoco) formed by a $[Fe_7S_9Mo$-homocitrate] center. FeMoco contains a cysteine residue coordinated to the terminal iron atom in a thiol manner, while the molybdenum atom is coordinated next to the sulfur bridges by a homocitrate moiety and a histidine residue.[28,29] The vanadium-nitrogenase enzyme, with a VFe-cofactor, is widely distributed with homologous genes to Mo-nitrogenase enzyme. It has been suggested that the vanadium system does not arise from a simple substitution of molybdenum from the MoFe-cofactor and the two enzymes present different reactivity at certain pH values and temperatures.[23] Investigations on V-nitrogenase isolated from *Azobacter chroococcum* showed that the catalyzed reduction of dinitrogen to ammonia takes place in a similar manner as with the Mo-nitrogenase enzyme, but instead a greater amount of $H_2$ is generated and more consume of ATP is required.[25]

$$N_2 + 12e^- + 12H^+ + 40MgATP \longrightarrow 2NH_3 + 3H_2 + 40MgADP + 40P_i$$

Based on several methods of characterization (EPR, MCD and Mössbauer studies[23]) and, later, according to crystallographic characterization of a $[VFe_3S_4Cl_3(dmf)_3]^-$ complex, the molecular structure of V-nitrogenases have been proposed to contain similar features to Mo-nitrogenases (see Figure 2). Several vanadium complexes with a $[VFe_3S_4]^{2+}$ core have been developed, but none of them have been reported to be capable of reducing nitrogen to ammonia. A structural Fe-V sulfur bridged cluster $[VFe_3S_4Cl_3(dmf)_3]^-$ has been reported as being able to catalyze the conversion of hydrazine to ammonia.[30,31]

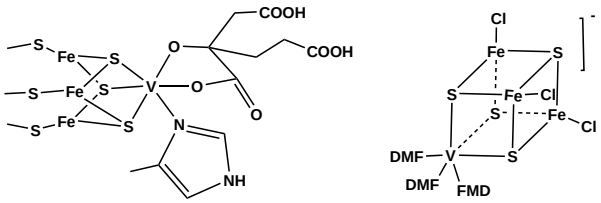


Figure 2: Proposed vanadium protein in vanadium-nitrogenase (left) and V-Fe model complex (right).

Amavadine is a vanadium(IV) complex that contain two equivalents of *S,S*-2,2'-hydroxy-iminodipropionic acid ($H_3$hidpa) and one equivalent of vanadium[32] (Figure 3). The natural product contains five chiral centers, four from chiral carbon atoms all in a *S* configuration and the fifth from the manner in which the ligand wraps around the vanadium.[33] The structural elucidation of amavadine was initially controversial, because it contains a rare example of non-oxovanadium(IV) compound.[34] The compound has great hydrolytic stability and can undergo an irreversible one electron redox transfer, and therefore it has been proposed as an electron-transfer agent in mushrooms.

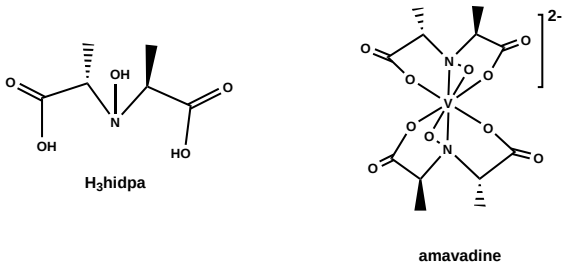


Figure 3: Schematic representation of the $H_3$hidpa ligand and its vanadium complex amavadine.

Further, amavadine has been reported as catalyst for thiol oxidation,[35] peroxidative halogenation, hydroxylation and oxygenation of alkyl and aromatic substrates.[36] Recently, it has been reported that amavadine can also convert methane to acetic acid in the presence of a perdisulfate salt and trifluoroacetic acid. Amavadine can be replaced by vanadium(V) complexes with ethanolamine, while the trifluoroacetic acid and the

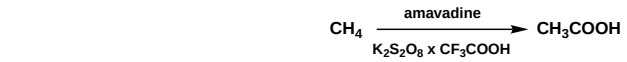


disulfate salt are necessary for reaction to proceed.[37]

Vanadium in its highest oxidation state has been found in vanadium-haloperoxidase enzymes isolated from marine algae[2,3] and terrestrial fungi.[38] Vanadate has been recognized as a structural and electronic analogue of phosphate and is most evident in the tetrahedral trianionic forms ($VO_4^{3-}$ and $PO_4^{3-}$). Vanadium(V) forms vanadate and vanadate derivates in aqueous solution and the analogy with phosphorus chemistry is extended to its electronic properties as a consequence of the similarity between the $pK_a$ values of vanadate and those of phosphate.[39]

$$H_3VO_4 + H_2O \rightleftharpoons H_2VO_4^- + H_3O^+ \; pK_a{=}3.5 \; (2.1 \text{ for } H_3PO_4)$$
$$H_2VO_4^- + H_2O \rightleftharpoons HVO_4^{2-} + H_3O^+ \; pK_a{=}7.8 \; (7.2 \text{ for } H_2PO_4^-)$$
$$HVO_4^{2-} + H_2O \rightleftharpoons VO_4^{3-} + H_3O^+ \; pK_a{=}12.5 \; (12.7 \text{ for } HPO_4^{2-})$$

A notable difference is the existence at physiological pH of vanadate as a mono-anion $H_2VO_4^-$, while phosphate exits primarily as the dianion $HPO_4^{2-}$. In contrast to phosphate chemistry, where $H_3PO_4$ is very stable, the similar $H_3VO_4$ is not well documented and its existence is doubtful. Under strongly acidic conditions (pH=1), $VO_2^+$ is the major species in aqueous vanadate solutions. This species is thermodynamically stable due to the hydration effect which increases its coordination number.[40] At around neutral pH, $H_2VO_4^-$ and $H_2VO_4^{2-}$ oligomerize to form dimers (**a**), tetramers (**b**) and pentamers (**c**).

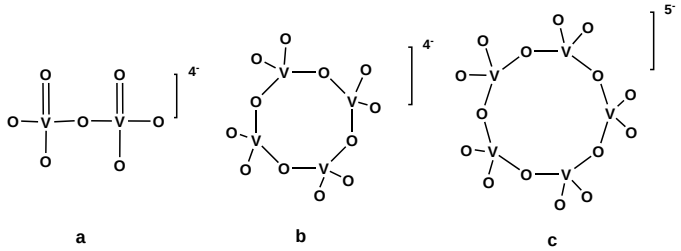

These vanadium anhydrides are analogous to pyrophosphate and polymeric phosphate anhydride. The tetrameric and pentameric vanadates are cyclic in solution and fail to show a linear analogy with biologically linear phosphates.

Both vanadium and phosphorus form esters varying from the tetra-coordinated phosphorus esters to the common five-coordinated vanadium esters. Four-coordinated V–P analogy exists in biphenolic diol,[41] phenoxide[42] and tri-tert-butyl-siloxide[43] when a bulky group introduced in the alkoxide molecules leads to a sterically restricted coordination number of the vanadium atom. Nevertheless, examples of four-coordinated vanadium atoms are quite rare and vanadium generally has a higher coordination number.

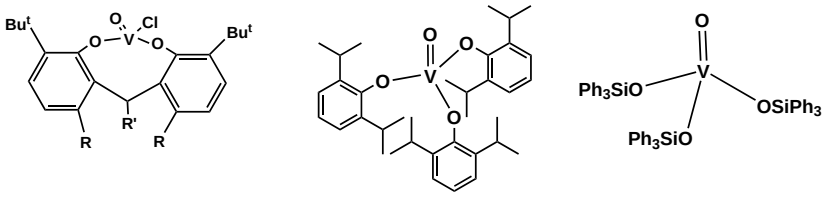


Vanadium esters (alkoxides) formed in aqueous solution have been reported to be substrates for phosphate-involving enzymes, such as dehydrogenase, isomerase and aldolase.[44–47]

$$\mathrm{ROH} + \mathrm{H_2VO_4^-} \rightleftharpoons \mathrm{ROVO_3H^-} + \mathrm{H_2O}$$

The formation of such esters take place rapidly at room temperature, while phosphate ester bond formation is much slower. Moreover, the vanadate-ester bond is more labile in aqueous solution than the analogues phosphorus bond.[48] A biologically important vanadate ester formation results from the reaction of vanadate with D-glucose, an organic ligand containing several hydroxyl groups capable of forming vanadate esters. Indeed $^{1}$H and $^{13}$C NMR investigations have confirmed the coexistence of several species in solution. However, it has been reported that a small amount of glucose-6-vanadate complex is also formed. This glucose-6-vanadate has been reported to be recognized by glucose-6-phosphate dehydrogenase, resulting in a rapid oxidation of D-glucose to D-gluconate in presence of the vanadate.[44,45]

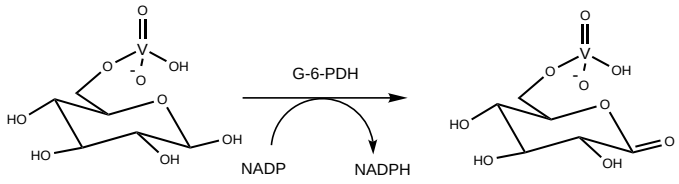


Although there are many parallels between vanadate and phosphate in their chemistry and biological action, there are also notable differences. For instance vanadium(V) can be easily reduced to V(IV), while phosphate cannot. Vanadium, due to its d-orbital, can adopt coordination numbers of 5, 6, 7 and 8, while phosphorus in biologically relevant compounds is four-coordinated. Penta-coordinated phosphate is thermodynamically unstable and has been reported only for high-energy intermediates, whereas penta-coordinated vanadate is a common feature for vanadium compounds. Penta-coordinated vanadium compounds are therefore regarded as analogues for phosphate transition states.[49]

A large variety of phosphate-metabolizing enzymes including phosphatases, ATPases and ribonucleases have been reported to be strongly inhibited by vanadium complexes. These enzymes catalyze the hydrolysis of phosphate ester bonds via a mechanism that involves the formation of penta-coordinated phosphate as high-energy transition state. The potent inhibition of these enzymes by vanadate is due to the chemical similarities between vanadate and phosphate,[50] with vanadate functioning as a transition state analogue.

Phosphatase enzymes can be divided into three main categories, according to the amino acid residue involved in the intermediate phosphate ester formation. Therefore, alkaline phosphatases have a nucleophilic serine residue in the active phosphate ester, acid phosphatases are based on a histidine residue linked to the ester and protein phosphatases contain a cysteine residue resulting in a thiophosphate ester (Figure 4).

The inhibition of phosphatases by vanadium compounds indicates that vanadate mimics the five-coordinate transition state of phosphate ester hydrolysis. Because the acid and alkaline phosphatases are compatible with vanadium(V) compounds, they have been particularly well studied.

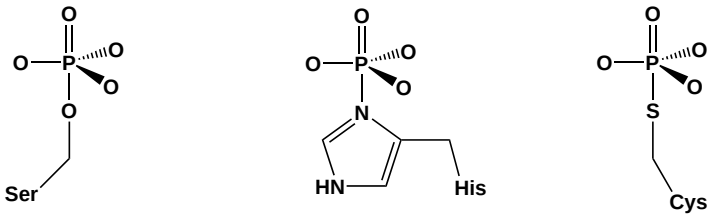


Figure 4: Schematic representation of the phosphointermediate esters in alkaline phosphatase (Ser residue), in acid phosphatase (His residue) and protein phosphatase (Cys residue).

The *cis*-dioxovanadium complex with dipicolinate, which contains a five-coordinated metal center, is known as the strongest inhibitor of these classes of phosphatases.[51] However, protein phosphatases are also inhibited by vanadium compounds and here it is worth mentioning the tyrosine-phosphatase, an enzyme involved in signal transduction mechanisms for controlling and regulating intracellular processes, e.g. in the insulin receptor system.[52] The inhibition of protein-phosphatases is likely to be important for the insulin enhancing effect of vanadium compounds and their therapeutic antidiabetic effect has been correlated with the possibility of increasing the autophosphorylation of the insulin receptor on a tyrosine residue, as well as to the stimulation of the translocation of the insulin-like growth receptor from an intracellular compartment to the plasma membrane.[53,54] This process is analogous to the insulin-induced movement of the glucose transporter from an intracellular compartment to the plasma membrane[55] and it has been postulated that, while vanadium complexes can not substitute insulin, they can manifest insulin enhancing actions.[9]

## 1.3 Vanadium-containing haloperoxidase enzymes

Haloperoxidases are enzymes capable of catalyzing the two-electron oxidation of halides by hydrogen peroxide forming hypohalous acid (HOX).[6,56] There are two main categories of haloperoxidases: those based on the heme group which are called heme-containing haloperoxidases and the second group is represented by non-heme haloperoxidases. The

latter class of haloperoxidases are subdivided into two categories: vanadium-containing haloperoxidases, with vanadate as prosthetic group, and "metal-free" haloperoxidases,[57] respectively. The nomenclature of haloperoxidases is established according to the most electronegative halide which can be oxidized catalytically. Therefore vanadium-containing chloroperoxidases (V-CPO) catalyze the oxidation of $Cl^-$, $Br^-$ and $I^-$; vanadium-containing bromoperoxidases can catalyze the oxidation of $Br^-$ and $I^-$ and vanadium-containing iodoperoxidases have been reported as catalyst for oxidation of $I^-$. The first report of an enzyme-based vanadate date from 1984, when Vilter discovered that the bromoperoxidase enzyme isolated from a brown algae, *Ascophyllum nodosum*, is inhibited by phosphate and the enzyme could not be re-activated by iron or other metals.[2] Thus, he established the existence of a new class of "non-heme" haloperoxidases. Since then, the interest in studying vanadium haloperoxidases has increased and several sources of isolation have been reported. Vanadium bromoperoxidases can be also isolated from the red seaweeds *Corralina pilulifera*[3] and *Corralina officinalis*[58] and from *Macrocystis pyrifera*.[59] Vanadium chloroperoxidases have been found in the terrestrial fungi *Curvularia inaequalis*.[6] More recently, vanadium-iodoperoxidases have been isolated from *Pelvetia canalicuta*[60] and the *Laminariaceae* family.[61]

Vanadium chloroperoxidase enzymes are the most studied vanadium-containing enzymes and crystal structure determination of the azide-substituted form, the apo-form (metal free) and the tungstate-containing enzyme are available.[62] The crystal structure determination of the native form of the enzyme was first reported in 1996[38] by Messerschmidt *et al.*, for the V-CPO enzyme isolated from *Curvularia Inaequalis*. This showed vanadate as the prosthetic group linked to the protein through only a covalently bonded histidine residue (His496). The protein fold is mainly $\alpha$-helical, with two four-helix bundles as structural motif. The vanadate moiety is located at the top of one of them, in a broad channel that is lined on one hydrophilic and one hydrophobic half, respectively. The proposed geometry of the vanadium atom is trigonal bipyramidal, with three non-proteinous oxygen atoms in the equatorial plane and the fourth, in the apical position, postulated as an OH group (V–O 193 pm). An extensive hydrogen bonding interaction has been observed, that is capable of fixing the vanadate in the protein shell. The equatorial oxygen atoms of the prosthetic group are in hydrogen bonding contact with

positively charged amino acid residues, such as Lys353, Arg360 and Arg490 (Figure 5). The lysine and one arginine amino acid are also used to compensate for the negative charge of the vanadate moiety. Moreover, the Arg490 residue is further stabilized and kept close to the active binding site by the formation of a salt-bridge with an aspartate residue, namely Asp292. Other key residues in the active site are Gly403 and Ser402, also forming hydrogen bonds with the equatorial oxygen atoms. Furthermore the His404 residue is the single amino acid hydrogen bonded to the apical hydroxy group. All these amino acids play a very important role in the chloroperoxidase activity.

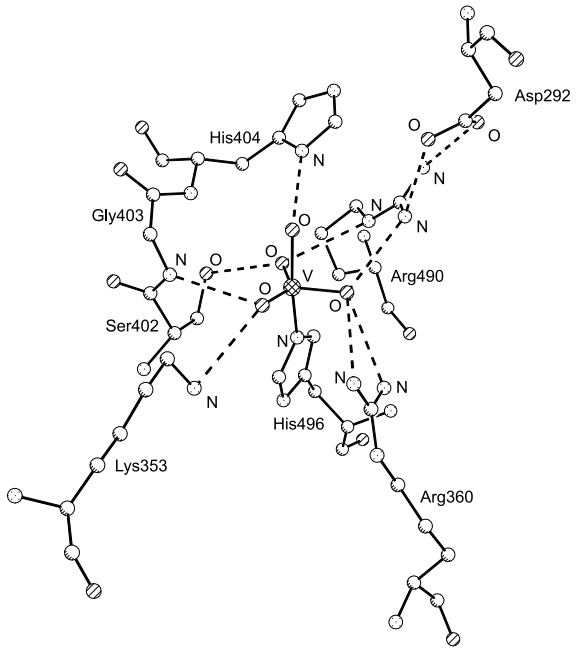


Figure 5: Crystal structure of the Vanadium chloroperoxidase isolated from *Curvularia Inaequalis*.

Mutagenesis studies performed by replacement His496 with alanine has been reported and support its vital role[63] in stabilizing the vanadate group through covalent bond of $N^{\epsilon}$ atom of the imidazole ring. The site-direct mutant with alanine yields the inactive apo-enzyme due to the incapacity of the enzyme to bind vanadate. A mutagenesis experiment on His404[38] with alanine resulted in the loss of chlorination activity, but the mutant still functions as a partial bromoperoxidase.[64] The vital role of the second histidine residue in the catalyzed chloride oxidation reaction has been explained

as a possible acid-base role during catalysis. Steady-state kinetic data suggests the acid-base role is played by vanadate-coordinated water or a histidine residue, due the determined $pK_a$ value of 5.6-6.5.[65] The single alanine mutant of the positively charged amino acids (Lys353, Arg490 and Arg360) have been also reported as inactive vanadium chloroperoxidases, but still with vanadium bromoperoxidase function.[63] Replacement of vanadate with other oxo-metals, such as molybdate and tungstate has also been studied. The crystal structure of vanadium chloroperoxidase with tungstate in the active site has been reported. By comparison to the vanadate-containing enzyme where the vanadium-histidine bond is strong (211 pm), the tungstate-containing enzyme contains a very weak W–N(His) (255 pm) bond.[62] When vanadate was replaced by molybdate, the molybdate-containing chloroperoxidase was incapable of performing the catalytic reaction, although the protein environment is able to bind molybdate.[62,66] This observation demonstrates the affinity of the enzyme for vanadate, while the results from site-direct mutagenesis studies clearly show the importance of the hydrogen bonding interaction in the catalytical activity of the enzyme. Apparently, any change in the vicinity of the prosthetic group converts V-CPO to V-BPO, while substitution of vanadate with similar oxometalates yields an inactive enzyme.

Spectroscopic and kinetic studies on the oxidative halogenation of V-CPO showed no change in the redox state of the transition metal during the catalytic cycle. The vanadate functions as a Lewis acid,[67] reacting first with hydrogen peroxide to form a side-on bound peroxide, which subsequently reacts with the halide.[6] Crystal structure determination of such a peroxo-chloroperoxidase has also been reported[6] and is depicted in Figure 6. The vanadium atom has a distorted tetragonal geometry with an apical oxygen atom, while the $\eta^2$ coordinated peroxide, the histidine residue and another non-proteinous oxygen atom are in the basal plane. The His404 is no longer in hydrogen bonding contact with the oxygen atoms of the peroxovanadate moiety, but instead the Lys353 residue is activating one of the peroxo-oxygen atoms through hydrogen bonding interaction.

Figure 6: Crystal structure of the peroxo form of vanadium chloroperoxidase.

The catalytic cycle proceeds through hydrogen bonding network. For instance *lys* residue activates the intermediate peroxide prior to halide attack by increasing the electrophilicity on the $O_{peroxo}$ oxygen.[68,69] Acid requirement for the catalytic turnover has been reported with the enzyme functioning optimally at pH 5.0 by forming a strong oxidizing intermediate with a protonated peroxide group (see Figure 9).

The X-ray structure determination of the vanadium bromoproxidase isolated from *Ascophyllum nodosum* has been also reported in 1999 by Vilter *et al.* at 2.0 Å.[70] There is a significant overlap of the active site between the two vanadium-containing enzymes, with a highly conserved vanadate binding site motif (see Figure 7). The vanadium atom has a distorted trigonal bipyramidal geometry with three non-proteinous oxygen atoms in the equatorial plane and the hydroxyl group and histidine ($His486^{V-BPO}$ and $His496^{V-CPO}$) residue in apical positions. The equatorial oxygen atoms of the vanadate moiety are also involved in hydrogen bonding interactions with the amino acid residues of the same chemical structure, i.e His418, Lys341, Arg349, Arg480, Ser416 and Gly417. The difference appears first in the further hydrogen bonding interactions of the arginine residues, respectively $Arg480^{V-BPO}$ and $Arg490^{V-CPO}$, that are part of vanadate-binding site. In V-CPO this arginine residue forms a salt-bridge to Asp292, while in V-BPO Arg480

is hydrogen bonded with an amino acid residue (Thr275) from the second shell of the protein environment. The main difference between the two enzymes is the presence of an additional histidine residue (His411) in V-BPO near the vanadate-binding site instead of Phe397 in V-CPO. In the peroxo-form of V-CPO, the peroxide moiety is directed towards Phe397 and forms a hydrogen bond with the Lys353 residue, whereas when the peroxovanadate is modelled into V-BPO, the additional His411 residue will be within hydrogen bonding distance. Therefore in V-BPO the additional histidine amino acid might be an additional donor/acceptor site.

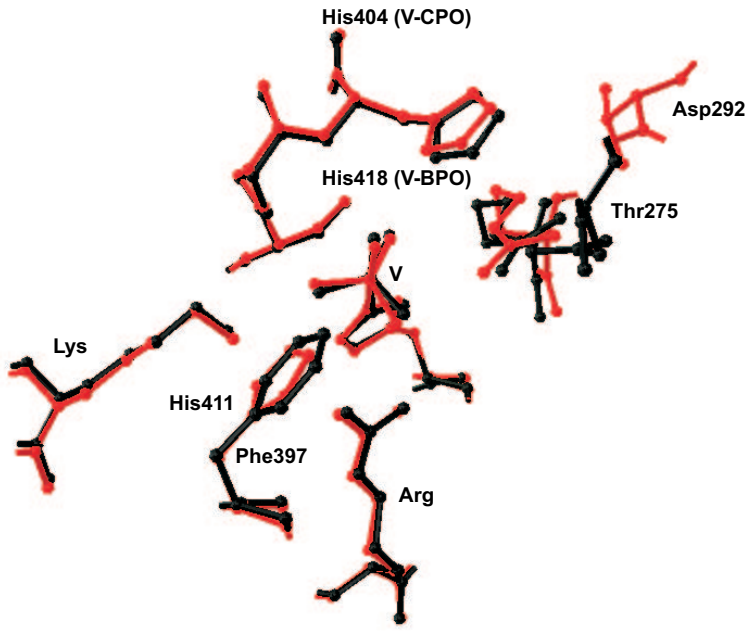


Figure 7: Overlay of the active site of V-CPO isolated from *Curvularia Inaequalis* (black drawings) with active site of V-BPO isolated from *Ascophyllum nodosum*.

Nevertheless, besides these differences, the two vanadium-containing enzymes have an $\alpha$-helical structure, formed by two four helix bundles with a common active vanadate-binding site feature that highlights the close relationship between them and could be an evidence of a common genetic origin. The substrate affinity of the enzymes for different halide oxidation reactions has been structurally attributed to the catalytic histidine residues ($His418^{V-BPO}$ and $His404^{V-CPO}$). These amino acids are stabilized differently in the two enzymes via hydrogen bonding interactions with the amino acids in their vicinity,

being tight in V-BPO and, therefore, leading to a different pH dependence.

The importance of these enzymes lie in their role in the halogenation of various organic substrates by HOX, formed in the enzyme-catalyzed reaction.[59,71,72] This can have industrial applications, since many halogenated derivatives are of pharmaceutical use and/or used for synthesizing active compounds. If no organic scavenger is present, the oxidized halide reacts with an additional hydrogen peroxide to form singlet oxygen.[73–75]

$$X^- + H_2O_2 + RH \overset{V-HPO}{\longrightarrow} RX + 2H_2O$$
$$X^- + H_2O_2 \overset{V-HPO}{\longrightarrow} 2H_2O + {}^1O_2$$

The vanadium-containing bromoperoxidases are enzymes with high thermal stability, presenting significant activity at temperature up to 70 °C. Moreover, this class of enzymes shows high tolerance to organic solvents, e.g. methanol, ethanol, iso-propanol and acetone do not inactivate the enzyme and can be used for enzyme purification.[71] Vanadium bromoperoxidases are also unaffected by detergents and their activity is still detectable after electrophoresis with sodium dodecyl sulfate.[76] Since crystallographic determination of the two enzymes shows high similarities in the vanadium-binding active site, it is most likely that these peroxidases share the same stability. Additionally, V-HPOs support a high concentration of both their substrate ($H_2O_2$) and their product (HOX), which would readily inactivate the corresponding heme-haloperoxidases. Thus, the haloperoxidases with vanadate as prosthetic group represent potent biocatalyst candidates for industrial applications in organic synthesis.

The Fe-heme moiety from heme-haloperoixdase isolated from the fungus *Caldariomyces fumago* is oxidized by hydrogen peroxide to form a $Heme^{+}Fe^{IV}{=}O$ intermediate capable of oxidizing the halide ion.[77] In this case, the mechanism involves a redox process, whereas in V-HPOs this mechanism is not operative and the vanadium atom does not change its oxidation state, rather it functions as Lewis acid.[78] Mechanistic investigations involving kinetic and product analysis suggest initial addition of $H_2O_2$, resulting in the formation of a side-on peroxide, followed by subsequent reaction with halide.[68] Spectroscopic investigations for $VO_2$-$O_2$ species were monitored by $^{17}O$ NMR and showed the formation of the peroxo-intermediate, but no evidence for an intermediate in which the

halide binds to the vanadium atom.[79] The rate-determining step in the catalytic cycle is the nucleophilic attack of the halide on the active peroxide-intermediate, generating HOX. This intermediate oxidized halide is able to halogenate a large variety of organic substrates. The proposed mechanism of the reaction is depicted in Figure 8.

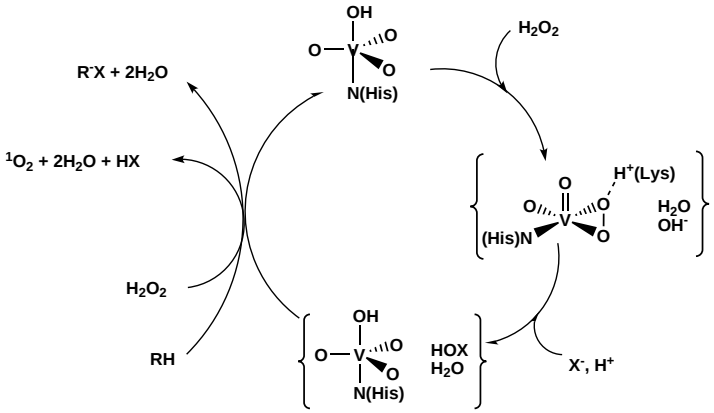


Figure 8: Schematic representation of the proposed mechanism of vanadium haloperoxidases catalyzed reactions.

A different pH dependence has been reported for the two types of vanadium haloperoxidases, varying from pH 5 for vanadium chloroperoxidase to pH 6.5 for vanadium bromoperoxidase. On these basis the intermediate peroxide was proposed to be different (see Figure 9). Protonation of the peroxo-intermediate has been proposed in the case of V-CPO, which requires an acidic medium for catalyzing the reaction. This is explained as a consequence of the higher electronegativity of the chloride compared to bromide.

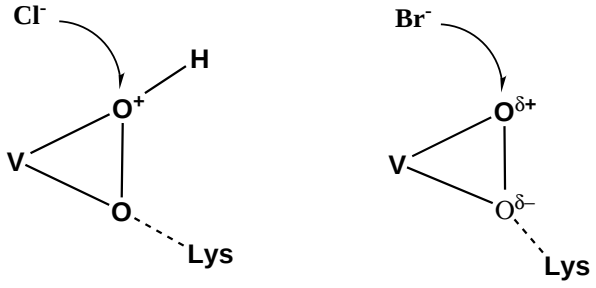


Figure 9: Peroxo-intermediate for V-CPOs (left) and V-BPOs (right).

The classic organic substrate for evaluating haloperoxidase activity is monochlordimedone (2-chloro-5,5-dimethyl-1,3-dimedone; MCD).[80] The reaction can be followed spectrophotometrically at 290 nm as a consequence of different absorption coefficient between the enol and ketone forms (Figure 10). In addition, phenol red can be used as organic substrate for oxidative bromination, resulting in the formation of bromphenol blue.[81]

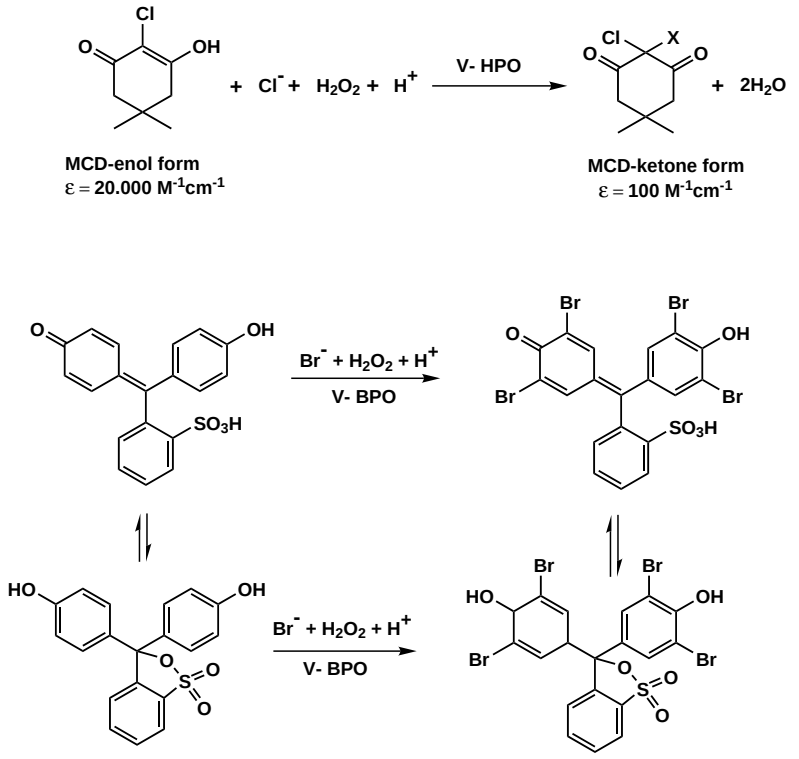


Figure 10: Halogenation of specific substrate, MCD, by vanadium-dependent chloroperoxidases (upper reaction) and the catalytic bromination of phenol red to bromophenol blue and their tautomerization equilibria (lower reaction).

Furthermore, V-HPOs exibit chemo-, regio- and stereoselectivity, which leads to the conclusion that the oxidized bromide is not diffusible, but is instead linked to the enzyme.[82] Competitive kinetic studies comparing the bromination of indoles and MCD as substrates in equimolecular amounts, using V-BPO/$H_2O_2$/$Br^-$, showed that the enzyme catalyzes preferentially the bromination of indole derivatives over MCD. In contrast, the same reaction performed with aqueous bromine showed the simultaneous bromination of all substrates present in solution.[82–84] The first regiospecific bromoperoxidative oxidation

was reported using 1,3-di-tert-butylindole as substrate, which, in the presence of $H_2O_2$ and $Br^-$, is oxidized quantitatively to 1,3-di-tert-butyl-2-indolinone with no brominated product (Figure 11). Conversely, the chemical reaction with aqueous bromine solution produces a mixture of brominated 2-indolinone derivatives.[85]

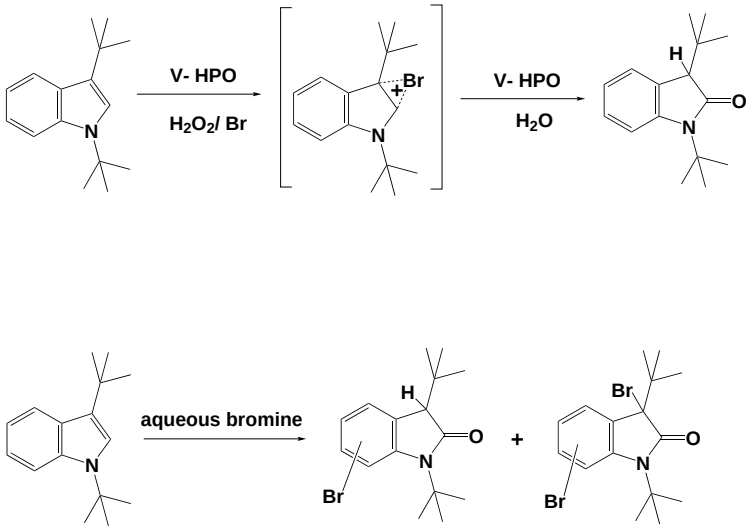


Figure 11: V-BPO catalyzed regiospecific bromoperoxidative oxidation of 1,3-di-tert-butylindole.

The only reported stereoselective reaction catalyzed by V-HPO is the oxidation of sulfides in the absence of halides. The oxidation of sulfides has been studied quite extensively in the recent times, especially when it proceeds in a stereospecific manner. Enantiopure sulfoxides are useful synthons in asymmetric synthesis and they have wide application in the pharmaceutical industry.[86] Methodologies for catalytic asymmetric sulfide oxidation are based on transition metal complexes, such as complexes of titanium, vanadium, chromium, iron and manganese with chiral Schiff base ligands. Vanadium haloperoxidases also catalyze the oxidation of sulfides to the corresponding sulfoxides, varying from an enantiolselective behavior in the case of the vanadium bromoperoxidases[87,88] to a racemic mixture of sulfoxides when vanadium chloroperoxidase[89] is used as catalyst (Figure 12). The reaction rate of enantioselective oxidation of methyl phenyl sulfide is rather slow (about 1 $min^{-1}$), but occurs with 96% *ee* for the (*R*)-enantiomer when the V-BPO is isolated from *Ascophyllum nodosum* and 55% *ee* of the (*S*)-enantiomer

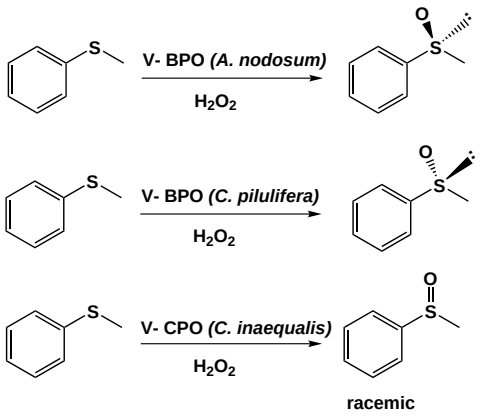


Figure 12: Enatioselective oxidation of thioanisole by vanadium bromoperoxidases.

when V-BPO is isolated from *Coralina pilulifera*.[87,88,90,91]

The ability of these vanadium-dependent bromoperoxidases to produce different enantiomers suggests that subtle differences present near the vanadium-binding site are also very important for the catalytic activity. This is also obvious when comparing the V-BPOs and V-CPOs, where different mechanisms have been suggested in order to explain the observed results. Nucleophilic attack of the sulfide at the peroxo intermediate take place when V-BPOs are used as catalyst, whereas a radical mechanism have been proposed in the case of V-CPOs-catalyzed sulfide oxidations. The later case consists in the formation of a positively charged sulfur radical $R_2S^{\bullet+}$ that is chemically oxidized. The suggested mechanism (see Figure 13) was confirmed by $H_2^{18}O_2$-labeled experiments and might explain the different reactivity of the two enzymes.[89]

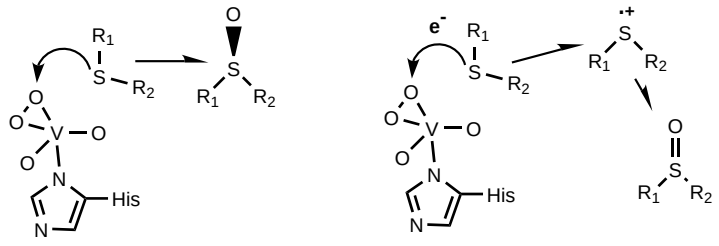


Figure 13: Schematic representation of the supposed mechanism of sulfur oxidation by vanadium bromoperoxidase (left) and vanadium chloroperoxidase (right).

## 1.4 From vanadium haloperoxidases to acid phosphatases

Hydrogen bonding interactions are of great biological relevance and their important role in the regulation of metal ion reactivity is well documented.[92] In the case of vanadium haloperoxidases, an example has been found in the activation of the peroxo form of the enzyme, where the coordinated peroxide is activated via hydrogen bonding interaction with the nearest amino acid residue. Another important role of the hydrogen bonding interactions in natural systems is related to the recognition and transport of ions. In this case, of particular interest is the analogy between vanadate and phosphate, the importance of the hydrogen bonding interaction on the mechanism of the phosphate transport system being well established.[93,94]

The prosthetic group vanadate of V-HPO can be removed by incubation of the enzyme in the presence of phosphate, resulting in the formation of apo-enzyme.[2] The reconstitution of the halo-form is achieved by back-reaction with vanadate at neutral pH, but the reconstitution is inhibited competitively by phosphate, molybdate and arsenate, which are structural analogs of vanadate. The inactivation of vanadium haloperoxidases by phosphate can be prevented by addition of $H_2O_2$ in line with the reported affinity of the active site of V-HPO for peroxovanadate.[95] On the other hand, phosphatase enzymes are also reported to be inhibited by vanadate, indicating a possible common architecture of the active site within these two different types of enzymes. Indeed the structural similarity between vanadate and phosphate results in a striking connection between vanadium haloperoxidase and several phosphatases,[96] with the amino acid sequence of the active site of V-HPO conserved within three families of acid phosphatases, including lipid phosphatases, mammalian glucose-6-phosphatase and bacterial nonspecific acid phosphatases. Several phosphatase enzymes have been crystallographically characterized with vanadate as transition state analog. The structurally characterized V-CPO shows vanadate linked to the protein only through an axially bound histidine residue and fixed in the protein shell via strong hydrogen bonding interactions. A similar motif has been found in rat prostatic acid phosphatase from *Escherichia blattae*, with vanadate as transition state analog covalently bound to His12 residue.[97]

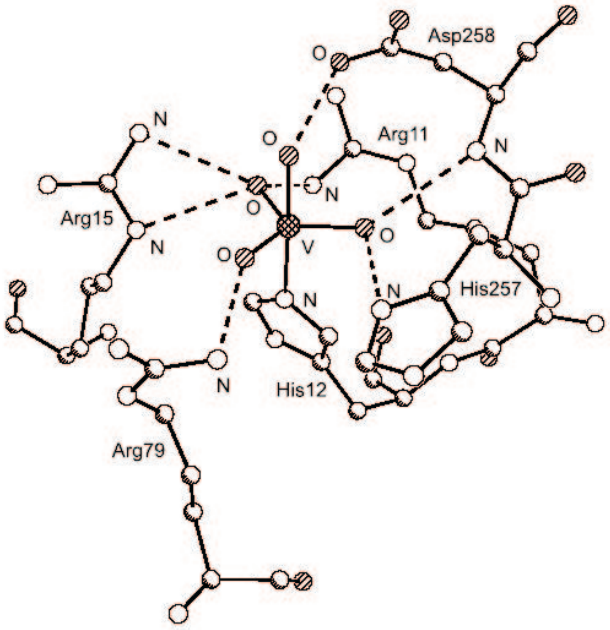


Figure 14: Crystal structure of the vanadate binding site in rat prostatic acid phosphatase from *Escherichia blattae*.

The vanadate forms a strong hydrogen bonding interaction with the nearby amino acid residues of the same chemical structure to the key amino acid residues that are hydrogen bonded to the prosthetic group in vanadium haloperoxidase enzymes. This similarity confirms that these two classes of enzymes are related evolutionarily and share the same ancestor.[98]

The most interesting acid phosphatase is mammalian glucose-6- phosphatase, a key enzyme in glucogenesis and glucose homeostasis, which is potently inhibited by vanadate.[99] Deficiency of this enzyme causes glycogen storage in the liver, leading to von Gierke disease and subsequent earlier patient death. Due to the problematic isolation and purification of this enzyme, a real crystal structure determination has not been reported, but, based on similarities between vanadium haloperoxidase and acid phosphatase, a prediction of the molecular structure is now possible.[96]

V-HPOs and phosphatases have different biological functions. The former catalyze the oxidation of halides, whereas the later catalyze the hydrolysis of phosphoesters and phosphor anhydride bonds. As previously described, since these two different types of

enzyme share the same supramolecular environment at their active sites, it is reasonable to assume that both may exhibit the dual activities. Indeed, the apo-form of V-CPO has been reported to exhibit phosphatase activity, catalyzing the hydrolysis of p-nitrophenyl phosphate with a turnover rate of 1.7 $min^{-1}$ of p-nitrophenol.[64] The possibility that peroxidase activity could be observed for vanadate-incorporated phosphatases has also been investigated. The vanadate-substituted acid phosphatases have also been reported to exhibit haloperoxidase activity, catalyzing the oxidative halogenation of bromide.[100] The turnover values for vanadium-substituted phosphatase enzymes have been reported to be 3.4 to 33 $min^{-1}$, depending on the vanadate-recombined acid phosphatase. This turnover rate is much slower than the catalytic activity of the native vanadium bromoperoxidase from *Ascophyllum nodosum*. At this time, analogy between these two classes of enzyme includes both structural and catalytic aspects, although it is obvious from kinetic data that the active site of vanadium haloperoxidase is not optimized for phosphatase activity and *vice versa*.

## 1.5 Model complexes for vanadium haloperoxidases

The discovery of V-HPOs has increased the interest in vanadium chemistry. A large number of vanadium complexes have been reported in recent decades as model compounds for the native enzymes and they contain both vanadium(V) and vanadium(IV) moieties. The crystallographic characterization and spectroscopic investigation of the native forms of V-CPO and V-BPO, as well as the peroxo-form, restricted the development of vanadium-model complexes with vanadium in the highest oxidation state only. It has been shown that these enzymes lose their activity on reduction[101] of the vanadate moiety and that the activity is fully restored by re-oxidation of vanadium atom,[2,81] demonstrating that vanadium(V) plays a vital role in the catalytic activity. Two general categories of complexes have been described as structural models for haloperoxidase enzymes. The first class, defined by oxo- and dioxo-vanadium(V) complexes based on ligands with oxygen and nitrogen donor atoms, contains the largest number of compounds. Within this class the Schiff base compounds are the largest group. Some examples are shown in Figure 15 (**1.1-1.4, 1.8**).

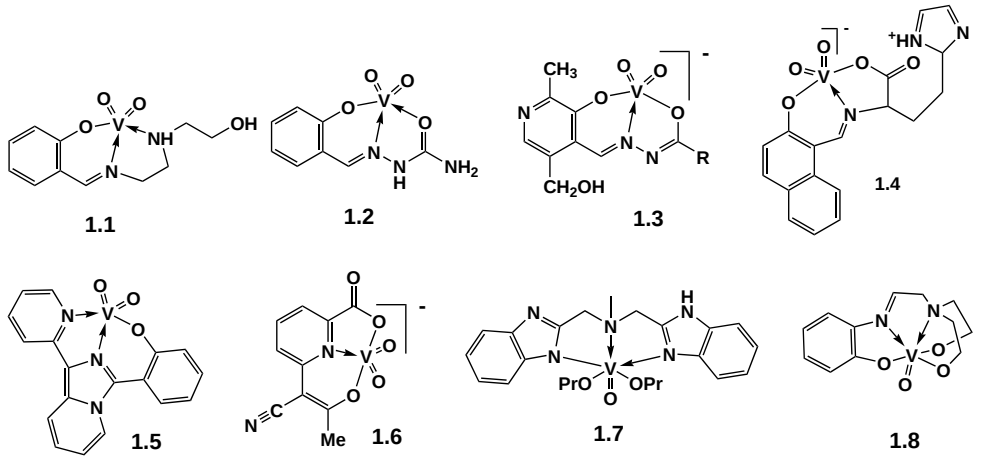


Figure 15: Structural model complexes for vanadium-dependent haloperoxidases. (**1.1**,[102] **1.2**,[103] **1.3**,[104] **1.4**,[105] **1.5**,[106] **1.6**,[107] **1.7**,[108] **1.8**[109]).

The second class of model compounds includes peroxovanadium(V) complexes. These complexes are of interest not only because they are able to model the peroxide intermediate of the catalytic cycle, but also because of their use as catalysts in organic synthesis. Numerous oxo-peroxo- and oxo-di- and/or tri-peroxovanadium complexes catalyze a variety of net two-electron oxidation reactions, e.g. epoxidation and hydroxylation of alkenes and allylic alcohols, oxidation of sulfides to sulfoxides, hydroxylation of benzene and other arenes, oxidation of primary and secondary alcohols.[110] Moreover, peroxovanadium complexes also perform the oxidation of a thiolato Co(III) complex to sulfenato complex, 2,2'-bipyridine to picolinic acid and the oxidation of sulfur dioxide to sulfate. An intriguing reaction is represented by a C6-substitution of nicotinic acid performed by peroxovanadium complexes in aqueous ethanol to give 6-(1-hydroxyethyl)nicotinic acid.[110] A wide range of peroxovanadium complexes has been reported with a side-on bound peroxide containing a V–O bond length of around 185 pm and an O–O bond of 140 pm, respectively, with a vanadium atom usually six or seven-coordinated. Some of these complexes have also been described as functional models capable of catalyzing the oxidation of bromide in acetonitrile with a turnover rate of *ca.* 300 product hour$^{-1}$.[111] In addition, peroxovanadium complexes have been reported as insulin-enhancing compounds. Administration to cell cultures was found to increase protein phosphorylation

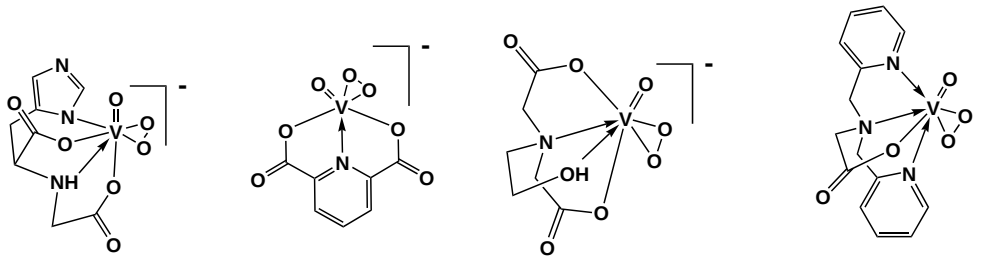

**1.9** **1.10** **1.11** **1.12**

Figure 16: Selected peroxo-vanadium model complexes for vanadium-dependent haloperoxidases. (**1.9**,[112,113] **1.10**,[114] **1.11**, **1.12**[111]).

of the insulin receptor presumably by inhibition of protein phosphatases.

A very important characteristic for structural models of vanadium dependent haloperoxidase enzymes is the existence of similar hydrogen bonding patterns. Unfortunately, at this time, only two reported systems exhibit hydrogen bonding network similar to that found in the natural system (Figure 17).

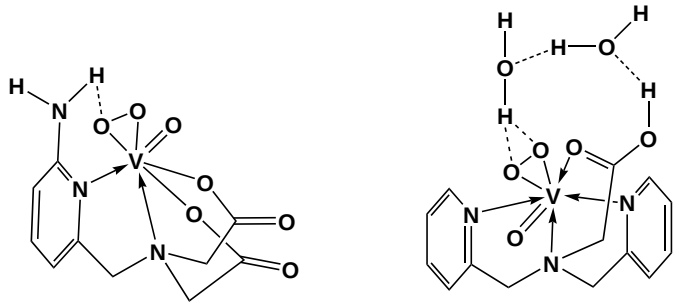

**1.13** **1.14**

Figure 17: Peroxovanadium complexes modelling the hydrogen bonding interaction found in the peroxide form of vanadium chloroperoxidases.

The first model complex, **1.13**, contains an intramolecular hydrogen bonding interaction established by a pendant amine functionality and the oxygen atom of the peroxide group,[115] while in the second case, **1.14**, the peroxo-oxygen atom is in hydrogen bonding contact with a water molecule.[116] Both peroxo-vanadium(V) complexes model structurally the peroxo-intermediate of the vanadium chloroperoxidase enzymes.

Besides structural similarities, an important role is attributed to functional model complexes and, in this direction insight into the mechanism of haloperoxidase reactions can be achieved using model compounds. This is due to their ease of isolation and the availability of many methods of characterization and monitoring, something not easily accessible with the enzymes. The first reported functional mimic of V-HPOs enzyme was reported by Butler *et al.* in 1992 for *cis*-dioxovanadium(V) species. Here, the peroxidative bromination of 1,3,5-trimetoxybenezene (TMB) was monitored.[117] A detailed mechanism involving the reactivity of ammonium vanadate with $H_2O_2$ under acidic conditions has been described (see Figure 18) and differences regarding the proposed mechanism of the enzymatic system have been presented. These comprise firstly the more acidic medium required for the synthetic model to catalyze the oxidation of bromide by hydrogen peroxide, with *cis*-$VO_2^+$ working optimally at pH around 2. The second difference concerns the active intermediates formed by reaction of vanadate with hydrogen peroxide. In this system, the reaction with $H_2O_2$ leads to formation of monoperoxo- or diperoxo vanadium species, in a ratio strongly dependent on hydrogen peroxide and acid concentrations. $^{51}V$ nuclear magnetic resonance monitoring of the catalytic reaction showed the formation of a mono-peroxovanadium ($VO(O_2)^+$) complex, independent of the pH conditions, while the formation of the diperoxo vanadium ($VO(O_2)_2^-$) species depends of the amount of acid used and is less favored at high acid concentrations (Figure 18). Neither $VO(O_2)^+$, nor $VO(O_2)_2^-$ oxidize bromide, rather they combine to form the dinuclear dioxo-triperoxo vanadium(V) complex, $(VO)_2(O_2)_3$, which is the actual oxidant.[118]

Analogous to the vanadate-catalyzed oxidation of bromide by $H_2O_2$, Secco carried out detailed kinetic studies on vanadate-catalyzed iodide oxidation. The reaction of *cis*-$VO_2^+$ with $H_2O_2$ yielded the mono- and diperoxovanadium(V) species, as described previously, but no dimerization was observed. On the other hand, a different reactivity towards reaction with halide, namely iodide, has been observed. Reduction of $VO(O_2)^+$ and $VO(O_2)_2^-$ by iodide takes place, resulting in the formation of vanadyl ($VO^{2+}$) species.[119]

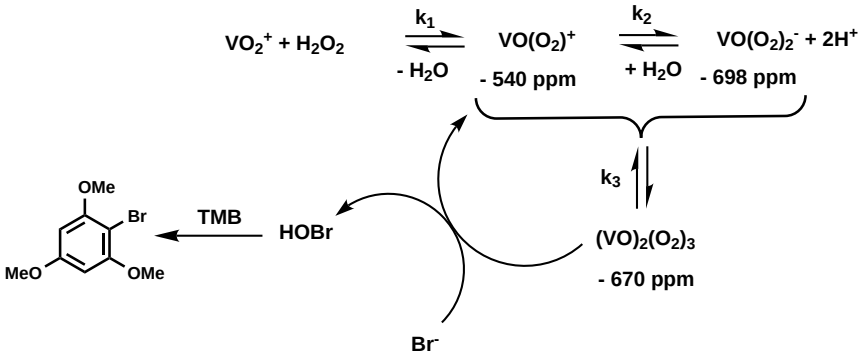


Figure 18; Proposed mechanism of vanadate-catalyzed peroxidative bromination of 1,3,5-trimethoxy benzene (TMB).

These reports demonstrate that even simple inorganic salts can catalyze the oxidation of halide by hydrogen peroxide, although they follow a different mechanism than the enzymatic system. Therefore vanadium coordination compounds are expected to enhance or to retard the catalytic reaction and, perhaps, to show closer mechanistic features to the enzymatic catalysis. The same author also investigated the peroxidative bromination reaction of TMB using N-(2-carboxyphenyl) salicylideneamine, [(HPS)VO(OEt)(EtOH)].[120] Using DMF as solvent and $HClO_4$ as the source of acidic conditions, the mechanism of the peroxidation of bromide was shown to take place by formation of a mono-peroxovanadium(V) complex, $[(HPS)VO(O_2)]^-$, as the active intermediate (Figure 19). The reaction has been proposed to proceed first by protonation of the oxo-vanadium(V) catalyst to form a [(HPS)VO(OH)] moiety that consequently reacts with hydrogen peroxide resulting in the formation of the mono-peroxovanadium(V) complex. Addition of bromide affords one turnover cycle of oxidized bromide which brominates one equivalent of TMB. The bromination reaction becomes catalytic when acid is present at least in equimolecular amounts with respect to $H_2O_2$. The reactivity of the mono-oxovanadium(V) complex in solution has been monitored by $^{51}V$ NMR and UV-Vis spectrophotometry, while the monitoring of the reaction was performed by GC determination of the formed Br-TMB compound. The catalytic activity was higher than for the previous described ammonium vanadate, but the acidic condition were still required for the reaction to be catalytic.

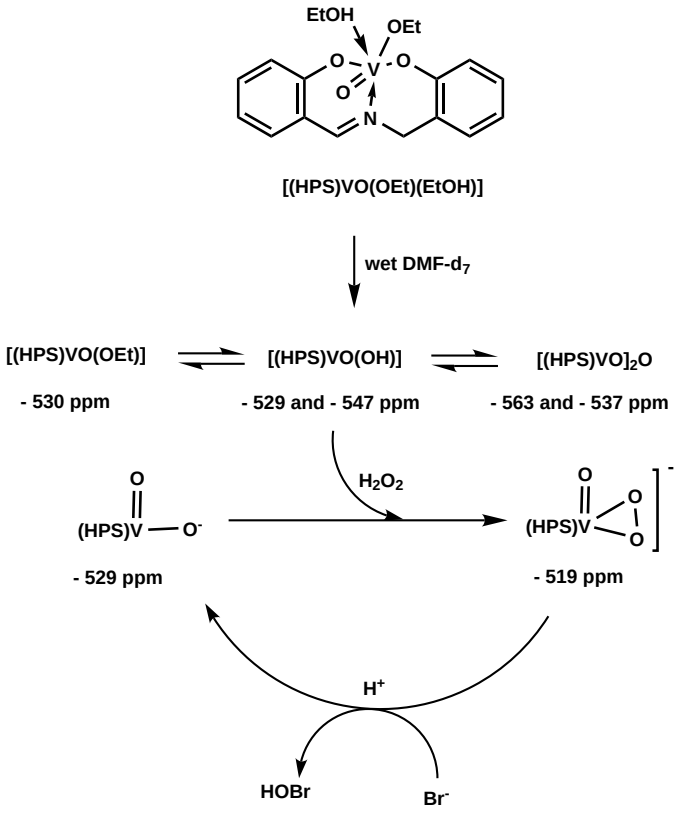


Figure 19: Proposed mechanism of peroxidative bromination reaction of 1,3,5-trimethoxy benzene (TMB) catalyzed by mono oxovanadium(V) complex.

Moreover, it has been proved that the bromination of an organic substrate in the above used conditions proceeds exclusively via an electrophilic mechanism and that no radical intermediates are involved in the reaction. Therefore, the chlorination of a toluene derivative has been performed and only the electrophilic products were detected, with no chlorination occurring at the methyl group.

The best catalytic results have been reported by Pecoraro *et al.* using the vanadium(V) complexes **1.11** and **1.12**, depicted in Figure 15. Starting from the corresponding *cis*-dioxovanadium(V) complexes, a detailed mechanism of the oxidation of bromide has been provided.[121] One key point in the catalytic reaction is the use of acetonitrile as solvent, as no reaction was observed in purely aqueous conditions. The kinetics of peroxide binding to *cis*-dioxovanadium(V) complexes, $VO_2L$, to form the oxo-peroxovanadium complexes is first order in $VO_2L$. One very important factor for performing the catalytic oxidation of bromide in acetonitrile was the need for one equivalent of acid. In the absence

of acid no reaction occurred, suggesting that the peroxo-complexes should be protonated, presumably at the peroxide group, in order to be activated. Further spectrophotometric investigations revealed a slight red-shift of the peroxo-to-vanadium charge transfer band when one equivalent of acid had reacted with the peroxo complex **1.12** (Figure 15). A mechanism consistent with that of the enzymatic system has been proposed and includes a partial positive charge on the protonated peroxide oxygen atom that will favor the nucleophilic attack of the halide[121] (Figure 20).

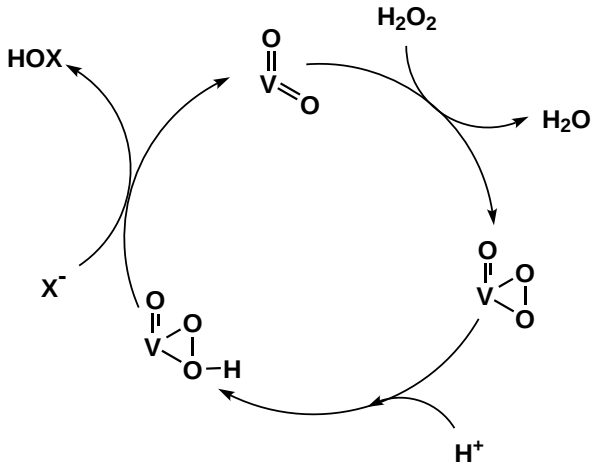


Figure 20: Proposed mechanism of halide oxidation by *cis*-dioxovanadium(V) complex.

Although much progress has been achieved in recent years towards oxidation of bromide by hydrogen peroxide using vanadium complexes as catalysts, the lack of structural similarities concerning the hydrogen bonding interaction and positively charged donor sites of the V-HPO active binding site limits their significance for mechanism comparison. Therefore, structural models which exhibit hydrogen bonding at the vanadate center related to the observed supramolecular environment of the native V-HPO proteins are expected to give further insight into the mechanism of the reaction and to be more appropriate functional models.

## 1.6 Design of vanadium(v) complexes with N-salicylidene hydrazides

Although the first reported crystal structure of a vanadium containing haloperoxidase dates from 1996 and much progress has been made since then, there remain a number of open questions. One such persisting question concerns the actual structure of the vanadate moiety: is it a monoprotonated vanadate $[VO_3(OH)]^{2-}$ as has been suggested or is it a diprotonated vanadate $[VO_2(OH)_2]^-$, in accordance with the observation that, under physiological conditions, vanadate exists in its diprotonated form? A possible answer to this question will be given by synthesis of **mono**- and **di-oxo**vanadium(v) complexes ($VO^{3+}$ or $VO_2^+$) obtained with ligand systems capable of accommodating both species, as described herein. Such a ligand system is represented by N-salicylidene hydrazides, a tridentate chelate ligand that can react towards complex formation in its mono- and di-anionic forms, thus making possible a variation of the protonation state in the obtained vanadium complexes. In vanadium-chloroperoxidase enzyme, a vital role has been attributed to the His404 residue suggested to play the acid-base role during the catalytic cycle. The vanadium model complexes with N-salicylidene hydrazide contain an amide functionality with a *NH* group which can be regarded as playing a similar role during vanadium-catalyzed bromide oxidation reaction.

A second question concerns the catalytic activity of the enzyme and is focused on the forces that enable the enzymatic system to catalyze the oxidation of halide by hydrogen peroxide so powerfully, with a turnover number in the range of $10^5$ mol product/h. An answer to this question came from the importance of the supramolecular hydrogen bonding interaction that fixes the prosthetic group in the protein shell. Single site-directed mutants of the amino acid residue of the active binding site showed the vital role of the hydrogen bonding interaction and proved that any small change in the vicinity of the vanadate moiety can change the affinity of the enzyme for its substrate, thus yielding an alteration on its reactivity. The functionalization of the N-salicylidene hydrazide ligands makes possible the isolation of bio-inspired vanadium complexes that mimic the hydrogen bonding interaction of the key amino acid residues with the vanadate moiety found in the natural system. A comparison between the active channel of the azide-substituted

vanadium chloroperoxidase and the substitution patterns of N-salicylidene hydrazide are depicted in Figure 21.

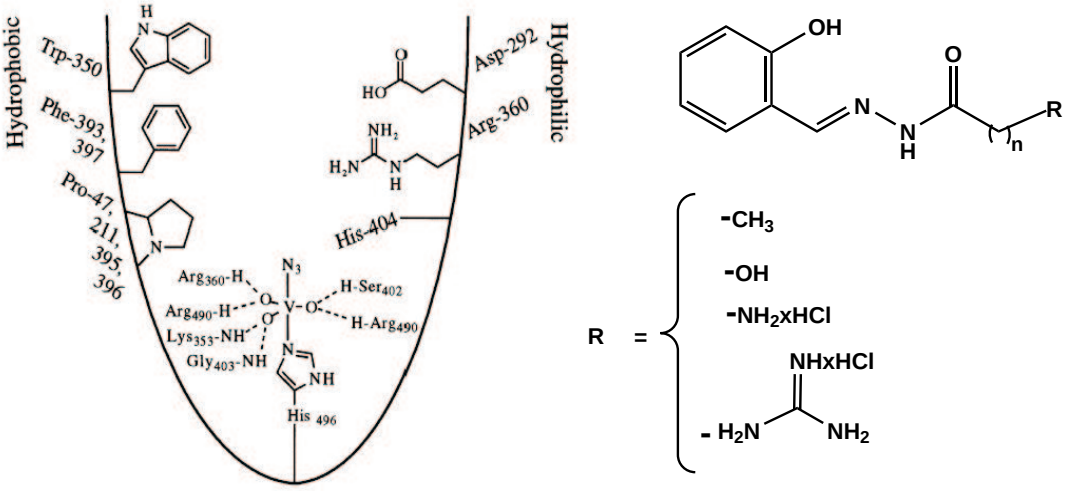


Figure 21: Schematic representation of the active channel of the azide form of V-CPO (left) and N-salicylidenehydrazide ligands with different substitution patterns (right).

Additionally, using the new synthetic vanadium analogues that approach significant properties of the protein active site, mechanistic investigations of the catalytic reaction, through isolation of oxo-monoperoxovanadium(V) complexes, will also bring new insights into the enzymatic catalytic reaction. Moreover, the possible influence of different aliphatic chain length in their reactivity is also investigated. Afterwards, the capacity of the isolated vanadium complexes to be functional models for the enzymatic system will also be discussed, together with solution studies that are relevant for the enzymatic catalytic reaction.

However, a difference in the vanadium coordination geometry between the vanadium haloperoxidase enzymes and the structural model systems that will be described here is obvious. Vanadium in the +5 oxidation state forms typically complexes with square-pyramidal geometry in five-coordinated compounds and has an octahedral geometry in six-coordinated complexes. In *cis*-dioxovanadium(V) complexes, the used tridentate chelate ligands prefer a planar arrangement of the donor atoms, yielding a square pyramidal geometry, whereas in the vanadium-containing enzyme, the protein environment is responsible for significant steric constraint, enforcing a distorted trigonal

bipyramidal geometry around the vanadium atom. However, vanadium complexes with a distorted trigonal bypiramidal geometry are also known, but distortion to both ideal geometries is present. To quantitatively compare these structures in terms of relative geometries around the vanadium atom, an angular structural parameter $\tau$ was defined.[122] The $\tau$ value is given by the difference of the largest angle values formed by the donor atoms which coordinate at the vanadium center. Therefore, $\tau$ is 0 when an ideal square pyramidal geometry is established around the metal center and has a value of 1 when the coordination sphere is arranged in an ideal trigonal bypiramidal geometry (Figure 22).

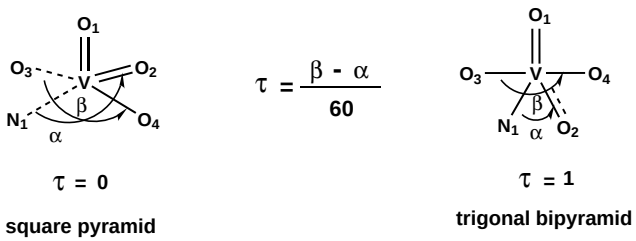


Figure 22: Schematic representation of the geometries around five-coordinated vanadium atom, with numbering of the donor atoms exemplified for the *cis*-dioxovanadium(V) complexes with N-salicylidenehydrazide ligand.

Nevertheless, despite the differences in geometrical arrangement around the vanadium center, the vanadium(V) complexes with N-salicylidene hydrazide present relevant hydrogen bonding interaction and, thus, they can be regarded as structural model complexes of the enzymatic system. On the other hand, N-salicylidene hydrazide ligands have also attracted interest due to their pharmacological importance. Benzoyl substituted N-salicylidene hydrazide has been reported to possess mild bacteriostatic activity, as well as being an inhibitor of DNA synthesis and cell growth.[123,124] The compound is used as drug for genetic disorders like thalassemia.[125,126] The potency of the ligand to inhibit DNA synthesis and cell growth was found to increase upon complexation of divalent transition metal ions. The Cu(II) complex was reported to be the most potent pharmacological agent,[124,126] whereas recently vanadium(V) complexes based on N-salicylidene semicarbazone ligand were reported to posses anti-tumor activity.[127]

# Chapter 2

# Vanadium(V) complexes based on N-salicylidene aliphatic acid hydrazides

Based on the reported crystal structure of vanadium chloroperoxidase,[38] vanadium complexes which exhibit hydrogen bonding interaction have been obtained using N-salicylidene aliphatic acid hydrazides. The ligand system acts as tridentate chelate ligand with a hydrophobic side-chain. Although various crystal structures of different vanadium haloperoxidases have been reported,[62,70,128] the real structure and the protonation state of the vanadate center remain uncertain. A monoprotonated vanadate moiety $[VO_3(OH)]^{2-}$ has been proposed as the active site in the native enzyme by analogy with phosphate chemistry although, the vanadate exists in the diprotonated form $[VO_2(OH)_2]^-$ at physiological pH as it has been mentioned. At this point, comparison with synthetic models is expected to give further insight into the mechanism of the reaction, as well as to establish the protonation state of the prosthetic group. Various *cis*-dioxo-[114,121] and monooxo-vanadium(V)[120,129] complexes have been reported as structural models for V-HPO enzymes, but the reports of a ligand system able to accommodate both species are rather scarce. Therefore, a versatile ligand system should be capable of accommodating both the *cis*-dioxo- and monooxovanadium(V) complexes regarded as structural models for the enzymatic system. Additionally, it should make possible variation

of the protonation state in the obtained complexes. The N-salicylidene aliphatic acid hydrazide ligand system reacts with ammonium metavanadate yielding anionic and/or neutral *cis*-dioxovanadium(V). Further, the neutral *cis*-dioxovanadium(V) complexes react stoichiometrically with 8-hydroxyquinoline to form mono-oxovanadium(V) complexes, thus proving the versatility of the chosen chelate system.

The synthesis of the N-salicylidene aliphatic acid hydrazides is relatively straightforward and involves, in the first step, the hydrazinolysis of aliphatic acid esters with near quantitative formation of the corresponding carbonic acid hydrazide. In the second step, the isolated $\omega$-aliphatic acid hydrazide reacts with salicylaldehyde via Schiff base condensation to form the title ligands. The schematic representation of the synthesis and substitution patterns described in this chapter are depicted in Figure 23. N-salicylidene aliphatic acid hydrazides act as a tridentate chelate systems, permitting coordination in both the mono- and dianionic forms due to the presence of the amide functionality, which makes possible an amide-iminole equilibrium.

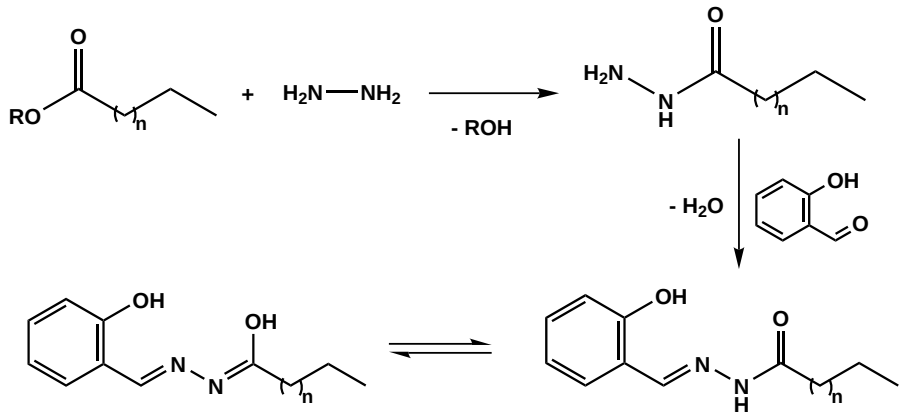


Figure 23: Schematic representation of the synthesis and tautomeric forms of N-salicylidene aliphatic acid hydrazides, where n=1 $H_2$salhyb, n=2 $H_2$salhyp and n=3 $H_2$salhyh.

## 2.1 *cis*-Dioxovanadium(V) complexes derived from N-salicylidene aliphatic acid hydrazides

Stoichiometric reaction of the Schiff base ligands with ammonium metavanadate in refluxing methanol for one day results in the formation of the ammonium salts of the anionic *cis*-dioxovanadium(V) complexes $NH_4[VO_2L]$. Over prolonged reaction time, the primarily formed ammonium salts were found to be converted to the neutral *cis*-dioxovanadium(V) complexes $VO_2HL$, with release of ammonia. A net difference regarding the solubility of the two types of complexes is obvious. The anionic species have a very good solubility in polar solvents and water, while the neutral complexes have a very poor solubility in polar solvents and are completely insoluble in water. Interconversion between these two *cis*-dioxovanadium species takes place, by modification of the protonation state of the hydrazide nitrogen atom of the amide functionality. The neutral *cis*-dioxovanadium complexes can be deprotonated by reaction with liquid ammonia, resulting in the reconversion to the anionic species.

$$NH_4VO_3 + H_2L \longrightarrow NH_4[VO_2L] + H_2O$$

$$NH_4[VO_2L] \longrightarrow [VO_2L] + H_2O + NH_3$$

$$[VO_2L] + NH_3(l) \longrightarrow NH_4[VO_2L]$$

### 2.1.1 Structural characterization

Crystallographic characterization of an anionic *cis*-dioxovanadium(V) complex, as well as a neutral *cis*-dioxovanadium(V) complex, has been achieved using N-salicylidene-5-pentanoic acid hydrazide as ligand ($H_2$salhyp). Stoichiometric reaction of $H_2$salhyp ligand with ammonium metavanadate in refluxing methanol yields the anionic *cis*-dioxovanadium(V) complex $NH_4[(salhyp)]$ (**1**), which crystallizes upon slow evaporation of the mother liquor at room temperature. Molecular structure determination of the anionic complex **1** shows two crystallographically distinct *cis*-dioxovanadium moieties, as depicted in Figure 24. The vanadium atoms are five-coordinated in a distorted square-

pyramidal geometry. The tridentate chelate system is fully deprotonated and coordinates in its dianionic form through the phenolate (O13 and O23) and iminolate (O14 and O24) oxygen atoms, as well as the imine nitrogen atoms (N11 and N21). The bond lengths C18–O14 and C28–O24 of 130 pm are consistent with the enolized form of the amide functionality and are in agreement with the observed V1–O14 and V2–O24 bond lengths of 195 and 197 pm, respectively. Relative to the mean plane given by the chelate ligand system, the vanadium atom is displaced toward the apical oxo group O11 by 33 pm and to O21 by 34 pm, whereas the oxo groups O12 and O22 are slightly distorted to the opposite side by 27 and 25 pm, respectively. This leads to a $\tau$ value of around 0.04 for both vanadium centers ($\tau = 0$ for an ideal square pyramid[122]) consistent with a distorted square pyramidal geometry at the metal centers. The vanadium to oxo group bond lengths (V=O) of 161 pm and 163 pm, respectively, are similar to reported bond distances in *cis*-dioxovanadium(V) complexes, as well as the V-N and V-O bond lengths.[130,131] Selected bond lengths and angles are listed in Table 1. Complex **1** crystallizes in the triclinic space group $P\bar{1}$ with two methanol molecules as solvent of crystallization and the ammonium cations placed in the vicinity of one vanadate center.

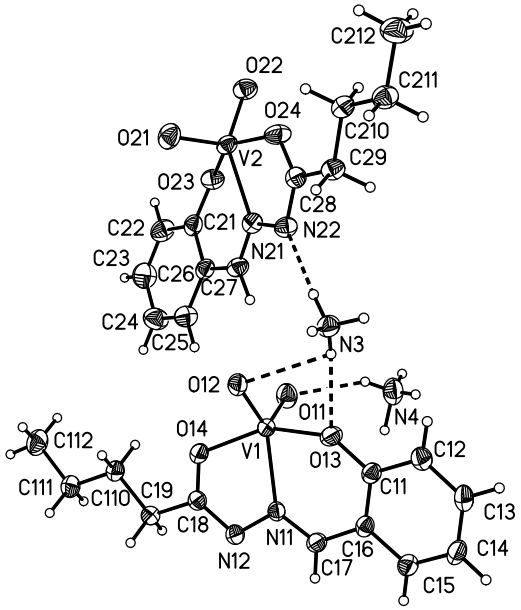


Figure 24: Molecular structure and numbering scheme of the anionic complex **1** in crystals of $NH_4[VO_2(salhyp)]\cdot MeOH$; displacement ellipsoids are drawn at 50% probability level.

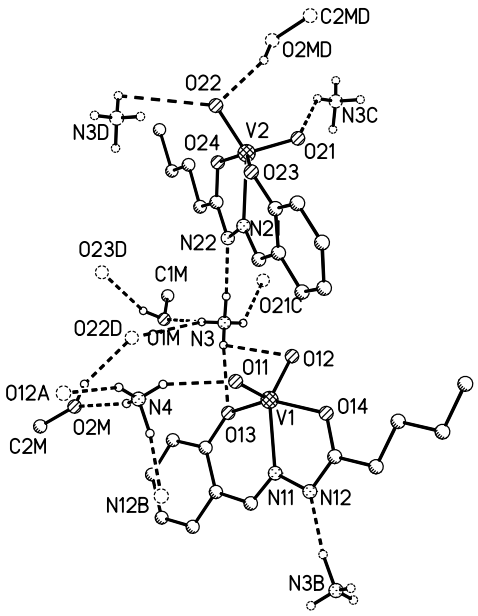


Figure 25: Representation of the hydrogen bonding interaction of the anionic complex **1** with the ammonium cations and methanol molecules in crystals of $NH_4[VO_2(salhyp)]\cdot MeOH$ (broken lines represent hydrogen bonds); relevant distances (in pm): N3···N22 291.8, N3···O1M 285.4, N3···O22D 295.1, N3···O13 301.7, N3···O12 296.7, N3···O21C 287.9, N4···O11 283.5, N4···O2M 278.4, N4···O12A 281.1, N4···N12B 293.2, O21···N3C 287.9, O22···N3D 295.1, O22···O2MD 279.9 and O1M···O23D 283.1 (symmetry transformations: A : x-1, y, z; B: -x+1, -y+1, -z+1; C: -x+2, -y+1, -z+2; D: -x+1, -y+1, -z+2).

In the solid state, an extensive hydrogen bonding interaction is observed, which involves particularly both double bonded oxo groups of the vanadate moiety, mimicking the environment found in the native enzyme. One ammonium cation connects, via a hydrogen bonding interaction, the two *cis*-dioxovanadium moieties by hydrogen bonding contacts with the hydrazide nitrogen atom N3···N22 (291.8 pm) of one molecule and the equatorial and phenolate oxygen atoms of the other moiety, N3···O12 (296.7 pm) and N3···O13 (301.7 pm), respectively. The apical double bonded oxygen atoms are in hydrogen bonding interactions with two different ammonium cations, N4···O11 (283.5 pm) and N3D···O22 (295.1 pm), respectively. A similar situation has been reported for the native enzyme, where the apical oxygen atom of the vanadate moiety is in hydrogen bonding

contact with His404, resulting in a V–O···N bridge formation. The hydrogen bonding network is completed by the methanol molecules, which are involved in bifurcated hydrogen bonding interaction with the ammonium cations and the equatorial oxygen atoms from neighboring molecules, as depicted in Figure 25. The observed vast hydrogen bonding interaction leads to the formation of a three-dimensional hydrogen bonded polymer with the ammonium cations establishing the layer, while the hydrophobic parts are oriented to the outside (see Figure 26).

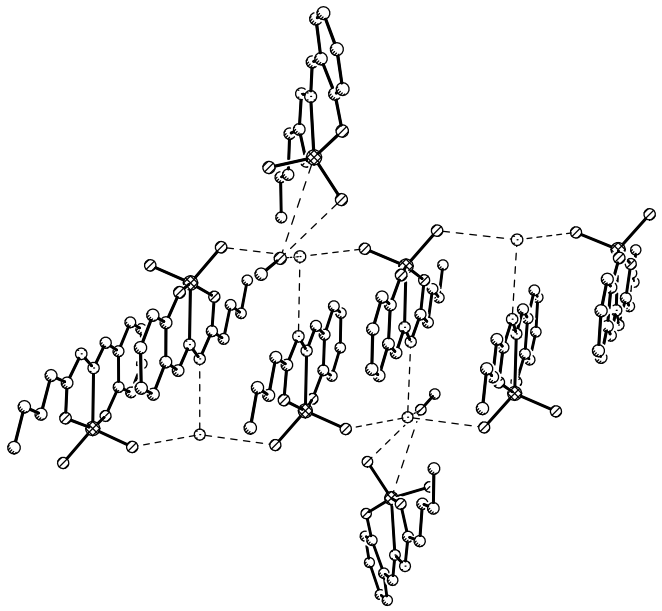

Figure 26: Representation of the hydrogen bonding network in crystals of $NH_4[VO_2(Hsalhyp)]\cdot MeOH$ (broken lines represent hydrogen bonds).

A very important role in the native vanadium haloperoxidases is attributed to the lysine residue that is hydrogen bonded to the equatorial oxygen atoms of the vanadate as the prosthetic group (V–O···$NH_3^+$). A similar situation is found in the case of the anionic complex described here, where the place of the *Lys* residue is taken by the ammonium cation, leading to a similar V–O···N bridge. On the other hand, hydrophobic components have been reported as parts of the active channel in both V-CPO and V-BPO. The amino acids constituting part of the channel of the helix bundle are different from V-CPO and V-BPO and are responsible for the specificity of these enzyme for certain substrates. The herein described anionic *cis*-dioxovanadium(V) complex has also a hy-

drophobic constitution formed by the aliphatic side-chain of the N-salicylidene hydrazide ligand, which is oriented to the outside part of the resulting polymer.

A neutral complex $[VO_2(Hsalhyp)]$ **2** has also been isolated after a prolonged time of the reaction between N-salicylidene 5-pentanoic acid hydrazide and ammonium metavanadate. The ligand coordinates in its monoanionic form, containing a protonated hydrazide nitrogen atom. Although the structure is also characterized by the presence of a *cis*-dioxovanadium(V) moiety, the protonation of the hydrazide atoms N12 and N22, respectively, leads to significant changes within the molecular structure of the vanadate fragment as compared to the $NH_4[VO_2(salhyp)]$ salt.

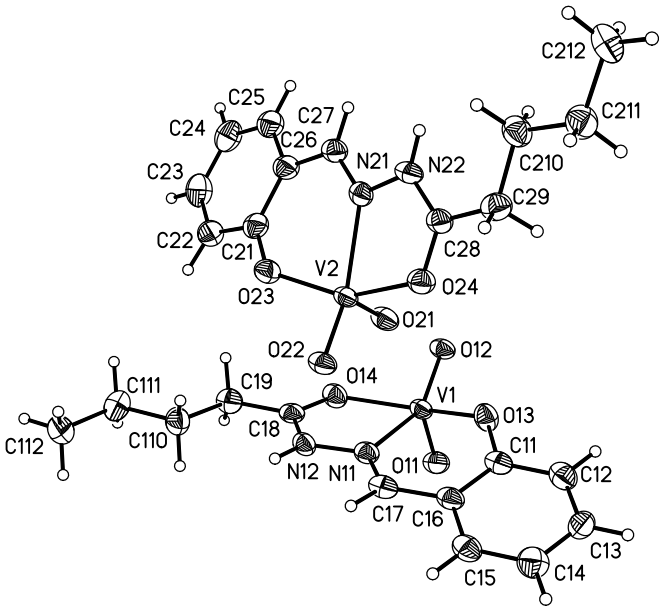


Figure 27: Molecular structure and numbering scheme of the neutral complex **2** in crystals of $[VO_2(Hsalhyp)]$: displacement ellipsoids are drawn at 50% probability level.

The N12–C18 bond length of 133 pm and N22–C28 of 132 pm, respectively, are elongated, as are the V1–O14 and V2–O24 (195 and 197 pm, respectively) bond lengths due to the weak coordination effect of the carbonyl oxygen atom. Moreover, the C–O bond length of the amide functionalities vary from 127 pm for C18–O14 to 128 pm for C28–O24, corresponding to partially double bond character. They are around 3 pm shorter than the iminol bond length observed in complex **1**. Similar to the previous case, the neutral *cis*-dioxovanadium(V) complex also crystallizes in the triclinic space group

$P\bar{1}$, with two very similar, but crystallographically different, moieties. The molecular structure and numbering scheme of complex **2** is depicted in Figure 27. The geometry around the vanadium center is also distorted square-pyramidal, with $\tau$ values of 0.25 and 0.26 pm, respectively. The distortion from an ideal square-pyramidal geometry is larger than that found in the anionic complex **1**. It is known that the local geometry at a *cis*-dioxovanadium(V) is rather flexible and can be varied by crystal packing effects.[130,131] Hydrogen bonding interactions are also observed in solid state, involving the protonated hydrazide nitrogen atoms N12 and N22, respectively, and the equatorial oxygen atoms of neighboring molecules.

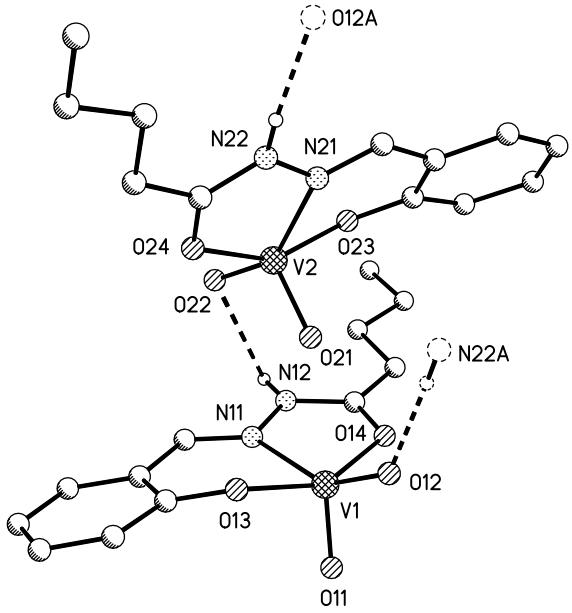


Figure 28: Representation of the hydrogen bonding interactions in the complex $[VO_2(Hsalhyp)]$ (broken lines represent hydrogen bonds); selected bond lengths (in pm): O22···N22 300.5, O12···N22A 272.7 (symmetry transformations: A : -x+1, -y, -z).

The two molecules are hydrogen bridged via the protonated hydrazide nitrogen atom and the equatorial double bonded oxygen atom N12···O22 (300.5 pm). The hydrogen bonding network is completed by hydrogen bonding contact between the equatorial oxygen atom O12 and protonated hydrazide nitrogen atom from the neighboring molecule O12···N22A (272.7 pm). Conversely to the anionic complex, no hydrogen bonding interaction involving the apical oxo groups (O11 and O12) are observed.

Table 1: Selected bond lengths (pm) and angles (°) in complexes **1** and **2**.

| | **1** | **2** | | **1** | **2** |
|---|---|---|---|---|---|
| V1−O11 | 161.6(2) | 161.1(4) | V2−O21 | 161.1(2) | 161.3(3) |
| V1−O12 | 164.6(2) | 163.1(3) | V2−O22 | 164.9(2) | 163.0(3) |
| V1−O13 | 190.8(2) | 192.1(4) | V2−O23 | 190.2(2) | 191.9(4) |
| V1−O14 | 195.6(2) | 203.0(4) | V2−O24 | 197.0(2) | 202.4(4) |
| V1−N11 | 213.8(2) | 216.8(4) | V2−N21 | 214.3(2) | 216.1(4) |
| O14−C18 | 129.9(3) | 127.3(6) | O24−C28 | 129.9(3) | 128.6(6) |
| N11−N12 | 140.9(3) | 137.6(6) | N21−N22 | 140.9(3) | 138.4(6) |
| N12−C18 | 130.8(3) | 133.1(7) | N22−C28 | 130.3(3) | 131.9(7) |
| O11−V1−O12 | 109.01(11) | 106.80(17) | O21−V2−O22 | 108.71(11) | 106.90(18) |
| O11−V1−O13 | 102.50(10) | 101.33(18) | O21−V2−O23 | 104.67(11) | 101.71(18) |
| O12−V1−O13 | 94.76(10) | 99.61(17) | O22−V2−O23 | 95.83(10) | 100.15(17) |
| O11−V1−O14 | 109.23(10) | 99.78(17) | O21−V2−O24 | 102.55(11) | 99.91(16) |
| O12−V1−O14 | 93.49(9) | 93.15(16) | O22−V2−O24 | 91.83(9) | 92.37(16) |
| O13−V1−O14 | 151.78(9) | 150.91(14) | O23−V2−O24 | 147.55(9) | 150.56(15) |
| O11−V1−N11 | 110.48(10) | 103.59(17) | O21−V2−N21 | 105.47(10) | 103.60(17) |
| O12−V1−N11 | 140.08(9) | 145.45(16) | O22−V2−N21 | 145.03(10) | 148.25(16) |
| O13−V1−N11 | 82.39(8) | 82.39(15) | O23−V2−N21 | 82.43(8) | 81.92(15) |
| O14−V1−N11 | 74.10(8) | 73.34(15) | O24−V2−N21 | 73.53(8) | 73.72(15) |

### 2.1.2 Spectroscopic data

The formation of the *cis*-dioxovanadium complexes is confirmed by strong IR vibrations corresponding to the $\nu(VO_2^+)$ group, which are observed at 894 and 908 $cm^{-1}$ in the anionic complexes and 893 and 919-921 $cm^{-1}$ in the neutral complexes. The coordination mode of the Schiff base ligands is obvious by comparison of the IR patterns of the free ligands with those of the complexes. Selected IR data for the *cis*-dioxovanadium complexes obtained with these ligands system are given in the experimental part of this

chapter, together with the IR data of the free ligands. The infrared spectra of the ligands exhibit bands around 1669-1673 $cm^{-1}$ due to the $\nu$ (C=O) stretch vibration. This band is shifted at 1628 $cm^{-1}$ upon complexation in the neutral *cis*-dioxovanadium(V) complexes and disappears in the IR spectra of the corresponding anionic complexes. The IR spectra of the ammonium salts shows instead a strong band at 1612 $cm^{-1}$, attributed to the stretching vibration of the conjugate –HC=N–N=C– group,[132,133] a characteristic IR feature of vanadium complexes with the enolized form of N-salicylidenehydrazide ligands.[134,135] A broad band for the free ligand, at approximately 3185 $cm^{-1}$, is assigned to intramolecular hydrogen bonds involving phenolic OH group. This band is not present in the IR spectra of both *cis*-dioxo complexes, indicating deprotonation of the phenol group on coordination of the metal center. However, the presence of a broad band at approximately 3435 $cm^{-1}$ in the complexes of type $NH_4[VO_2L]$ indicates the presence of the ammonium cations. Whereas in the IR spectrum of the neutral *cis*-dioxovanadium complexes the vibration assigned to the $\nu$(NH) stretching vibration appears at 3210 $cm^{-1}$. Solution characterization of the complexes has been achieved through $^1H$ and $^{51}V$ NMR measurements. The $^1H$ data for the novel *cis*-dioxovanadium(V) complexes are consistent with the proposed structures and exhibit shifted resonances in comparison with the corresponding proton resonances of the free ligands. In particular, the full deprotonation of the free N-salicylidene hydrazide ligands in the anionic complexes is confirmed by the absence of the downfield $^1H$ NMR resonances corresponding to the O−H and N−H protons. Moreover, the $^1H$ NMR spectra of the Schiff base ligands always show two sets of resonances at 8.33 and 8.99 ppm, attributable to the azomethine (-CH=N) proton due to the E-Z isomerism. The azomethine bond is present as one conformer through vanadium coordination proved by an observed deshielded resonance of its singlet at 8.75 ppm in the $^1H$ NMR of the complexes (see Experimental part). A net difference between the neutral and the ammonium salts of the *cis*-dioxovanadium(V) complexes is observed in their $^1H$ NMR. A broad resonance at 7.11 ppm is observed in the $^1H$ NMR of the ammonium salt of the *cis*-dioxovanadium(V) complexes and is attributed to $NH_4^+$ protons. This resonance is absent in the $^1H$ NMR of the corresponding neutral *cis*-dioxo- complexes which exhibit instead the specific resonance of the N*H* proton at around 11 ppm. Furthermore, $^{51}V$ NMR is indicative of the *cis*-$VO_2^+$ formation. $^{51}V$ NMR performed in DMSO-$d_6$ shows

one resonance for the ammonium salts of *cis*-dioxovanadium(V) complexes at -534 ppm ($\nu_{1/2} \sim 615$ Hz) and two resonances for the neutral complexes at -535 ppm ($\nu_{1/2} \sim 590$ Hz) and -572 ppm ($\nu_{1/2} \sim 600$ Hz). While the first resonance is certainly specific for *cis*-dioxovanadium(V) complexes with this type of ligand, the -572 ppm resonance may be due to association of the molecules in solution, leading to the formation of a dimeric *cis*-dioxovanadate structure.

### 2.1.3 Oxidative bromination

Vanadium bromoperoxidases, isolated mainly from marine organisms catalyze the oxidation of bromide[75] and iodide[2] by hydrogen peroxide. The oxidized halide species can subsequently react with appropriate organic substrates to yield halogen-containing derivates.[56,81] Although several vanadium complexes have been reported as structural models for vanadium haloperoxidases, little is known about the vanadium-catalyzed peroxidative halogenation reactions. The first functional mimic of the V-BPO enzyme is represented by ammonium vanadate.[117] This is able to catalyze the peroxidative halogenation of 1,3,5-trimetoxybenzene (TMB) in acidified DMF solution with a maximum turnover rate of 15 mol Br-TMB×(mol catalyst×h)$^{-1}$.[117] V-BPO enzymes have been reported to catalyze the same reaction with a turnover rate of $4.7\times10^5$ mol Br-TMB×(mol enzyme×h)$^{-1}$ at pH 6.5.[59,72,75] Contrary to the native enzyme, all the reported functional vanadium complexes catalyze the oxidation of bromide at lower pH, with turnover rates $10^4$ slower.[120] The herein reported *cis*-dioxovanadium(V) complexes have been also tested towards their capacity to catalyze the oxidative bromination of trimethoxybenezene using hydrogen peroxide as oxidant and $HClO_4$ as the source of acidic medium.

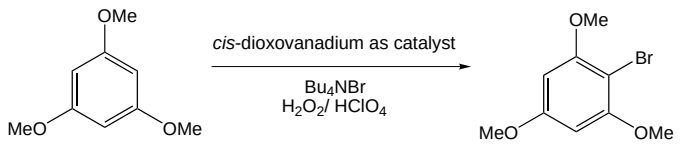


Figure 29: Oxidative bromination of 1,3,5-trimethoxybenzene catalyzed by *cis*-dioxovanadium(V) complexes.

In a typical experiment, 10 mol% complex was added to a DMF solution containing 5 mM TMB and an excess of tetra-butylammonium bromide (50 mM). The reactions were initiated by simultaneous addition of perchloric acid and hydrogen peroxide. Aliquots of the reaction solution were quenched with NaOH and extracted with ethyl acetate for GC measurements. The results are summarised in Table 2. In contrast to the natural system, which functions optimally at approximately neutral pH,[71,117] both types of *cis*-dioxovanadium(V) complexes catalyze the oxidative bromination of TMB only in the presence of acid at a rate much slower than vanadium bromoperoxidase enzymes. The turnover rate lay in the range 45-58 mol product×(mol catalyst×h)$^{-1}$, similar to those reported for other vanadium complexes based on Schiff base ligands.[120,136] At this point, it should be mention that the blank reaction produced no Br-TMB in the measuring period.

Table 2. Catalytic oxidative bromination of TMB

| Compound | % Br-TMB after 5 min. (µmol] | TON (mol Br-TMB/ mol catalyst $h^{-1}$ |
|---|---|---|
| 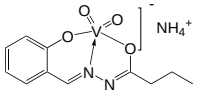 | 37.4 % (56.1 µmol) | 45 |
| 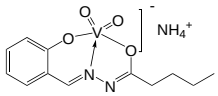 | 37.9 % (56.8 µmol) | 46 |
| 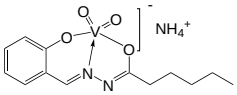 | 44.1 % (66.1 µmol) | 53 |
| 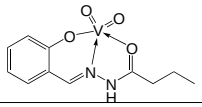 | 48.1 % (72.1 µmol) | 58 |

A small difference in reactivity was observed between the anionic complex $NH_4$[$VO_2$-(salhyb)] compared to the neutral one [$VO_2$(Hsalhyb)]. No big influence in the reactivity was observed by increasing the length of the aliphatic side-chain by one or two methylene groups, showing that this part of the ligand does not interfere with the reactivity of the vanadate center. It is known that electronic effects are less effective over more than four bonds, particularly inductive effects, and most likely an increase in reactivity of the model

complexes can be achieved by insertion of electron-withdrawing and/or electron-donating groups on the aromatic ring of the N-salicylidene aliphatic acid hydrazides.

## 2.2 Mono-oxovanadium(V) complexes based on N-salicylidene aliphatic acid hydrazides

Reaction between equimolar amounts of neutral *cis*-dioxovanadium (V) complexes $[VO_2(HL)]$ and 8-hydroxyquinoline in refluxing methanol yields the desired mono-oxovanadium(V) complexes $[VO_2(L(Q)]$. These complexes have a very good solubility in oxygen- and halogen-containing organic solvents and acetonitrile. The mono-oxovanadium(V) complexes can also be obtained by *in situ* stoichiometric reaction of N-salicylidene hydrazide ligands, ammonium metavanadate and 8-hydroxyquinoline in refluxing methanol. The *in situ* reaction can also be performed starting from a vanadium(IV) precursor as a source of vanadium. Thus, addition of a methanolic solution of the Schiff base ligand to a suspension of vanadyl acetylacetonate under aerobic conditions yields a brown-colored solution as a consequence of the fast oxidation of the vanadium(IV) precursor to vanadium(V) complex. Stepwise addition of 8-hydroxyquinoline to this solution yields dark violet solutions from which the dark-colored mono-oxovanadium(V) complexes were separated. Here should be mentioned that the equimolar reaction of N-salicylidenehydrazide with $VO(acac)_2$ results in the formation of the neutral *cis*-dioxovanadium(V) complexes upon air oxidation of the vanadium(IV) precursor. This method represents an alternative method to synthesize $[VO_2(HL)]$ complexes and has the advantage of shorter reaction times due to the higher reactivity towards complexation of the vanadyl acetylacetonate precursor and its better solubility properties compared to the ammonium metavanadate precursor.

$$[VO_2(HL)] + HQ \longrightarrow [VO(Q)(L)] + H_2O$$

$$HL + HQ + NH_4VO_3 \longrightarrow [VO(Q)(L)] + H_2O$$

$$HL + HQ + VO(acac)_2 \longrightarrow [VO(Q)(L)] + Hacac + H_2O$$

$$HL + VO(acac)_2 \longrightarrow [VO_2(HL)] + Hacac + H_2O$$

### 2.2.1 Structural characterization

The molecular structures of all mono-oxovanadium(V) complexes using the three N-salicylidenehydrazide ligands were determined by X-ray crystallography and are depicted in Figures 30-32.

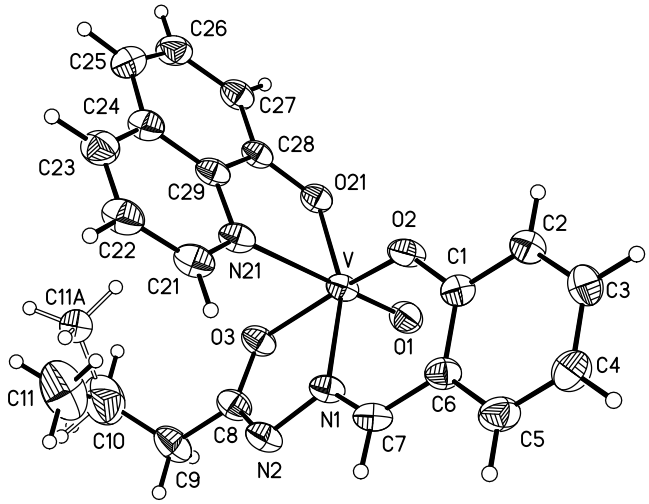


Figure 30: Molecular structure and numbering scheme for [VO(salhyb)(Q)] (**3**); displacement ellipsoids are drawn at 50% probability. Distorted $CH_3$ group in a ratio of 80% C11 and 20 % C11A.

In all cases the vanadium atom is six-coordinated as a VO(ONO)ON moiety in a distorted octahedral geometry. The fully deprotonated N-salicylidene hydrazide ligands form a tetragonal plane through the phenolate oxygen atom O2, the imine nitrogen atom N1 and the iminolate oxygen atom O3 together with the oxygen atom O21 of the bidentate 8-hydroxyquinoline ligand. Relative to this plane, the vanadium atom is displaced toward the terminal oxygen atom O1 by 31.5, 31.7 and 30.9 pm in complexes **3**, **4** and **5**, respectively. *Trans* to the oxo group O1 is located the nitrogen atom N21 of the 8-hydroxyquinoline ligand with the angle O1–V–N21 being 176.6°, 176.2° and 175.6° in complexes **3**, **4** and **5**, respectively. The vanadium to terminal oxo group (O1) bond lengths is of around 159 pm in complex **3**, **4** and **5**, respectively. These distances are slightly longer than those reported for $VO^{3+}$ complexes with hydrazones and 8-hydroxyquinoline as coli-

gand (158 pm),[137] but are within the range of 157-160 pm reported for monooxovanadium complexes when catechol,[138] hydroxamates[139,140] or polyols[141] are used as coligands. The Schiff base ligands form five- and a six-membered chelate rings with bite angles of around 84° (O2–V–N1) and 75° (O3–V–N1), respectively. Selected bond lengths and angles for complexes **3**, **4** and **5** are given in Tables 3.

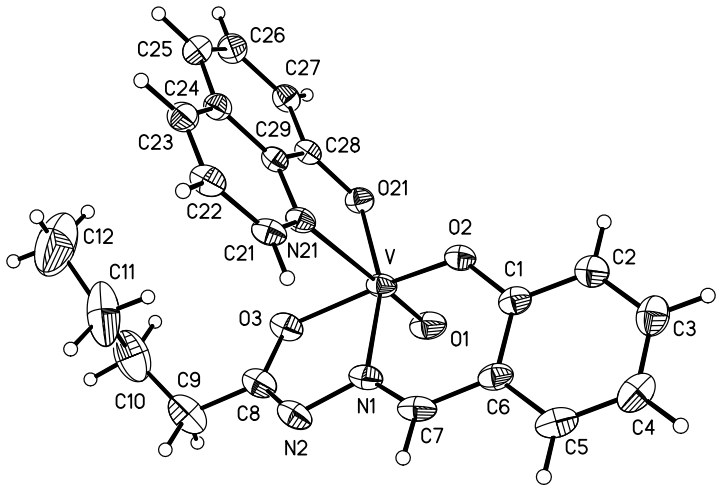


Figure 31: Molecular structure and numbering scheme for [VO(salhyp)(Q)] (**4**); displacement ellipsoids are drawn at 50% probability.

The coordination of N-salicylidenehydrazide ligands containing the enolized amide functionality in the dianionic form is consisting with 130 pm bond length for N2–C8 and 131 pm for C8–O2 bond, respectively. These bond lengths are comparable with the distances found in the ammonium salts of the *cis*-dioxovanadium(V) complex $NH_4[VO_2(salhyp)]$ (**1**). The vanadium to oxygen bond lengths in the defined tetragonal plane follow the order V–O21 (quinoline oxygen)<V–O2 (phenol oxygen)<V–O3 (iminolate oxygen). This can be explained as a consequence of the *trans* position of the quinoline oxygen O21 to the weak donor nitrogen atom N1, while the phenol oxygen atom O2 of the Schiff base ligand is located *trans* to the iminolate oxygen atom O3 of the same ligand. On the other hand, the bond length for vanadium to nitrogen atom N21 of the 8-hydroxyquinoline co-

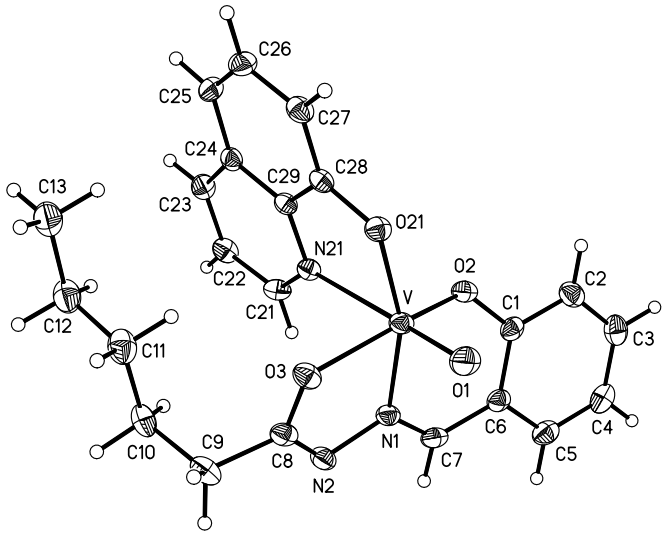


Figure 32: Molecular structure and numbering scheme for [VO(salhyh)(Q)] (**5**); displacement ellipsoids are drawn at 50% probability.

ligand is also lengthened due to the *trans* location to the terminal oxo group O1, which is strongly covalently bound to the vanadium atom.

Finally, all the mono-oxovanadium(V) complexes shown here crystallized in the monoclinic space group $P2_1/n$ with common structural features. Nevertheless, small differences between them are present, regarding the orientation of the aliphatic side chain. In complex **3** a distorted methyl group is present, as a consequence of the crystal packing, in a ratio of 80% for C11 and 20% for C11A, respectively. Further, increase of the side-chain with one and respectively two methylene groups did not afford the same effect, but a different torsion angle for N2-C8-C9-C10 was observed. This varied from 123° in complex **3** to 136° in complex **4** and 97° in complex **5**, resulting in a different orientation of the methylene group close to the enolized amide functionality. The flexibility of the aliphatic side chain is depicted in Figure 33 by the overlay of the molecular structures of complex **4** and **5**.

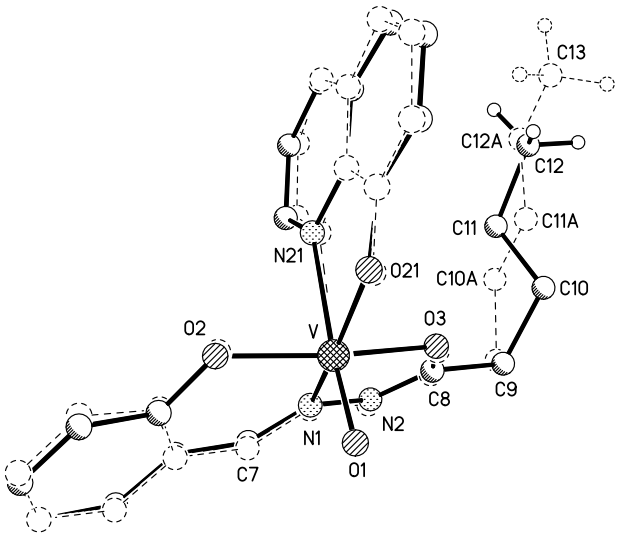


Figure 33: Overlay of the molecular structures of [VO(salhyp)(Q)] **4** (thick lines) and [VO(salhyh)(Q)] **5** (atoms extension A, broken lines).

### 2.2.2 Spectroscopic studies

The $^{1}$H and $^{13}$C NMR data for the novel mono-oxovanadium complexes summarized in the experimental section are consistent with the determined molecular structures. In particular, deprotonation of the dianionic form of the N-salicylidene hydrazide ligands upon coordination to vanadium is confirmed by the absence of the downfield $^{1}$H NMR resonances corresponding to the O−H and N−H protons. The azomethine (-CH=N) proton resonate at 9.15 ppm, a dieshielding effect of 0.16-0.82 ppm upon coordination to vanadium being observed. The methylene hydrogen atoms located in the vicinity of the carbonyl group present upfield resonances in the $^{1}$H NMR spectra of the vanadium complexes and exhibit one resonance corresponding to the existence of only one isomer when the vanadium atom is coordinated. Moreover, the aromatic region is accompanied by additional resonances that are indicative of the coordination of 8-hydroxyquinoline. Further characterization of the complexes is given by the $^{51}$V NMR spectra, recorded in DMSO-$d_6$ and $CDCl_3$. The $^{51}$V NMR spectra of all three mono-oxovanadium(V) complexes is somehow solvent dependent, i.e. in DMSO-$d_6$ a shift at -471 ppm with a width at half height of $\nu_{1/2} = 310$ Hz is observed, while in $CDCl_3$ the peak appears at -482 ppm with a width at half height of $\nu_{1/2} = 145$ Hz. The obtained complexes are stable in solu-

Table 3. Selected bond lengths (pm) and angles (°) in complexes **3**, **4** and **5**.

| | **3** | **4** | **5** |
|---|---|---|---|
| V−O1 | 159.41(18) | 158.99(17) | 159.01(14) |
| V−O2 | 185.69(16) | 185.98(17) | 186.37(13) |
| V−O3 | 194.34(16) | 195.00(17) | 195.29(13) |
| V−O21 | 184.55(16) | 185.98(17) | 184.86(13) |
| V−N1 | 208.1(2) | 208.35(19) | 207.84(15) |
| V−N21 | 237.0(2) | 235.70(19) | 236.04(15) |
| C8−O3 | 131.0(3) | 131.0(3) | 131.0(2) |
| C8−N2 | 130.0(3) | 129.9(3) | 130.3(2) |
| O1−V−O2 | 99.11(9) | 99.04(9) | 99.72(7) |
| O1−V−O3 | 97.48(8) | 98.12(8) | 98.53(7) |
| O1−V−O21 | 101.31(8) | 101.27(8) | 100.84(7) |
| O1−V−N1 | 99.46(9) | 99.15(8) | 97.35(7) |
| O1−V−N21 | 176.59(8) | 176.22(8) | 175.63(7) |
| O2−V−O21 | 101.86(7) | 103.45(7) | 102.14(5) |
| O2−V−O3 | 155.23(8) | 154.54(7) | 153.38(6) |
| O2−V−N1 | 84.19(7) | 83.91(7) | 83.65(6) |
| O3−V−O21 | 92.73(7) | 91.43(7) | 93.24(6) |
| O3−V−N1 | 75.01(7) | 74.90(7) | 74.91(6) |
| O3−V−N21 | 80.59(7) | 79.11(7) | 78.54(5) |
| O21−V−N1 | 157.09(8) | 156.84(8) | 159.61(6) |
| O21−V−N21 | 76.05(7) | 76.34(7) | 76.22(5) |
| N1−V−N21 | 82.80(7) | 82.68(7) | 85.06(6) |
| N2−V−C9 | 119.6(2) | 119.6(2) | 118.71(17) |

tion and no decomposition was observed in the presence of water. The oxovanadium(V) complexes can be converted in *cis*-dioxovanadium(V) complexes by reaction with NaOH. $^{51}$V NMR monitoring of the reaction with 0.5 equivalents of base in a DMSO-$d_6$/$D_2O$ (9:1) mixture showed the coexistence of both species ($\delta$ = -472 ppm ($\nu_{1/2}$ = 300 Hz) and

$\delta$ = -535 ppm ($\nu_{1/2}$ = 600 Hz)). One equivalent of NaOH generates only the anionic *cis*-dioxovanadium(V) complexes which resonate at -538 ppm ($\nu_{1/2}$ = 600 Hz). Further addition of base, up to two equivalents, did not produce any further change in the $^{51}$V NMR spectra. The difference of 3 ppm between the resonances of the *cis*-dioxocomplexes can be explained by the influence of more than one species existing in solution when 0.5 equivalents of base have been added.

The coordination modes of the N-salicylidene hydrazide ligands were further confirmed by comparison of the IR patterns of these ligands with those of the complexes, as well as with 8-hydroxyquinoline spectra. The characteristic ligand stretching vibrations at 3185 cm$^{-1}$ and 1673-1669 cm$^{-1}$ due to the $\nu$(NH) and $\nu$(C=O) vibrations, respectively, were not observed in the IR spectra of the complexes, indicating enolization of the amide functionality to the iminol form and its involvement in coordination to vanadium. Instead a strong band at 1605 cm$^{-1}$ is observed in the IR spectra of the complexes. This can be attributed to the asymmetric vibration of the conjugated $\nu$(-CH=N-N=C-) group[132,133] and is 6 cm$^{-1}$ shifted to a lower frequency compared to the corresponding vibration found in the ammonium salts of *cis*-dioxovanadium(V) complexes (see Experimental Part). Further differences are observed for the IR vibrations of the 8-hydroxyquinoline, used here as a coligand, namely the disappearance of the $\nu$(OH) characteristic vibration at 3152 cm$^{-1}$. For all complexes, a strong vibration is observed at 970 cm$^{-1}$ and is assigned as stretching vibration of V=O moiety. Further information was gained by electronic absorption studies carried out on acetonitrile solutions. All the vanadium complexes exhibit strong absorption maxima at 241, 273, 322 and 540 nm (see experimental part). The N-salicylidenehydrazide ligands exhibit absorption maxima at 278, 288 and 319 nm (see experimental part for $\varepsilon$ value), while 8-hydroxyquinoline absorbs at 241 ($\varepsilon$ = 39.2 $\times 10^3$ cm$^{-1}$M$^{-1}$) and 328 ($\varepsilon$ = 0.9 $\times 10^3$ cm$^{-1}$M$^{-1}$) nm in acetonitrile solution. From comparison of the UV-Vis spectra of the complexes and the organic ligands, it is obvious that, except for 540 nm band, all the other absorption maxima are shifted due to coordination. The visible absorption maxima in the UV-Vis spectra of the complexes appears most likely due to a ligand-to-metal charge transfer.

### 2.2.3 Electrochemical investigations

A characteristic feature of the vanadate moiety in vanadium bromoperoxidases is the reducible capacity of the prosthetic group to form an EPR-active vanadium center.[101,142] The reduced state, $[V^{IV}O(ONO)(ON)]^-$, of the [VO(L)(Q)] complexes can be generated in acetonitrile solutions by electrochemical reduction at 0.355V *vs.* Ag/AgCl electrode as reference electrode. All three mono-oxovanadium(V) complexes presented here showed the same electrochemical behavior. In particular, the potentials of the charge transfer processes were within ± 2 mV of each other. The square wave voltammograms (SWV), measured with a drop hanging mercury electrode, were obtained using 2.4 mM acetonitrile solutions using square wave frequencies of 25, 50, 100, 200, 400, 800 and 1500 Hz, respectively. The cyclic voltammograms exhibit in all cases two reversible one-electron reduction steps at 0.355 V and -1.638V. The SWV for complex **4** will be discussed in detail and is shown in Figure 34.

The first one-electron reduction step can be expressed as:

$$ML + e^- \rightleftharpoons ML^- \text{ (reaction 1)}$$

and occurs at a positive potential $E^\circ$ = 0.355 V, being fully reversible for square wave frequencies up to 1500 Hz.

The second reduction step occurs at a negative potential of $E^\circ$ = -1.638 V and is accompanied by a pre-wave. This can be expressed as:

$$ML^- + e^- \rightleftharpoons ML^{2-} \text{ (reaction 2)}$$

Looking at the frequency dependence of the second reduction peak and of the accompanying pre-wave shown in Figure 35, it is clear that this second reduction process remains diffusion-controlled over the entire frequency range. The accompanying pre-wave tends to become equal to the diffusion-controlled current if the square wave frequency moves towards zero, while a steady state current appears to be reached for very high square wave frequencies. This indicates that the pre-wave results from the reduction of a species produced in a preceding chemical equilibrium.

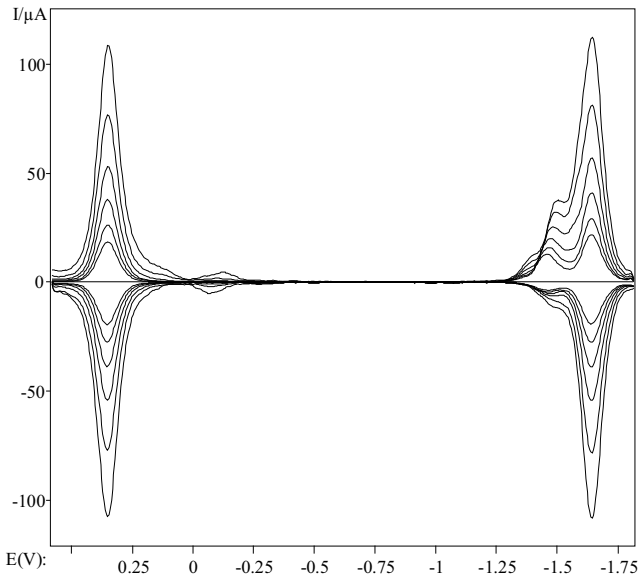


Figure 34: Square wave voltammogram of complex **4** using square wave frequencies from 25, 50, 100, 200, 400, 800 and 1500 Hz.

In other words, the height of the plateau current ($i_k$) is at least partly under kinetic control and satisfies the Bard-Faulkner equation:[143]

$$i_d/i_k = 1.02 + K\tau^{-1/2}$$

where $i_d$ is the diffusion control peak current, $\tau$ the time scale and K is a parameter that depends on the thermodynamic and kinetic constants associated with the previous chemical equilibrium from which the electrochemically active species are produced. Because the time scale, $\tau$, is inversely proportional to the square wave frequency, f, a linear dependence could be obtained as depicted in Figure 36.

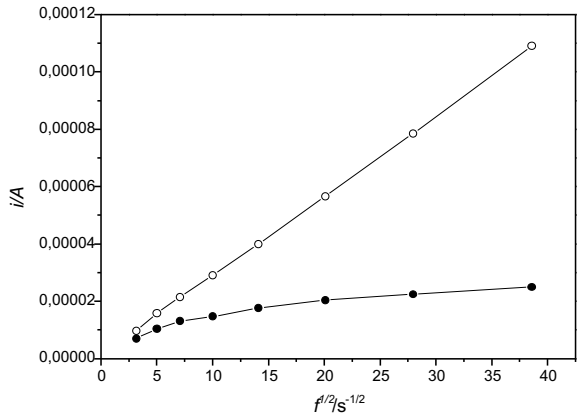


Figure 35: Height of the peak current (white circles) and the plateau of the accompanying pre-wave (black circles) associated with the second reduction step for complex **4**. The peak current associated with the first reduction step exhibits virtually the same frequency dependence as that indicated by white circles.

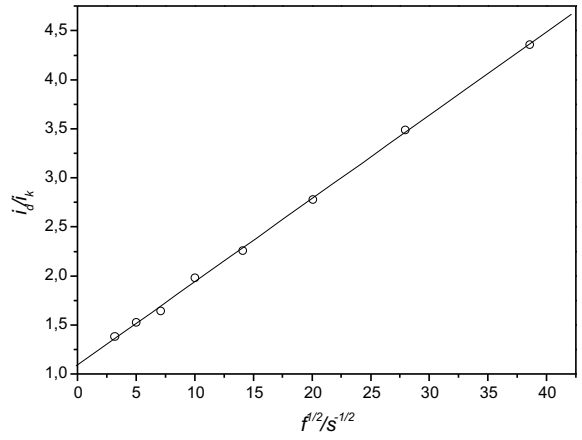


Figure 36: Ratio between the diffusion controlled peak current and the kinetically controlled plateau current as a function of the square wave frequency. If the pre-wave results from a previous chemical reaction this ratio should satisfy the Bard-Faulkner equation with $\tau^{-1/2} = \sqrt{f}$.

This once more confirmed that the pre-wave which accompanies the second reduction process is really an effect of a preceding chemical reaction. Taking into account that the 8-hydroxyquinoline anion itself shows a reversible reduction process, which take place at potential - 1.52 V, this could lead to the conclusion that a split off/addition reaction is responsible for the appearance of the pre-wave. This can be expressed as:

$$ML^- \rightleftharpoons M + L^- \text{ (reaction 3)}$$

where $L^-$ is the reduced 8-hydroxyquinoline ligand as a radical anion.

However, since the production of the species $L^-$ consumed in the pre-wave goes at the consuming of $ML^-$ which is coupled with $L^-$ by the chemical reaction 3, the above finding is not in agreement with the observation that the reduction of $ML^-$ at about -1.64 V remains fully diffusion-controlled over the entire frequency range. Also in disagreement with the simple pre-equilibrium expressed in reaction 3 is the shift of the pre-wave to more positive potentials with the increased period of time of the underlying electrochemical method (i.e. the lower the square wave frequency), because the opposite shift would be expected theoretically. Reasonable agreement with the experimental data was obtained (at least qualitatively) by taking an additional ligand addition/elimination reaction for the vanadium(V) complex into consideration

$$ML \rightleftharpoons M + L \text{ (reaction 4)}$$

where L is the deprotonated quinoline anion.

It is important to emphasize that the equilibrium for both reactions, i.e. reaction 3 and 4 is far to the left. Actually, reaction 3 is slightly pushed to the right site, only because any (infinitesimal) small amount of $L^-$ is immediately re-oxidized to L if the potential is moving between the first reduction step and the pre-wave. Although L then reacts with M, so that the resulting ML is immediately reduced again, the difference in the equilibrium/rate constants of reactions 3 and 4 (as well as the differences of the diffusion coefficients of the underlying species- the latter effect has been neglected in simulations) results in an accumulation of effects. This means that the second reduction step is accompanied by a pre-wave exhibiting an unusual frequency dependence of the

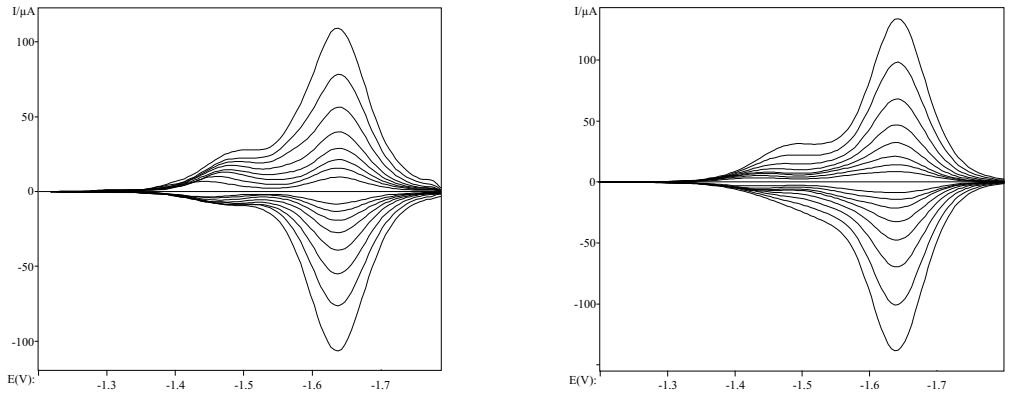


Figure 37: Comparison between measured SWVs (left) and simulated SWVs based on chemical equations (right) using the conditions quoted in Figure 34.

potential shift and an almost diffusion-controlled growth of the peak current associated with the charge transfer process (reaction 2).

Moreover, the reduction of the mono-oxovanadium(V) complexes was also achieved using Zn-Hg amalgam, a reducing agent which does not interfere with the second reduction process described in the cyclic voltametry experiments. EPR studies on this reduced form of complexes showed a specific eight-line EPR signal with a g value of 1.992 and A value of 96 G, as one would expect for a vanadium(IV) complex.

### 2.2.4 Peroxidative bromination reaction of 1,3,5-trimethoxybenzene catalyzed by mono-oxovanadium(v) complexes

Following the procedure described in 2.1.3, the mono-oxovanadium(V) complexes described here were also tested regarding their capacity to catalyze the oxidation of bromide, monitored by GC determination of mono-brominated TMB product. Unfortunately, the results showed almost no catalytic activity of these mono-oxovanadium complexes. From the entries listed in Table 4, it is obvious that the complexes present a lower catalytic activity than vanadyl acetylacetonate. The slow peroxidative bromination of TMB catalyzed by these complexes can be attributed to the high stability of the six-coordinated vanadium center, which does not permit side-on bonding of the peroxide ligand to form the active intermediate necessary for the reaction to proceed. This can lead to the con-

clusion that a five-coordinated metal center is favored for the catalytic reactivity and/or the six-coordination site of the vanadium center should be occupied by a weak donor ligand, such as solvent molecules.

Table 4. Catalytic oxidation experiments using mono-oxovanadium(V) complexes- **3**, **4** and **5** as catalysts.

| Complex | % Br-TMB ($\mu$mol) (after 5 min.) | % Br-TMB ($\mu$mol) (after 10 min.) |
|---|---|---|
| **3** | 3.2(4.8) | 9.0(13.5) |
| **4** | 3.0(4.5) | 7.5(11.2) |
| **5** | 4.6(6.9) | 11.1(16.6) |
| $VO(acac)_2$ | 16.0(24.0) | 17.2(25.8) |

## 2.3 Conclusions

N-salicylidenehydrazide ligands with aliphatic side chain are capable of accommodating mono-oxovanadium(V) complexes and *cis*-dioxovanadium(V) complexes, both types of compounds being regarded as structural model complexes for vanadium-dependent haloperoxidases. The reaction of N-salicylidene n-aliphatic acid hydrazides with ammonium metavanadate results in the formation of anionic *cis*-dioxovanadate, as well as neutral *cis*-dioxovanadium(V) complexes. An extensive hydrogen bonding interaction has been observed in the solid state in the crystal structure determined for two such *cis*-dioxovanadium complexes. The hydrogen bonding network involves hydrogen bonding contacts between oxo groups of the vanadate center and the donor atoms of the Schiff base ligand and/or the ammonium cations. Moreover, the neutral *cis*-dioxovanadium(V) complexes can be reacted with 8-hydroxyquinoline in refluxing methanol to form the six-coordinated mono-oxovanadium(V) complexes. Conversion of the mono-oxovanadium(V) to the corresponding *cis*-dioxovanadium(V) complexes has been achieved in solution by reaction with NaOH in different ratios. $^{51}V$ NMR monitoring of the reaction with base in deuterated DMSO:$D_2O$ solution showed that one equivalent of NaOH is sufficient to yield the dioxovanadium complexes. Moreover, addition of simple deuterated water to

a solution of oxovanadium(V) complexes in DMSO-$d_6$ did not yield any decomposition of the complexes. Electrochemical investigations on acetonitrile solutions of the mono-oxovanadium(V) complexes showed quasi-reversible cyclic voltammograms with two one-electron reduction steps. The first consists in the formation of a vanadium(IV) complex $[V^{IV}O(ONO)(ON)]^-$ and occurs at positive potential, while the second process seems to be most likely generated by the reduction of the split off coligand.

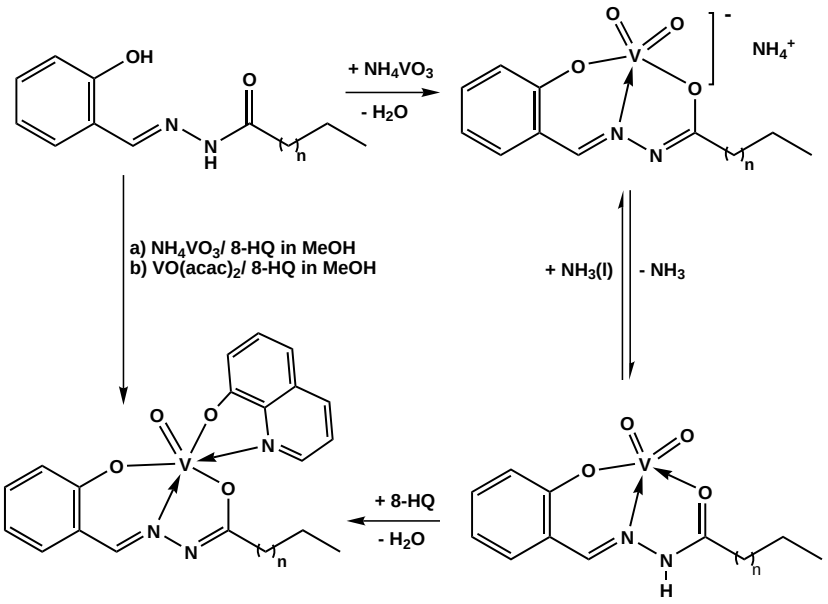


Figure 38: Schematic representation of reactivity pathways described in this chapter.

A different reactivity between the *cis*-dioxovanadium and monooxovanadium complexes has been observed towards vanadium-catalyzed peroxidative bromination of 1,3,5-trimetoxybenezene. *Cis*-dioxovanadium(V) complexes are also functional models of vanadium bromoperoxidase enzymes, being capable of catalyzing the peroxidative bromination of 1,3,5-trimetoxybenzene with a turnover rate ranging from 45-53 mol Br-TMB×(mol catalyst×h)$^{-1}$, when the anionic complexes were used as catalysts, to 58 mol Br-TMB× (mol catalyst×h)$^{-1}$ when neutral *cis*-dioxovanadium(V) complex catalyzed the biomimetic reaction. Attempts to perform the same catalytic reaction with mono-oxovanadium(V) complexes were not very successful due to the slow turnover rate of the reaction. Therefore, a five-coordinated vanadium center seems to be more appropriate for the oxidative bromination reaction, due to the presence of empty sites at the vanadium atom, favoring

thus, the addition of $H_2O_2$ to form a side-on bound peroxo-complex. As the mono-oxovanadium(V) complexes described here contain a six-coordinated vanadium center, the formation of the peroxo-vanadium(V) complex requires most likely the splitting off of the bidentate coligand (8-HQ).

## 2.4 Experimental Part

### 2.4.1 Materials

Abbreviations used throughout the text: $H_2$salhyb = butyric acid (2-hydroxy benzylidene) hydrazide, $H_2$salhyp = pentanoic acid (2-hydroxy benzylidene) hydrazide, $H_2$salhyh = hexanoic acid (2-hydroxy benzylidene) hydrazide; HQ = 8-hydroxyquinoline, TMB = 1,3,5-trimethoxybenzene. $\omega$-Carbonic acid hydrazides were prepared by reaction of the corresponding n-alkyl esters with 1.2 equivalents of hydrazine hydrate. All other chemicals were used as received. Cyclic voltametry measurements and square wave voltametric measurements were conducted by a three-electrode technique using a homemade computer-controlled instrument based on the PCI 6110-E data acquisition board (National Instruments). The experiments were performed in acetonitrile solutions containing 0.25 M tetra-butylammonium hexafluorophosphate under a blanket of solvent saturated with argon. The ohmic resistance to be compensated for was determined by measuring the impedance of the system at potentials where the Faraday current was negligible. Background corrections were accomplished, only for cyclic voltammograms, by subtracting the current curves of the blank electrolyte containing the same concentration of the supporting electrolyte from the experimental cyclic voltammograms. Ag/AgCl was used as reference electrode in acetonitrile containing 0.25 M tetra-butylammonium chloride. The potential of this reference system was calibrated by measuring the potential of the couple ferrocenium/ferrocene at the end of each experiment and was found to be 0.812±0.002 V throughout the measurements. The working electrode was hanging drop mercury ($m_{Hg-drop}$= 4 mg) produced by a CGME instrument from Bioanalytical Systems Inc., West Lafayette, USA. Theoretical square wave voltammograms were simulated using the DigiElch package, available from www.DigiElch.de.

### 2.4.2 Synthesis of N-salicylidene $\omega$-carbonic acid hydrazides

**$H_2$salhyb**

To a solution of butyric acid hydrazide (6.6 g, 64.7 mmol) in 30 mL methanol, salicylaldehyde (7.9 g, 14.3 mL, 64.7 mol) was added dropwise under continuous stirring at room temperature. The resulting slightly yellow solution was stirred at r.t. for additional 12 hours. The formed precipitate was filtered and the solvent removed under reduced pressure. Yield: 12.2 g (59.1 mmol, 91%). Anal. Calc. for $C_{11}H_{14}N_2O_2$ (206.24): C 64.06, H 6.84, N 13.58; Found C 63.94, H 7.26, N 13.33. $^1$H NMR (200 MHz, DMSO-$d_6$): $\delta = 0.91$ (dt, 3H, C$H_3$, $^3$J=7.31 Hz), 1.53-1.61 (m, 2H, C$H_2$CH$_3$), 2.18 and 2.54 (t, 2H, C$H_2$CO, $^3$J=7.22 Hz and $^3$J=7.31 Hz, ratio 1.4:0.8), 6.80-6.95 (m, 2H, arom. C$H$), 7.17-7.30 (m, 1H, arom. C$H$), 7.44-7.66 (m, 1H, arom. C$H$), 8.24 and 8.33 (s, total 1H, C$H$=N, ratio 0.3:0.7), 10.24, 11.18, 11.57 (N$H$, O$H$, total 2H in a ratio of 0.3:1.0:0.6) ppm. Selected IR data (cm$^{-1}$): $\nu$= 3185 (s; NH, OH$_{ass}$), 1673 (s, C=O), 1623 (s, CH=N). UV/Vis ($CH_3CN$ solution, $\lambda_{max}$ in nm ($\varepsilon$ in $10^3$ M$^{-1}$ cm$^{-1}$)): 278 (18.5), 288 (17.3), 319 (8.7).

**$H_2$salhyp**

This ligand was prepared as described above from pentanoic acid hydrazide (7.7 g, 66.0 mmol) and salicylaldehyde (8.1 g, 7.0 mL, 66.0 mmol) in methanol. Yield: 13.8 g (62.6 mmol, 95%). Anal. Calc. for $C_{12}H_{16}N_2O_2$ (220.27): C 65.43, H 7.32, N 12.72; Found C 65.57, H 7.34, N 12.89. $^1$H NMR (200 MHz, DMSO-$d_6$): $\delta = 0.87$ (t, 3H, C$H_3$, $^3$J=7.13 Hz), 1.28-1.35 (m, 2H, C$H_2$CH$_3$), 1.51-1.59 (m, 2H, C$H_2$CH$_2$CO), 2.20 and 2.56 (t, 2H, C$H_2$CO, $^3$J=7.31 Hz, ratio 1.4:0.7), 6.80-6.99 (m, 2H, arom. C$H$), 7.17-7.30 (m, 1H, arom. C$H$), 7.44-7.60 (m, 1H, arom. C$H$), 8.24 and 8.33 (s, total 1H, C$H$=N, ratio 0.4:0.6), 10.12, 11.18, 11.56 (N$H$, O$H$, total 2H in a ratio 0.3:1.0:0.6) ppm. Selected IR data (cm$^{-1}$): $\nu$= 3185 (s; NH, OH$_{ass}$), 1669 (s, C=O), 1623 (s, CH=N). UV/Vis ($CH_3CN$ solution, $\lambda_{max}$ in nm ($\varepsilon$ in $10^3$ M$^{-1}$ cm$^{-1}$)): 278 (18.4), 288 (17.6), 319 (8.9).

**$H_2$salhyh**

$H_2$salhyh was obtained analogously to the other ligands from hexanoic acid hydrazide (7.6 g, 58.0 mmol) and salicylaldehyde (7.1 g, 6.1 mL, 58.0 mmol) using the same solvent.

Yield: 12.1 g (51 mmol, 89%). Anal. Calc. for $C_{13}H_{18}N_2O_2$ (234.29): C 66.64, H 7.74, N 11.96; Found C 66.66, H 7.76, N 11.97. $^1$H NMR (200 MHz, DMSO-$d_6$): $\delta$ = 0.85 (t, 3H, C*H*$_3$, $^3$J=6.68 Hz), 1.22-1.31 (m, 4H, C*H*$_2$), 1.49-1.64 (m, 2H, C*H*$_2$CH$_2$CO), 2.19 and 2.60 (t, 2H, C*H*$_2$CO, $^3$J=7.40 Hz and $^3$J=7.50 Hz, ratio 1.2:0.8), 6.80-6.99 (m, 2H, arom. C*H*), 7.21-7.30 (m, 1H, arom. C*H*), 7.44-7.60 (m, 1H, arom. C*H*), 8.24 and 8.33 (s, total 1H, C*H*=N, ratio 0.4:0.6), 10.12, 11.18, 11.56 (N*H*, O*H*, total 2H in a ratio 0.3:1.0:0.6) ppm. Selected IR data (cm$^{-1}$): $\nu$= 3186 (s; NH, OH$_{ass}$), 1669 (s, C=O), 1623 (s, CH=N). UV/Vis ($CH_3CN$ solution, $\lambda_{max}$ in nm ($\varepsilon$ in $10^3$ M$^{-1}$ cm$^{-1}$)): 278 (19.0), 288 (17.3), 319 (8.0).

### 2.4.3 Synthesis of the ammonium salts of *cis*-dioxovanadium complexes

#### Preparation of $NH_4$[$VO_2$(salhyb)]

To a solution of $H_2$salhyb (1.0 g, 4.8 mmol) in 100 mL MeOH was added $NH_4VO_3$ (0.6 g, 4.8 mmol). The resulting mixture was refluxed with continuous stirring for 24 hours and filtered hot for removal of unreacted ammonium metavanadate. The resulting solution volume was reduced under reduced pressure to about half of its original volume. After standing overnight at room temperature in an open flask, a yellow precipitate was formed. Additional material could be obtained by removal of the solvent to dryness and washing the yellow-brownish solid with chloroform (3x20 ml). Total yield: 0.5 g (1.5 mmol, 30%). $^1$H NMR (400 MHz, DMSO-$d_6$): $\delta$ = 0.89 (t, 3H, C*H*$_3$), 1.58-1.60 (m, 2H, C*H*$_2$), 2.22 (t, 2H, C*H*$_2$CO), 6.73-6.75 (m, 2H, arom. C*H*), 7.12 (m, 4H, arom. N$H_4^+$), 7.28-7.47 (m, 2H, arom. C*H*), 8.74 (s, 1H, C*H*=N) ppm. $^{51}$V NMR (105 MHz, DMSO-$d_6$): -533.8 ppm ($\nu_{1/2}$=585 Hz). Selected IR data (cm$^{-1}$): $\nu$= 3434 (br, $NH_4^+$), 1612 (s, -CH=N-N=CH-), 908 and 894 (s, $VO_2$).

#### Preparation of $NH_4$[$VO_2$(salhyp)](1)

To a solution of $H_2$salhyp (1.0 g, 4.5 mmol) in 100 mL MeOH was added $NH_4VO_3$ (0.5 g, 4.5 mmol). The resulting mixture was refluxed with continuous stirring for one day and filtered hot for removal of unreacted ammonium metavanadate. The work-up of the

resulting solution is similar to that described previously for $NH_4[VO_2(Hsalhyb)]$. Total yield: 0.5 g (1.5 mmol, 35%). $^1$H NMR (400 MHz, DMSO-$d_6$): $\delta$ = 0.87 (t, 3H, C$H_3$), 1.29-1.36 (m, 2H, C$H_2$), 1.52-1.59 (m, 2H, C$H_2$), 2.26 (t, 2H, C$H_2$CO), 6.73-6.77 (m, 2H, arom. C$H$), 7.08 (m, 4H, arom. N$H_4^+$), 7.28-7.48 (m, 2H, arom. C$H$), 8.75 (s, 1H, C$H$=N) ppm. $^{51}$V NMR (105 MHz, DMSO-$d_6$): -534.3 ($\nu_{1/2}$=610 Hz) ppm; Selected IR data (cm$^{-1}$): $\nu$= 3434 (br, $NH_4^+$), 1611 (br, -CH=N-N=CH-), 895, 908 (s, $VO_2$).

**Preparation of $NH_4[VO_2(salhyh)]$**

This complex was prepared analogously, using the above described procedure, from $H_2$salhyh (1.0 g, 4.3 mmol) and $NH_4VO_3$ (0.5 g, 4.3 mmol). Total yield: 0.4 g (1.2 mmol, 30%). $^1$H NMR (400 MHz, DMSO-$d_6$): $\delta$ = 0.85 (m, 3H, C$H_3$), 1.28 (m, 4H, C$H_2$), 1.57 (m, 2H, C$H_2$), 2.24 (m, 2H, C$H_2$CO), 6.73-6.76 (m, 2H, arom. C$H$), 7.11 (br., 4H, N$H_4^+$), 7.17-7.19 (m, 1H, arom. C$H$), 7.47-7.51 (m, 1H, arom. C$H$), 8.76 (s, 1H, C$H$=N) ppm. $^{51}$V NMR (105 MHz, DMSO-$d_6$): -534.2 ($\nu_{1/2}$=615 Hz) ppm. Selected IR data (cm$^{-1}$): $\nu$= 3434 (br, $NH_4^+$), 1612 (s, -CH=N-N=CH-), 895, 908 (s, $VO_2$).

### 2.4.4 Synthesis of the neutral *cis*-dioxovanadium complexes

The synthesis of these complexes follows the procedure describe above for each ammonium salt of *cis*-dioxovanadium(V) complexes with the reflux period prolonged to about three days.

**Preparation of $[VO_2(Hsalhyb)]$**

Yield: 0.6 g (2.1 mmol, 44%). *Anal.* Calc. for $C_{11}H_{13}N_2O_4V$ (288.170): C 45.85, H 4.55, N 9.72. Found: C 45.85, H 4.58, N 9.61. This complex was alternatively prepared by reaction of $H_2$salhyb (0.42 g, 2 mmol) with $VO(acac)_2$ (0.52 g, 2 mmol) in 50 mL methanol under continuous stirring and reflux for about four hours. Removal of the solvent to about third of the initial volume lead overnight a yellow precipitate. Yield: 0.34 g (1.18 mmol, 60%). $^1$H NMR (400 MHz, DMSO-$d_6$): $\delta$ = 0.94 (t, 3H, C$H_3$, $^3$J=7.2 Hz), 1.60-1.67 (m, 2H, C$H_2$), 2.36 (t, 2H, C$H_2$CO, $^3$J= 7.2 Hz), 6.82-6.98 (m, 2H, arom. C$H$), 7.43-7.71 (m, 2H, arom. C$H$), 8.80 (s, 1H, C$H$=N) ppm and 11.15, 11.58 (br. N$H$); $^{51}$V NMR

(105 MHz, DMSO-$d_6$): -533.9 (shoulder), -541 ($\nu_{1/2}$=790 Hz), -570.6 ($\nu_{1/2}$=870 Hz) ppm in a ratio 0.7:1.0. MS (ESI-negative mode): m/z = 287.3 [M - $H^+$](100%). Selected IR data ($cm^{-1}$): $\nu$= 3434 (br, NH), 1628 (s, CO), 1611 (s, -CH=N), 921 and 893 (s, $VO_2$).

**Preparation of [$VO_2$(Hsalhyp)] (2)**

Yield: 0.5 g (1.8 mmol, 40%). *Anal.* Calc. for $C_{12}H_{15}N_2O_4V$ (302.201): C 47.69, H 5.00, N 9.27. Found: C 46.90, H 5.10, N 10.21. $^{51}$V NMR (105 MHz, DMSO-$d_6$): -537.3 ($\nu_{1/2}$=570 Hz) and -570.1 ppm in a ratio 1.0:0.2. Selected IR data ($cm^{-1}$): $\nu$= 3435 (br, NH), 1628 (s, CO), 1611 (s, -CH=N), 921 and 892 (s, $VO_2$).

**Preparation of [$VO_2$(Hsalhyh)]**

Yield: 0.9 g (2.9 mmol, 67%). *Anal.* Calc. for $C_{13}H_{17}N_2O_4V$ (316.221): C 49.38, H 5.42, N 8.86. Found: C 49.36, H 5.27, N 8.84. $^1$H NMR (400 MHz, DMSO-$d_6$): $\delta$ = 0.95 (t, 3H, C$H_3$), 1.28-1.35 (m, 4H, C$H_2$), 1.60-1.66 (m, 2H, C$H_2$), 2.34 (t, 2H, C$H_2$CO), 6.80-6.98 (m, 2H, arom. C$H$), 7.24-7.70 (m, 2H, arom. C$H$), 8.79 (s, 1H, C$H$=N) and 10.10, 11.15, 11.60 (br. N$H$). $^{51}$V NMR (105 MHz, DMSO-$d_6$): -540.6 ($\nu_{1/2}$=665 Hz) and -570.7 ($\nu_{1/2}$=780 Hz) ppm in a ratio 1.0:0.8. MS (FAB in nba): m/z = 235.3 [L + $H^+$](20%), 300 (58%), 317 [M + $H^+$](44%), 438 (20%). Selected IR data ($cm^{-1}$): $\nu$= 3437 (br, NH), 1627 (s, CO), 1610 (s, -CH=N), 919 and 893 (s, $VO_2$).

### 2.4.5 Synthesis of the mono-oxovanadium(V) complexes

**Preparation of [VO(salhyb)(Q)] (3)**

**Method 1:** To a suspension of [$VO_2$(Hsalhyb)] (0.49 g, 1.71 mmol) in 30 mL methanol was added dropwise (15 minutes), under reflux and continuous stirring, a solution of 8-hydroxyquinoline (0.24 g, 1.70 mmol) in 10 mL methanol. The resulting dark-violet solution was refluxed for additional two hours and the solution was filtered hot. The solvent was reduced to dryness under reduced pressure and redissolved in 5 mL methanol. Upon standing at room temperature overnight, a dark-violet solid was formed. Yield: 0.40 g (0.96 mmol, 56%).

**Method 2:** A solution of $H_2$salhyb (0.21 g, 1.00 mmol) in 15 mL methanol was added under stirring to a suspension of $VO(acac)_2$ (0.26 g, 1.00 mmol) in 15 mL methanol. The resulting reaction mixture was refluxed for two hours under continued stirring, during which time the color changed from green to brown. 8-Hydroxyquinoline (0.14 g, 1.00 mmol), dissolved in 10 mL methanol, was added dropwise over a period of 15 minutes and the reaction solution was refluxed and stirred for an additional 30 minutes. The reaction mixture was reduced to dryness under reduced pressure and redissolved in 5 mL methanol. Upon standing at room temperature, overnight a dark-violet solid is formed. Yield: 0.32 g (0.77 mmol, 77%).

**Method 3:** To a suspension of $NH_4VO_3$ (0.24 g, 2.00 mmol) in 10 mL methanol was added $H_2$salhyb (0.42 g, 2.00 mmol) dissolved in 30 mL methanol, followed by immediate addition of a solution of 8-hydroxyquinoline (0.29 g, 2.00 mmol) in 10 mL methanol. The reaction mixture was refluxed with continuous stirring over a period of two hours. The reaction volume was reduced to around 10 mL and kept at room temperature in an open flask. Yield: 0.60 g (1.44 mmol, 72%).

*Anal.* Calc. for $C_{20}H_{18}N_3O_4V$ (415.321): C 57.84, H 4.36, N 10.11. Found: C 58.08, H 4.18, N 10.15. $^1$H NMR (400 MHz, DMSO-$d_6$): $\delta$ = 0.48 (t, 3H, C$H_3$, $^3$J=7.31 Hz), 1.09-1.22 (m, 2H, C$H_2$CH$_3$), 1.99-2.11 (m, 2H, C$H_2$CO), 6.73-6.75 (d, 1H, arom. C$H$), 6.99-7.02 (m, 1H, arom. C$H$), 7.17-7.19 (m, 1H, arom. C$H$), 7.46-7.50 (m, 1H, arom. C$H$), 7.56-7.59 (m, 1H, arom. C$H$), 7.69-7.72 (m, 2H, arom. C$H$), 7.78-7.81 (m, 1H, arom. C$H$), 8.09-8.11 (m, 1H, arom. C$H$), 8.50-8.53 (m, 1H, arom. C$H$), 9.15 (s, 1H, C$H$=N) ppm. $^{13}$C NMR (50 MHz, DMSO-$d_6$): $\delta$ = 12.9 ($C$H$_3$), 19.1 ($C$H$_2$CH$_3$), 31.3 ($C$H$_2$CO), 111.5, 115.5 (arom.$C$H), 119.5 (arom.$C$), 120.4, 122.5, 123.0, 128.3, 129.0, 133.3, 135.3, 138.3, 138.8, 146.3 (arom.$C$H and $C$), 154.2 (arom.$C$H=N) ppm), 162.3, 163.3 (arom.$C$O–V), 175.8 ($C$O–V). $^{51}$V NMR (105 MHz, DMSO-$d_6$): - 471.7 ppm ($\nu_{1/2}$=315 Hz); $^{51}$V NMR (105 MHz, $CDCl_3$): - 481.3 ppm ($\nu_{1/2}$=145 Hz). Selected IR data (cm$^{-1}$): 1605 (s, -CH=N-N=C-), 1553 (s, -CH=N arom., quinoline), 969 (s, VO). UV/Vis ($CH_3CN$ solution, $\lambda_{max}$ in nm ($\varepsilon$ in $10^3$ M$^{-1}$ cm$^{-1}$)): 241 (41.5), 273 (19.1), 322 (8.5), 540 (6.8).

**Preparation of [VO(salhyp)(Q)] (4)**

Complex **4** was prepared as described above from $[VO_2(Hsalhyp)]$ (**2**) (0.51 g, 1.71 mmol) and 8-hydroxyquinoline (0.24 g, 1.70 mmol) in refluxing methanol. The *in situ* reactions were similar to the previously described. *Method 1*: $H_2$salhyp (0.22 g, 1.00 mmol), $VO(acac)_2$ (0.26 g, 1.00 mmol) and 8-hydroxyquinoline (0.14 g, 1.00 mmol) in methanol or alternatively by *Method 3* by reaction of $H_2$salhyp (0.44 g, 2.00 mmol) with stoichiometric amounts of $NH_4VO_3$ and 8-hydroxyquinoline in methanol solution. Yield: 0.53 g (1.23 mmol; 72 %) (method 1), 0.41 g (0.95+mmol; 95 %) (method 2) and 0.58 g (1.35 mmol; 67.5 %) (method 3). *Anal.* Calc. for $C_{21}H_{20}N_3O_4V$ (429.347): C 58.75, H 4.70, N 9.79. Found: C 58.73, H 4.60, N 9.92. $^1$H NMR (400 MHz, DMSO-$d_6$): $\delta$ = 0.50 (t, 3H, C*H*$_3$, $^3$J=7.33 Hz), 0.71-0.83 (m, 2H, C*H*$_2$CH$_3$), 1.02-1.08 (m, 2H, C*H*$_2$CH$_2$CO), 2.02-2.09 (m, 2H, C*H*$_2$CO), 6.72-6.76 (m, 1H, arom. C*H*), 6.99-7.02 (m, 1H, arom. C*H*), 7.17-7.20 (m, 1H, arom. C*H*), 7.47-7.59 (m, 2H, arom. C*H*), 7.68-7.74 (m, 2H, arom. C*H*), 7.79-7.81 (m, 1H, arom. C*H*), 8.09-8.10 (m, 1H, arom. C*H*), 8.49-8.53 (m, 1H, arom. C*H*), 9.14 (s, 1H, C*H*=N) ppm. $^{13}$C NMR (100 MHz, DMSO-$d_6$): $\delta$ = 13.4 (*C*H$_3$), 21.1 (*C*H$_2$), 27.7 (*C*H$_2$), 29.2 (*C*H$_2$CO), 111.0, 115.4 (arom.*C*H), 119.5 (arom.*C*), 120.4, 122.5, 123.0, 128.2, 129.1, 133.3, 135.3, 138.3, 138.6, 146.3 (arom.*C*H and *C*), 154.2 (*C*H=N) ppm), 162.3, 163.4 (arom.*C*O–V), 176.1 (*C*O–V). $^{51}$V NMR (105 MHz, DMSO-$d_6$): - 471.5 ppm ($\nu_{1/2}$=310 Hz); $^{51}$V NMR (105 MHz, $CDCl_3$): - 482.3 ppm ($\nu_{1/2}$=145 Hz). Selected IR data ($cm^{-1}$): 1605 (s, -CH=N-N=C-), 1552 (s, -CH=N arom., quinoline), 972 (s, VO). UV/Vis ($CH_3CN$ solution, $\lambda_{max}$ in nm ($\varepsilon$ in $10^3$ $M^{-1}$ $cm^{-1}$)): 241 (42.9), 273 (19.8), 322 (8.8), 540 (7.0).

**Preparation of [VO(salhyh)(Q)] (5)**

Complex **5** was prepared by analogous methods. *Method 1*: $[VO_2(Hsalhyh)]$ (0.54 g, 1.71 mmol) in 30 mL methanol and 8-hydroxyquinoline (0.24 g, 1.70 mmol); *Method 2*: from $H_2$salhyh (0.23 g, 1.00 mmol), $VO(acac)_2$ and 8-hydroxyquinoline in stoichiometric amounts; and *Method 3*: reaction of $H_2$salhyh (0.47 g, 2.00 mmol) with equimolar amounts of $NH_4VO_3$ and 8-hydroxyquinoline in methanol. Yield: 0.61 g (1.37 mmol; 80 %) (method 1), 0.38 g (0.85 mmol; 85 %) (method 2) and 0.68 g (1.53 mmol; 76.5 %)

(method 3). *Anal.* Calc. for $C_{22}H_{22}N_3O_4V$ (443.373): C 59.60, H 5.00, N 9.48. Found: C 59.55, H 5.11, N 9.79. $^1$H NMR (400 MHz, DMSO-$d_6$): $\delta$ = 0.54 (m, 3H, C$H_3$, $^3$J=7.31 Hz), 0.60-0.91 (m, 4H, C$H_2$), 1.05-1.12 (m, 2H, C$H_2$CH$_2$CO), 2.00-2.14 (m, 2H, C$H_2$CO), 6.73-6.76 (m, 1H, arom. C$H$), 6.99-7.03 (m, 1H, arom. C$H$), 7.17-7.19 (m, 1H, arom. C$H$), 7.47-7.51 (m, 1H, arom. C$H$), 7.56-7.59 (m, 1H, arom. C$H$), 7.69-7.74 (m, 2H, arom. C$H$), 7.79-7.81 (m, 1H, arom. C$H$), 8.09-8.11 (m, 1H, arom. C$H$), 8.51-8.54 (m, 1H, arom. C$H$), 9.14 (s, 1H, C$H$=N) ppm. $^{13}$C NMR (100 MHz, DMSO-$d_6$): $\delta$ = 13.4 ($C$H$_3$), 21.5 ($C$H$_2$), 25.3 ($C$H$_2$), 29.3 ($C$H$_2$), 30.1 ($C$H$_2$CO), 111.9, 115.4, 119.5 (arom.$C$H and $C$), 120.4, 122.4, 122.9, 128.2, 129.1, 133.2, 135.2, 138.2, 138.6, 146.2 (arom.$C$H and $C$), 154.1 ($C$H=N) ppm), 162.3, 163.3 (arom.$C$O–V), 176.1 ($C$O–V). $^{51}$V NMR (105 MHz, DMSO-$d_6$): - 472.6 ppm ($\nu_{1/2}$=310 Hz); $^{51}$V NMR (105 MHz, $CDCl_3$): - 481.1 ppm ($\nu_{1/2}$=145 Hz). Selected IR data (cm$^{-1}$): 1605 (s, -CH=N-N=C-), 1551 (s, -CH=N arom., quinoline), 973 (s, VO). UV/Vis ($CH_3CN$ solution, $\lambda_{max}$ in nm ($\varepsilon$ in $10^3$ M$^{-1}$ cm$^{-1}$)): 241 (42.8), 273 (19.5), 322 (8.6), 540 (7.1).

## Reduction of [VO(salhyp)(Q)] (4) complex

Complex **4** (0.05 g, 0.12 mmol) was dissolved in 5 mL acetonitrile under argon atmosphere in presence of an excess of Zn-Hg amalgam. The resulting violet solution was stirred at r.t. for about 30 minutes when a green precipitate was formed. The precipitate was filtered off under argon atmosphere and redissolved in dried DMF for EPR measurement.

### 2.4.6 Catalytic oxidative bromination of TMB

TMB (25 mg, 0.15 mmol) was dissolved in 10 mL DMF. 10 mL of stock solution of tetrabutylammonium bromide (48.3g/L) (1.5 mmol, 10 equiv.) were added, followed by addition of 1 mL of vanadium complex, 0.15 mol% in DMF (0.015 mmol), $HClO_4$ (0.15 mmol) and $H_2O_2$ (0.15 mmol) in this order. Aliquots of the reaction (250 $\mu$L) were quenched in 2 mL of NaOH 2 mM aqueous solution and extracted with 3 mL ethyl acetate. The reaction products were identified by gas-chromatography using the following temperature programm: 80 °C to 240 °C with a heating rate of 15 °C per minute, followed by 5 minutes holding of 240 °C temperature.

# Chapter 3

# Vanadium complexes based on N-salicylidene hydrazides with hydroxyl substituted aliphatic side chains

The hydroxy-functionalization of the aliphatic side chain of the N-salicylidene hydrazide ligands has been achieved in order to design a ligand system capable of mimicking the hydrogen bonding interaction of the vanadate moiety from the natural system with the serine residue. The synthesis of this ligand system involves, in the first step, the reaction between lactone and two equivalents of hydrazine hydrate. The reaction was performed under reflux and continuous stirring for 12 hours to form the n-hydroxy aliphatic acid hydrazides. In the second step, Schiff base condensation with salicylaldehyde affords N-salicylidene hydrazides that contain hydroxyl substituted aliphatic side chains. The schematic representation of the synthesis pathway is depicted in Figure 39.

The synthesis of vanadium(V) complexes with these type of Schiff base ligands follows in general the procedure outlined in Chapter 2 with some differences regarding the synthesis of oxovanadium(V) complexes.

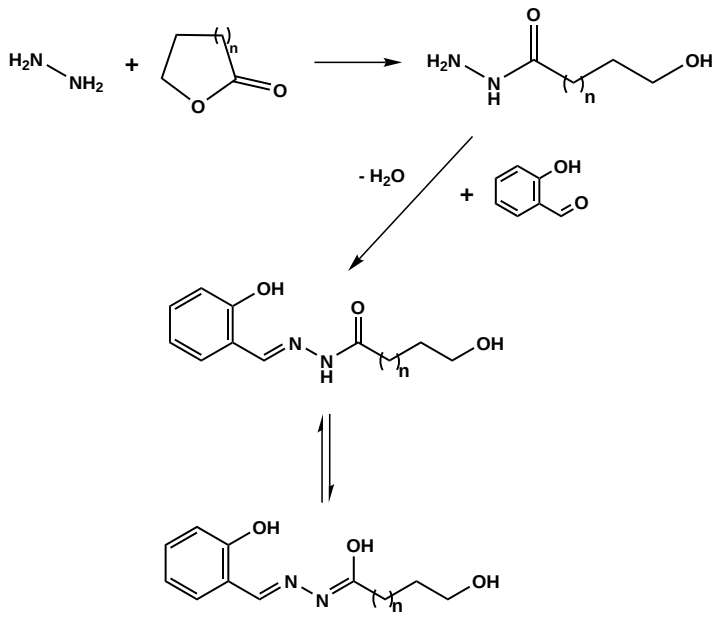

Figure 39: Schematic representation of the synthesis and tautomeric forms of hydroxyl-substituted N-salicylidene hydrazides. n=1 $H_2$salhyhb; n=2 $H_2$salhyhp; n=3 $H_2$salhyhh.

Every attempt to perform the *in situ* reaction using stoichiometric amounts of the new N-salicylidene hydrazide ligands, ammonium metavanadate and 8-hydroxyquinoline failed. Instead a mixture of the ammonium salt of *cis*-dioxovanadium(V) complexes[134,135] and methoxy-bis-(8-quinolinato)-oxovanadium(V)(**6**) has been obtained. Complex **6** crystallizes overnight from the reaction mixture as violet prisms. Removal of the reaction solvent to dryness and redissolving of the residue in chloroform, afforded a good separation of the two complexes due to the insolubility of the anionic *cis*-dioxovanadium complex in the chosen solvent. Complex **6** has been reported first time by Blair *et al.* in 1958[144] and later on by Riechel *et al.*,[145] Giacomelly *et al.*[146] and it has been crystallographically characterized by Scheidt[147] as an oxo-isopropoxo-bis-(8-quinolinato) vanadium(V) complex. The similar complex **6** crystalizes in the monoclinic space group $C_2/c$ with two crystallographically distinct oxovanadium moieties. Each molecule contains an octahedrally six-coordinated vanadium atom with the two nitrogen atoms of the hydroxyquinoline ligand placed in *trans* position to the oxo (O3) and methoxy (O4C) ligands (Figure 40).

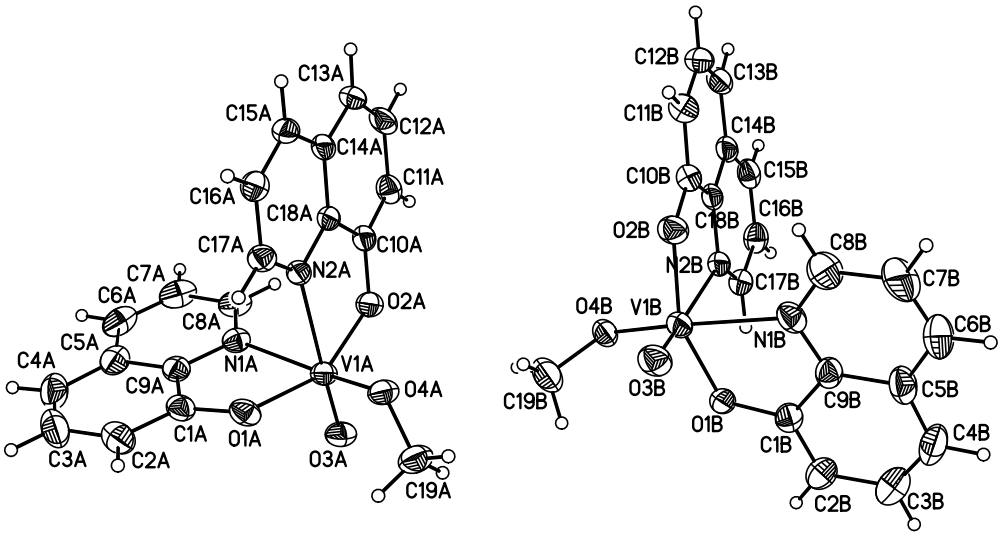


Figure 40: Molecular structure and numbering scheme for $[VO(Q)_2(OCH_3)]$ **6**; displacement ellipsoids are drawn at the 50% probability level.

The bond lengths and angles are very similar to those previous reported for isopropoxy-vanadium complex except the vanadium to nitrogen atom located *trans* to the oxo group. This bond length is slightly shortened to around 230 pm, compared to 231.7 pm reported by Scheidt. Selected bond lengths and angles for complex **6** are given in Table 5.

Complexes of type **6** represent the first models of vanadium(V) complexes able to behave as the corresponding organic ester. This complex can be converted in vanadium(V) anhydrides, as well as in the corresponding acids of type oxo-hydroxo-vanadium(V) quinolinate complex-$[VO(OH)Q_2]$ when reacted with acid.[146,148]

This is a significant difference to the ligand system outlined in Chapter 2, since in the case of the alcoholic side chain, the reaction of the ammonium salt of *cis*-dioxovanadium complexes with 8-hydroxyquinoline did not afford the desired mono-oxovanadium(V) complexes. However the reaction was successful by performing *in situ* reaction using a vanadium(IV) precursor and equimolecular amounts of N-salicylidene hydrazides and 8-hydroxyquinoline in methanol and/or acetonitrile solution.

Table 5. Selected bond lengths (pm) in complex **6**.

| | | | |
|---|---|---|---|
| V1A−O1A | 191.98(18) | V1B−O1B | 192.82(18) |
| V1A−O2A | 189.93(17) | V1B−O2B | 190.21(18) |
| V1A−O3A | 159.91(17) | V1B−O3B | 160.27(18) |
| V1A−O4A | 178.16(17) | V1B−O4B | 176.80(17) |
| V1A−N1A | 220.1(2) | V1B−N1B | 220.6(2) |
| V1A−N2A | 230.1(2) | V1B−N2B | 229.7(2) |
| O3A−V1A−O4A | 101.07(9) | O3B−V1B−O4B | 101.73(9) |
| O3A−V1A−O2A | 97.15(8) | O3B−V1B−O2B | 95.84(9) |
| O4A−V1A−O2A | 102.92(8) | O4B−V1B−O2B | 102.20(8) |
| O3A−V1A−O1A | 101.31(8) | O3B−V1B−O1B | 101.59(9) |
| O4A−V1A−O1A | 91.46(8) | O4B−V1B−O1B | 91.83(8) |
| O2A−V1A−O1A | 153.93(8) | O2B−V1B−O1B | 154.91(8) |
| O3A−V1A−N1A | 93.17(8) | O3B−V1B−N1B | 92.75(9) |
| O4A−V1A−N1A | 163.39(8) | O4B−V1B−N1B | 163.13(9) |
| O2A−V1A−N1A | 83.53(8) | O2B−V1B−N1B | 84.68(8) |
| O1A−V1A−N1A | 77.27(8) | O1B−V1B−N1B | 76.65(8 |
| O3A−V1A−N2A | 172.50(8) | O3B−V1B−N2B | 171.11(9) |
| O4A−V1A−N2A | 84.23(7) | O4B−V1B−N2B | 84.47(7) |
| O2A−V1A−N2A | 76.36(7) | O2B−V1B−N2B | 76.48(7 |
| O1A−V1A−N2A | 83.72(7) | O1B−V1B−N2B | 84.42(7) |
| N1A−V1A−N2A | 82.45(7) | N1B−V1B−N2B | 82.20(8) |

The vanadium(V) complexes synthesized using the title ligand system represent a side-chain functionalized model system for vanadium dependent haloperoxidases, namely regarding the serin residue. In the native enzyme structure this serine residue is most likely used as a hydrogen bonding acceptor, whereas in the apo-protein the serine residue can be involved in phosphatase activity.[98] Moreover, this Ser402 residue became a matter of considerable interest recently. EXAFS studies on vanadium bromoperoxidase isolated from *Ascophylum nodosum*, suggested that serine plays a vital role in the catalysis, being

the actual site of bromination, forming a carbon-bromide bond during the turnover.[149] This proposed essential role could not be verified by site-directed mutagenesis experiment performed on the vanadium chloroperoxidase enzyme from the fungus *Curvularia inaequalis*.[150] Although, the basic activity of the enzyme is retained by mutation of the active serine with alanine, a significant decrease of the enzyme activity has been reported for both the chlorination and the bromination activity. The catalytic activity of the appropriate active site-mutant decreased to about 4% and 20%, respectively. The role of the serine residue has also been addressed using synthetic model, namely the ammonium salt of the *cis*-dioxovanadium(V) complex based on N-salicylidene 5-hydroxy pentanoic acid hydrazide $NH_4[VO_2(salhyhp)]$, a catalyst which contains a similar hydroxyl group which was proposed to be halogenated.[135]

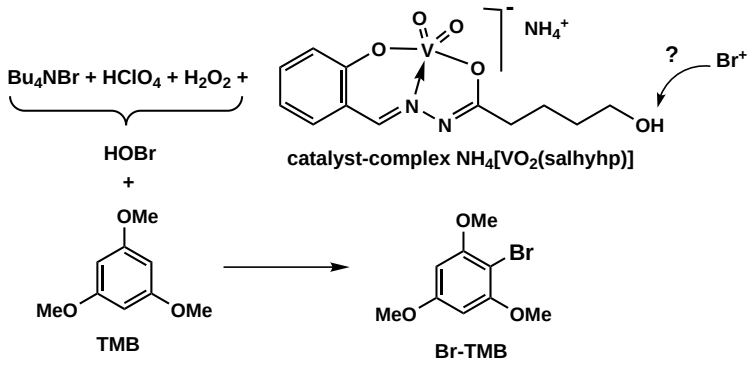


Figure 41: Schematic representation of the oxidative bromination reaction catalyzed by $NH_4[VO_2(salhyhp)]$.

In a typical experiment using 10 mM TMB, 10 equivalents bromide, one aliquot hydrogen peroxide and 10 mol% catalyst in DMF solution acidified with perchloric acid, the possible formation of the carbon-bromide bond by a hypothetic bromination of the aliphatic hydroxyl group was verified. After three hours of reaction, at room temperature, the formed Br-TMB was extracted with ethyl acetate and the DMF solvent removed under strong vacuum by partial frozen. $^1$H NMR performed on the isolated catalyst using DMSO-$d_6$ as solvent showed a free *OH* group which resonated at 4.26 ppm. This is consistent with the results reported by Tanaka et al.[150] that such a bromination does not occur during the catalytic cycle.

In the following parts of this chapter the discussions will be focused on the vanadium(V) complexes derived from N-salicylidene 4-hydroxy-butanoic acid hydrazide due to the crystallographic characterization of the whole series of vanadium(V) complexes involved in the mechanism of the oxidative halogenation of an organic substrate; whereas all the other corresponding complexes with 5-hydroxy and 6-hydroxy-N-salicylidene hydrazides have been spectroscopically characterized and there are presented in the experimental part of this chapter.

## 3.1 *cis*-Dioxovanadium(V) complexes derived from N-salicylidene 4-hydroxy-butanoic acid hydrazide

The reaction of N-salicylidene 4-hydroxy-butanoic acid hydrazide with ammonium metavanadate in methanol, under reflux for about 24 hours results in the formation of the corresponding ammonium salt of the anionic *cis*-dioxovanadium(V) complex $NH_4[VO_2(salhyhb)]\cdot H_2O$ (**7**). Complex **7** is soluble in water and polar organic solvents such as DMSO and DMF. For prolonged reaction times the primarily formed ammonium salt was found to be converted to the corresponding neutral complex $[VO_2(Hsalhyhb)]$ (**8**) by release of ammonia. $[VO_2(Hsalhyhb)]$ (**8**) was isolated as yellow crystalline compound which is poorly soluble in organic solvents and insoluble in water. The neutral complex **8** can be de-protonated by reaction with neat ammonia resulting in formation back of the anionic complex,[151] as depicted below:

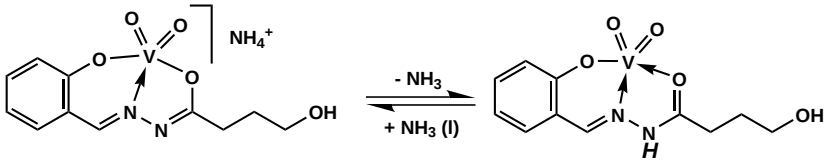


### 3.1.1 Structural characterization

The molecular structure of the anionic complex $NH_4[VO_2(salhyhb)]\cdot H_2O$ (**7**) has been reported by Pohlmann *et al.*[134,151,152] and is shown in Figure 42, while selected bond

lengths and angles are listed in Table 6. For the vanadium atom a distorted square pyramidal coordination is found with the equatorial plane formed by the ONO donor atoms of the Schiff base ligand together with one oxo group O2. The apical position at the vanadium atom is occupied by the other oxo group O1 with a V=O1 bond distance of 163 pm. This bond distance is only 2 pm longer than that of the anionic complex **1** described previously and within the reported range of vanadium to axial oxygen atom distances in *cis*-dioxovanadium(V) complexes.[103,153,154] The distortion to an ideal square pyramidal geometry is larger than in the similar anionic complex **1**, with a $\tau$ value of 0.12. This observation demonstrates the flexibility of the geometry at the vanadium center dictated by hydrogen bonding interactions. The molecular structure of the ammonium salt $NH_4[VO_2(salhyhb)]\cdot H_2O$ (**7**) shows high similarity with that observed for the corresponding $NH_4[VO_2(salhyp)]$ (**1**). The Schiff base ligand coordinates as dianionic tridentate system with deprotonated hydrazide nitrogen atom N2, hence is the partial double bond character of N2–C8 of around 131 pm. This is further in agreement with O4–C8 and V–O4 bond lengths of 130 and 196 pm, respectively. These values are consistent with the enolate form of the amide functionality and are in good agreement with the corresponding bond distances found for the pentanoic analog **1**.

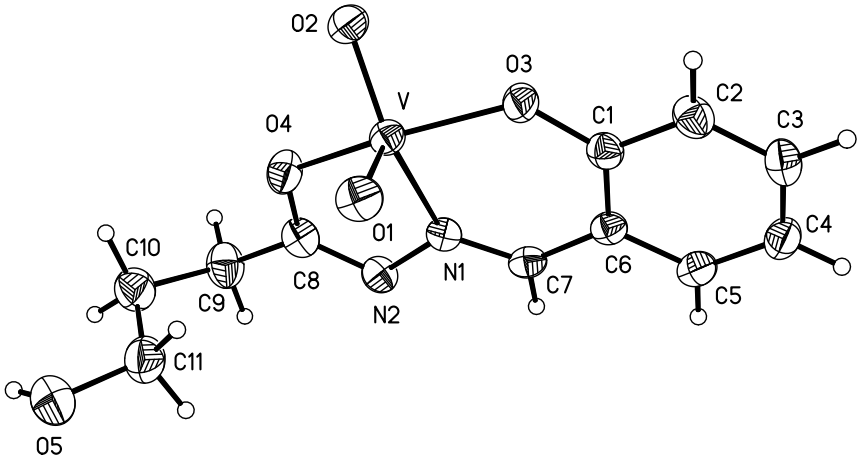


Figure 42: Molecular structure and numbering scheme for $NH_4[VO_2(salhyhb)]$ (**7**); displacement ellipsoids are drawn at the 50% probability level.

The complex crystalizes in the monoclinic space group $P2_1/c$ with a water molecule as solvent of crystallization. As observed for the ammonium salt of the pentanoic-derivative complex **1**, both oxo groups of the *cis*-dioxovanadium(V) moiety are parts of the hydrogen bonding network.

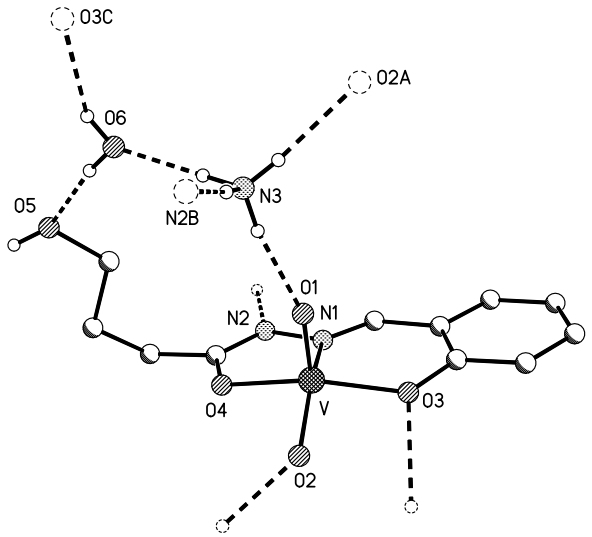


Figure 43: Hydrogen bonding interaction in crystals of complex **7** (broken lines represent hydrogen bonds); relevant distances (in pm): N3···O1 289.1, N3···O6 274.3, N3···O2A 281.4, N3···N2A 290.2, O5···O6 272.6 and O6···O3A 292.3 (symmetry operators: A: x-1, y, z; B: -x+1, -0.5+y, -1.5-z; C: x-1, 0.5-y, -0.5+z).

The important difference between the pentyl and the hydroxy butanoic derivative is, that, the network observed for $NH_4[VO_2(salhyhb)]\cdot H_2O$ contains an additional donor group, namely hydroxyl functionality which is in hydrogen bonding contact with the water molecule (O5···O6 272.6 pm). The water of crystallization establishes further an intramolecular hydrogen bonding interaction with the ammonium cation (O6···N3 274.3 pm) and the phenol oxygen atom (O6···O3C 292.3 pm) of a neighboring molecule. The ammonium cation completes this hydrogen bonding network by hydrogen bonding interactions with the apical oxo group O1 (N3···O1 289.1 pm), with each of the symmetrical equivalent oxo group O2 (N3···O2A 281.4 pm) and the hydrazide nitrogen atom N2 (N3···N2B 274.3 pm) of neighboring molecule.

Over prolonged reaction time, the stoichiometric reaction of N-salicylidene 4-hydroxy butanoic acid hydrazide with ammonium metavanadate to around three days, results in

the formation of the neutral *cis*-dioxovanadium(V) complex (**8**). Slow evaporation at room temperature of the mother liquor yielded yellow crystals, suitable for X-ray measurement.[151] Molecular structure and numbering scheme for $[VO_2(Hsalhyhb)]$ is shown in Figure 44 and presents a *cis*-dioxovanadium moiety with a five-coordinated vanadium atom. The two oxo groups are in *cis* position to each other, one in the apical position and the other forming the equatorial plane together with the phenolate and carbonyl oxygen atoms (O3 and O4), respectively, as well as the weakly coordinated imine nitrogen atom (N1) of the tridentate chelate ligand. The vanadium atom is displaced out from the plane, formed by the ligand, with 27 pm toward the apical oxygen atom O1, while the equatorial oxo group O2 is slightly distorted on the opposite side by 25 pm. This leads to a $\tau$ value of 0.14 consistent with a distorted square-pyramidal geometry around the vanadium atom. The distortion to an ideal-square pyramidal geometry of the vanadium atom in the neutral complex **8** is very similar with the distortion found in the anionic complex **7**. This indicates, that within similar hydrogen bonding network, the geometry is conserved. The vanadium to apical oxygen atom O1 bond distance of 161 pm is very similar with the corresponding bond length in complex **2**. Relevant bond distances and angles in complex **8** are listed in Table 6.

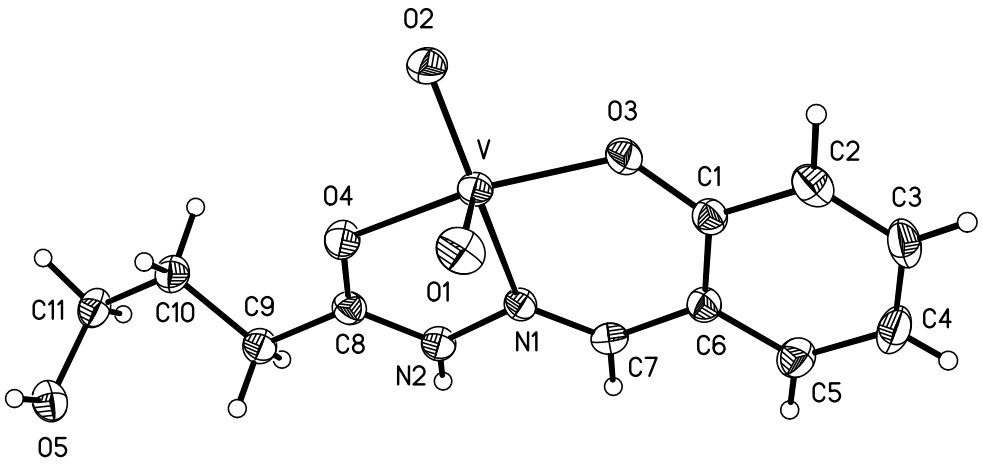


Figure 44: Molecular structure and numbering scheme for $[VO_2(Hsalhyhb)]$ (**8**); displacement ellipsoids are drawn at the 50% probability level.

The complex crystallizes in the monoclinic space group $P2_1/c$ with the N-salicylidene 4-hydroxy butanoic acid hydrazide containing the protonated hydrazide nitrogen atom N2H. This is in agreement with the shortening of the C8–O4 bond length to 126 pm and elongation of the V–O4 bond length to 203 pm compared to corresponding bond distances of the anionic complex **7**.

At first glance the molecular structure of complex **8** shows high similarity with the one determined for non-substituted 5-pentanoic chain [$VO_2$(Hsalhyp)] (**2**). This is particularly obvious as the hydrogen bonding interactions are concerned, since in both cases the same functional groups of the vanadium coordination environment are constituing parts; i.e. the equatorial oxo group O2 and the protonated hydrazide nitrogen atom N2. However, the additional hydroxyl group of the substituted side-chain present in [$VO_2$(Hsalhyhb)] also constitutes part of the hydrogen bonding network. This bridges the equatorial oxygen atom (O5···O2A 281.6 pm) and the protonated hydrazide nitrogen atom (O5···N2C 273.3 pm) of two neighboring molecules (Figure 45).

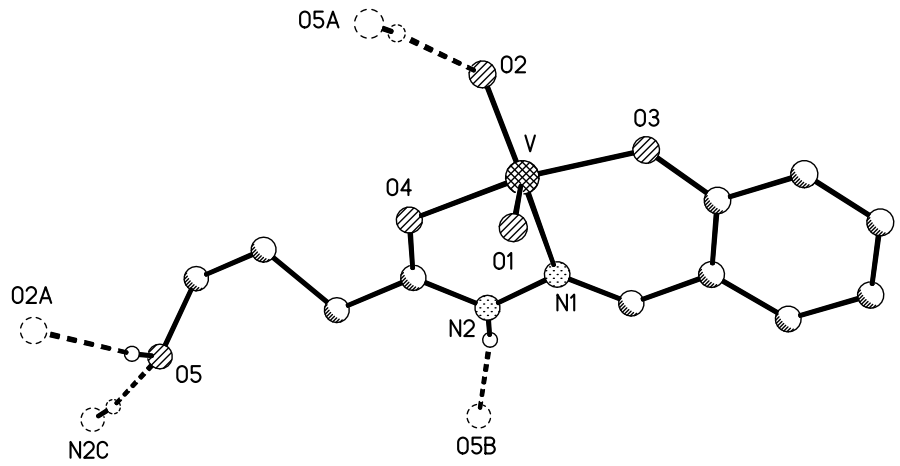


Figure 45: Hydrogen bonding interaction in complex [VO(HSahyb)] (**8**) (broken lines represent hydrogen bonds); relevant distances (in pm): O2···O5A 281.6 and N2···O5B 273.3 (symmetry aperators: A: -x, -y, -z; B: -x, 0.5+y, -0.5-z; C: -x, -0.5+y, -0.5-z).

Moreover, at first sight, the molecular structure of [$VO_2$(Hsalhyhb)](**8**) shows also high similarity with that observed for the corresponding anionic complex **7**. The overlay of the covalent parts of the two structures shown in Figure 46 confirms this but however it is also obvious, that there are significant differences regarding the orientation of the

alkylic side chain of the ligand system. The hydroxy-alkyl side chain deviates from the mean plane by an angle (C9–C10–C11–O5) of 62° in complex **8**, whereas in complex **7** the hydroxyl substituted side-chain is orientated on the opposite site with an angle value of 168°. This, clearly indicates, the importance of the hydrogen bonding interactions which can have an influence on the actual molecular structure.

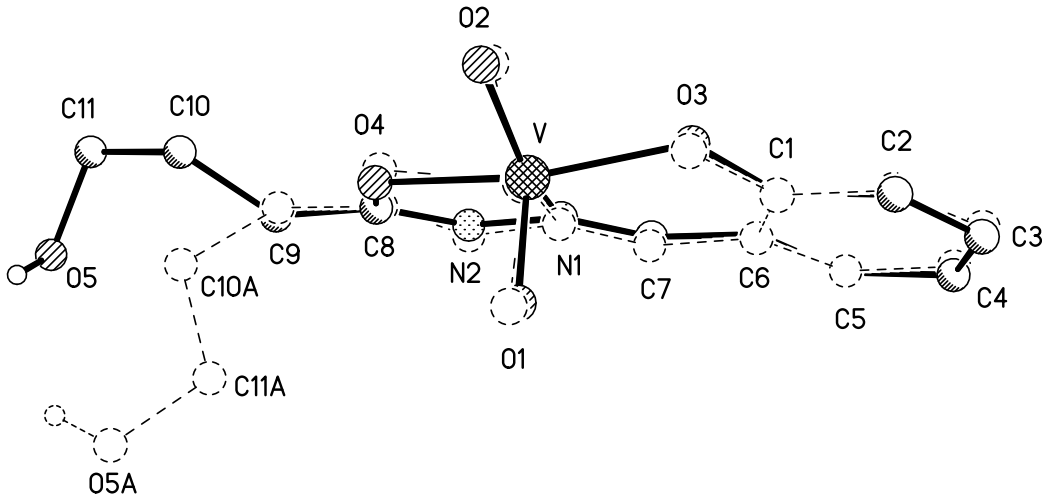


Figure 46: Overlay of the covalent backbone of the molecular structures of $[VO_2(Hsalhyhb)]$ **8** (thick lines) and $NH_4[VO_2(salhyhb)]$ **7** (broken lines).

Table 6. Selected bond lengths (pm) and angles (°) in complexes **7** and **8**.

| | **7** | **8** | | **7** | **8** |
|---|---|---|---|---|---|
| V−O1 | 163.22(16) | 161.41(15) | O1−V−O2 | 109.93(9) | 108.85(8) |
| V−O2 | 163.58(16) | 164.22(14) | O1−V−O3 | 104.14(8) | 103.97(7) |
| V−O3 | 189.12(15) | 189.92(14) | O1−V−O4 | 103.00(8) | 98.94(7) |
| V−O4 | 196.09(16) | 203.01(15) | O2−V−O3 | 94.07(7) | 98.00(7) |
| V−N1 | 213.25(18) | 216.39(17) | O2−V−O4 | 91.67(7) | 91.15(7) |
| C8−O4 | 130.6(3) | 126.4(2) | O3−V−O4 | 148.39(7) | 150.27(6) |
| C8−N2 | 130.7(3) | 132.2(3) | O1−V−N1 | 108.16(7) | 107.81(7) |
| O2−V−N1 | 141.43(8) | 141.97(7) | O3−V−N1 | 82.36(6) | 81.60(6) |
| O4−V−N1 | 73.99(6) | 73.45(6) | | | |

### 3.1.2 Spectroscopic data

The spectroscopic characterization of the complex is consistent with the proposed structures. The extension of the aliphatic side-chain to 5-hydroxy- and 6-hydroxy- derivatives made possible the isolation of anionic and neutral *cis*-dioxovanadium(V) complexes. The IR spectra contain strong stretching vibration in the region 885-927 $cm^{-1}$ for the anionic complexes and 892-910 $cm^{-1}$ for the neutral complexes. These stretching vibrations were assigned to the *cis*-$VO_2$ moiety and the vibrations are similar with reported values for $\nu(VO_2^+)$ group.[104,121,155] Similarly with *cis*-dioxovanadium(V) complexes described in Chapter 2, the Schiff base ligands coordination mode is identical. When neutral *cis*-dioxovanadium(V) complexes are formed, the $\nu$(NH) vibration is observed at 3217 $cm^{-1}$ as a broad band, together with the $\nu$(CO) vibration at 1627 $cm^{-1}$. These stretching modes are shifted compared to their vibrations at 3185 and 1669-1673 $cm^{-1}$ in the free ligands. However, these vibrations are absent in the IR spectra of the ammonium salt of *cis*-dioxovanadium(V) complexes due to the enolization of the amide functionality and, instead the 1613 cm $^{-1}$ band assigned as $\nu$(–CH=N–N=CH–) vibrates in the same region as was described in previous chapter. Further evidence of the coordination mode of the Schiff base ligands was obtained from the $^1$H and $^{13}$C NMR spectra, which are summarized in the experimental section. The resonances of O*H* and N*H* protons of the free ligands are absent in the $^1$H NMR of the anionic *cis*-dioxovanadium(V) complexes, indicating the enolization of the amide functionality upon complexation. Instead, a new resonance at 7.11 ppm, corresponding to $4H^+$, is observed, indicative of the formation of the ammonium salts of complexes. A significant downfield shift of *ca.* 0.4 ppm for the azomethine (–CH=N–) proton in the $^1$H NMR of anionic complexes, relative to the corresponding free ligand, supports the coordination of the azomethine nitrogen atom. A very good indication of the integrity of complexes in solution is represented by $^{51}$V NMR spectra. Both types of *cis*-dioxovanadium(V) complexes resonate at $\delta$ = -533 ppm region in DMSO-$d_6$ solution, being what one would expect for a dioxovanadium complex containing a rich O/N environment.[11] The $^{51}$V NMR data for the ammonium salt of the anionic *cis*-dioxovanadium(V) complex is somehow solvent dependent; for example an up-field shift of around 5 ppm has been observed in $D_2O$ solution ($\delta$ = -538 ppm)

compared to the resonance recorded in DMSO-$d_6$ solution. Unfortunately, the neutral complexes have a very poor solubility in organic solvents and their characterization in solution was limited.

### 3.1.3 Oxidative bromination of 1,3,5-trimethoxybenzene

Following the procedure outlined in Chapter 2, the ammonium salts of *cis*-dioxovanadium(V) complexes were tested for their capacity to catalyze the oxidative bromination of 1,3,5-trimetoxybenzene (TMB).

From the entries presented in Table 7, it is clear that the vanadium complex obtained with N-salicylidene 4-butanoic acid hydrazide $NH_4[VO_2(salhyhb)]$, is the most potent catalyst of this serie. The turnover rate of about 55 mol Br-TMB$\times$(mol catalyst$\times$h)$^{-1}$, is superior compared to that performed by ammonium salt of *cis*-dioxovanadium complex with non-substituted aliphatic side-chain $NH_4[VO_2(salhyb)]$ (Table 2, Chapter 2). This observation is in agreement with the observed influence of the hydrogen bonding interactions in the reactivity of the prosthetic group in V-HPO enzymes.

Table 7. Catalytic oxidation experiments using ammonium salts of *cis*-dioxovanadium(V) complexes as catalysts.

| Complex | 2 min. | 5 min. | 10 min. | 15 min. | TON |
|---|---|---|---|---|---|
| $NH_4[VO_2(salhyhb)]$ | 13.5(20.2) | 46.1(69.1) | - | - | 55 |
| $NH_4[VO_2(salhyhp)]$ | 9.5(14.2) | 28.0(42.0) | 54.3(81.4) | 70.3(105.4) | 34 |
| $NH_4[VO_2(salhyhh)]$ | 11.5(17.2) | 34.7(52.0) | 68.1(102.1) | 74.1(111.1) | 41 |

Note: The results are given in obtained % Br-TMB and as $\mu$mol Br-TMB within parenthesis. The turnover numbers were calculated taking into account the conversions obtained within 5 minutes.

### 3.1.4 Reactivity of the complexes towards HCl

The formation of an oxo-hxdroxy-vanadate moiety $[V^{V}O(OH)]^{2+}$ became a matter of considerable interest in the last period. The metal to hydroxy group bond is in general a common feature in metal-containing enzymes. M–OH units have been proposed as active species in iron and cobalt nitrile hydratases,[156] iron-containing lipoxygenases,[157,158] zinc and nickel hydrolytic enzymes,[159,160] acid phosphatases[161] and vanadium haloperoxidases.[6] Synthetic models that contain a $M^{II/III}$-OH bond were often reported, either as monomeric structure or as hydroxy-bridged complexes of type M–$(OH)_n$–M. The synthesis of such compounds requires either the presence of water or base as a source of hydroxyl ligand and complexes with $Co^{II/III}$–OH,[162,163] $Fe^{II/III}$–OH[50,164,165] and $Zn^{II}$–OH[166] moiety have been crystallographically characterized. In vanadium chemistry, only $V^{IV}$–OH units are known, both as monomer[167,168] as well as dimer complexes.[169,170] The formation of a vanadium to terminal hydroxyl group moiety has been reported in vanadium(IV) compounds based on pyrazolyl and bi-pyridine rings after hydrolysis of V–OCl or V–Cl bonds of the starting inorganic salts. Based on similarities between the vanadium and molybdenum chemistry, a $Mo^{V}$–$(OH)_n$–$Mo^{V}$ moiety has also been crystallographically identified.[171] Moreover, the reported crystal structure of V-ClPO contains a metal-to-terminal hydroxy unit. Various attempts to isolate or to identify the intermediates $[V^{V}O(OH)]^{2+}$ species have been reported.[104,155] The first reported vanadium(V) complex of this type was proposed in 1958[144,148] for the bis-(8-quinolinato)-oxo-hydroxy vanadium complex. The complex was generated *in situ* using first acetic acid as a source of hydroxyl ligand and, later by stoichiometric reaction of complexes of type **6** with hydrochloride acid.[145,146] Although later reports are known,[104,155,172] the molecular structure determination of such $[V^{V}O(OH)]$-containing compound has not been reported. Pecoraro *et al.* reported the spectrophotometric titration of a *cis*-dioxovanadium(V) (see also Figure 14, compound **1.1**) complex with HCl in acetonitrile solution suggesting the formation of a $[V^{V}O(OH)]^{2+}$ unit, based on the stoichiometry of the reaction.[102] The protonation reaction takes place preferentially at the *cis*-dioxovanadate center (Figure 47) and secondly, at the secondary amine which leads to an unstable compound. Addition of HCl as acetonitrile diluted solution to the dioxo-complex solution leads to red-shifts of

the absorption maxima, generating a red-colored material with an absorption maxima at 496 nm, whereas further addition of HCl generated a violet, very unstable compound.

In accordance with the structure of the starting *cis*-dioxovanadium(V) complex, it is plausible that the protonation occurs first at the vanadate center, whereas the protonation of the secondary amine will lead to an unstable complex due to the breakdown of the weak covalent bound V–N through involvement of the nitrogen pair electron in binding hydrogen.

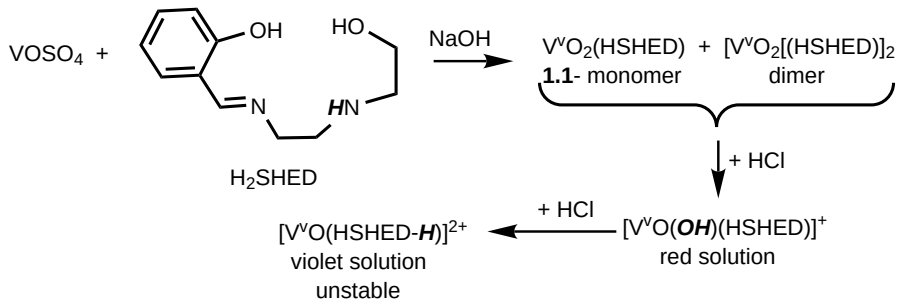


Figure 47: Schematic representation of the reactivity of complex (**1.1**) toward HCl in acetonitrile solution in accordance with reference 38.

In order to confirm or deny the formation of such $[V^{V}O(OH)]^{2+}$ moiety in vanadium model-complexes based on N-salicylidene hydrazide, investigation regarding the reactivity towards hydrochloric acid has been performed. The reaction of the anionic *cis*-dioxovanadium(V) $NH_4[VO_2(salhyhb)]$, with HCl in aqueous solution has been spectrophotometrically investigated. Spectrophotometric titration of an aqueous solution of complex **7** has been monitored by stepwise addition of 5 equivalents of HCl, 0.01 M standardized aqueous solution. The complex itself has a very good solubility in water with a high stability and exhibits three absorption maxima at: 214 ($\varepsilon$= $22.3\times10^3$ $M^{-1}cm^{-1}$), 281 ($\varepsilon$= $11.0\times10^3$ $M^{-1}cm^{-1}$) and 371 ($\varepsilon$= $3.2\times10^3$ $M^{-1}cm^{-1}$) nm, respectively. Stepwise addition of 0.25 equivalents HCl generates a constant decrease in absorbance of 371 nm band, accompanied by a slight split of the 281 nm band. The spectrum presents an isosbestic point at 294 nm, which can be interpreted as an equilibrium between the existing species in solution.

Most likely only one protonation step takes place, which occurs at the hydrazide

nitrogen atom: This hydrazide site is more basic compared to vanadate moiety and its protonation takes place preferentially. The reconversion of the initial spectrum can be achieved by back-titration with NaOH 0.01 M aqueous solution and it has been found that 6.5 equiv. of base were necessary to recover the initial UV-Vis spectra of the anionic complex. Theoretical interpretation of data set using a programme based on one developed by Zuberbühler (SPECFIT-32)[173,174] is in agreement with the proposed reaction.

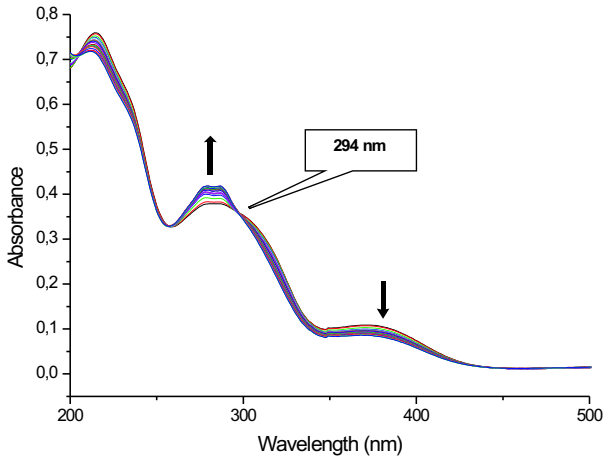


Figure 48. Spectrophotometric titration of $NH_4[VO_2(Salhyhb)]$ **7** (33.4$\mu$M) with 5 equivalents HCl 0.01 M in water. Successive addition of 0.25 equivalent of acid was performed at 18 °C with an equilibration time of 2 minutes within acid additions.

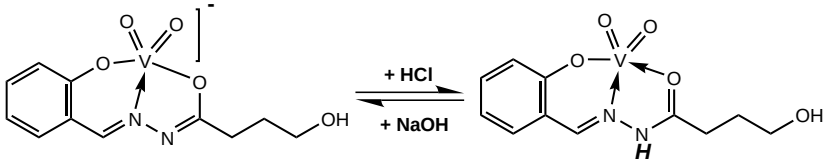


Figure 49. Proposed reactivity of $NH_4[VO_2(salhyhb)]$ with HCl in aqueous solution at 18 °C.

A reasonable fit of the measured data when 5 equivalents of acid have been used, was obtained by taking into account one protonation step, resulting in a value of 10 000

of the equilibrium constant which corresponds to a calculated $pK_b$ value of 10.0±0.2. The standard deviation was found to be around $1\times10^{-3}$ and it increases to around $1.5\times10^{-3}$ when an additional protonation reaction had been taken into account. Further confirmation of the proposed one step protonation reaction has been achieved by $^{51}V$ NMR monitoring of the reaction in $D_2O$. The *cis*-dioxovanadium complex exhibits one resonance at -538 ppm. This resonance remains unchanged when up to one equivalent of HCl 1M is added, whereas further increase of the amount of hydrochloric acid to 1.5 and 3 equivalents, generated an insoluble yellow material. This is indicative of the protonation of the hydrazide nitrogen atom upon neutral vanadium complex formation (Figure 49). The neutral complex is known as having a poor solubility in organic solvent and it is completely insoluble in water. Moreover, it should be mentioned that the resonance of the $^{51}V$ nuclei in *cis*-dioxovanadium(V) complexes based on N-salicylidene hydrazide, are independent of counter ions. Thus, the two *cis*-dioxospecies, anionic and neutral complexes, exhibit the same $^{51}V$ resonance. Therefore, it can be concluded that, in aqueous solution, the protonation reaction with HCl occurs at the hydrazide nitrogen atom, the most basic site comparing to the oxo groups of the vanadium center.

### 3.1.5 Reactivity of the complexes towards $H_2O_2$

Vanadium haloperoxidases are enzymes capable of catalyzing halide oxidation by hydrogen peroxide to hypohalous acid.[6] This oxidized halogen intermediate is able to halogenate various organic substrate,[68] or to react with a second equivalent of hydrogen peroxide to produce singlet oxygen.[73–75] Moreover, these enzymes can also catalyze the oxidation of organic sulfides to corresponding sulfoxides.[89,90,175] The mechanism of these catalytic reactions involves a peroxo-intermediate formation. Spectroscopic and kinetic studies on the native enzyme showed no change in the redox state of the prosthetic group during the catalytic cycle. Thus, the vanadate was proposed to function as a Lewis-acid catalyst, reacting firstly with hydrogen peroxide to form a side-on bonded peroxo moiety. This peroxide may be activated through hydrogen-bonding interactions with the first shell of amino acids and nearby water molecules.[78] An rearrangement of the geometry of the prosthetic group occurs during the turnover, varying from a trigonal bipyramidal

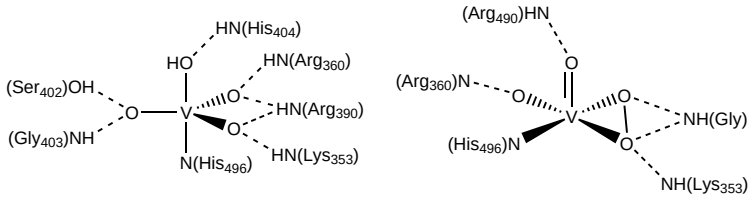


Figure 50: The active site in V-CPO: native form (left), peroxo form (right).

geometry in the native form to a tetragonal arrangement in its peroxo form.[78]

A vital role for the peroxide-intermediate activation has been attributed to lysine residue which is in hydrogen bonding contact with one of the peroxide-oxygen atom. It has been suggested that this hydrogen bonding interaction is responsible for an increased electrophilicity on the peroxide moiety, favoring therefore, the subsequent attack of the halide. Based on this aspect of the biological function of the vanadate in VHPO, the synthesis of structural models with relevant hydrogen bonding interaction has recently been reported[115,116] (Figure 17). Both vanadium(V) peroxo complexes are designed to model the corresponding intermediate of vanadium haloperoxidases. Nevertheless the knowledge about peroxo-vanadium(V) complexes capable to mimic the hydrogen bonding interaction found in the natural system is limited.

Renirie *et al.*[95] monitored spectrophotometrically the formation of the peroxo-form of vanadium chloroperoxidase enzyme. The native enzyme presents a near-UV absorption maxima which is pH dependent, varying from 315 nm at pH value of 8.3 (similar with UV-Vis spectra of V-BPO) to 305-310 nm at pH around 5. Spectrophotometric titration with $H_2O_2$ cause a decrease in intensity of this band accompanied by a red-shift of the absorption maxima at 389 nm, indicative of the addition of hydrogen peroxide at the vanadate moiety.

The anionic complex $NH_4[VO_2(salhyhb)]$ was also reacted with hydrogen peroxide in order to mimic the reactivity of the V-CPO enzyme. The reactivity of $NH_4[VO_2(salhyhb)]$ towards $H_2O_2$ has been studied using UV-Vis spectroscopy in different solvents medium. Spectrophotometric titration of complex **7** with $H_2O_2$ in aqueous solution was monitored by stepwise addition of the oxidant. The UV-Vis spectra showed a constant decrease of the 371 nm maxima of the *cis*-dioxovanadium complex with the added amount of hydrogen peroxide. A slight splitting of the 278 nm maxima into two new bands (278 and 287 nm) is also obvious (Figure 51). At this point similarity between the resulting spectra by titration with hydrogen peroxide and the characteristic UV-Vis absorption maxima of the free ligand becomes apparent.

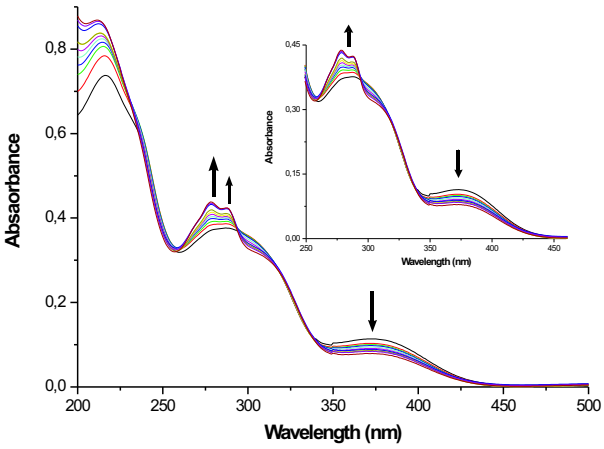


Figure 51: Spectrophotometric titration of $NH_4[VO_2(salhyhb)]$ with 10 equivalents $H_2O_2$ in water solution at 20 °C. The titration was performed by successive addition of 0.25 equivalents of $H_2O_2$ (25 mM) aqueous solution after every two minutes.

Further addition of hydrogen peroxide up to 20 equivalents yielded an increase of the new 278 ($\varepsilon$= 16.2×10$^3$ M$^{-1}$cm$^{-1}$), and 287 ($\varepsilon$= 15.6×10$^3$ M$^{-1}$cm$^{-1}$) nm bands, whereas the 315 nm shoulder also increased in intensity ($\varepsilon$= 8.6×10$^3$ M$^{-1}$cm$^{-1}$). This excess of hydrogen peroxide (20 equivalents) yielded an UV-Vis spectrum which exhibits the features of the free ligand (Figure 52), recorded as 50 $\mu$M aqueous solution. The Schiff base ligand ($H_2$salhyhb) exhibited three absorption maxima in water solution, detected at 215 ($\varepsilon$=

14.8×10$^3$ M$^{-1}$cm$^{-1}$), 278 ($\varepsilon$= 19.7×10$^3$ M$^{-1}$cm$^{-1}$), 287 ($\varepsilon$= 17.7×10$^3$ M$^{-1}$cm$^{-1}$) and 318 ($\varepsilon$= 8.8×10$^3$ M$^{-1}$cm$^{-1}$) nm, respectively. Therefore, the result of the spectrophotometric titration of complex **7** with 20 equivalents of hydrogen peroxide in water solution can be interpreted as a decomposition of the anionic *cis*-dioxovanadium(V) complex. This might be due to the presence of excess water which makes the azomethine bond very sensitive to hydrolysis.

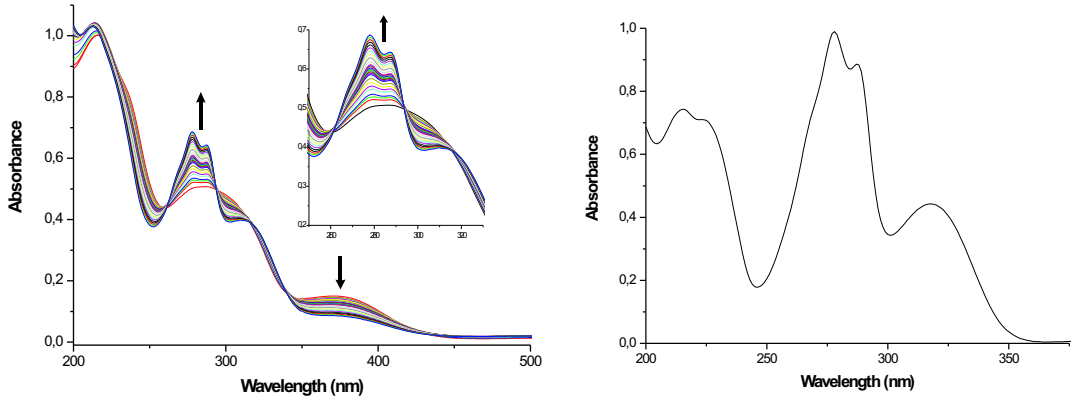


Figure 52: Spectrophotometric titration of $NH_4[VO_2(salhyhb)]$ with 20 equivalents $H_2O_2$ in water solution at 20 °C (left panel) and the UV-Vis spectrum of the free ligand ($H_2$salhyhb as 50 $\mu$M aqueous solution) (right panel).

Moreover, such an interpretation is sustained by $^{51}$V NMR monitoring of the reaction using $D_2O$ as solvent. The anionic complex resonate at -538 ppm. Addition of 2.5 equivalents of $H_2O_2$ generates a decrease in intensity of this resonance accompanied by the appearance of a new resonance at -691 ppm. The later resonance becomes predominant by increasing the amount of $H_2O_2$ to 5 equivalents. The further increase of the added amount of hydrogen peroxide cause a single resonance, the one at -691 ppm ($\nu_{1/2}$= 136 Hz), assigned to the inorganic oxo-di-peroxovanadium(V) $[VO(O_2)_2(H_2O)]_2^-$ (Figure 18).[118] This value of the $^{51}$V resonance coincide with the resonance reported by Conte *et al.* for inorganic $[VO(O_2)_2(H_2O)]_2^-$ in water solution.[176] These results are in agreement with the UV-Vis interpretation of the reaction and they showed the decomposition of the *cis*-dioxovanadium(V) complex in presence of excess of water.

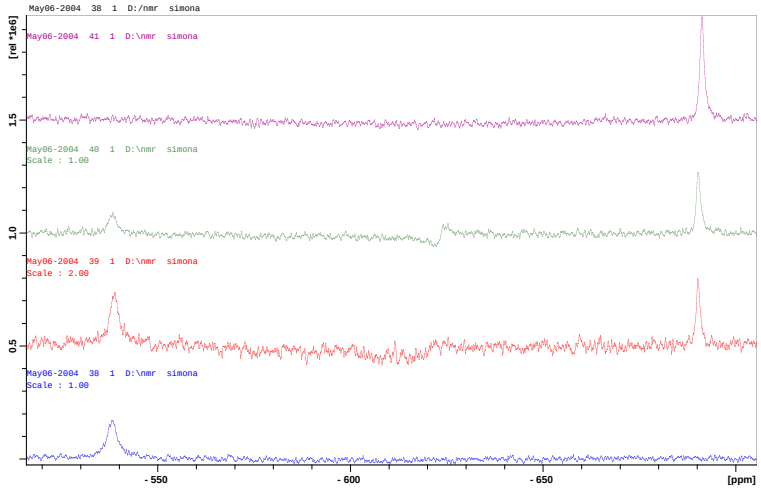


Figure 53: Titration of $NH_4[VO_2(salhyhb)]$ with $H_2O_2$ in $D_2O$ solution monitored by $^{51}V$ NMR; complex (blue spectra), complex + 2.5 equiv. $H_2O_2$ (red spectra), complex + 5.0 equiv. $H_2O_2$ (green spectra), complex + 10.0 equiv. $H_2O_2$ (violet spectra).

The spectrophotometric titration of complex **7** with $H_2O_2$ has also been performed in methanol solution. Stepwise addition of $H_2O_2$ causes a red-shift of the 384 nm band to 392 nm which increases in intensity with the increasing amount of added $H_2O_2$. The 278 nm broad band is increasing also in intensity accompanied by sharpening and splitting into two new bands. The 310 nm shoulder observed in the initial spectrum of the anionic *cis*-dioxovanadium(V) complex is also increasing in intensity during the titration with $H_2O_2$ (Figure 54). This behavior of the reaction differs to one described in water solution and it can be interpreted as the formation of a desired peroxo complex of type $[VO(O_2)salhyhb]^-$.

Taking into account that the vanadium-catalyzed bromide oxidation is performed in DMF solution, the UV-Vis monitoring of the reaction of $NH_4[VO_2(salhyhb)]$ (**7**) with $H_2O_2$ have also been performed in DMF solution. An increase in intensity of the 385 nm band has been observed accompanied by a very small red-shift(Figure 55), similarly with the spectrophotometric titration performed in methanol solution and is consistent with the formation of the peroxo complex $[VO(O_2)salhyhb]^-$.

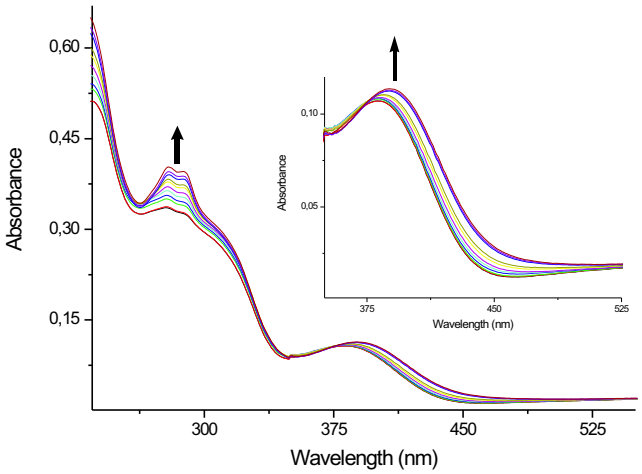


Figure 54: Spectrophotometric titration of $NH_4[VO_2(salhyhb)]$ with $H_2O_2$ (25 mM) in methanol solution at 20 °C. The titration shows the formation of the peroxovanadium complex with strong absorbance at 392 nm using the conditions quoted in Figure 51.

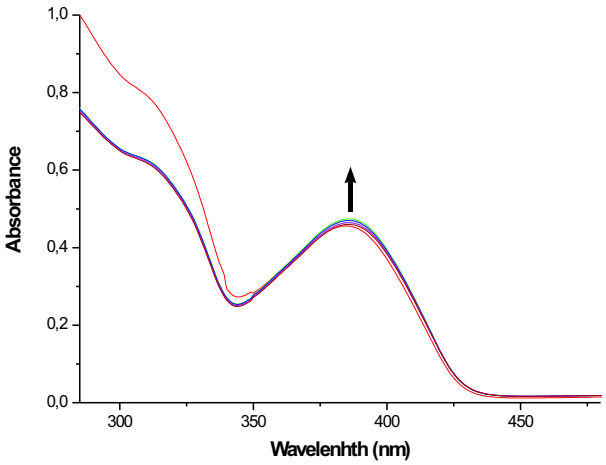


Figure 55: Spectrophotometric titration of $NH_4[VO_2(salhyhb)]$ with $H_2O_2$ in DMF solution at 20 °C. The titration shows the formation of the peroxovanadium vanadium complex through addition of 0.5 equivalents of hydrogen peroxide up to 2 equivalents, followed by at once addition of other two equivalents.

It can be concluded that the reactivity of the *cis*-dioxovanadium(V) complex towards $H_2O_2$ is strongly dependent on the solvent and this dependence can be caused especially by the imine-bond presence which is hydrolytically unstable.

Based on the results from the spectrophotometric titrations, the reaction of the $NH_4[VO_2(salhyhb)]$ with $H_2O_2$ was performed also in large amounts using ethanol-water 4:1 mixture at 0° C. This reaction of the ammonium salt of *cis*-dioxovanadium(V) complex with 2 equivalents of hydrogen peroxide yielded the neutral oxo-monoperoxovanadium complex $[VO(O_2)(Hsalhyhb)H_2O]\cdot H_2O$ (**9**) upon release of ammonia due to the water presence. The complex crystalizes as orange-red crystals from cold solution overnight and it is unstable in solution for a prolonged time hydrolyzing to the corresponding neutral *cis*-dioxo complex. The oxo-peroxovanadium complex **9** has also been obtained by *in situ* reaction of potassium vanadate, hydrogen peroxide and N-salicylidene 4-hydroxy butanoic acid hydrazides in methanol-water solution at 0 °C, in presence of perchloric acid. Due to the acidic reaction conditions in the latter case, the tridentate Schiff base ligand was expected to coordinate in its monoanionic form via protonation of the hydrazide nitrogen atom N2.

Complex **9** is soluble in various organic solvents like alcohols, acetonitrile and DMF without decomposition. The $^{51}V$ NMR spectrum recorded in $CD_3OD$ reveals a single resonance in the typical range, i.e. at -551 ppm ($\Delta\nu_{1/2}$=105 Hz), whereas in DMSO-$d_6$ a fast decomposition takes place immediately after dissolution of the complex, indicated by the detection of two resonance peaks in the $^{51}V$ NMR spectrum. The peak at -539 ppm ($\Delta\nu_{1/2}$=860 Hz) is attributed to the corresponding *cis*-dioxocomplex and the second peak at -572 ppm ($\Delta\nu_{1/2}$=1100 Hz) is attributed to the corresponding dimeric *cis*-dioxocomplex, respectively. The intensity ratio for the two resonance peaks observed in deuterated DMSO is approximately 10:1. The molecular structure of complex **9** determined by X-ray crystallography reveals a pentagonal-bipyramidal geometry for the coordination around the vanadium atom as depicted in Figure 56. The ligand coordinates in its monoanionic form, providing an ONO donor set. In the equatorial plane, the vanadium atom is coordinated by the side-on bonded peroxo group with O2 and O3 as well as the donor atoms O4, N1 and O5 of the tridentate hydrazide ligand. The axial positions of the coordination polyhedra are occupied by oxo group O1 and by the oxygen

atom O7 of the coordinated water molecule. The structural parameters given in Table 8 are consistent with those observed for the vanadium(V) complex with hydrazide ligand and and in good agreement with those reported for vanadium(V) oxo-peroxo complexes, which generally feature a coordination at the vanadium atom with the oxo group in axial position and an equatorial side-on bonded peroxide.[111,115,116,177]

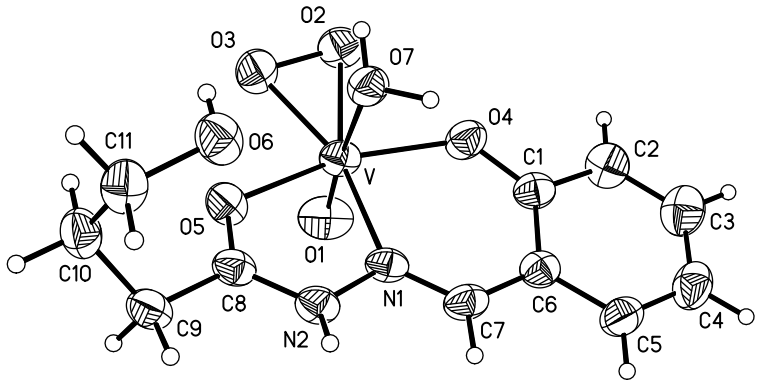


Figure 56: Molecular structure of **9**; displacement ellipsoids are drawn at the 50% probability level.

Complex **9** crystallizes with one water molecule (O8) leading to an extensive hydrogen bonding network in the solid state as depicted in Figure 57. The first sphere of hydrogen bonding interactions given in Figure 57 is solely located below the planar ligand arrangement in a *trans* orientation with respect to the oxo group O1. Consequently the oxo group O1 and the carbonyl group O5 of the hydrazide ligand are not involved in the hydrogen bonding network, which is in agreement with their relatively low donor ability. Both enantiomers present in the crystal structure of **9**·$H_2O$ form a hydrogen bonded chain via the interaction between the protonated hydrazide nitrogen atom N2 and the peroxo group of a neighboring complex with the same enantiomeric symmetry (N2···O2A 280, N2···O3A 305 pm). These two enantiomeric chains set up a bilayer which incorporates the hydrogen bonding network shown in Figure 58 and in turn leads to an one-dimensional hydrogen bonded chain along the [010] direction (Figure 58).

A situation reminescent of the role of the active site lysine residue in VHPO[78] is found by the hydrogen bonding interaction between the peroxo ligand (O2 and O3) and the acidic N–H group of the hydrazide ligand (N2).

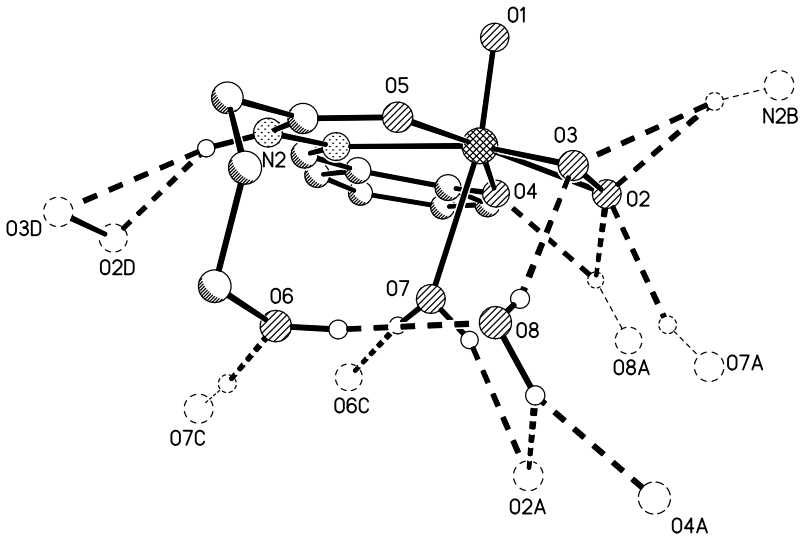


Figure 57: Hydrogen bonding network for complex $\mathbf{9}\times H_2O$. Only hydrogen atoms bonded to non-carbon atoms are shown, broken lines represent hydrogen bonds, dashed circles and lines represent symmetry equivalent atoms and bonds between them, respectively (symmetry operators A: 1-x, -y, -z; B: x, y-1, z; C: 1-x, 1-y, -z; D: x, 1+y, z). Selected hydrogen bond distances (pm): N2···O2D 280.2, N2···O3D 305.2, O6···O8 286.0, O7···O2A 282.7, O7···O6C 271.1, O8···O2A 306.0, O8···O3 299.8, O8···O4A 295.8.

A second type of hydrogen bonding pathway related to the peroxo group originates from the hydroxy side chain (O6) of the Schiff base ligand system. This side-chain is involved in hydrogen-bonding cascade that includes the water oxygen atom O8 (O6···O8 286 pm); this leads to an intramolecular interaction with the oxygen atom O3 of the peroxo group (O8···O3 299 pm), and an intermolecular interaction with the peroxo oxygen atom O2 (O8···O2A 306 pm) of a neighboring complex. The later of these hydrogen bonds is part of a bifurcated interaction between O8 towards O2 (Figure 57). The hydrogen-bond network is completed by the coordinated water molecule, O7, which forms intermolecular contacts with the hydroxy side chain oxygen atom O6 (O6C···O7 271 pm) and with the peroxo oxygen atom O2 (O7···O2A 283 pm) from two different neighboring molecules of opposite enantiomeric chains. The observed hydrogen bonding interaction are of specific interest due to the presence of the Ser402 in the active site of vanadium haloperoxidases, in particular, they are of possible relevance for proton transfer reactions.

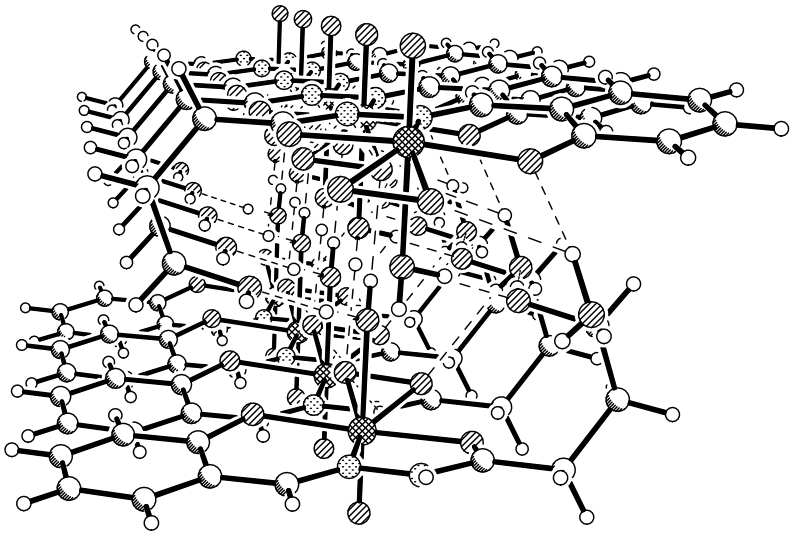

Figure 58: Representation of the hydrogen-bonded bilayer for neutral oxo-peroxo-complex **9**, as viewed approximately along the [010] direction.

The structure of the mono-peroxovanadium(V) complex was also confirmed by IR spectroscopy. Comparison between the IR patterns of the $NH_4[VO_2(salhyhb)]$ with IR spectrum of $[VO(O_2)(Hsalhyhb)]$ showed different stretching vibration of the vanadate moiety. While the $\nu(VO_2^+)$ vibrates at 909 $cm^{-1}$, the V=O group of the peroxo-complex **9** present stretching vibration at 978 $cm^{-1}$ and the region is completed by the stretching vibration corresponding to $\nu(O–O_{peroxo})$ at 921 $cm^{-1}$ as well as the asym. and sym. vibration corresponding to $\nu(V(O)_2)$ group at 765 and 562 $cm^{-1}$, respectively. Solution investigations on anionic oxo-monoperoxovanadium complex has also been performed using NMR technique as well as UV-Vis spectrophotometry. The $^{51}V$ NMR performed in DMSO-$d_6$ solution is indicative of the instability of the complex in solution for a prolonged period of time. At room temperature, independent of solvent, the orange-red solution of the peroxovanadium complex **9** becomes yellow colored from which neutral cis-dioxovanadium(V) complex is separating in a matter of hours. The UV-Vis spectra of complex **9** in DMF and MeOH solution presents absorbtion maxima at 392 nm due to the peroxo-to-metal charge transfer and 278, 288 and 319 nm. The later three absorption maxima closely resembles the maxima of the free ligand. This UV-Vis spectra is in agreement with the obtained results of the spectrophotometric reaction of the corresponding ammonium salt of the *cis*-dioxovanadium(V) with $H_2O_2$, confirming the interpretation of the results.

Table 8. Selected bond lengths (pm) and angles (°) for complex **9**.

| | | | |
|---|---|---|---|
| V−O1 | 157.8(3) | V−O7 | 225.8(3) |
| V−O2 | 189.1(3) | V−N1 | 213.2(3) |
| V−O3 | 187.6(3) | O2−O3 | 142.9(4) |
| V−O4 | 197.6(3) | C8−O4 | 125.7(4) |
| V−O5 | 207.6(3) | C8−N2 | 132.3(5) |
| O1−V−O2 | 103.48(13) | O2−V−O3 | 44.57(12) |
| O1−V−O3 | 101.94(14) | O2−V−O4 | 79.39(12) |
| O1−V−O4 | 97.52(15) | O2−V−O5 | 119.93(12) |
| O1−V−O5 | 94.26(14) | O2−V−O7 | 86.31(12) |
| O1−V−O7 | 170.08(13) | O2−V−N1 | 155.91(12) |
| O1−V−N1 | 94.13(13) | O3−V−O4 | 123.41(13) |
| O4−V−O5 | 154.21(12) | O3−V−O5 | 75.86(12) |
| O4−V−O7 | 82.58(11) | O3−V−O7 | 86.08(12) |
| O4−V−N1 | 82.17(12) | O3−V−N1 | 146.81(13) |
| O5−V−O7 | 81.95(11) | O5−V−N1 | 74.14(12) |
| O7−V−N1 | 76.01(11) | | |

## 3.2 Reactivity of the oxo-monoperoxovandium(V) complex

Renirie et all.[95] determined spectrophotometrically the stability and reactivity of the peroxo intermediate of vanadium chloroperoxidases. The peroxo form is very stable at a pH value of 8 and persists for a long period of time, whereas it is less stable at a pH value of 5 (the activity optimum for the native enzyme). However in both conditions the peroxo form of the enzyme is capable to oxidize $Cl^-$ ions to hypochloric acid under a pseudo-first order reaction. To probe the ability of the peroxo complex towards haloperoxidase activity, the formation of an oxidized bromide species was tested. This was monitored by the

formation of bromo derivate Br-TMB. The peroxo complex-[VO($O_2$)HSalhyhb)$H_2O$]·$H_2O$ reacts with one equivalent of TMB in presence of an excess of tetra-n-butylammonium bromide and one equivalent of perchloric acid to yield 2-bromo-1,3,5-trimetoxybenzene. About 90% of TMB was converted in the corresponding brominated compound in less than 30 minutes as monitored by HPLC. In the absence of acid, as well as without the complex no brominated products could be observed. This could lead to the conclusion that the oxidation of bromide by hydrogen peroxide involves the formation of an oxo-monoperoxovanadium complex as intermediate. Due to the requirement of stoichiometric amounts of acid in the equimolecular reaction between peroxo-complex **9** and organic substrate (here TMB) is most likely that an activation via protonation of the peroxide moiety is necessary.

For the vanadium haloperoxidases catalyzed sulfide oxidation reaction the mechanism is also proposed to proceed through a peroxo intermediate. To probe the sulfoxidation reactivity of this peroxo-vanadium(V) complex, an equimolecular reaction with phenyl-methyl-sulfide have been performed in a dichloromethane-methanol mixture. The methyl phenyl sulfoxide was oxidized very slowly leading to about 75% conversion in about 48 hours. It is interesting to note, that this is about the same time usually observed for catalytic turnover in model systems with only 1 mol-% of the vanadium catalyst present. The oxidative capacity of the peroxo complex was further tested by investigating its reaction with triphenylphosphane in acetonitrile solution. $^{31}$P NMR spectroscopy monitoring of the reaction showed the phosphane oxide readily formed together with the corresponding *cis*-dioxovanadium(V) complex, implying that full conversion of the reactants had occurred.

## 3.3 Mono-oxovanadium(V) complexes based on N-salicylidene hydrazides that contain an hydroxyl-substituted aliphatic side-chain

Mono-oxovanadium(V) complexes based on hydroxyl-substituted N-salicylidene carbonic acid hydrazide can be synthesized starting from the corresponding neutral *cis*-dioxovana-

dium(V) complexes in reaction with equimolecular amount of 8-hydroxyquinoline in refluxing methanol solution. The second method consists of *in situ* stoichiometric reaction of the Schiff base ligands, vanadyl acetyacetonate in refluxing methanol and/or acetonitrile, followed by stepwise addition of 8-hydroxyquinoline. The equimolecular reaction of $VO(acac)_2$ with N-salicylidene hydroxyl-substituted aliphatic acid hydrazide proceed by aerial oxidation of the vanadium(IV) precursor to yield a brown colored solution. Further on, addition of 8-hydroxyquinoline cause a violet colored solution. Variation of the aliphatic chain length of the Schiff base ligand afforded three oxovanadium(V) complexes which have a very good solubility in polar solvents (alcohols, DMF and DMSO), halogenated solvents (chloroform and dichlormethane) and acetonitrile, behaving very similar with the corresponding mono-oxovanadium(V) complexes described in Chapter 2.

### 3.3.1 Structural characterization

Using N-salicylidene hydrazide ligand derived from 4-hydroxy butanoic acid hydrazide and following the reactions outlined above, the corresponding oxovanadium(V) [VO(Q)(salhyhb)] (**10**) complex could be isolated as microcrystalline compound by recrystallization from a methanol/acetonitrile 1:1 mixture. The complex crystallize in the triclinic space group $P\bar{1}$ with two very similar molecules per unit cell. The other two oxovanadium(V) complexes derived from 8-hydroxyquinoline and N-salicylidene of 5-hydroxy-pentanoic [VO(Q)(salhyhp)] (**11**), and 6-hydroxy hexanoic acid hydrazides [VO(Q)(salhyhh)] (**12**), respectively have been spectroscopically characterized and presented in the experimental part of the chapter. The molecular structure of complex **10** determined by X-ray crystallography features two structurally very similar but crystallographically distinct oxovanadium(V) moieties in an oxygen and nitrogen rich environment as depicted in Figure 59. The vanadium atom is six-coordinated in a distorted octahedral geometry. The dianionic N-salicylidenehydrazide acts as tridentate chelate system coordinating through ONO donor atoms that form a basal plane together with the oxine oxygen O21 and O41, respectively of the bidentate 8-hydroxyquinoline ligand. Relative to this plane, the vanadium atom V1 is displaced toward the terminal oxygen atom O11 by 31.5 pm, while the other vanadium atom V3 is distorted towards the oxygen atom

O31 by 30 pm. *Trans* to the terminal oxo groups O11 and O31 are located the nitrogen atom N21 and N41, respectively, of the 8-hydroxyquinoline ligand with the bond length of around 235 pm, very similar with the corresponding bond lengths found in the previously described mono-oxovanadium complexes. These bond lengths are around 27.5 pm longer than the vanadium to imine nitrogen atom of the Schiff base ligand (N11 and N31) bond distances, due to the *trans* position of the quinoline nitrogen atom to the terminal double bonded oxygen atom. The V=O (oxo) bond length of around 159 pm is very similar with the corresponding bond distance found in the oxovanadium(V) complexes with non-substituted aliphatic side-chain.

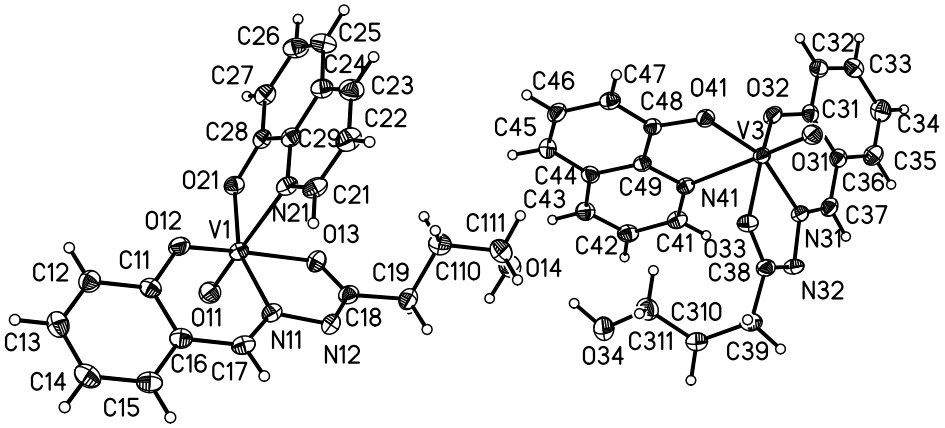


Figure 59: Molecular structure of the two crystallographically distinct [VO(Q)(salhyhb)] (**10**) molecules; displacement ellipsoids are drawn at the 50% probability level.

The Schiff base ligand forms a six- and a five-membered chelate ring with bite angles of 83.8° (O12–V1–N11, O32–V3–N31) and around 75° (O13–V1–N11 and O33–V3–N31), respectively, consistent with observed distortion of the vanadium geometry. Selected bond lengths and angles for complex **10** are given in Table 9. The coordination mode of the N-salicylidene hydrazide ligand is very similar with that described in vanadium complexes which contain the enolized form of the amide functionality with the C–O bond lengths of around 131 pm and V–O3 distance of 195 pm.

The difference to the mono-oxovanadium(V) complexes described in Chapter 2, is the presence of a medium-to strong hydrogen bonding network observed in solid state in complex **10**. The two crystallographically distinct oxovanadium(V) moieties are in hydrogen bonding contact via hydroxyl groups of the side-chain substituted N-salicylidene hydrazide ligands of 286.0 pm (O14···O31A). Moreover, the terminal oxo group O31 of the enantiomeric molecule is in hydrogen bonding interaction with hydroxy oxygen atoms from neighboring molecules (O31···O14A) as depicted in Figure 60.

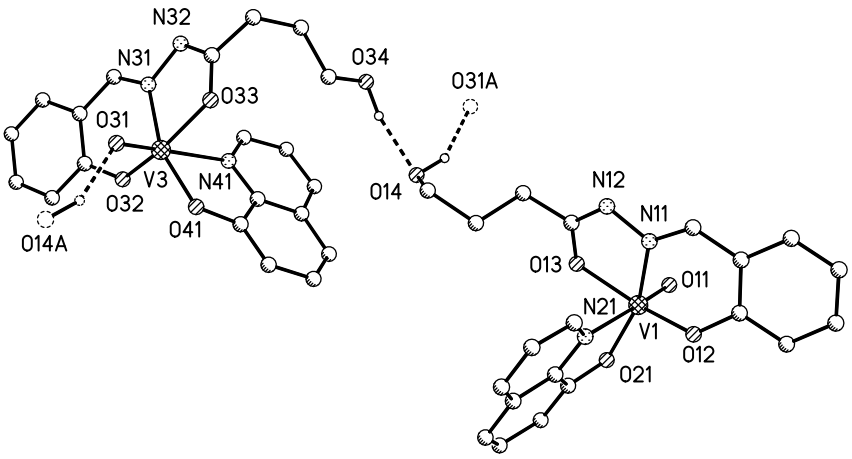


Figure 60: Representation of the hydrogen bonding interaction of complex **10** (broken lines represent hydrogen bonds); relevant hydrogen bond distances (pm): O31···O14A 286.0, O14···O31A 287.5 (symmetry operators A: x-1, y, z).

The hydrogen bonding interaction observed leads to the formation of a two-dimensional network along the crystallographic (010) plane as depicted in Figure 61. The orientation of the oxygen atoms involved in hydrogen bonding results in formation of a polymeric chain, while the non hydrogen bonded oxo groups are located on outside.

Complex **10** is one of the rare example of oxovanadium(V) complex which contains a hydrogen bonded terminal oxo moiety. Similar interaction was found in the natural enzyme where the apical hydroxyl group of the vanadate center is in hydrogen bonding interaction with an nitrogen atom of an imidazole ring of a His404 residue.[6]

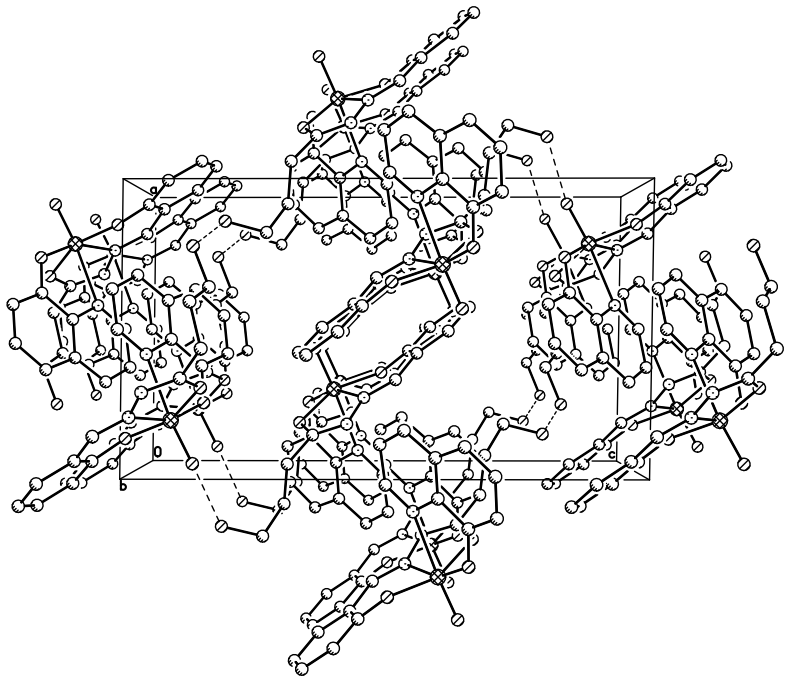

Figure 61: Representation of the hydrogen bonding network in crystals of complex **10** as viewed along the [010] direction; broken lines represent hydrogen bonding interactions.

### 3.3.2 Spectroscopic studies

The IR spectra of the complexes are consistent with the proposed formation of the oxo-vanadium(V) complexes and presents a strong vibration at 969-972 assigned to $\nu$(VO) stretching vibrations. The enolized form of the Schiff base ligand is consistent with the vibration of the conjugated -CH=N–N=C- system observed at 1604 cm$^{-1}$. In general the IR patterns of these mono-oxovanadium(V) complexes are very similar with the IR patterns of the mono-oxovanadium(V) complexes described in Chapter 2. The difference is the appearance of a broad band at 3443 cm$^{-1}$ assigned to $\nu$(OH aliphatic) vibration involved in intermolecular hydrogen bonding interaction. The $^{1}$H and $^{13}$C NMR data for all complexes are summarized in the experimental section and are consistent with the formation of the proposed mono-oxovanadium(V) complexes. The coordination of the

Table 9. Selected bond lengths (pm) and angles (°) for complex **10**.

| | | | |
|---|---|---|---|
| V1–O11 | 159.38(15) | V3–O31 | 159.79(14) |
| V1–O12 | 186.09(14) | V1–O32 | 185.04(14) |
| V1–O13 | 195.77(14) | V1–O33 | 195.09(14) |
| V1–O21 | 184.28(14) | V1–O41 | 184.97(14) |
| V1–N11 | 207.89(17) | V1–N31 | 207.91(17) |
| V1–N21 | 235.44(17) | V1–N41 | 235.35(16) |
| O13–C18 | 130.8(2) | O33–C38 | 131.3(2) |
| N12–C18 | 130.3(3) | N32–C38 | 130.1(3) |
| O11–V1–O12 | 98.88(7) | O31–V3–O32 | 99.59(7) |
| O11–V1–O13 | 99.02(7) | O31–V3–O33 | 97.04(7) |
| O11–V1–O21 | 101.26(7) | O31–V3–O41 | 99.21(7) |
| O12–V1–O13 | 153.98(6) | O32–V3–O33 | 155.27(6) |
| O12–V1–O21 | 103.33(6) | O32–V3–O41 | 101.34(6) |
| O13–V1–O21 | 91.50(6) | O33–V3–O41 | 93.89(6) |
| O11–V1–N11 | 98.05(7) | O31–V3–N31 | 99.95(7) |
| O11–V1–N21 | 176.51(7) | O31–V3–N41 | 173.81(7) |
| O12–V1–N11 | 83.83(6) | O32–V3–N31 | 83.79(6) |
| O12–V1–N21 | 84.26(6) | O32–V3–N41 | 85.47(6) |
| O13–V1–N11 | 75.09(6) | O33–V3–N31 | 75.37(6) |
| O13–V1–N21 | 78.51(6) | O33–V3–N41 | 79.33(6) |
| O21–V1–N11 | 158.01(6) | O41–V3–N31 | 159.03(6) |
| O21–V1–N21 | 76.46(6) | O41–V3–N41 | 76.18(6) |
| N11–V1–N21 | 83.73(6) | N31–V3–N41 | 84.05(6) |

8-hydroxyquinoline ligand, used here as a coligand is in agreement with observed resonances corresponding to its aromatic protons. $^{51}$V NMR measurements present a single resonances at -472 ppm ($\Delta\nu_{1/2}$ = 350 Hz) in DMSO-$d_6$ solutions and -482 ppm ($\Delta\nu_{1/2}$ = 145 Hz) in deuterated chloroform solutions being similar with previously described $VO^{3+}$ complexes with $N_2O_4$ environment. A similar reactivity towards NaOH in solution have

been found (see Chapter 2). $^{51}$V NMR monitoring of the reaction shows two vanadium species which resonate at -472 ppm ($\Delta\nu_{1/2}$ = 350 Hz) and -535 ppm ($\Delta\nu_{1/2}$ = 600 Hz) when 0.5 equivalents of base were used. These two resonances were attributed to the oxo-vanadium(V) complex and *cis*-dioxovanadium(V),[135] respectively. Further increase of the amount of base to one equivalent, generated only the cis-dioxovanadium complex which resonates at -536 ppm ($\Delta\nu_{1/2}$ = 600 Hz). No further change of the resonance shift was observed when up to two equivalents of base were used. The reaction with NaOH, when *cis*-dioxovanadium(V) complexes are generated, is very similar with corresponding one described in Chapter 2, proving the similarities in reactivity of the mono-oxovanadium(V) species.

### 3.3.3 Electrochemical investigations

The mono-oxovanadium(V) complexes were also electrochemically investigated by cyclic voltmametry experiments in acetonitrile solutions using Ag/AgCl as reference electrode. All three complexes presented here showed the same electrochemical behavior and very similar with previous described in Chapter 2, in particular the potential of the charge transfer processes. The square wave voltammogram (SWV) measured with a drop hanging mercury electrode were obtained using 0.25 M $Bu_4NCl$ as electrolyte and square wave frequencies of 25, 50, 100, 200, 400, 800 and 1500 Hz, respectively. The potential values for the three mono-oxovanadium(V) complexes are tabulated in Table 10 and the cyclic voltametry experiment for complex **12** is shown in Figure 62.

Table 10. Potential values (in V) for cyclic voltametry measurements

| | $1^{st}$ reduction | $2^{nd}$ reduction |
|---|---|---|
| complex **10** | + 0.403 | - 1.575 |
| complex **11** | + 0.393 | - 1.582 |
| complex **12** | + 0.388 | - 1.580 |

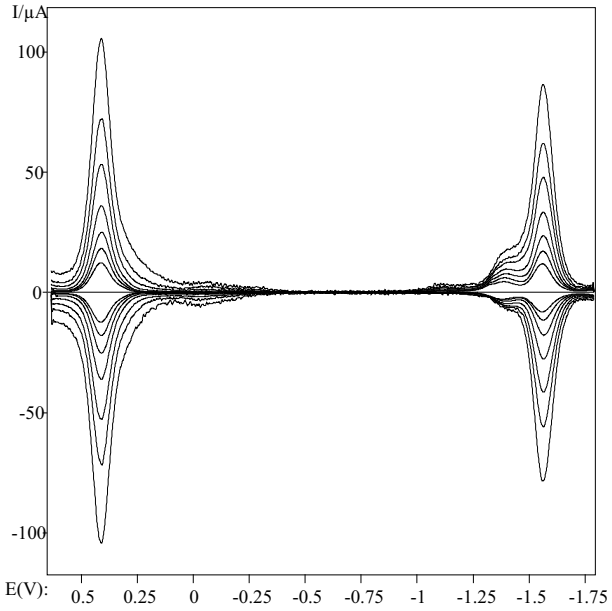


Figure 62: Square wave voltammogram of complex **2** using square wave frequencies of 25, 50, 100, 200, 400, 800 and 1500 Hz.

The first electron reduction step ($ML + e^- \rightleftharpoons ML^-$) occurs at higher positive potential ($E^\circ = 0.393$ V) in comparison with 0.355 V reported previously, while the second reduction step occurs at negative potential of $E^\circ$ = - 1.582 V and is also accompanied by a pre-wave ($ML^- + e^- \rightleftharpoons ML^{2-}$). As depicted in Figure 62, the two reduction processes take place preferentially with the first reduction step occurring with higher current values. This differs from previous square wave voltammograms of oxovanadium complexes based on non-substituted aliphatic side-chain, where the two reduction processes occurred with equal current rates.

Nevertheless, the frequency dependence of the two reduction peaks and of the accompanying pre-wave also shows a linear behavior versus time indicating that the second reduction process remains diffusion controlled over the entire frequency range. As can be seen from Figure 63, the accompanying pre-wave tends to become equal to the diffusion controlled current when the square wave frequency moves towards zero, while a steady state current seems to be reached for very high square wave frequencies. This is a similar situation with previously described cyclic voltammetry experiment, suggesting analogue electrochemical behavior in the given conditions.

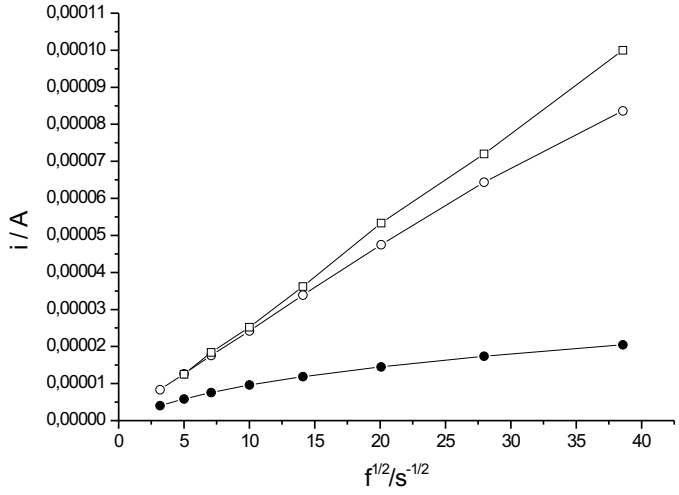


Figure 63: Height of the peak current at positive potential (white rhombus), at negative potential (white circles) and the plateau of the accompanying pre-wave (black circles) associated with the second reduction processes in complex **12**

The pre-wave which accompanies the second reduction process can be an effect of a chemical reaction involving the 8-hydroxyquinoline anion, which also shows a reversible reduction process at -1.52 V. Therefore a split off/addition reaction of this coligand in the mono-oxovanadium complexes might be responsible for the appearance of the pre-wave. The reaction can be expressed as:

$$ML^- \rightleftharpoons M + L^-$$

where $L^-$ is the reduced 8-hydroxyquinoline ligand as a radical anion. The equilibrium of this reaction is slightly pushed to the right side, only because infinitesimal amount of $L^-$ is immediately re-oxidized to L if the potential is moving between the first reduction step and the pre-wave.

However, since the production of the species $L^-$ consumed in the pre-wave goes at the consuming of $ML^-$ which is coupled with $L^-$ following the last equilibrium, the above finding is not in agreement with the observation that the reduction of $ML^-$ at about -1.58 V remains fully diffusion-controlled over the entire frequency range. This disagreement is also supported by the shift of the pre-wave to more positive potentials by increasing the time window of the underlying electrochemical method (i.e. the lower the square

wave frequency), because the opposite shift would be theoretically expected. Reasonable agreement with the experimental data was obtained when an additional ligand addition/elimination reaction was taking into consideration for the mono-oxovanadium(V) complex:

$$ML \rightleftharpoons M + L$$

where L is the deprotonated quinoline anion.

The equilibrium for this last reaction is far moved towards the left. Although L reacts with M, so that the resulting ML is immediately reduced again, the difference in the equilibrium/rate constants of the last two reactions (as well as the differences of the diffusion coefficients of the underlying species) results in an accumulation of effects. This means that the second reduction step is accompanied by a pre-wave exhibiting an unusual frequency dependence of the potential shift and an almost diffusion-controlled growth of the peak current associated with the charge transfer process.

At this point, it can be concluded that the quasi-reversible cyclic voltammograms showed two one-electron reduction steps. The first one consists of the formation of a vanadium(IV) complex and occurs at positive potential, while the second reduction process takes place at negative potential and is accompanied by a pre-wave. The pre-wave seems to be most likely generated by the reduction of the splitted off coligand.

## 3.4 Conclusions

Vanadium(V) complexes with N-salicylidenehydrazide ligands that contain hydroxyl substituted aliphatic side chain represent a functionalized side-chain model complexes for vanadium haloperoxidase. The structural model complexes obtained with these Schiff base ligands are based on both mono-oxo- and *cis*-dioxo-vanadium(V) complexes. Reactivity of the ammonium salts of *cis*-dioxovanadium(V) complexes towards HCl in aqueous solution showed a single protonation step which occurs at the more basic hydrazide nitrogen atom, resulting in the formation of the corresponding neutral *cis*-dioxovanadate complex. Furthermore, investigations regarding the mechanism of vanadium-catalyzed bromide oxidation reaction by hydrogen peroxide proved the formation of a peroxo-intermediate when the reaction is performed in nonaqueous solutions. Reactivity of a

neutral oxo-monoperoxovanadium(V) towards its capacity to function as active intermediate of the *cis*-dioxovanadium-catalyzed oxidation reaction showed the necessity of a stoichiometric amount of acid for proceeding the reaction, manifesting a similar behavior with the one described for the natural system.

The neutral *cis*-dioxovanadium(V) complexes can react with 8-hydroxyquinoline to form the mono-oxovanadium complexes. In both oxo- and dioxo- vanadium complexes relevant hydrogen bonding interaction for the enzymatic system have been observed. The mono-oxovanadium(V) complex represents the first example of an oxo-vanadium compound with hydrogen bonded apical oxo-group. Moreover, the inter-conversion of the oxovanadium(V) complexes in the corresponding *cis*-dioxovanadium complexes have also been shown to be possible. Monitoring of the reaction by $^{51}$V NMR showed that one equivalent of NaOH yield the splitting off of the coligand, resulting in re-formation of the *cis*-dioxovanadium complex.

## 3.5 Experimental Part

Abbreviations used throughout the text: $H_2$salhyhb = 4-hydroxy butyric acid (2-hydroxy benzylidene) hydrazide, $H_2$salhyhp = 5-hydroxy pentanoic acid (2-hydroxy benzylidene)-hydrazide, $H_2$salhyhh = 6-hydroxy hexanoic acid (2-hydroxy benzylidene) hydrazide, HQ = 8-hydroxyquinoline, TMB = 1,3,5-trimethoxybenzene, Br-TMB = 2-bromo 1,3,5-trimethoxybenzene.

### 3.5.1 Synthesis of $\omega$-hydroxy aliphatic acid hydrazide

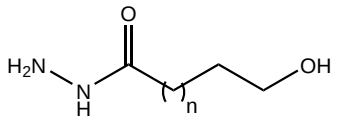


Hydrazide hydrate (2 equiv.) was added to 25 g lactone and the resulting solution was refluxed under continuous stirring for about 4 hours. The solution was cooled down

at room temperature when a colorless precipitate was formed. The resulting precipitate was filtered and recrystallized from absolute ethanol.

**Synthesis of 4-hydroxy butanoic acid hydrazide**

This compound was prepared from $\gamma$-butyrolactone (0.29 mol) and hydrazine hydrate (29.0 g 0.6 mol) following the general method described above. Yield: 26.8 g (0.2 mol, 76%).

**Synthesis of 5-hydroxy pentanoic acid hydrazide**

This hydrazide was synthesized from $\delta$-valerolactone (0.25 mol) and hydrazine hydrate (25.0 g 0.5 mol) following the general method described above. Yield: 21.3 g (0.15 mol, 64%).

**Synthesis of 6-hydroxy hexanoic acid hydrazide**

$\epsilon$-Caprolactone (0.22 mol) and hydrazine hydrate (22.00 g 0.44 mol) were reacted following the general method described above. Yield: 27.04 g (0.18 mol, 82%).

### 3.5.2 Synthesis of N-salicylidene $\omega$-hydroxyl aliphatic hydrazides

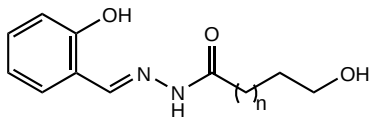


**Synthesis of N-salicylidene 4-hydroxy butanoic acid hydrazide (n=1) $H_2$salhyhb**

To a solution of 4-hydroxy-butanoic acid hydrazine (7.8 g, 66.0 mmol) in 50 mL methanol, salicylaldehyde (8.10 g, 14.3 mL, 66.0 mol) was added dropwise under continuous stirring at room temperature. The resulting slightly yellow solution was stirred at r.t. for an additional 12 hours. The formed precipitate was filtered and the solvent removed under reduced pressure. Yield: 10.3 g (59.1 mmol, 69%). $^1$H NMR (200 MHz, DMSO-$d_6$): $\delta$ =

1.71 (q, 2H, C$H_2$, $^3$J=7.3 Hz), 2.26 and 2.60 (t, 2H, C$H_2$CO, $^3$J=7.5 Hz, ratio 1.3:0.7), 3.46-3.48 (m, 2H, C$H_2$OH), 4.50-4.54 (m, 1H, O$H$), 6.84-6.91 (m, 2H, arom. C$H$), 7.21-7.26 (m, 1H, arom. C$H$), 7.44-7.66 (m, 1H, arom. C$H$), 8.24 and 8.32 (s, 1H, C$H$=N, ratio 0.4:0.6), 10.12, 11.18, 11.59 (N$H$, O$H$, total 2H in ratio 0.3:1.0:0.6) ppm. $^{13}$C NMR (50 MHz, DMSO-d$_6$): $\delta$ = 27.5, 28.2 (all $C$H$_2$), 28.7, 30.6 (both $C$H$_2$CO), 60.0, 60.2 (both $C$H$_2$OH), 116.1, 116.3, 118.6, 119.2, 119.4, 120.0, 126.8, 129.5, 130.8, 131.1 (all arom.$C$H and $C$), 140.8, 146.4 (both $C$H=N), 156.3, 157.3, 168.5 (all arom.$C$), 173.9 ($C$=O). Selected IR data (cm$^{-1}$): $\nu$= 3185 (s; NH, OH$_{ass}$), 1673 (s, C=O), 1623 (s, CH=N).

**Synthesis of N-salicylidene 5-hydroxy pentanoic acid hydrazide (n=2) H$_2$salhyhp**

The N-salicylidene-5-hydroxy-pentanoic acid hydrazide (H$_2$salhyhp) ligand has been synthesized by Schiff base condensation of salicylaldehyde (17.6 g, 1.44 mol) with 5-hydroxy-pentanoic acid hydrazide (19.1 g, 1.44 mol) in 100 mL methanol. Yield: 30.7 g (1.3 mol, 90%). $^1$H NMR (200 MHz, DMSO-d$_6$): $\delta$ = 1.32-1.62 (m, 4H, C$H_2$), 2.17 and 2.53 (t, 2H, C$H_2$CO, $^3$J=7.3 Hz, ratio 1.4:0.6), 3.33-3.44 (m, 2H, C$H_2$OH), 4.37-4.40 (m, 1H, O$H$), 6.78-6.87 (m, 2H, arom. C$H$), 7.13-7.26 (m, 1H, arom. C$H$), 7.41-7.57 (m, 1H, arom. C$H$), 8.24 and 8.33 (s, 1H, C$H$=N, ratio 0.4:0.6), 10.11, 11.14, 11.53 (N$H$, O$H$, total 2H in a ratio 0.3:1.0:0.7) ppm. $^{13}$C NMR (50 MHz, DMSO-d$_6$): $\delta$ = 20.8, 21.6, 31.8 ($C$H$_2$), 32.0, 32.1 (both $C$H$_2$CO), 60.4, 60.5 (both $C$H$_2$OH), 116.1, 116.3, 118.6, 119.3, 119.4, 120.0, 126.8, 129.4, 130.9, 131.1 (arom.$C$H and $C$), 140.8, 146.4 ($C$H=N), 156.3, 157.3, 168.5 (arom.$C$), 173.9 ($C$=O). Selected IR data (cm$^{-1}$): $\nu$= 3185 (s; NH, OH$_{ass}$), 1673 (s, C=O), 1623 (s, CH=N). UV/Vis (CH$_3$CN solution, $\lambda_{max}$ in nm ($\varepsilon$ in 10$^3$ M$^{-1}$ cm$^{-1}$)): 278 (16.4), 288 (14.9), 319 (7.7).

**Synthesis of N-salicylidene 6-hydroxy hexanoic acid hydrazide (n=3) H$_2$salhyhh**

The H$_2$salhyhh ligand has been synthesized from salicylaldehyde (15.6 mL, 1.5 mol) and 6-hydroxy-pentanoic acid hydrazide (21.6 g, 1.5 mol) in 100 mL methanol. Yield: 30.0 g (1.20 mol, 80%). $^1$H NMR (200 MHz, DMSO-d$_6$): $\delta$ = 1.23-1.65 (m, 6H, C$H_2$), 2.21 and 2.55 (t, 2H, C$H_2$CO, $^3$J=7.3 Hz, ratio 1.4:0.7), 1.32-3.42 (m, 2H, C$H_2$OH), 4.36 (br, 1H, O$H$), 6.81-6.91 (m, 2H, arom. C$H$), 7.16-7.30 (m, 1H, arom. C$H$), 7.44-7.60 (m, 1H,

arom. C*H*), 8.24 and 8.32 (s, 1H, C*H*=N, ratio 0.3:0.7), 10.15, 11.18, 11.57 (N*H*, O*H*, total 2H in ratio 0.3:1.0:0.7) ppm. $^{13}$C NMR (50 MHz, DMSO-$d_6$): $\delta$ = 24.1, 24.9, 25.2, 25.4 (all $CH_2$), 32.3, 34.0 (both $CH_2CO$), 60.6 ($CH_2OH$), 116.1, 116.3, 118.6, 119.2, 119.5, 120.0, 126.8, 129.5, 130.8, 131.1 (arom.*C*H and *C*), 140.9, 146.5 (*C*H=N), 156.4, 157.3, 168.5 (arom.*C*), 173.9 (*C*=O). Selected IR data ($cm^{-1}$): $\nu$= 3185 (s; NH, $OH_{ass}$), 1673 (s, C=O), 1623 (s, CH=N).

### 3.5.3 Synthesis of ammonium salts of *cis*-dioxovanadium(V) complexes

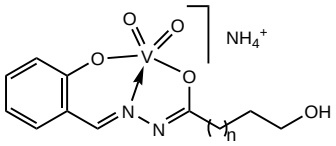


To a solution of 2 g of Schiff base ligand in 50 mL methanol, ammonium metavanadate in stoichiometric amount was added. The resulting mixture was refluxed for one day with vigourous stirring, when the color of the solution turned brown. After filtration of the unreacted inorganic salt, the solution volume was reduced under reduced pressure to about half. From this mother liquor, yellow product precipitated by slow evaporation of the solvent at room temperature. Additional material can be obtained by removal of the solution volume to dryness when a brown-yellowish residue is formed. This residue can be purified by extraction with chloroform.

**$NH_4$[$VO_2$(salhyhb)]**(**7**); Yield: 1.72 g (5.3 mmol, 59%). $^1$H NMR (200 MHz, DMSO-$d_6$): $\delta$ = 1.70-1.73 (m, 2H, C$H_2$), 2.32 (t, 2H, C$H_2$CO), 3.33 (br, $H_2$O), 3.38-3.42 (m, 2H, C$H_2$OH), 4.36 (br, 1H, O*H*), 6.73-6.88 (m, 2H, arom. C*H*), 7.08 (br, 4H, arom. N$H_4^+$), 7.30-7.61 (m, 2H, arom. C*H*), 8.74 (s, 1H, C*H*=N) ppm. $^{13}$C NMR (50 MHz, DMSO-$d_6$): $\delta$ = 28.5 ($CH_2CO$), 29.4 ($CH_2CH_2OH$), 60.5 ($CH_2OH$), 116.6, 119.4, 120.1, 132.3, 132.8 (all arom.*C*H and *C*), 154.1 (*C*=N), 164.2 (arom.*C*O–V), 176.3 (*C*O–V) ppm. $^{51}$V NMR (105 MHz, DMSO-$d_6$): -534.4 ppm ($\nu_{1/2}$ = 575 Hz). $^{51}$V NMR (105 MHz, $D_2O$):

-538.1 ($\nu_{1/2}$ = 575 Hz). Selected IR data ($cm^{-1}$): $\nu$= 3400 (br, $NH_4^+$, $H_2O$), 1613 (s, -CH=N-N=CH-), 909 (s, $VO_2$). MS (ESI-negative mode in MeOH): 303.1 ($M^-$-$NH_4^+$-$H^+$) (100%), 590(10%), 629.0 ($2M^-$-$NH_4^+$-$H^+$+Na) (10%). UV/Vis ($CH_3OH$ solution, $\lambda_{max}$ in nm ($\varepsilon$ in $10^3$ $M^{-1}$ $cm^{-1}$)): 235 (13.7), 278 (9.2), 288 (8.3), 310 (shoulder), 384 (2.5). UV/Vis (DMF solution, $\lambda_{max}$ in nm ($\varepsilon$ in $10^3$ $M^{-1}$ $cm^{-1}$)): 308 (9.7), 389 (6.2).

**$NH_4$[$VO_2$(salhyhp)]**; Yield: 1.88 g (5.6 mmol, 62%). *Anal.* Calc. for $C_{12}H_{19}N_3O_5V$ (336.24): C 42.87, H 5.70, N 12.50. Found: C 42.85, H 5.41, N 12.51. $^1$H NMR (200 MHz, DMSO-$d_6$): $\delta$ = 1.41-1.63 (m, 4H, C$H_2$), 2.24 (t, 2H, C$H_2$CO, $^3$J=7.1 Hz), 3.36-3.41 (m, 2H, C$H_2$OH), 4.40 (br, 1H, O$H$), 6.70-6.77 (m, 2H, arom. C$H$), 7.13 (br, 4H, arom. N$H_4^+$), 7.25-7.49 (m, 2H, arom. C$H$), 8.74 (s, 1H, C$H$=N) ppm. $^{13}$C NMR (50 MHz, DMSO-$d_6$): $\delta$ = 22.7 ($CH_2$), 31.7 ($CH_2$C=O), 32.3 ($CH_2CH_2$OH), 60.5 ($CH_2$OH), 116.7, 119.4, 119.8, 132.3, 132.7 (all arom.$C$H and $C$), 154.2 ($C$H=N), 164.3 (arom.$C$O–V), 176.4 ($C$O–V) ppm. $^{51}$V NMR (105 MHz, DMSO-$d_6$): -533.3 ($\nu_{1/2}$=600 Hz) ppm; $^{51}$V NMR (105 MHz, $D_2O$): -537.5 ($\nu_{1/2}$ = 638 Hz). Selected IR data ($cm^{-1}$): $\nu$= 3400 (br, $NH_4^+$), 1614 (br, -CH=N-N=CH-), 927 and 887 (s, $VO_2$). MS (ESI-negative mode in MeOH): 317 ($M^-$-$NH_4^+$-$H^+$) (100%), 657 ($2M^-$-$NH_4^+$-$H^+$+Na) (10%).

**$NH_4$[$VO_2$(salhyhh)]**; Yield: 0.42 g (1.2 mmol, 13%). $^{51}$V NMR (105 MHz, DMSO-$d_6$): -533.4 ($\nu_{1/2}$=615 Hz) ppm. Selected IR data ($cm^{-1}$): $\nu$= 3434 (br, $NH_4^+$), 1612 (s, -CH=N-N=CH-), 895 and 908 (s, $VO_2$).

### 3.5.4 Synthesis of neutral *cis*-dioxovanadium(V) complexes

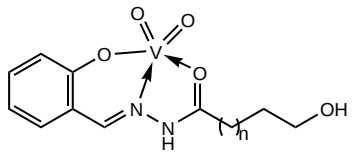


The synthesis and and purification of the neutral *cis*-dioxoxvanadium(V) complexes follows the same procedure described above with the difference of the reaction time which

was prolonged for about three days.

**[$VO_2$(Hsalhyhb)]**(**8**); Yield: 1.2 g (3.9 mmol, 43%). $^{51}$V NMR (105 MHz, DMSO-$d_6$): -533.3 ($\nu_{1/2}$=600 Hz) ppm. Selected IR data (KBr): $\nu$ = 3435 (br, NH), 1628 (s, CO), 1612 (s, br; HC=N), 910 ($VO_2$), 892 (s, $VO_2$).

**[$VO_2$(Hsalhyhh)]**; Yield: 0.80 g (2.4 mmol, 27%). *Anal.* Calc. for $C_{13}H_{17}N_2O_4V$ (333.22): C 47.00, H 5.16, N 8.43. Found: C 46.83, H 4.88, N 8.30. $^{51}$V NMR (105 MHz, DMSO-$d_6$): -534.2 ($\nu_{1/2}$=645 Hz). Selected IR data ($cm^{-1}$): $\nu$= 3435 (br, NH, OH), 1627 (s, CO), 1610 (s, -CH=N), 892 (s, $VO_2$). MS (ESI-negative mode): m/z = 331 ($M^-$) (100%), 685 ($2M^-$+Na)(20%).

### 3.5.5 Synthesis of neutral oxo-monoperoxovanadium(V) complexes

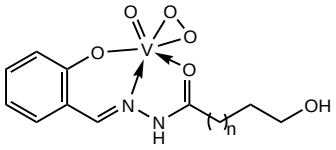


To an aqueous solution of $KVO_3$ (0.69 g, 5 mmol) in 20 mL water and $H_2O_2$ (0.75 mL 30% aqueous solution), the Schiff base ligand (5 mmol) dissolved in 25 mL methanol was added dropwise at 0° C under constant stirring. The pH of the resulting orange-red solution was adjusted to about pH∼2 with $HClO_4$ 0.1M solution. The solution was stirred on ice-bath for an additional 30 minutes while an orange solid precipitate. This was filtered off and washed with cold methanol. The filtrate solution was kept at 5° C in a closed vessel for about one week when additional solid is formed.

**[$VO(O_2)$(Hsalhyhb)$H_2O$]·$H_2O$**(**9**); Yield: 1.38 g (3.9 mmol, 77%) general method and 0.9 g (2.5 mmol, 33%) second method. Anal. Calc. for $C_{11}H_{17}N_2O_8V$ (**9**·$H_2O$) (356.21):

C 37.09, H 4.81, N 7.86; Found C 37.73, H 4.71, N 8.09. $^{1}$H NMR (400 MHz, $CD_3OD$): $\delta$ = 1.96 (tt, 2H, C$H_2$, $^{3}$J=6.8 Hz), 2.52 (t, 2H, C$H_2$CO, $^{3}$J=7.6), 3.67 (t, 2H, C$H_2$OH, $^{3}$J=6.4), 4.83 (s, $H_2$O), 6.91-7.01 (m, 2H, arom. C$H$), 7.49-7.58 (m, 2H, arom. C$H$), 8.56 (s, 1H, C$H$=N) ppm. $^{13}$C NMR (50 MHz, $CD_3OH$): $\delta$ = 29.0 ($C$H$_2$CO), 30.5 ($C$H$_2$CH$_2$OH), 62.4 ($C$H$_2$OH), 117.7, 121.4, 121.5, 133.4, 133.7 (all arom.$C$H and $C$), 153.2 ($C$=N), 165.1 (arom.$C$O–V), 179.7 ($C$=O) ppm. $^{51}$V NMR (105 MHz, $CD_3OD$): -551.4 ppm ($\nu_{1/2}$ = 105 Hz). Selected IR data (cm$^{-1}$): $\nu$= 3400 (br, NH, $H_2O$), 978 (s, V=O), 921 (s, O–O, peroxo), 765 (asym. $V(O)_2$), 562 (sym. $V(O)_2$). MS (ESI-negative mode in MeOH): m/z = 318.9 ($M^-$-$H^+$-$H_2$)(100%).

**[VO(O$_2$)(Hsalhyhp)]**; Yield: 0.87 g (2.6 mmol, 52%). Anal. Calc. for $C_{12}H_{15}N_2O_6V$ (334.22): C 43.13, H 4.52, N 8.38; Found C 43.47, H 4.77, N 8.51. $^{1}$H NMR (200 MHz, $CD_3OD$): $\delta$ = 1.65-1.85 (m, 4H, C$H_2$) 2.46 (t, 2H, C$H_2$CO, $^{3}$J=7.2), 3.60 (t, 2H, C$H_2$OH, $^{3}$J=6.4), 6.89-7.01 (m, 2H, arom. C$H$), 7.44-7.58 (m, 2H, arom. C$H$), 8.55 (s, 1H, C$H$=N) ppm. $^{13}$C NMR (50 MHz, $CD_3OH$): $\delta$ = 23.9 ($C$H$_2$), 32.0 ($C$H$_2$CO), 33.2 ($C$H$_2$), 62.5 ($C$H$_2$OH), 117.7, 121.3, 121.4, 133.6, 135.3 (all arom.$C$H and $C$), 153.2 ($C$=N), 166.9 (arom.$C$O–V), 179.9 ($C$=O) ppm. $^{51}$V NMR (105 MHz, $CD_3OD$): -550.7 ppm ($\nu_{1/2}$ = 105 Hz). Selected IR data (cm$^{-1}$): $\nu$= 3400 (br, NH, OH), 978 (s, V=O), 921 (s, O–O, peroxo), 765 (asym. $V(O)_2$), 562 (sym. $V(O)_2$). MS (ESI-negative mode in MeOH): 318.9 ($M^-$-$H^+$-$H_2$)(100%).

**[VO(O$_2$)(Hsalhyhh)]·2H$_2$O**; Yield: 0.42 g (1.2 mmol, 24%). Anal. Calc. for $C_{13}H_{21}N_2O_8V$ (complex·$H_2O$) (384.26): C 40.06, H 5.50, N 7.29; Found C 39.89, H 5.41, N 7.08. $^{51}$V NMR (105 MHz, $CD_3OD$): -551.4 ppm ($\nu_{1/2}$ = 110 Hz). Selected IR data (cm$^{-1}$): $\nu$= 3400 (br, NH, $H_2O$, OH), 978 (s, V=O), 921 (s, O–O, peroxo), 765 (asym. $V(O)_2$), 562 (sym. $V(O)_2$).

**Alternative method for synthesis of $[VO(O_2)(Hsalhyhb)H_2O]\cdot H_2O$(9)**

To a solution of $NH_4[VO_2(salhyhb)]$ (**7**) (2.4 g, 7.5 mmol) in 25 mL mixture ethanol:water 4:1, hydrogen peroxide (1.5 ml 30%, 15 mmol) was added dropwise at 0°C under continuous stirring. The resulting clear, orange colored solution was stirred for additional 15 minutes. 5 mL cold ethanol were added additionally to the reaction mixture and the solution was kept in the refrigerator where overnight orange crystals were formed. Yield: 0.90 g (2.5 mmol, 33%). Anal. Calc. for $C_{11}H_{17}N_2O_8V$ (**9**·$H_2O$) (356.20): C 37.09, H 4.81, N 7.86; Found C 37.82, H 4.82, N 8.03. $^{51}V$ NMR (105 MHz, $CD_3OD$): -551.4 ppm ($\nu_{1/2}$ = 125 Hz).

### 3.5.6 Reactivity of the oxo-monoperoxovanadium(V) complex

**Bromide oxidation**

The oxidative bromination of 1,3,5-trimethoxybenzene (25 mg, 0.15 mmol) with complex **9** (54 mg, 0.15 mmol) in the presence of 10-fold excess of tetrabutylammonium bromide (0.483 g, 1.5 mmol) and one equivalent perchloric acid, was performed in DMF (30 mL). The brominated derivative (Br-TMB) was monitored by HPLC measurement using a Sperisorb ODS-2 column and a mixture $H_2O$:MeOH (50:50 v/v) as eluent.

**Sulfuroxidation reaction**

A solution of complex **9** (19 mg, 0.05 mmol) in a dichloromethane:methanol (7:3 v/v) mixture (10 mL) was reacted with one equivalent phenyl methyl sulfide at room temperature. The progress of the reaction was monitored qualitatively using thin layer chromatography (eluent mixture: ethyl acetate/chloroform/methanol-5:10:3 (v/v/v)) and quantitatively by gas chromatography.

**Reaction with triphenylphosphine**

Triphenyl phosphine (13 mg, 0.05 mmol) was added to a solution of **9** (19 mg, 0.05 mmol) in acetonitrile (15 mL) and the resulting solution was refluxed for around one hour. Upon cooling at room temperature, a yellow precipitate was formed. This was removed by filtration and, the mother liquor kept at 5 °C when additional precipitate is formed. The

overall yield is 9.8 mg (0.03 mmol, 64%) of the *cis*-dioxovanadium(V) complex **8**. $^{51}$V NMR (105 MHz, DMSO-$d_6$): -539.0 ppm.

### 3.5.7 Synthesis of mono-oxovanadium(V) complexes

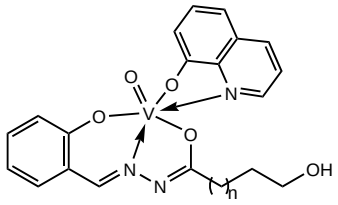


**Method 1:** To a suspension of neutral *cis*-dioxovanadium(V) omplex (1.71 mmol) in 30 mL methanol was added dropwise (over 15 minutes) under reflux and continuous stirring a solution of 8-hydroxyquinoline (0.24 g, 1.70 mmol) in 10 mL methanol. The resulting dark-violet solution was refluxed for an additional 2 hours and the solution was filtered hot. The solvent was removed to dryness under reduced pressure and the obtained solid redissolved in 5 mL methanol.

**Method 2:** A solution of Schiff base ligand (2 mmol) in 25 mL methanol was added to a suspension of $VO(acac)_2$ (0.53 g, 2 mmol) in 10 mL methanol. The resulting reaction mixture was refluxed for 2 hours with continuous stirring when the color changed from green to brown. 8-Hydroxyquinoline (0.29 g, 2 mmol) dissolved in 10 mL methanol was added dropwise over a period of 30 minutes and the reaction solution was refluxed and stirred for an additional 2 hours. The solvent was removed under pressure to dryness and the resulting solid dried under strong vacuum.

**Method 3:** The same procedure as Method 2 has been repeated using acetonitrile as reaction solvent.

**[VO(salhyhb)(Q)]** (**10**): Yield: *Method 1*: 0.40 g (1.06 mmol, 62%); *Method 2*: 0.32 g (0.77 mmol, 77%) and *Method 3*: 0.63 g (1.42 mmol, 71.0%). *Anal.* Calc. for

$C_{20}H_{18}N_3O_5V$ (443.40): C 56.69, H 4.21, N 9.74. Found: C 56.29, H 4.26, N 9.92. $^1$H NMR (400 MHz, DMSO-$d_6$): $\delta$ = 1.26 (q, 2H, *CH*$_2$, $^3$J=6.95 Hz), 2.09 (tt, 2H, C*H*$_2$CO, $^3$J=7.39 Hz), 3.09 (t, 2H, C*H*$_2$OH, $^3$J=6.28 Hz), 4.26 (br, 1H, *OH*), 6.72-6.74 (m, 1H, arom. C*H*), 6.98-7.00 (m, 1H, arom. C*H*), 7.17-7.18 (m, 1H, arom. C*H*), 7.45-7.80 (m, 5H, arom. C*H*), 8.09-8.10 (m, 1H, arom. C*H*), 8.50-8.52 (m, 1H, arom. C*H*), 9.14 (s, 1H, C*H*=N) ppm. $^{13}$C NMR (100 MHz, DMSO-$d_6$): $\delta$ = 26.3 (*C*H$_2$CO), 29.1 (*C*H$_2$), 59.6 (*C*H$_2$OH), 110.9, 115.4, 119.5 (arom.*C* and *C*H), 120.4, 122.5, 123.0, 128.2, 129.0, 133.2, 135.2, 138.2, 138.5, 146.1 (arom.*C*H and *C*), 154.2 (*C*H=N) ppm), 162.3, 163.3 (arom.*C*O–V), 176.1 (*C*O–V). $^{51}$V NMR (105 MHz, DMSO-$d_6$): - 471.4 ppm ; $^{51}$V NMR (105 MHz, $CDCl_3$): - 482.8 ppm. Selected IR data (cm$^{-1}$): 3446 (sh, OH), 3048 (arom. CH), 2935, 2869 ($CH_2$ aliphatic), 1605 (s, -CH=N-N=C-), 969 (s, VO). UV/Vis ($CH_3CN$ solution, $\lambda_{max}$ in nm ($\varepsilon$ in $10^3$ M$^{-1}$ cm$^{-1}$)): 241 (43.5), 273 (20.8), 321 (9.1), 540 (6.8).

**[VO(salhyhp)(Q)]** (**11**): Yield: *Method 1*: 0.38 g (0.85 mmol, 49%); *method 2* 0.41 g (0.95 mmol; 95 %) and *Method 3*: 0.69 g (1.55 mmol, 77.5%). *Anal.* Calc. for $C_{21}H_{20}N_3O_5V$ (445.346): C 56.64, H 4.53, N 9.44. Found: C 57.00, H 4.43, N 8.97. $^1$H NMR (200 MHz, DMSO-$d_6$): $\delta$ = 1.04-1.17 (m, 4H, C*H*$_2$), 2.07 (t, 2H, C*H*$_2$CO, $^3$J=6.60 Hz), 3.09 (t, 2H, C*H*$_2$OH, $^3$J=6.28 Hz), 4.26 (br, 1H,O*H*), 6.72-6.76 (d, 1H, arom. C*H*), 6.97-7.04 (m, 1H, arom. C*H*), 7.16-7.21 (m, 1H, arom. C*H*), 7.45-7.60 (m, 2H, arom. C*H*), 7.70-7.73 (m, 3H, arom. C*H*), 7.79-7.82 (m, 1H, arom. C*H*), 8.08-8.11 (m, 1H, arom. C*H*), 8.50-8.54 (m, 1H, arom. C*H*), 9.15 (s, 1H, C*H*=N) ppm. $^{13}$C NMR (50 MHz, DMSO-$d_6$): $\delta$ = 22.3 (*C*H$_3$), 29.2 (*C*H$_2$CO), 31.3 (*C*H$_2$), 59.9 (*C*H$_2$OH), 110.8, 115.4, 119.4 (arom.*C* and *C*H), 120.4, 122.5, 123.0, 128.2, 129.0, 133.2, 135.2, 138.3, 138.5, 146.2 (arom.*C*H), 154.2 (*C*H=N), 162.3, 163.2 (arom.*C*O–V), 176.0 (*C*O–V). $^{51}$V NMR (105 MHz, DMSO-$d_6$): - 472.4 ppm; $^{51}$V NMR (105 MHz, $CDCl_3$): - 483.0 ppm. Selected IR data (cm$^{-1}$): 3435 (sh, OH), 3048 (arom. CH), 2936, 2930, 2862 ($CH_2$ aliphatic), 1604 (s, -CH=N-N=C-), 973 (s, VO). UV/Vis ($CH_3CN$ solution, $\lambda_{max}$ in nm ($\varepsilon$ in $10^3$ M$^{-1}$ cm$^{-1}$)): 241 (43.9), 273 (21.4), 321 (9.5), 540 (6.8).

**[VO(salhyhh)(Q)]** (**12**): Yield: *Method 1*: 0.62 g (1.35 mmol, 79%); *Method 2*: 0.38 g

(0.85 mmol; 85 %) and *Method 3*: 0.67 (1.43 mmol, 71.5%) (*method 2*). *Anal.* Calc. for $C_{22}H_{22}N_3O_5V$ (459.372): C 57.52, H 4.83, N 9.15. Found: C 57.33, H 4.83, N 8.37. $^1$H NMR (400 MHz, DMSO-$d_6$): $\delta$ = 0.80-0.92 (m, 2H, C$H_2$), 1.02-1.10 (m, 4H, $CH_2$), 1.99-2.31 (m, 2H, C$H_2$CO, $^3$J=6.28 Hz), 3.10 (t, 2H, C$H_2$OH, $^3$J=6.80 Hz), 4.26 (br, 1H, O$H$), 6.73-6.75 (d, 1H, arom. C$H$), 6.97-7.03 (m, 1H, arom. C$H$), 7.16-7.21 (m, 1H, arom. C$H$), 7.39-7.51 (m, 1H, arom. C$H$), 7.56-7.59 (m, 1H, arom. C$H$), 7.59-7.69 (m, 2H, arom. C$H$), 7.69-7.79 (m, 1H, arom. C$H$), 8.09-8.10 (m, 1H, arom. C$H$), 8.51-8.53 (m, 1H, arom. C$H$), 9.15 (s, 1H, C$H$=N) ppm. $^{13}$C NMR (50 MHz, DMSO-$d_6$): $\delta$ = 24.6, 25.6 ($C$H$_2$), 29.5 ($C$H$_2$CO), 31.9 ($C$H$_2$), 60.3 ($C$H$_2$OH), 110.9, 115.4, (arom. $C$H), 119.5 (arom.$C$), 120.4, 122.4, 122.9, 128.2 (arom. $C$H), 129.1 (arom. $C$), 133.2, 135.2, 138.2 (arom. $C$H), 138.6 (arom. $C$), 146.2 (arom.$C$H), 154.1 ($C$H=N) ppm), 162.3, 163.3 (arom.$C$O–V), 176.0 ($C$O). $^{51}$V NMR (105 MHz, DMSO-$d_6$): - 472.0 ppm; $^{51}$V NMR (105 MHz, $CDCl_3$): - 482.9 ppm. Selected IR data (cm$^{-1}$): 3430 (sh, OH), 3060 (arom. CH), 2930, 2859 ($CH_2$ aliphatic), 1605 (s, -CH=N-N=CH-), 973 (s, VO). UV/Vis ($CH_3CN$ solution, $\lambda_{max}$ in nm ($\varepsilon$ in $10^3$ M$^{-1}$ cm$^{-1}$)): 241 (43.2), 273 (20.1), 321 (9.1), 540 (6.6).

### 3.5.8 Catalytic oxidative bromination of TMB

TMB (25mg, 0.15 mmol) was dissolved in 10 mL DMF. 10 mL of stock solution of tetrabutylammonium bromide (48.3g/L) (1.5 mmol, 10 equiv.) was added, followed by addition of 1 mL of vanadium complex, 0.15 mol% in DMF (0.015 mmol), $HClO_4$ (0.15 mmol) and $H_2O_2$ (0.15 mmol) in this order. Aliquots of the reaction (250 $\mu$L) were quenched in 2 mL of NaOH 0.002 M aqueous solution and extracted with 3 mL ethyl acetate. The reaction products were identified by gas-chromatography using the temperature programme described in Chapter 2.

# Chapter 4

# Vanadium(V) complexes based on N-salicylidene hydrazides that contain an amino-functionalized aliphatic side-chain

Investigations concerning the actual structure of the vanadate in vanadium dependent haloperoxidases were performed on the native enzyme as well as its reduced vanadium(IV) form.[101] Recent theoretical studies on models in comparison with spectroscopic data of vanadium haloperoxidases propose the vanadate moiety to be double protonated $[VO_2(OH)_2]^-$, which makes the *cis*-dioxovanadium(V) complexes, appropriate model complexes for the enzymatic system.[178,179] The amino-functionalization of the aliphatic side-chain of the used tridentate chelate system has been achieved in order to mimic the hydrogen bonding interaction of the prosthetic group of the V-HPOs and the lysine residue.[38] A vital role for the catalytic chloride oxidation reaction has been attributed to Lys353, an amino acid hydrogen bonded to one of the equatorial oxygen atom of the prosthetic group in the native enzyme.[63,180] Mutagenesis studies, performed by replacement of Lys353 amino acid with alanine, leaded to a drastic loss of the enzyme activity.[63] Additionally this vital role of the lysine amino acid is sustained by X-ray crystal structure determined for the peroxide-form of V-CPO that reveals lysine in hydrogen bonding

interaction with the peroxo-oxygen atom via its protonated amino group.[6] The catalytic cycle is proposed to proceed through hydrogen bonding network, e.g. the peroxide intermediate is activated by hydrogen bonding interaction with the lysine residue. In this manner the electrophilicity on the peroxo group is increased favoring the subsequent attack of the halide.[111]

The synthesis of the amino-functionalized N-salicylidene hydrazide ligand system follows the pathway depicted in Figure 64. The amino aliphatic esters as hydrochloride salts react with hydrazine hydrate in equimolecular amounts, resulting in the formation of $\omega$-amino aliphatic acid hydrazide hydrochloride. Subsequent reaction with salicylaldehyde affords almost quantitatively the desired N-salicylidene hydrazide that contain a "protected amino" functionalized aliphatic side-chain.

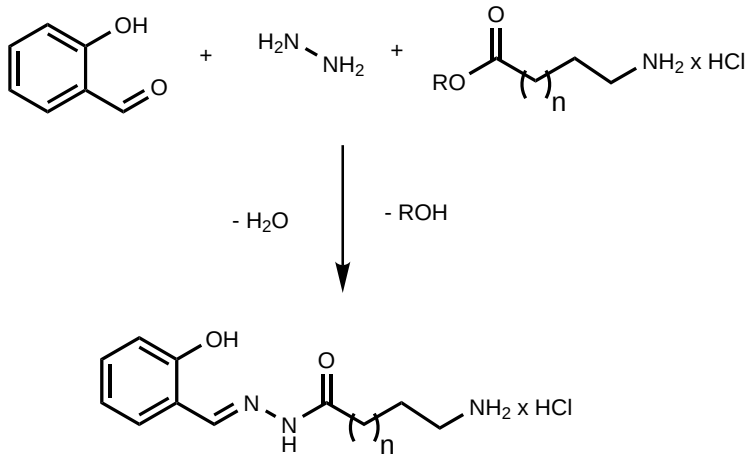


Figure 64: Schematic representation of the synthesis of amino functionalized N-salicylidene hydrazides. n=1 $H_2$salhab×HCl and n=3 $H_2$salhah×HCl.

The important step of the ligand synthesis is the stoichiometric reaction between the aliphatic amino ester hydrochloride and hydrazine hydrate. The protection of amino functionality in the carbonic acid hydrazide prevents the second Schiff base condensation reaction between the salicylaldehyde and the aliphatic amino group. At this point should be mentioned that, 6-amino hexanoic acid was recommended as a specific reagent for aldehydes recognition, giving better recovery than bisulphite.[181] Moreover, it is known that the amino acids in general can very easy eliminate water through reaction between

the carboxylate functionality and the free amino group resulting in the formation of lactam. If excess of hydrazide is used in the reaction with the amino acid esters, a mixture of lactam and hydrazide-hydrochloride was isolated as a consequence of the ester hydrolysis in strong basic medium.

Stoichiometric reactions of these new Schiff base ligands with ammonium metavanadate yield *cis*-dioxovanadium(V) complexes which can be regarded as appropriate structural models for the enzymatic system. The synthesis pathway of vanadium complexes is very similar with previous described procedure, but nevertheless, significant differences are obvious since, the presence of the amino-functionality makes possible cyclisation reactions. Moreover, a different reactivity of the two Schiff base ligands upon vanadium coordination have been observed, varying from favored nitrogen-containing ring closure in the case of N-salicylidene 4-amino butanoic acid hydrazide hydrochloride $H_2$salhab×HCl, to an intact ligand in the anionic *cis*-dioxovanadium complexes of N-salicylidene 6-amino hexanoic acid hydrazide $H_2$salhah×HCl.

## 4.1 *cis*-Dioxovanadium(v) complexes based on N-salicylidene 4-amino butanoic acid hydrazide hydrochloride

Stoichiometric reaction of the Schiff base ligand $H_2$salhyab×HCl, with ammonium metavanadate in refluxing methanol solution for about two days, results in the formation of neutral *cis*-dioxovanadium(V) complex as a dimeric compound-$[VO_2(Hsalhycab)]_2$. The reaction takes place by an intramolecular imine bond formation accompanied by a five-membered ring closure resulting in a dihydro-pyrrole structure (Figure 65).

Although, alternatives to prepare the *in situ* formed hydrazide have been reported,[182] the knowledge about ring closure upon ligand complexation in vanadium chemistry is rather scarce. A lactone ring closure has been formed by reaction of peroxovanadate with N-(2-hydroxyethyl) ethylenediaminetriacetic acid in acidic aqueous solution,[183] whereas more recently an imidazole ring formation upon vanadium coordination has been also reported.[106,184]

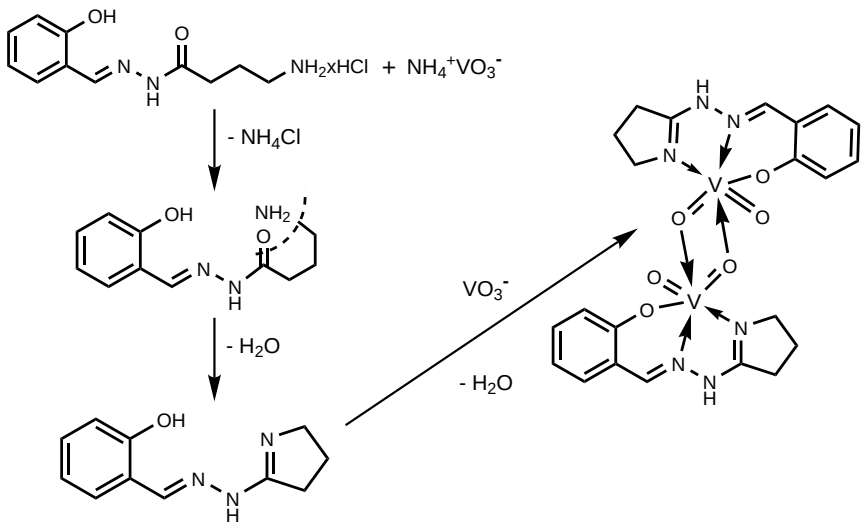


Figure 65: Mechanism for the formation of the dimeric *cis*-dioxovanadium(V) complex from N-salicylidene hydrazides-4-amino-butanoic hydrazide hydrochloride ($H_2$salhab×HCl).

The herein described *cis*-dioxovanadium(V) complex is the first vanadium compound with *in situ* formed pyrrole-like structure. The complex crystallizes from the mother liquor, within a week, as yellow needle crystals, suitable for X-ray measurement. Molecular structure determination reveals a dimeric structure $[VO_2(Hsalhycab)]_2$ **13**, when the complex is crystallized from methanol, and a monomeric structure $[VO_2(Hsalhycab)]$ **14**, when it is crystallized from water-methanol mixture. Molecular structure determination of complex **13** is depicted in Figure 66 and it shows two *cis*-$VO_2^+$ units forming a bis-($\mu$-oxo)-bridged vanadium(V) Schiff base dimer. Each vanadium atom is six-coordinated in a distorted octahedral geometry. The two oxo groups of the vanadate center are distinct and occupy different positions. The first of these O1 is placed in the apical position with a typical V=O bond distance of 161.6 pm, while the second is part of the basal plane and it is involved in the bridge between V and V0A where, it is strongly coordinated to V (V=O2 169.3 pm) and weakly associated with V0A (V0A–O2 245.8 pm). The coordination sphere of vanadium atom is completed by the phenolate oxygen atom O3 and two imine nitrogen atoms (N1 and N3) which fulfill the basal plane of the octahedra. The vanadium to nitrogen bond lengths are also distinct, varying from

a typical vanadium to imine nitrogen atom distance V–N1 of 222 pm to V–N3 bond length of about 14.5 pm shorter. The shortness of V–N3 bond length (207.5 pm) is a consequence of more covalent bonded nitrogen atom which is part of a conjugated system and which can be protonated and deprotonated due to the lability of the double bond (Figure 67). An additional reason for the observed difference in V–N bond lengths is given by their position in the coordination sphere of vanadium. For example, the N1 atom is place in *trans* position to double bonded oxygen atom O2, whereas the N3 atom is located *trans* to a weaker coordinated oxygen atom, namely the phenolate oxygen O3 atom.

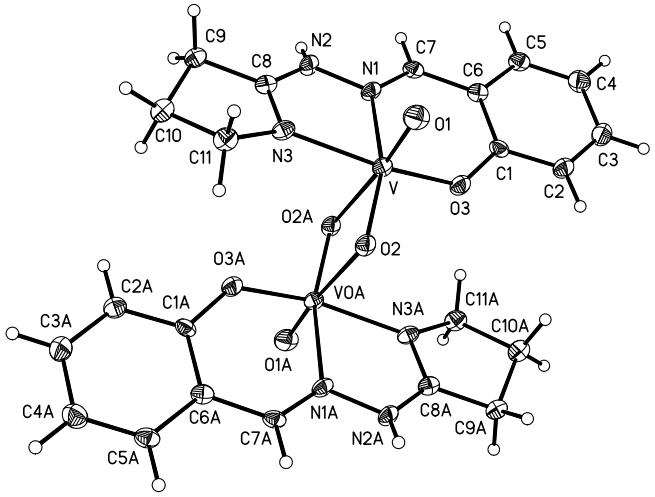


Figure 66: Molecular structure and numbering scheme of the dimeric complex $[VO_2(Hsalhycab)]_2$ (**13**); displacement ellipsoids are drawn at 50% probability level.

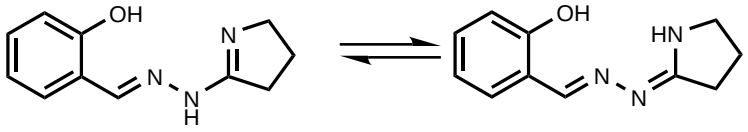


Figure 67: Tautomeric forms of the *in situ* formed cyclic ligand.

The two *cis*-dioxovanadium units, observed in the crystal structure of **13**, are related by an inversion center with the two vanadium atoms apart from each other by 327.3 pm. This separation distance is 20 pm longer than similar vanadium separation found in

reported binuclear-($\mu$-hydroxy)-bridged vanadium(IV) pyrazolyl complexes.[169] The O2–V–O2A angle is around 77.5°, while the V–O2–V0A is obtuse and it has a value of 102.4° as it is expected for an oxo-bridged dimer.[102,184] The O1–V–O2 angle of 106.9° is similar with corresponding angle in previous described *cis*-dioxovanadium(V) complexes, while the O1–V–O2A angle is larger and has a value of 174.5°. Although numerous *cis*-dioxovanadium(V) complexes have been reported, the reports of dimeric vanadium(V) structures are rather scarce. Nevertheless, Pecoraro *et al.* published in 1988 a similar dimeric *cis*-dioxovanadium complexes formed with N-salicylidene-N'-(2-hydroxyethyl)-ethylenediamine ($H_2$SHED) ligand[102] and more recently, Parajón-Costa reported a bis-(oxo-bridged) binuclear vanadium(V) complex based on dipicolinic acid.[185] The reported bond lengths and angles characteristic for the vanadium atoms are in good agreement with the parameters found in similar complex **13**. Selected bond lengths and angles in dimeric *cis*-dioxovanadium(V) complex **13** are given in Table 11.

The N-salicylidene dihydro-pyrrole hydrazide coordinates in its monoanionic form containing a protonated hydrazide nitrogen atom N2 that is involved in hydrogen bonding interaction with the oxo bridging oxygen atom (N2···O2 268.4 pm), leading to a polymer-like association (Figure 68).

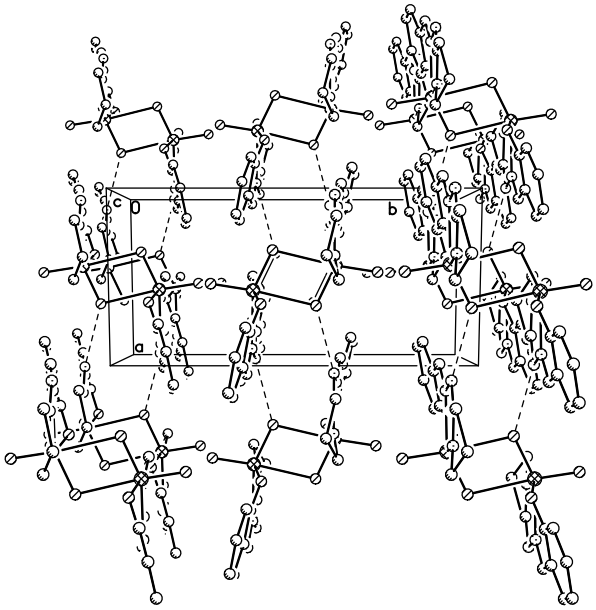


Figure 68: Representation of the hydrogen bonding interactions represented by broken lines, in complex **13** as viewed along the [001] axis.

This is a similar situation to one found in the neutral *cis*-dioxovanadium complexes obtained with N-salicylidene hydrazide that contain a hydroxyl and/or non-substituted aliphatic side-chain, where the protonated hydrazide nitrogen atom establishes hydrogen contacts with the equatorially double-bonded oxygen atom.

When the stoichiometric reaction of the N-salicylidene 4-amino butanoic acid hydrazide hydrochloride with ammonium metavanadate was performed in a mixture methanol-water (2:1 v/v), the monomeric *cis*-dioxovanadium(V) complex [$VO_2$(Hsalhycab)] (**14**) has been isolated. The molecular structure determination is shown in Figure 69, while selected bond lengths and angles are listed in Table 11. The vanadium atom is five-coordinated in a distorted square pyramidal geometry. The *in situ* formed ligand coordinates via ONN donor atoms forming the equatorial plane together with the double bonded oxygen atom O2, while the other oxo group O1 occupies the apical position. The N-salicylidene dihydro-pyrrole hydrazide ligand lies in one plane with the vanadium atom displaced out of the plane by 25 pm towards the apical oxo-group O1.

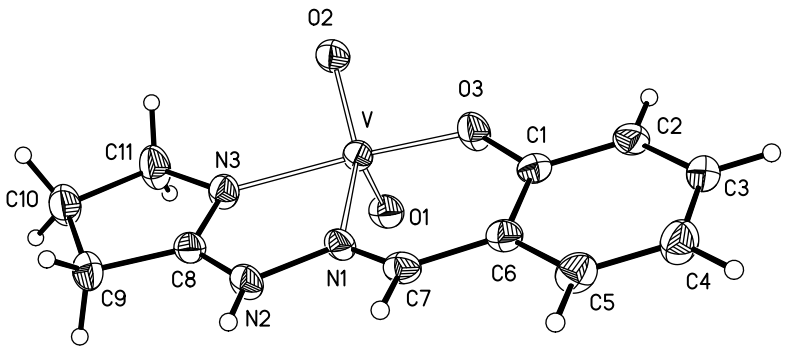


Figure 69: Molecular structure and numbering scheme of the monomer complex [$VO_2$(Hsalhycab)] (**14**); displacement ellipsoids are drawn at 50% probability level).

The equatorial oxo group O2, is distorted by 69 pm in the opposite direction to vanadium. This results in a $\tau$ value of 0.20 pm, consistent with a slight distortion to an ideal square pyramidal geometry of the vanadium atom. The vanadium to oxo group distances V–O1 and V–O2 are almost equal with the two oxygen atoms in *cisoid* positions forming a O1–V–O2 angle of 107°. On the other hand, the vanadium to nitrogen atom bond lengths, as well as vanadium to phenolate oxygen atom (O3) bond distance are shortened compared to those distances in the dimeric structure **13**, due to a different

coordination number of the vanadium atom.

A vital role for the catalytic activity of V-HPOs enzyme has been attributed to histidine residue (His486$^{\text{V-BPO}}$ and His496$^{\text{V-CPO}}$) as the single amino acid residue covalently bonded to the vanadium atom. The described herein complex contain also a vanadium to nitrogen-containing heterocycle bond of 222 pm, that can be regarded as similar bond structure with the one found in enzymatic system. A net difference between these two bond lengths is obvious, varying from a strong covalent bond in the native V-CPO of around 211 pm to a weaker V–N bond distance of around 11 pm longer in complex **14**. However, complex **14** presents also important hydrogen bonding interactions. The protonated hydrazide nitrogen atom is in hydrogen bonding interaction with the equatorial oxo ligand resulting in the formation of a 1D-polymer build up by hydrogen bonding interactions (N2$\cdots$O2 282.9 pm).

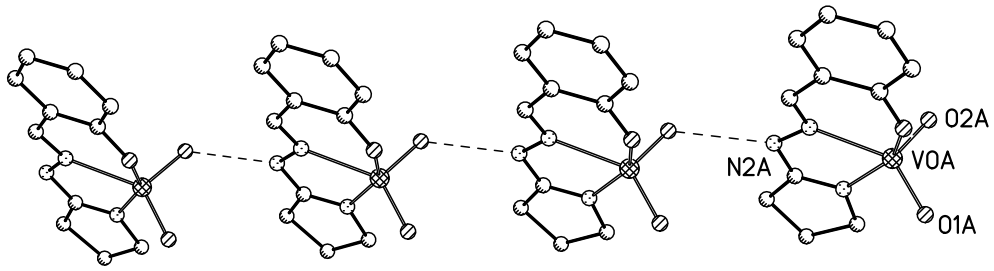


Figure 70: One dimensional polymer build up by hydrogen bonding interactions (broken lines) in crystals of complex **14**.

### 4.1.1 Spectroscopic characterization

The spectroscopic characterization of the two *cis*-dioxovanadium(V) complexes is in agreement with the crystallographically determined structure, although no difference can be made among them in solution. No difference between the $^{1}$H NMR and the $^{51}$V NMR spectra of the two complexes has been observed. The $^{1}$H NMR spectrum of the free ligand exhibits specific R-N$H_3^+$Cl$^-$ resonance at 8.04 ppm, which was absent in the $^{1}$H NMR spectra of complexes. This is consistent with the cyclisation of the ligand system upon vanadium coordination. Moreover, the imine protons of the Schiff base ligand are deshielded by around 0.3 ppm as a consequence of their involvement in coordination.

Table 11. Selected bond lengths (pm) and angles (°) in complexes **13** and **14**.

| | **13** | **14** | | **13** | **14** |
|---|---|---|---|---|---|
| V−O1 | 161.67(17) | 161.97(18) | V−N1 | 222.0(2) | 221.5(2) |
| V−O2 | 169.34(17) | 162.98(19) | V−N3 | 207.5(2) | 204.2(2) |
| V−O3 | 191.32(2) | 189.75(18) | N1−N2 | 139.0(3) | 131.0(3) |
| V−O2A | 245.88(16) | - | C8−N3 | 131.4(3) | 131.0(3) |
| C8−N2 | 134.6(4) | 129.9(3) | | | |
| O1−V−O2 | 106.89(9) | 107.41(10) | O2−V−O3 | 102.27(8) | 99.93(9) |
| O1−V−O3 | 99.62(9) | 102.51(9) | O2−V−N1 | 153.92(7) | 137.97(9) |
| O1−V−N1 | 97.77(8) | 113.53(9) | O2−V−N3 | 94.94(8) | 91.95(9) |
| O1−V−N3 | 95.64(9) | 99.77(9) | O2−V−O2A | 77.54(7) | - |
| O1−V−O2A | 174.54(7) | - | N3−V−N1 | 73.94(8) | 72.55(8) |
| O3−V−N1 | 81.37(8) | 80.49(7) | N3−V−O2A | 80.65(7) | - |
| O3−V−N3 | 152.48(8) | 150.20(9) | N1−V−O2A | 77.40(6) | - |
| O3−V−O2A | 82.30(7) | - | V−O2−V0A | 102.46(7) | - |

While in the $^{1}$H NMR spectra of the free ligand, this group exhibits two sets of signals, the vanadium complexation yielded only one conformer of the imine bound illustrated in the resonance of its proton as a single singlet. Unfortunately, due to their neutral character, these complexes have a poor solubility in organic solvents and the $^{13}$C NMR measurements requires a large number of scans. Nevertheless, a comparison between the $^{13}$C NMR patterns of the free ligand and the corresponding $^{13}$C NMR spectra of complex **14** proved the coordination mode of the ligand. The most indicative resonance is the down field shift at 152 ppm of the imine carbon atom (*C*H=N), that resonate around 140 ppm and 146 ppm, respectively in the free N-salicylidene amino-functionalized acid hydrazides as a consequence of the E-Z isomers. The 173 ppm specific carbonyl resonance is absent in the $^{13}$C NMR spectrum of the complexes owing to dihydro-pyrrole formation with the *C*H=N resonance at 169 ppm. The formation of the *cis*-$VO_2^+$ is apparent by $^{51}$V NMR measurements performed in DMSO-$d_6$ and DMF-$d_7$ solutions. Both the dimeric and the monomeric *cis*-dioxovanadium complexes resonate at -577 ($\nu_{1/2}$=316

Hz) in DMSO-$d_6$ and -574 ($\nu_{1/2}$=450 Hz) ppm in DMF-$d_7$, respectively. As can be seen no solvent dependence have been observed, the two resonances in deuterated DMSO and DMF solutions being very similar. The existence of the monomeric structure in solution is more likely and MS measurements performed on dimer **13** in methanol solution, using ESI positive mode, shows as major species the monomer complex with m/z 286.2 (50%) and 308.0 (100%) signals attributed to [**14**+$H^+$] and [**14**+Na], while the m/z signal corresponding to the molecular weight of the dimeric structure are less abundant: 575.0 (5%) [**13**+$H^+$] and 593.3 (10%) [**13**+Na].

The IR spectrum of the complexes is indicative of the proposed structures. Two strong vibrations are observed in the IR spectra of complex **14** at 902 and 936 $cm^{-1}$ assigned to stretching vibrations of the *cis*-$VO_2^+$ group, comparable with the stretching vibrations found for the previous described *cis*-dioxovanadium(V) with N-salicylidene hydrazide ligands. For the dimeric complex **13** the corresponding strong vibrations appear at 885 and 943 $cm^{-1}$, respectively being in according with a six coordinated vanadate stretching vibrations in dimeric complexes.[102,185] Furthermore, a comparison between the IR patterns of the free ligand and the IR spectrum of complexes are consistent with the proposed coordination mode of the ligand. The IR spectrum of the free ligand exhibits strong vibration at 3450 $cm^{-1}$ and 1690 $cm^{-1}$ attributed to the stretching vibrations of the amino functionality and to carbonyl group, respectively. These vibrations were absent in the IR spectrum of the complexes, but instead two strong vibrations, equal in intensity were observed at 1656-1622 and 1610-1613 $cm^{-1}$ attributed to the asymmetric vibration of the two conjugated -C=N- groups. In both type of complexes stretching vibration owing to the protonated hydrazide nitrogen atom, N2H, have been detected at around 3435-3447 $cm^{-1}$.

### 4.1.2 Peroxidative bromination of TMB

The catalytic bromide-oxidation reaction performed by complex **14** has also been examined. Following the established procedure, the oxidative bromination of TMB by $H_2O_2/Br^-$ system was performed with 20 mol% catalyst **14** in acidified DMF solution. The progress of the reaction was proved to be, in this case, very slow. The conversion of

TMB to the corresponding Br-TMB took place with around 15% conversion in the first two minutes of reaction time and developing maximum 36% Br-TMB within 5 minutes. The catalytic activity of complex **14** is lower than previous examples, taking into account that double amount of catalyst has been used for proceeding the reaction. The maximum turnover rate is 22 mol Br-TMB×(mol catalyst×h)$^{-1}$. Therefore, complex **14** catalyze the oxidative bromination of TMB, similarly to the inorganic salts, such as vanadyl acetylacetonate and ammonium metavanadate, for which a turnover rate of maximum 15 mol Br-TMB×(mol catalyst×h)$^{-1}$ was found.[117] The vanadium-catalyzed oxidative bromination of TMB was also followed by $^{51}$V NMR. The $^{51}$V resonance of 50mM DMSO-$d_6$ solution complex **14** is -577 ppm ($\nu_{1/2}$=315 Hz). Addition of $H_2O_2$, up to five equivalents, caused no change of the chemical shift. When six equivalents of $H_2O_2$ have been reacted with the *cis*-dioxovanadium complex, two additional resonances appeared at -608 ($\nu_{1/2}$=410 Hz) and -619 ppm ($\nu_{1/2}$=505 Hz), but with the -579 ppm ($\nu_{1/2}$=410 Hz) resonance still predominant. Increased amount of $H_2O_2$, up to 10 equivalents, caused a decrease in intensity of the -579 ppm resonance and the increasing of the other two resonances with the -622 ppm one being predominant. The latter predominant resonance can be attributed to oxo-peroxovanadium complex formation [VO($O_2$)(Hsalhycab)]. The observed upfield shifts for peroxovanadium complex is in accordance with reported upfield resonances by Tracey *et al.* who examined the aqueous formation of complexes of type [VO($O_2$)L] where L was an amino acid ligand.[186] The presence of the resonance corresponding to the starting *cis*-dioxovanadium(V) complex, when excess of hydrogen peroxide was used, it is not surprising. The isolated oxo-peroxovanadium complex **9**, showed a high instability in DMSO-$d_6$ solution, with a very fast decomposition to the corresponding dioxovanadium complex. Therefore, the observed reactivity of **14** towards $H_2O_2$ can be interpreted as the formation of an unstable peroxovanadium complex. Further increase of the added amount of $H_2O_2$ to 30 equivalents, caused completely new species. This is sustained by the disappearance of all previous detected $^{51}$V resonances and the appearance of a two overlapped resonances at -636 and -640 ppm, respectively. The latter $^{51}$V shifts might be given by vanadate oligomers, formed by decomposition of the peroxo species when excess of hydrogen peroxide is used. Another possible reason for the last two observed resonances in DMSO-$d_6$ solution might be due to the known

high hygroscopicity of the solvent. Therefore, the existence of excess of water leads to decomposition of the peroxovanadium complex as was described in Chapter 3.

On the other hand, the $^{51}$V NMR monitoring of the reaction of *cis*-dioxovanadium(V) complex with $HClO_4$ was also performed, in deuterated DMF and DMSO solutions. Addition of 10 equivalents of $HClO_4$ to a DMF-$d_7$ solution of **14** caused an upfield resonance of vanadium nucleus, shifted from -574 ppm ($\nu_{1/2}$=450 Hz) to -487 ppm resonance ($\nu_{1/2}$=1907 Hz); whereas in DMSO-$d_6$ solution the resulting resonance was detected at -474 ppm ($\nu_{1/2}$=1160 Hz), respectively. At this point, it is tempting to assume that a [VO(OH)(Hsalhycab)] complex is formed through protonation reaction of the vanadate center. This assumption will be further supported by reported -483 ppm resonance of the $[VO(OH)Q_2]$ complex in $CDCl_3$ solution.[11] Further investigation of the reactivity of the complex has been performed by UV-Vis monitoring of the reaction. In this case, $HClO_4$ aqueous solution 9.2 M was diluted in DMF and, therefore the amount of water introduced in the system was reduced. Spectrophotometric titration of 70$\mu$M DMF solution of complex **14** with $HClO_4$ has been performed, using different acid concentrations. The UV-Vis spectra of the *cis*-dioxovanadium(V) complex exhibits two absorption maxima; at 418 nm ($\varepsilon$=7.4×10$^3$ M$^{-1}$ cm$^{-1}$) and 332 nm ($\varepsilon$=5.8×10$^3$ M$^{-1}$ cm$^{-1}$). Addition of 0.5 equivalents of $HClO_4$ 0.09 M DMF solution caused a blue shifts of both maxima, at 406 ($\varepsilon$=5.7×10$^3$ M$^{-1}$ cm$^{-1}$) and 311 ($\varepsilon$=6.7×10$^3$ M$^{-1}$ cm$^{-1}$) nm, respectively. The spectrum exhibits further formation of the new species and 1.5 equivalent of acid caused the appearance of a new band at 394 nm ($\varepsilon$=3.5×10$^3$ M$^{-1}$ cm$^{-1}$) and an increase of intensity of the 310 nm absorption maxima ($\varepsilon$=5.7×10$^3$ M$^{-1}$ cm$^{-1}$). Further addition of acid, up to two equivalents caused a new shift of the 394 nm band to 389 nm. The final UV-Vis spectrum exhibits, therefore two new absorption maxima, at 389 nm ($\varepsilon$=5.0×10$^3$ M$^{-1}$ cm$^{-1}$) and 310 nm ($\varepsilon$=8.5×10$^3$ M$^{-1}$ cm$^{-1}$) (Figure 71). The isosbestic point at 330 nm, is indicative of an equilibrium between the existing species in solution. The resulting spectra closely resembles the characteristic absorption of *cis*-dioxovanadium(V) complex **7** which contains an intact N-salicylidene hydrazide ligand. Therefore, a possible hydrolysation of the *in situ* formed ligand might occur. The proposed reaction of complex **14** with $HClO_4$ is shown in Figure 72.

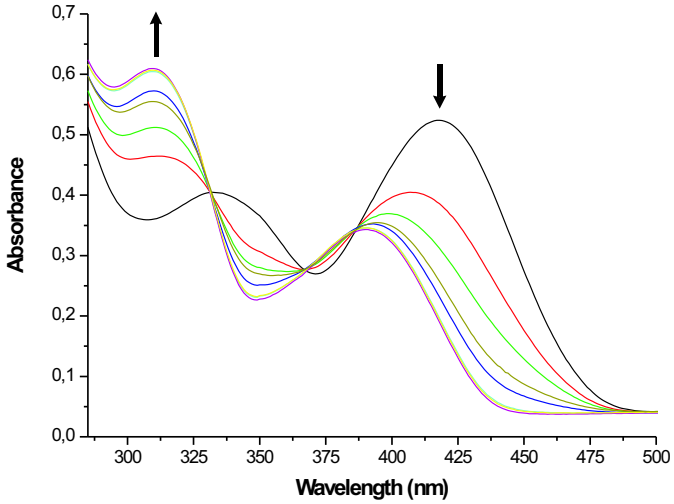


Figure 71: Spectrophotometric titration of **14** with two equiv. $HClO_4$ in DMF solution at 18 °C; 0.50 equivalents acid 0.09 M solution were added successively from two to two minutes under continuous stirring (black spectrum represents the starting point of the titration). The titration shows the proposed equilibrium depicted in Figure 72.

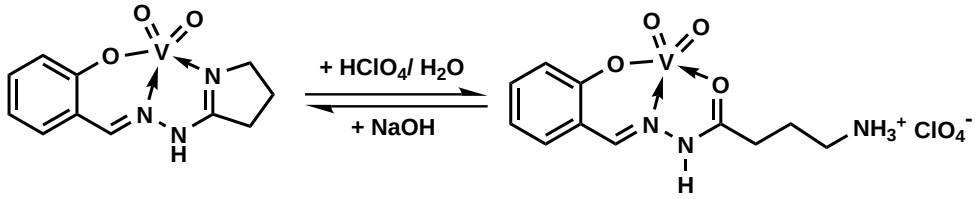


Figure 72: Proposed reactivity of $[VO_2(Hsalhycab)]$ (**14**) with 2 equivalents of $HClO_4$ in DMF solution.

The reaction is fully reversible and backwards titration with NaOH 0.1 M, aqueous solution, generates the initial spectra of complex **14**. The requirement of base for a complete recovering was instead higher compared to the used amount of acid and three equivalents of base were necessary to regenerate the initial spectra of complex **14** (Figure 73).

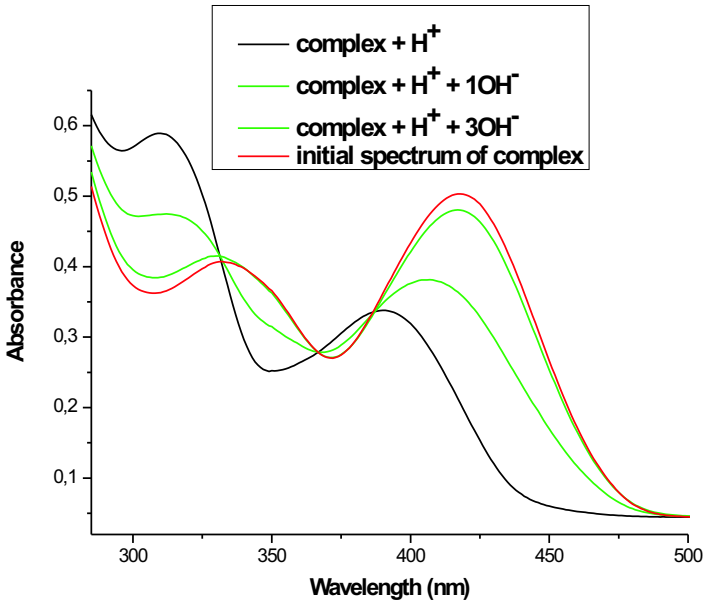


Figure 73: Spectrophotometric backwards titration with NaOH 0.1 M aqueous solution; base was added as indicated in the legend from two to two minutes at 18 °C under continuous stirring.

A detailed monitoring of the reaction was achieved by stepwise addition of 0.1 equivalents $HClO_4$ 9 mM solution. In this case, the gradually generation of the new species was more obvious, with the isosbestic point clearly present (Figure 74). The less intense absorption maxima, observed at 310 nm, compared to previous described spectrophotometric titration (Figure 71), could be caused by a high dilution of the final complex as a consequence of the used diluted acid solution.

If an excess of $HClO_4$ 0.09 M solution (five equivalents) is stepwise added, the UV-Vis spectrum of the resulting solution does not exhibit significant changes (Figure 75) compared to spectrophotometric titration performed with only two equivalents of acid. The progress of the reaction, from about two equivalents to five equivalents of acid, is insignificant and few amount of the new species is generated. The UV-Vis spectra exhibits a constant decrease of the 389 nm absorption maxima and an increase in intensity of the 310 nm maxima (Figure 75, right pictogram). Therefore, the hydrolysis of the dihydro-pyrrole ring to form N-salicylidene amino acid hydrazide is most likely to occur.

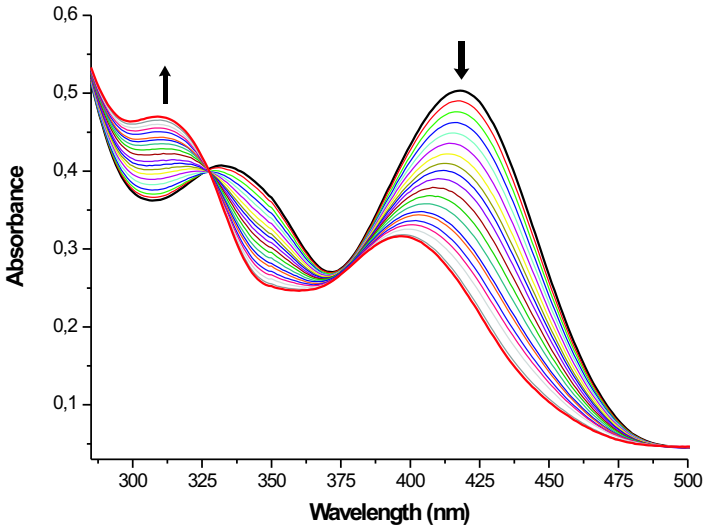


Figure 74: Spectrophotometric titration of **14** with two equiv. diluted $HClO_4$ in DMF solution at 18 °C; 0.1 equivalents acid 9 mM solution were added successively from 1.3 to 1.3 minutes under continuous stirring.

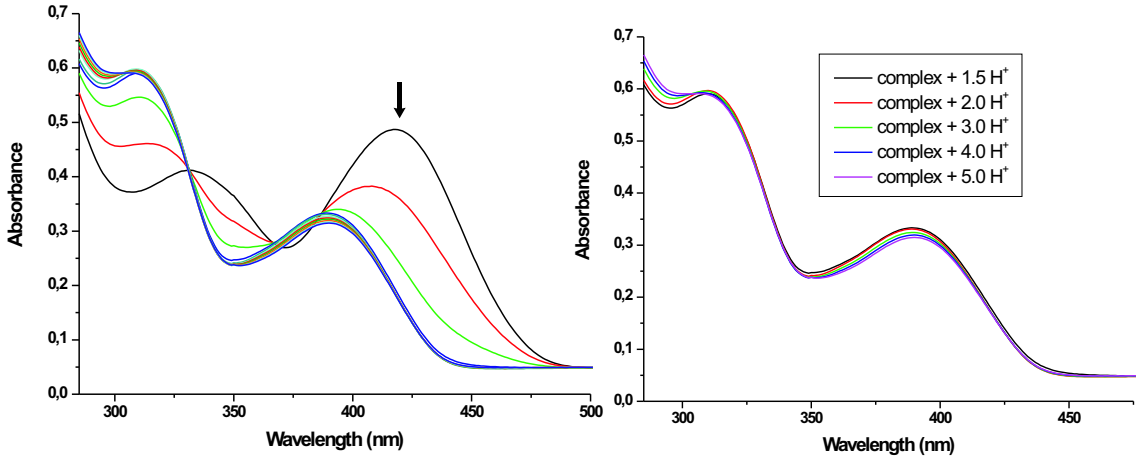


Figure 75: Spectrophotometric titration of **14** with five equiv. $HClO_4$ in DMF solution at 18 °C; 0.5 equivalents of acid 0.09 M solution were added successively from two to two minutes.

Unfortunately, when five equivalents of $HClO_4$ were used for the titration, the back-reaction with NaOH did not yield the complete recovering of the initial spectra of the complex. The addition of NaOH gave the initial absorption maxima, characteristic for complex **14**, but the intensity is much lower and the amount of required base is of around eight equivalents. Therefore, maybe some decomposition of complex might occur when excess of acid is present with the complex partially reformed in basic conditions.

Therefore, the reactivity of complex **14** towards $HClO_4$ in DMF solution take place, most likely by hydrolysation of the *in situ* formed dihydropyrrole structure to form an amino-substituted N-salicylidene hydrazide which contains a protonated hydrazide nitrogen atom (Figure 72). A $^{51}V$ NMR monitoring of the reaction, following the conditions of the UV-Vis spectrophotometric titration is expected to give further insight into the system.

## 4.2 *cis*-Dioxovanadium(V) complexes derived from N-salicylidene 6-amino hexanoic acid hydrazides

Further extension of the aliphatic side-chain of the starting amino acid ester with two methylene groups afforded the N-salicylidene 6-amino hexanoic acid hydrazide. The ligand is capable to react with ammonium metavanadate in refluxing methanol solution to yield the anionic *cis*-dioxovanadium(V) complex. By comparison to the shorter amino-functionalized N-salicylidene hydrazide, no cyclization has been occurred during the reaction with ammonium metavanadate. This can be explained due to the instability of the possible 7-membered ring closure. According with the used solvent of crystallization, two types of crystals could be isolated. Crystallization from methanol affords complex $[VO_2(salhyah)]$ (**15a**) (see Figure 76), while crystallization from a 1:1 mixture methanol-water leads to complex $[VO_2(salhyah)]\cdot 0.5H_2O$ (**15b**) (see Figure 77). The latter mentioned compound contains half molecule of water of crystallization per formula unit. In both cases the protonated amino functionalized side-chain compensates the negative charge on the vanadate moiety, similar to the lysine residue in the vanadium dependent haloperoxidase enzymes.

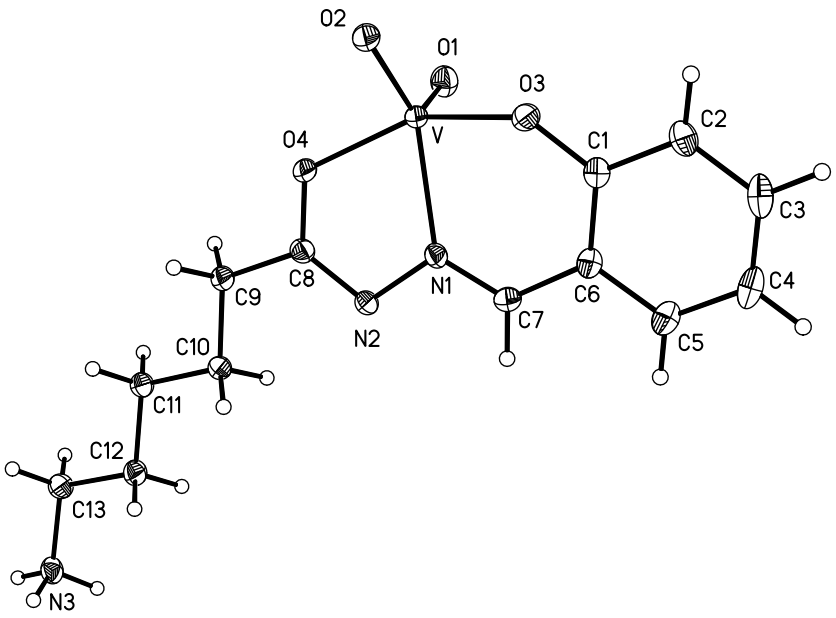


Figure 76: Molecular structure of $[VO_2(salhyah)]$ (**15a**); displacement ellipsoids are drawn at the 50% probability level.

The molecular structure of both complexes determined by X-ray crystallography feature a *cis*-dioxovanadium(V) moiety in a distorted square pyramidal environment with a $\tau$ value of 0.14 for complex **15a** and 0.18 for complex **15b**. The distortion to the ideal square pyramidal geometry is similar with previous described geometry of the vanadium atom in *cis*-dioxovanadium(V) complexes based on N-salicylidene hydrazide ligand. The Schiff base ligand coordinates in its dianionic form, providing an ONO donor set which form the equatorial plane together with one of the double bonded oxygen atom O2, whereas the other oxo group O1 occupies the apical position. The V=O (O1 and O2) bond lengths, as well as the V-N1 and V-O (O3 and O4) bond distances are almost the same for both complexes (see Table 12) and within the expected range for *cis*-dioxovanadium(V) complexes.[103,187] Complex **15a** crystalizes in the monoclinic space group $P2_1/n$, whereas complex **15b** crystallizes in the orthorhombic space group Pbcn. The two crystal structures shows high similarity. The anionic nature of the complex and, therefore the presence of the iminole form of the ligand is consistent with the observed V-O4 and C8-O4 bond lengths of around 195.5 and 130 pm, respectively.

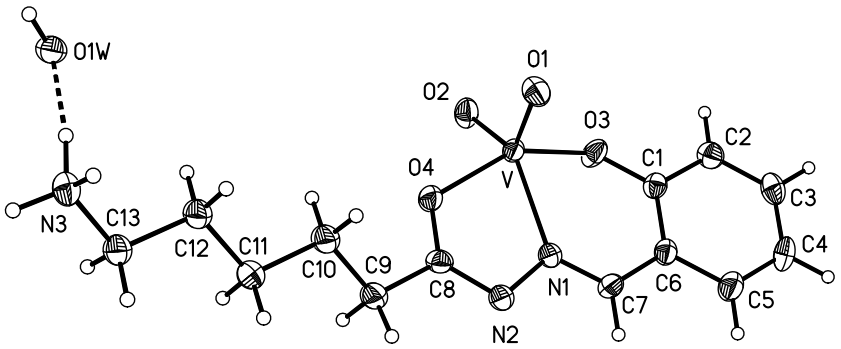


Figure 77: Molecular structure of $[VO_2(salhyah)]\cdot 0.5H_2O$ (**15b**); displacement ellipsoids are drawn at the 50% probability level.

The nitrogen atom and the three coordinated oxygen atoms at the pyramid base are nearly in the plane with the relative deviation of $O_3N$ atoms from the least-square plane of 9.2 pm in complex **15a** and 12.2 pm in complex **15b** with the vanadium atom around 50 pm apart from this plane towards the apical oxo group O1. In both cases the protonated amino group compensates the negative charge of the vanadate center and is involved in strong hydrogen bonding interaction.

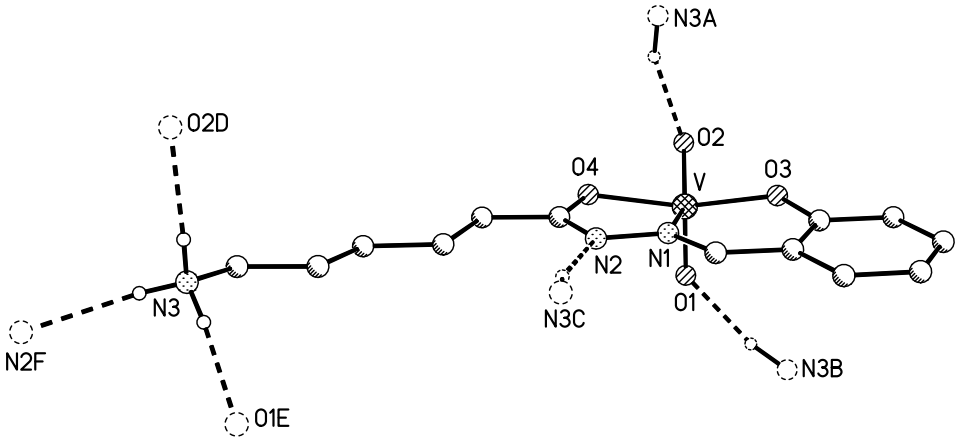


Figure 78: Hydrogen bonding interaction in crystals of complex **15a** (broken lines represent hydrogen bonds); relevant distances (in pm): N3···O2D 284.1, N3···N2F 302.4, N3···O1E 279.1 (symmetry transformations: A: 0.5 - x, 0.5 + y, 1.5 - z; B: 1.5 - x, 0.5 + y, 1.5 - z; C: 0.5 + x, - 0.5 - y, 0.5 + z; D: 0.5 - x, - 0.5 + y, 1.5 - z; E: 1.5 - x, - 0.5 + y, 1.5 - z; F: - 0.5 + x, - 0.5 - y, - 0.5 + z).

In complex **15b** an intermolecular hydrogen interaction is established between the protonated amino group and the water of crystallization (N3···O1w 283.4 pm), which is hydrogen bonded towards a nitrogen atom N2 of the hydrazide group from a neighboring molecule (Figure 79). In complex **15a**, this hydrogen interaction is established directly between the amino group and the nitrogen atom of the hydrazide from a neighboring molecule (Figure 78).

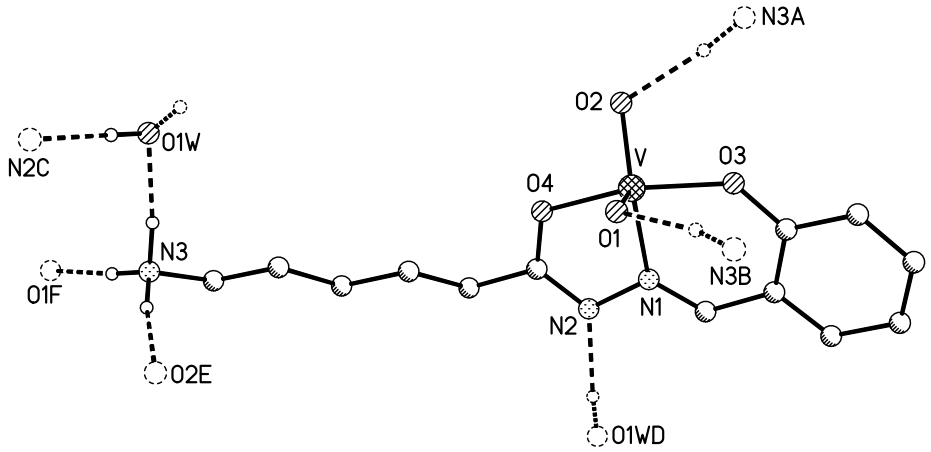


Figure 79: Hydrogen bonding interaction in crystals of complex **15b** (broken lines represent hydrogen bonds); relevant distances (in pm): N3···O2E 278.9, N3···O1F 276.3, N3···O1W 283.4, O1W···N2C 276.4 (symmetry transformations: A: 0.5 - x, 1.5 + y, - 0.5 - z; B: 0.5 + x, 0.5 - y, 0.5 + z; C: - 0.5 + x, 0.5 - y, 0.5 + z; D: 0.5 + x, - 0.5 - y, 0.5 + z; E: 0.5 - x, 1.5 + y, 0.5 - z; F: - 0.5 + x, - 0.5 - y, 0.5 + z).

A vital role for the catalytic activity of the vanadium chloroperoxidase enzyme is attributed to the lysine residue that is hydrogen bonded to the equatorial oxygen atom of the prosthetic group. A similar situation has been found in *cis*-dioxovanadium(V) complex with N-salicylidene 6-amino hexanoic acid hydrazide. In both complexes the protonated amino group is in hydrogen bonding interaction with the oxo groups O1 (N3···O1 279.1 pm in complex **15a** and N3···O1 276.3 pm in complex **15b**) and O2 (N3···O2 284.1 pm in complex **15a** and N3···O2 280 pm in complex **15b**). Moreover, the compensation of the negative charge on vanadium center by protonated functionalities of the ligand system is quite rare and only one more example is known in the literature.

This is represented by a similar described *cis*-dioxovanadium(V) complex based on N-salicylidene dimethyl-amino acetic hydrazide, which contains a substituted quaternary amine group.[188]

Table 12. Selected bond lengths (pm) and angles (°) in complexes **15a** and **15b**.

| | **15a** | **15b** | | **15a** | **15b** |
|---|---|---|---|---|---|
| V−O1 | 163.26 | 163.04 | V−N1 | 214.76 | 213.77 |
| V−O2 | 164.39 | 163.31 | C8−O4 | 130.13 | 129.48 |
| V−O3 | 189.87 | 190.44 | C8−N2 | 130.61 | 130.48 |
| V−O4 | 195.46 | 195.57 | N1−N2 | 131.4(3) | |
| O1−V−O2 | 111.25(6) | 110.18(8) | O2−V−O3 | 96.11(5) | 94.03(7) |
| O1−V−O3 | 103.30(5) | 102.38(7) | O2−V−O4 | 90.33(5) | 93.79(7) |
| O1−V−O4 | 102.22(5) | 101.17(7) | O2−V−N1 | 140.49(5) | 140.19(8) |
| O1−V−N1 | 107.24(5) | 109.32(8) | O3−V−N1 | 82.96(5) | 82.22(6) |
| O3−V−O4 | 148.73(5) | 150.82(7) | O4−V−N1 | 72.96(4) | 73.87(6) |

### 4.2.1 Spectroscopic studies

The IR spectra of the complexes are consistent with the determined molecular structures and presents the strong bands related to *cis*-$VO_2^+$ stretching vibrations at 931 and 909 $cm^{-1}$. The enolization of the amide functionality is consistent with the observed 1610 $cm^{-1}$ vibration assigned to the conjugated -CH=N–C=N- group. Strong vibration, but rather broad have been detected at 3435 $cm^{-1}$ corresponding to amino group. The intact coordination mode of the ligand was further confirmed by comparison of the $^1H$ NMR patterns of the ligand with the complexes as well as with the NMR patterns of complex **14**. By comparison with $^1H$ NMR spectra of complex **14** the specific R-$NH_3^+$ resonance has been observed at 7.59 ppm as a broad signal with the integration area corresponding of $3H^+$, in agreement with crystallographically solved structure. The azomethine proton is deshielded by 0.3 ppm comparing to its original resonances in the free ligand in accordance with the weakly coordinated nitrogen atom at the vanadium atom. While the -CH=N proton is present as E and Z isomer in the free Schiff base ligand

in a ratio 1.6:1, the coordination of the metal atom leads a single isomer consistent with observed one resonance in the $^{1}$H NMR of the complexes. Consequently, the resonance of the methylene group C$H_2$CO which also exhibits two resonances in $^{1}$H NMR spectra of the free ligand at 2.26 and 2.54 ppm due to a amide-iminole equilibrium, shows only one resonance for the iminole form at 2.26 ppm in $^{1}$H NMR spectra of the complex. The other methylene protons, as well as the aromatic protons resonate in the expected regions (see Experimental Section) with minor variations in their positions. The formation of the *cis*-dioxovanadium complex is further given by the -532 ppm resonance ($\Delta\nu_{1/2}$ = 600 Hz) in $^{51}$V NMR spectra recorded in DMSO-$d_6$. This resonance is upfield shifted by -45 ppm comparing to previous *cis*-dioxovanadium (V) complex obtained with N-salicylidene 4-butanoic acid hydrazide, but it is very similar with previous found $^{51}$V resonances for *cis*-dioxovanadium(V) complexes with an intact N-salicylidene aliphatic acid hydrazides.

### 4.2.2 Reactivity of the complex

The reactivity of complex **15a** was tested in solution by reaction with standard hydrochloric acid aqueous solutions, as well as its capacity to form a monoperoxovanadium complex, postulated as active intermediate for the reaction catalyzed by vanadium compounds as model for vanadium-dependent haloperoxidases.[121]

#### Protonation Reaction

The protonation reaction of complex **15a** was monitored by spectrophotometric titration of an aqueous solution of the complex with standard HCl solutions. Titration of 50 $\mu$M solution of the complex with two equivalents of HCl 0.1 M, monitored by stepwise addition of 0.5 equivalents acid, yields gradually a decrease in intensity of the 370 nm band and an increase in intensity of 282 nm band accompanied by a slight splitting (Figure 80). The isosbestic point at 297 nm demonstrates the existence of an equilibrium between components in solution. The reversibility of the reaction was accomplished by titration with NaOH 0.1 M (Figure 81) and two equivalents were required for recovering of the initial spectra. This differs to the situation found for the similar complex **7** described in Chapter 3, were a slight excess of base comparing to used amount of acid was necessary

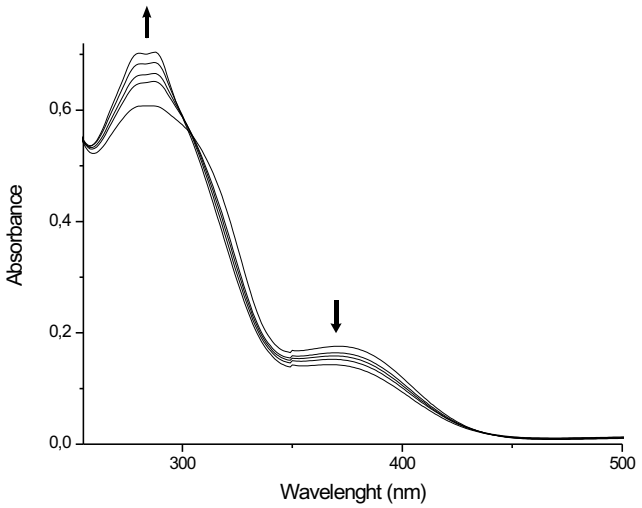


Figure 80: Spectrophotometric titration of [$VO_2$(salhyah)] (50$\mu$M) with two equivalents HCl 0.1 M in water; 0.5 equivalents of acid were added successively from two to two minutes at 18 °C. Isosbestic point is observed at 297 nm for the proposed equilibrium depicted in Figure 82.

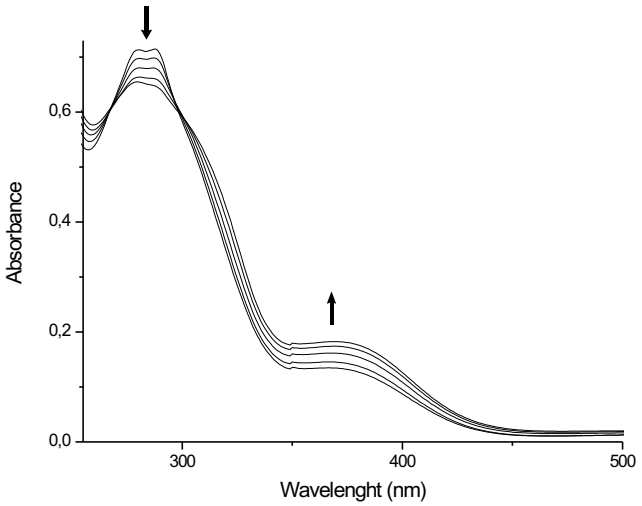


Figure 81: Spectrophotometric backwards titration of protonated [$VO_2$(Hsalhyah)] with two equivalents NaOH 0.1 M in water; 0.5 equivalents of base were added successively from two to two minutes at 18 °C.

to recover the anionic complex.

Despite this difference in the amount of required base for the back-titration, the UV-Vis spectra presents very high similarities and the interpretation of the results is analogues with previous described in Chapter 3. One protonation reaction occurs that takes place at the hydrazide nitrogen atom N2 which is the most basic site compared to the oxo groups of the vanadium ion (Figure 82).

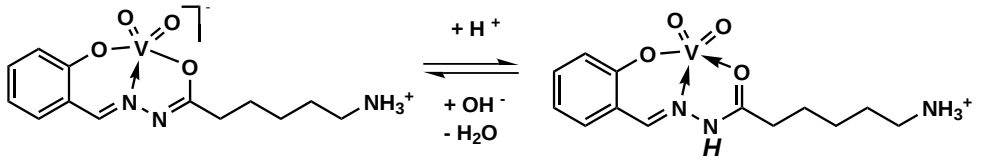


Figure 82: Proposed protonation reaction of complex **15** with HCl in water solution.

For a more closer investigation on the used system, the spectrophotometric titration has been performed on a diluted complex solution (33.4 $\mu$M) with 0.01 M HCl solution using a higher excess of acid, similarly with the used conditions for spectrophotometric titration of complex **7** with hydrochloric acid. The reaction was monitored by stepwise addition of 0.25 equivalents of HCl 0.01 M aqueous solution and performed first with five equivalents of acid and further addition of acid up to 10 equivalents (Figure 83). The initial spectra of the complex presents three absorbtion maxima at 214 ($\varepsilon$= 21.00×10$^3$ M$^{-1}$cm$^{-1}$), 282 ($\varepsilon$= 9.93×10$^3$ M$^{-1}$cm$^{-1}$) and 370 ($\varepsilon$= 3.30×10$^3$ M$^{-1}$cm$^{-1}$) nm. When five equivalents of acid have been added to the aqueous solution of the complex, an increase in intensity of the 282 nm band was observed ($\varepsilon$= 10.64×10$^3$ M$^{-1}$cm$^{-1}$), while the absorption maxima of 370 nm is constantly decreasing in intensity ($\varepsilon$= 3.02×10$^3$ M$^{-1}$cm$^{-1}$). Further addition of acid up to 10 equivalents caused a constant decrease of the intensity of the absorption maxima of the 370 nm band ($\varepsilon$= 2.79×10$^3$ M$^{-1}$cm$^{-1}$) and no shift of the wavelengths in general (Figure 83). The reaction is also fully reversible and the back-titration with base (10 equivalents), added stepwise affords the initial spectrum of the complexes (Figure 84).

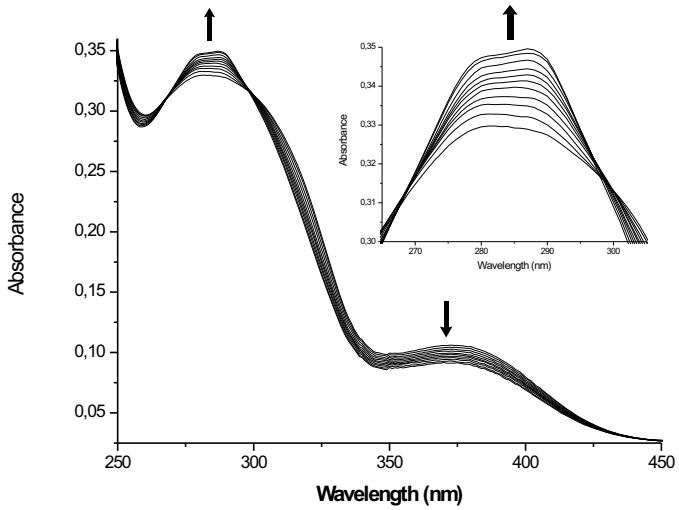


Figure 83: Spectrophotometric titration of [$VO_2$(salhyah)] (33.4$\mu$M) with 10 equivalents HCl 0.01 M in water; 0.25 equivalents of acid were added successively from two to two minutes at 18 °C.

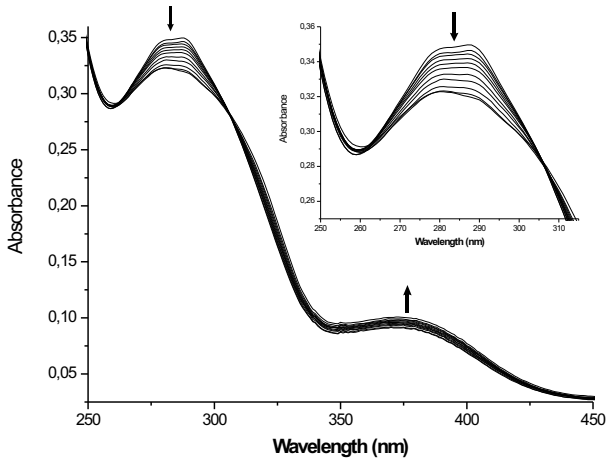


Figure 84: Spectrophotometric backwards titration of protonated [$VO_2$(Hsalhyah)] complex through reaction with 1o equivalents HCl 0.01 M. The titration is shown through addition of 10 equivalents NaOH 0.01 M aqueous solution; 0.25 equivalents of base were added successively from two to two minutes at 18 °C.

The obtained final UV-Vis spectra of the mixture complex **15** with acid, were also theoretically interpreted with the programm based on Zuberbühler mathematical background.[173,174] The formation of the protonated species at the hydrazide nitrogen atom

was confirmed for both five and ten equivalents of HCl titration data. A reasonable fit of the measured data, when five equivalents of acid have been used, was obtained by taking into account one protonation step. This gives a value of 630 for the equilibrium constant with a standard deviation of $5\times10^{-4}$. Further addition of acid up to 10 equivalents leads an decrease of the equilibrium constant to 580 and also an increase of the standard deviation to $8\times10^{-4}$, value which could not be improved by calculations with a possible second equilibrium process. The calculated $pK_b$ value is 11.2±0.2 for the spectrophotometric titration depicted in Figure 83. This confirmed once again the proposed process shown in Figure 82 and it leads the conclusion that, for this system, in aqueous solution, there is no protonation at the di-oxo groups of the vanadium atom. Moreover up to date, there have been crystallographically characterized only the corresponding oxo-hydroxo vanadium(IV) complexes.[167,169] For the N-salicylidene carbonic acid hydrazide system used here, the protonation of the hydrazide nitrogen atom is further in agreement with a similar reported *cis*-dioxovanadium system.[131]

**Reaction with hydrogen peroxide**

The formation of a peroxovanadium complex in solution has also been established by electronic absorption spectroscopy. Stepwise addition of 0.5 equivalents of $H_2O_2$ 25 mM methanol solution to 40 $\mu$M methanol solution of the complex yields the progressive generation of an orange material ($\lambda$ = 392 nm) (Figure 85). The titration reaction of **15** with 10 equivalents of hydrogen peroxide exhibits an isosbestic behavior. The spectral changes consist in a red shift of the 380 nm ($\varepsilon$= $2.6\times10^3$ $M^{-1}cm^{-1}$) band to 392 nm ($\varepsilon$= $2.9\times10^3$ $M^{-1}cm^{-1}$) accompanied by an increase of the absorption maxima due to the peroxo-to-vanadium charge transfer band. The 278 nm ($\varepsilon$= $8.2\times10^3$ $M^{-1}cm^{-1}$) broad band of the *cis*-dioxovanadium complex is also increasing in intensity with sharpening and splitting into two new bands (278 ($\varepsilon$= $11.7\times10^3$ $M^{-1}cm^{-1}$) and 288 ($\varepsilon$= $11.5\times10^3$ $M^{-1}cm^{-1}$) nm).

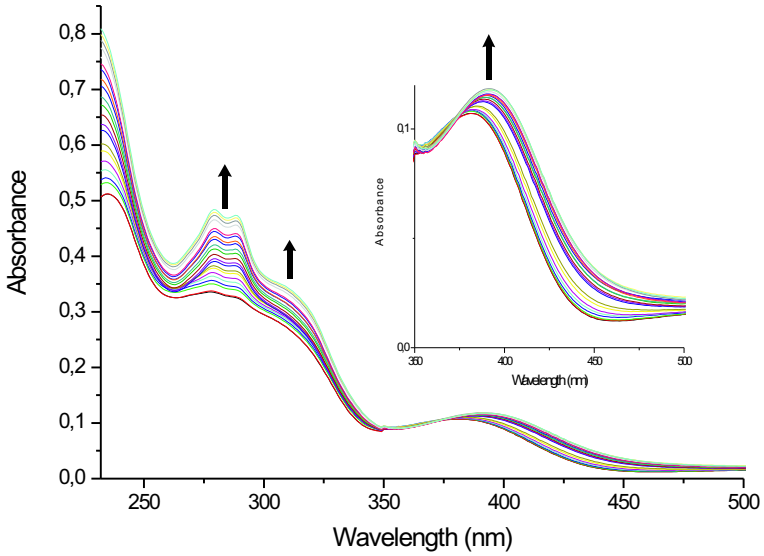


Figure 85: Spectrophotometric titration of $[VO_2(salhyah)]$ (40$\mu$M) with 10 equivalents $H_2O_2$ 25 mM in methanol; 0.5 equivalents of hydrogen peroxide were added successively at every two minutes at 20 °C. The titration shows the formation of the peroxovanadium complex with specific absorbance at 392 nm.

The final spectra pattern is similar to that of the isolated peroxovanadium complex **9** recorded in methanol solution. This is a very important observation, since a peroxovanadium complex has been postulated as active intermediate of the catalytic reactions, not only for the enzymatic system,[95] but also for the vanadium model complexes.[111]

The oxidative-bromination reaction of TMB catalyzed by *cis*-dioxovanadium(V) complex (**15**), has also been performed. Following the typical experiment, 10 mol% catalyst has been reacted with hydrogen peroxide in acidified DMF solution, to yield an active peroxo-intermediate able to catalyze bromide oxidation. This resulting oxidized bromide has been monitored by GC dosage of mono-brominated TMB product compared with non-reacted TMB. The reaction has been initiated by succesive addition of perchloric acid and hydrogen peroxide to a DMF solution containing 1,3,5-trimethoxybenzene, catalyst and excess of tetra-butylammonium bromide. A 41.8% conversion of the TMB to BrTMB has been achieved within 5 minutes, corresponding to a turnover rate of 50 mole of brominated TMB per mol of catalyst and hour, which is about 3 times faster than the reported ammonium vanadate[117] and two times faster than complex **14**. The amount of brominated TMB increase to 79.3% after 10 minutes of reaction time, similar catalytic activity to

previous described anionic *cis*-dioxovanadium(V) complexes with hydroxyl-functionalized N-salicylidene hydrazide. Thus, the bioinspired *cis*-dioxovanadium(V) complex with N-salicylidene hydrazide which contains an amino substituted aliphatic side-chain catalyze the oxidative bromination of TMB following analogous pathway to vanadium bromoperoxidases. The vanadium complex reacts with $H_2O_2$ to form a peroxovanadium species as was proved by spectrophotometric titration with hydrogen peroxide. The synthetic complex **15a** requires instead more acidic conditions and also performs lower turnover rate compared to the natural system.

## 4.3 Oxidation of sulfides catalyzed by *cis*-dioxovanadium(V) complexes

Vanadium haloperoxidase enzymes are also capable to catalyze the oxidation of sulfides to sulfoxides, varying from an enantioselective behavior in the case of vanadium bromoperoxidases to a non-selective reaction when vanadium chloroperoxidase has been used to mediate the reaction.[88,89] Various vanadium complexes have been also reported[189,190] as catalysts for sulfides oxidation reaction with the complexes involving mainly Schiff base ligation. The capacity of the new *cis*-dioxovanadium(V) complexes to function as catalysts for the oxidation reaction of methyl phenyl sulfide by hydrogen peroxide was also investigated. Following the reported procedure,[191] 1 mol-% catalyst has been used for the reaction and a slight excess (1.2 equivalents) of hydrogen peroxide, in a mixture $CH_2Cl_2/CH_3OH$ 7:3. Methanol was used as co-solvent due to the bad solubility of the complex in non-polar solvents and moreover, for a better miscibility of the aqueous oxidant with the halogenated solvent. After 16 hours of reaction time, 100% of the corresponding sulfoxide was obtained when complex **14** was used as catalyst, whereas 89% conversion was established by the catalyst **15a** within 18 hours. Reports of vanadium-catalyzed sulfur oxidation reactions range from 58 to 92% conversion in the period of time of 14-16 hours[189–192] when oxo- or *cis*-dioxovanadium(V) complexes were used as catalysts. The yields of the catalytic reaction raise to 60% conversion of sulfide within two hours, when peroxovanadium (V) complexes catalyzed the reaction.[193] Efficient vanadium-based

catalyst for the sulfide oxidation reaction was reported as salan-type oxovanadium(IV) complex which accomplished 91% conversion after six hours of reaction in acetonitrile solution.[189]

## 4.4 Conclusions

The new *cis*-dioxovanadium(V) complexes with N-salicylidene-hydrazides that contain an amino-functionalized side-chain have been synthesized and fully characterized. These complexes can be regarded as structural model for the enzymatic system due to the relevant hydrogen bonding interaction which involves the oxygen atoms of the vanadate moiety. When N-salicylidene 4-amino butanoic hydrazide has been used as ligand system, dimeric and monomeric *cis*-dioxoanadium(V) complexes have been isolated. The reaction took place by an intramolecular cyclisation reaction, resulting in the formation of neutral *cis*-dioxovanadium complexes based on dihydro-pyrrole N-salicylidene hydrazide. Complex **14** showed instead a low efficiency as catalyst of the bromide oxidation reaction. Reactivity of the complex towards $HClO_4$ in DMF solution showed the hydrolysis of the dihydro-pyrrole formed structure, resulting in the formation of 4-amino aliphatic acid hydrazide which contains a protonated hydrazide nitrogen atom. However, **14** was instead capable to catalyze the oxidation of sulfides with a quantitative conversion of methyl phenyl sulfide into the corresponding sulfoxide after 16 hours.

Further increase of the aliphatic side chain with two methylene groups yield the formation of anionic *cis*-dioxovanadium(V) complexes. The compensation of the negative charge at the vanadium atom is now achieved by the protonated amino group that takes the place of the ammonium cation found in the previous examples. The complex allows for a variation of the protonation state that occurs at the basic amide nitrogen. Spectroscopic investigations regarding the reactivity of the complex towards HCl showed that the protonation in aqueous solution occurs only at the hydrazide nitrogen atom. Peroxidative bromination of TMB in acidified DMF solution showed high efficiency of the complex to function as catalyst of the reaction. Therefore, complex **15** can be regarded as both structural and functional model complex for vanadium haloperoxidases. Moreover, **15** showed significant catalytic capacity for sulfide oxidation reaction accomplishing

89% conversion of thioanisole within 18 hours. Thus, using very simple conditions (room temperature and no exclusion of air) together with low excess and inexpensive oxidant (hydrogen peroxide) these complexes were capable of oxidizing thioanisole to the corresponding thioanisole sulfoxide with high efficiency.

## 4.5 *cis*-Dioxomolybdenum(VI) complexes based on N-salicylidene hydrazides that contain an amino-functionalized aliphatic side-chain

Molybdenum has been reported as an important metal in biological systems and, numerous molybdenum containing enzymes are known.[194] The existence of molybdenum in oxotransferase enzymes had increased the interest for the reactivity and coordination chemistry of *cis*-dioxomolybdenum complexes.[92,195] Moreover, various molybdenum(VI) complexes have been reported as efficient catalysts for epoxidation and hydroxylation of olefines,[196–199] oxidation of sulfides[200] and alcohols[201] and as catalysts of oxygen transferring reaction.[202,203] In addition, $MoO_3(aq)$[204,205] and $[MoO(O_2)_2(oxalate)]^{2-}$[206] are known as functional mimics for V-HPOs enzyme, being capable to catalyze the oxidation of halides by hydrogen peroxide. At this point should be mentioned that, molybdate showed a higher catalytic activity, compared to the inorganic vanadate. The reported turnover rate for the catalytic bromide oxidation reaction is *ca.* 180 mol Br-TMB×(mol Mo catalyst×h)$^{-1}$ which is about 45 times faster than ammonium metavanadate.[205] However, the number of molybdenum-based catalyst for the haloperoxidase reaction is very limited and there are reports of molybdenum coordination compounds as analogs of vanadium complexes, which were incapable to mediate the catalytic halide oxidation.[207] The vanadate as the prosthetic group of vanadium haloperoxidases, has been found to be vital for the catalytic reaction, since its removal or reduction leads an inactive (apo)protein derivate.[2,101] Replacement of vanadate with molybdate did not restore the haloperoxidase activity of the enzyme,[101] although the protein environment of the V-HPO enzymes was capable of binding molybdate.[62]

In order to address the question whether *cis*-dioxomolybdenum complexes with

N-salicylidene hydrazide ligand can serve as catalysts of the oxidative bromination reaction, the corresponding *cis*-dioxomolybdenum(VI) complexes were also isolated. Based on similar chemistry of molybdate and vanadate, there are already reports which proved the versatility of the used Schiff base system towards molybdenum accommodation.[151] Therefore, the N-salicylidene hydrazide that contain an amino functionalized side chain were also reacted, in equimolecular amounts, with molybdenyl acetylacetonate in presence of one equivalent of sodium hydroxide. The presence of base was a compulsory requirement for the reaction to proceed as a consequence of the used Schiff base ligand as hydrochloride salt. The reaction was performed in refluxing methanol when *cis*-dioxomolybdenum(VI) complexes were isolated. Using the short aliphatic side chain of the amino-funtionalized N-salicylidene hydrazide precursor, suitable crystals for X-ray measurement of the *cis*-dioxomolybdenum(VI) complex **16**, were obtained. The molecular structure determination reveals a *cis*-dioxomolybdenum moiety (Figure 86) with the molybdenum atom in a distorted octahedral geometry. Due to the base presence for the reaction, the ligand is also present as N-salicylidene dihydropyrrole hydrazide and coordinates via the phenolate oxygen atom O3 and the two imine nitrogen atoms (N1 and N3). A net difference conservely to corresponding *cis*-dioxovanadium(V) complexes is the deprotonation of the hydrazide nitrogen atom of the *in situ* formed ligand. This consist with the observed Mo–N3 bond length of 201 pm that is shortened comparing to the corresponding V–N3 of 222 pm found in complex **14**. The coordination sphere of the molybdenum atom is completed by the two oxo groups placed in *cis*-position to each other and a coordinated methanol molecule (Figure 86). The molybdenum to oxo group bond distances are almost equal (Mo–O1 of 169.8 pm and Mo–O2 of 170.3 pm) and similar with corresponding bond distances reported for *cis*-dioxomolybdenum complexes.[202,203,208] The coordinated oxygen atom O1M of the methanol molecule, located *trans* to oxo group O1, is weakly bonded at the molybdenum center (Mo–O1M 215 ppm). The structural differences between the *cis*-dioxomolybdenum complex **16** and the analog vanadium complex **14** is that the molybdenum atom has a six-coordination number, fulfilling, in general its sixth coordination site with solvent molecule. Selected bond lengths and angles for complex **16** are given in Table 13.

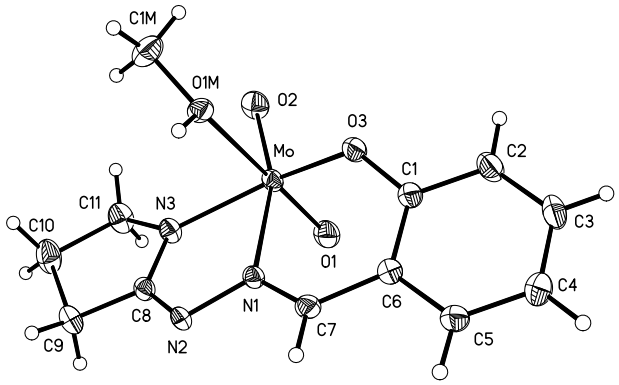


Figure 86: Molecular structure and numbering scheme of complex $[MoO_2(salhycab)(MeOH)]$ (**16**); displacement ellipsoids are drawn at 50% probability level.

However, hydrogen bonding interaction in complex **16** were also observed, but with the involvement of different donor patterns. The coordinated methanol molecule is in hydrogen bonding interaction with the hydrazide nitrogen atom N2 of neighboring molecule (N2$\cdots$OC 289 pm), whereas in the corresponding *cis*-dioxovanadium complex the hydrogen bonding interaction involved the strong covalently bonded oxo group. The hydrogen bonding interaction established in the crystal packing of *cis*-dioxomolybdenum complex results in the formation of layered polymeric structure (Figure 87).

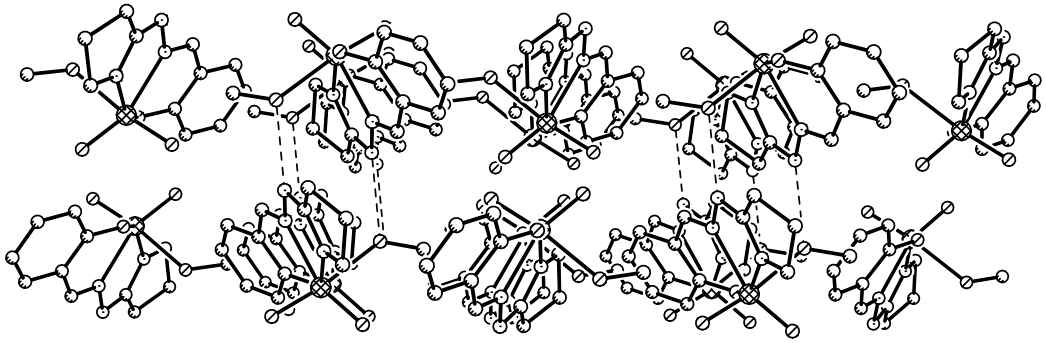

Figure 87: Representation of the hydrogen bonding network (drawn as broken lines) observed in the crystals of the *cis*-dioxomolybdenum complex **16** viewed along the [100] axis.

Table 13. Selected bond lengths (pm) and angles (°) in complex **16**.

| | | | |
|---|---|---|---|
| Mo−O1 | 169.84(15) | Mo−N1 | 227.67(16) |
| Mo−O2 | 170.29(14) | Mo−N3 | 206.09(18) |
| Mo−O3 | 195.42(15) | C8−N2 | 131.0(3) |
| Mo−O1M | 231.36(14) | C8−N3 | 134.0(3) |
| O1−Mo−O2 | 105.19(7) | O2−Mo−O3 | 106.44(7) |
| O1−Mo−O3 | 96.27(7) | O2−Mo−N1 | 159.02(7) |
| O1−Mo−N1 | 93.43(6) | O2−Mo−N3 | 95.94(7) |
| O1−Mo−N3 | 100.43(7) | O2−Mo−O1M | 83.20(6) |
| O1−Mo−O1M | 170.81(7) | N3−Mo−N1 | 70.79(6) |
| O3−Mo−N1 | 80.49(6) | N3−Mo−O1M | 82.12(6) |
| O3−Mo−N3 | 147.40(7) | N1−Mo−O2A | 79.00(5) |
| O3−Mo−O1M | 77.46(6) | | |

### 4.5.1 Spectroscopic characterization

The formation of the *cis*-dioxomolybdenum(VI) complex has been also confirmed by spectroscopic methods. The $^{1}$H NMR of the complex is in agreement with the proposed coordination of the ligand, in particular the absence of the down field resonance corresponding to NH proton found in the corresponding $^{1}$H NMR spectrum of vanadium(V) complexes. The azomethine proton (-CH=N) is upfield shifted by around two ppm compared to vanadium complexes. A similar effect, but in opposite direction of the NMR scale, was observed for the methylene protons placed in vicinity of the molybdenum atom, namely $CH_2N$–Mo. The other aliphatic and aromatic protons resonate in expected region with insignificant differences. The $^{13}$C NMR presents instead strong differences regarding the position of the resonances of the carbon atoms close to the nitrogen and oxygen atoms which are covalently bonded at molybdenum atom. A resonance at 176.5 ppm corresponding to $CH_2$ group place in vicinity of the coordinated nitrogen atom has been observed in the case of *cis*-dioxomolybdenum complex; this is about seven ppm downfielded compared with the resonance found in vanadium complex **14**. On the other hand, the phenolic carbon atom is four ppm shifted upfield, whereas the azomethine carbon

resonate in similar region according to a weak covalently bonded nitrogen atom. The presence of the coordinated methanol is confirmed by the specific resonances of the $CH_3$ protons at 3.15-3.16 ppm and 4.08 pmm for the OH proton with the $^{13}C$ resonance at 48.6 ppm. Furthermore, the IR spectrum is consisting with the crystallographically determined structure and contains strong stretching vibration at 909 and 930 $cm^{-1}$ corresponding to *cis*-$MoO_2$ group. Contrary to the IR spectrum of *cis*-dioxovanadium(V) complex only one vibration was observed at 1605 $cm^{-1}$ assigned to the -CH=N-N=C group and thus, is confirmed the deprotonation of the hydrazide nitrogen atom N2 on molybdenum coordination.

Similar spectroscopic patterns were detected for the *cis*-dioxomolybdenum(VI) complex **17**, obtained with N-salicylidene 6-amino hexanoic acid hydrochloride ligand. Comparison between $^1H$ and $^{13}C$ NMR of **17** with the $^1H$ and $^{13}C$ NMR patterns of the corresponding vanadium complex **15a**, follows in general the differences described above. The molybdenum atom is also six-coordinated as a consequence of the specific NMR resonances of the methanol nuclei detected in both the $^1H$ and $^{13}C$ NMR of complex **17**. Similarly to the corresponding *cis*-dioxovanadium(V) complex, the molybdenum complex **17** contains an intact N-salicylidene 6-amino hexanoic acid hydrazide showed by characteristic resonances detected in both $^1H$ and $^{13}C$ NMR spectra of the molybdenum complex. By comparison with the vanadium complex **15a**, the *cis*-dioxomolybdenum complex **17** has a neutral character with the amino functionality resonating at 7.58 ppm with the integration area corresponding to two protons. The other aliphatic and aromatic protons of the tridentate ligand coordinates in the expected regions with insignificant differences compared with their resonances in the *cis*-dioxovanadium(V) complex **15a**.

### 4.5.2 Catalytic tests

The haloperoxidase activity of the *cis*-dioxomolybdenum complex **16**, has been performed following the procedure described for vanadium complexes. Unfortunately no catalytic activity of the molybdenum complex has been found towards the peroxidative bromination of 1,3,5-trimethoxybenzene, although the ligand system is capable to coordinate molybdenum in a similar manner with vanadium complexes. This observation is in agree-

ment with the results reported for vanadium haloperoxidase enzyme where the molybdate bonded enzyme was reported as inactive.[62] Compared to the inorganic molybdate and vanadate, were the molybdate proved to be an efficient catalyst of the haloperoxidase reaction, the replacement of vanadate with molybdate in this case did not afford the same positive effect. Instead, the *cis*-dioxomolybdenum(VI) complex (**16**) functions as efficient catalyst for the sulfide oxidation. 1 mol% complex in a dichlormethane-methanol mixture catalyzed the oxidation of phenyl methyl sulfide to around 83% sulfoxide after 18 hours using $H_2O_2$ as oxidant. Contrary to vanadium-catalyzed reaction, sulfone as over oxidation product, has been obtained. Every attempt to decrease and/or to avoid completely the sulfone formation failed and an decrease from around 25% to 10% was achieved by stepwise addition of hydrogen peroxide over a period of at least 5 minutes at 0 °C.

Thus, it can be concluded that *cis*-dioxomolybdenum(VI) complex with N-salicylidene hydrazide that contain an amino functionalized side-chain can be prepared in a similar manner with vanadium complexes, resulting in dihydropyrrole hydrazide sequence formed *in situ* upon reaction with metal salts when 4-amino butanoic substituted Schiff base is used as ligand system. This molybdenum complex showed no catalytic activity of the oxidative bromination of 1,3,5-trimethoxybenzene by hydrogen peroxide, contrary to the *cis*-dioxovanadium(V) complexes. Instead the *cis*-dioxomolybdenum complex is capable to catalyze the oxidation of sulfides to corresponding sulfoxides with a slight over oxidation capacity. When N-salicylidene 6-amino hexanoic acid hydrazide had been used as ligand system, the resulting *cis*-dioxomolybdenum(VI) complex has been spectroscopically characterized. The reaction between the Schiff base ligand as hydrochloride salt and molybdenyl acetylacetonate as a source of molybdenum salt takes place with a very low yield and requires the presence of one equivalent of base. When no base have been used for reaction mixture to proceed, a molybdenum(V) complex as a greenish-blue material could be isolated, which presents an specific one-line EPR signal with a g value of 1.92, as a specific characteristics for paramagnetic molybdenum(V) complex.[209]

## 4.6 Experimental Section

**Materials:** Diluted perchloric acid (0.09 M) for spectrophotometric titration was obtained by dilution of a standard $HClO_4$ 9.21 M (aqueous solution) in DMF. NaOH and HCl 0.1 M and 0.001 M were used as standardized aqueous solutions. All other reagents were used as received, without further purification. Abbreviations used throughout the text: $H_2$salhyab = 4-amino butyric acid (2-hydroxy-benzylidene) hydrazide hydrochloride, $H_2$salhyah = 6-amino hexanoic acid (2-hydroxy-benzylidene) hydrazide, Hsalhycab = 2-(2-hydroxy-benzylidene) 4,5-dihydro-pyrrole hydrazide, TMB = 1,3,5-trimethoxybenzene, Br-TMB = 2-bromo 1,3,5-trimethoxybenzene, Q = 8-hydroxyquinoline.

The programm used for theoretical interpretation of UV-Vis data was an C++ adaption of the original SPECFIT-32, which was initially developed in Basic. The used programm keeps the original mathematical background and is capable using ASCII files to calculate the equilibrium constants from multiwavelength spectroscopic data based on a factor analysis.

### 4.6.1 Synthesis of amino-aliphatic hydrazide as hydrochloride salts

#### Synthesis of 4-amino butanoic acid hydrazide hydrochloride

To a solution of ethyl 4-aminobutanoate hydrochloride (7.68 g, 0.05 mmol) in absolut ethanol (10 mL), hydrazine hydroxide 100 % (2.50 g, 2.50 mL, 0.05 mmol) was added under continuous stirring, followed by addition of ethanol (40 mL) and water (5 mL). The resulting solution was refluxed under continuous stirring overnight. After cooling at room temperature diethyl ether (50 mL) was added which caused a turbulence of the solution. Stirring at room temperature for 12 hours yields a colorless precipitate. (Note: in the case of an oil formation, the reaction mixture is dried under strong vacuum and it is extracted three times with hot absolut ethanol and precipitated by stirring with diethyl ether (100 mL)). Yield: 6.45 g (0.04 mol; 84 %). *Anal. for* $C_4H_{12}N_3OCl$ (153.61): calcd. C 31.28, H 7.87, N 27.36; found C 32.20, H 7.68, N 26.37.

**Synthesis of 6-amino hexanoic acid hydrazide hydrochloride**

To a solution of methyl 6-aminohexanoate hydrochloride (9.08 g, 0.05 mmol) in absolut ethanol (25 mL), hydrazine hydroxide 100 % (2.50 g, 2.45 mL, 0.05 mmol) was added with reflux and stirring overnight. The resulting solution was rotary evaporated to dryness and extracted five times with absolut ethanol (50 mL) when an oily compound was formed. Titruration with diethyl ether (150 mL) yields the desired solid product. Yield: 8.30 g (0.04 mol; 91 %). *Anal. for* $C_6H_{16}N_3OCl$ (181.66): calcd. C 39.67, H 8.87, N 23.13; found C 39.90, H 8.72, N 23.13. $^1$H NMR (200 MHz, $D_2O$): $\delta$ = 1.06-1.28 (m, 2H, C$H_2$), 1.34-1.59 (m, 4H, C$H_2$), 2.08 (t, 2H, C$H_2$CO, $^3$J= 7.22 Hz), 2.83 (t, 2H, C$H_2$NH$_2\times$HCl, $^3$J= 7.50). $^{13}$C NMR (50 MHz, $D_2O$): $\delta$ = 24.4, 24.9, 26.3 (all $C$H$_2$), 33.3 ($C$H$_2$CO), 39.2 ($C$H$_2$NH$_2\times$HCl), 175.4 ($C$=O).

## 4.6.2 Synthesis of Schiff base ligands as hydrochloride salts

**Synthesis of N-salicylidene 4-amino butanoic acid hydrazide hydrochloride ($H_2$Salhyab$\times$HCl)**

To a solution of 4-amino butanoic acid hydrazide hydrochloride (3.20 g, 0.02 mol) in refluxing absolut ethanol (50 mL), salicylaldehyde (2.42 g, 0.02 mol, 2.07 mL) was added dropwise. The resulting yellow solution was cooled down and stirred at room temperature overnight. The formed precipitate was filtered off and dried in vacuo. Additional material can be obtained by reduction under strong vacuum of the solution to about half followed by addition of diethylether (100 mL). Total yield: 4.12 g (0.016 mol; 80 %). *Anal. for* $C_{11}H_{16}N_3O_2Cl$ (257.72): calcd. C 51.27, H 6.26, N 16.30; found C 51.81, H 6.31, N 15.96. $^1$H NMR (400 MHz, DMSO-$d_6$): $\delta$ = 1.80-1.90 (m, 2H, C$H_2$), 2.36 and 2.70 (t, total 2H, C$H_2$CO, $^3$J= 7.20 and $^3$J= 7.28 Hz, ratio 1.2:0.9), 2.79-2.85 (m, 2H, C$H_2$N$H_3^+Cl^-$), 6.87-6.99 (m, 2H, arom. C$H$), 7.19-7.40 (m, 1H, arom. C$H$), 7.46-7.69 (m, 1H, arom. C$H$), 8.04 (br, 3H, N$H_3^+Cl^-$), 8.28 and 8.42 (s, 1H total, C$H$=N, ratio 0.4:0.6), 10.16, 11.17, 11.29 and 12.02 (N$H$, O$H$, total 2H in ratio 0.4:0.6:0.4:0.6) ppm. $^{13}$C NMR (50 MHz, DMSO-$d_6$): $\delta$ = 21.8, 22.8 (all $C$H$_2$), 29.0 and 30.6, ($C$H$_2$CO), 38.2 ($C$H$_2$N$H_3^+Cl^-$), 116.1, 116.3, 118.6, 119.2, 120.0, 126.5, 130.6, 130.9, 131.1, 133.1 (all arom. $C$H and $C$), 140.8, 146.5 (both $C$H=N), 156.4, 157.3, 158.6, 162.5, 167.6 (arom. $C$), 172.9 ($C$=O)

ppm. Selected IR data ($cm^{-1}$): $\nu$= 3461 ($NH_3^+Cl^-$), 3169 (NH); 1689 (s; C=O), 1621 and 1606 (C=N).

**Synthesis of N-salicylidene 6-amino-hexanoic acid hydrazide hydrochloride ($H_2$Salhyah×HCl)**

To a solution of 6-amino hexanoic acid hydrazide hydrochloride (7.27 g, 0.04 mol) in refluxing absolut ethanol (100 mL), salicylaldehyde (4.84 g, 0.04 mol, 4.15 mL) was added dropwise. The resulting yellow solution was cooled down and stirred at room temperature overnight. The formed precipitate was filtered off and dried in vacuo. Additional material can be obtained by reduction under reduce pressure of the solution to about half of its initial volume followed by addition of diethylether (100 mL). Total yield: 11.25 g (0.04 mol; 97.5 %). *Anal. for* $C_{13}H_{19}N_3O_2Cl$ (284.765): calcd. C 54.83, H 6.72, N 14.75; found C 55.05, H 6.62, N 14.25. $^1$H NMR (200 MHz, DMSO-$d_6$): $\delta$ = 1.31-1.41 (m, 2H, C$H_2$), 1.50-1.61 (m, 4H, C$H_2$), 2.35 and 2.57 (t, 2H, C$H_2$CO, $^3$J= 7.22 Hz, ratio 1.2:0.8), 2.66-2.82 (m, 2H, C$H_2NH_3^+Cl^-$), 6.80-6.93 (m, 2H, arom. C$H$), 7.17-7.29 (m, 1H, arom. C$H$), 7.42-7.60 (m, 1H, arom. C$H$), 7.94 (br, 3H, $NH_3^+Cl^-$), 8.26 and 8.41 (s, 1H total, C$H$=N, ratio 0.3:0.6), 10.18, 11.22, 11.89 (N$H$, O$H$, total 2H a ratio 0.3:1.0:0.6) ppm. $^{13}$C NMR (50 MHz, DMSO-$d_6$): $\delta$ = 23.4, 24.3, 25.4, 25.5 26.6 (all $C$H$_2$), 31.6, 33.6 (both $C$H$_2$CO), 38.2 ($C$H$_2NH_3^+Cl^-$), 116.1, 116.2, 118.5, 119.1, 119.3, 120.0, 126.5, 129.2, 130.7, 131.0 (all arom. $C$H and $C$), 140.7, 146.3 (both $C$H=N), 156.3, 157.2, 158.6, 168.2 (arom. $C$), 173.6 ($C$=O) ppm. Selected IR data ($cm^{-1}$): $\nu$= 3461 ($NH_3^+Cl^-$), 3169 (NH); 1689 (s; C=O), 1621 and 1606 (C=N).

### 4.6.3 Synthesis of *cis*-dioxovanadium(V) complexes

**Synthesis of complex [$VO_2$(Hsalhycab)]$_2$ (13)**

To a solution of Schiff base ligand-$H_2$Salhyab×HCl (0.50 g, 1.94 mmol) in methanol (25 mL) was added $NH_4VO_3$ (0.23 g, 1.96 mmol) when a brown colored mixture was formed. The resulting mixture was refluxed for around 2 days when a clear solution was obtained. The volume of the solution was concentrated to about half under reduce pressure and left at room temperature when a yellow precipitate is formed overnight.

The resulting precipitate was filtered off and the solution volume removed under reduce pressure for additional material. Recrystallization of the yellow precipitate from methanol afford suitable crystals for X-ray measurement. Yield: 0.60 g (1.05 mmol; 54 %).*Anal. for* $C_{22}H_{24}N_6O_6V_2$ (570.35): calcd. C 46.33, H 4.24, N 14.73; found C 45.57, H 3.81, N 14.58. $^1$H NMR (400 MHz, DMSO-$d_6$): $\delta$ = 2.17-2.21 (m, 2H, C$H_2$), 2.63-2.82 (m, 2H, C$H_2$C=N), 3.67-3.71 (m, 2H, C$H_2$C-N-V), 6.81-6.83 (m, 2H, arom. C$H$), 7.40-7.56 (m, 2H, arom. C$H$), 8.64 (s, 1H, C$H$=N), 12.9 (br, 1H, N$H$) ppm. $^{51}$V NMR (105 MHz, DMSO-$d_6$): $\delta$ = -577.2 ppm ($\Delta\nu_{1/2}$ = 325 Hz). ESI-MS (positive mode): m/z = 286.2 [monomer + $H^+$](45%), 308.2 286.2 [monomer + Na](100%), 553.3 [M - $O^{2-}$](90%), 593.3 [M + Na](20%). Selected IR data ($cm^{-1}$): $\nu$= 3447 (br, NH), 1656 and 1610 (s, -C=N-N=C-), 944 and 885 (s, $VO_2$).

**Synthesis of complex [$VO_2$(Hsalhycab)] (14)**

To a solution of Schiff base ligand-$H_2$Salhyab×HCl (0.50 g, 1.94 mmol) in methanol (25 mL) was added a slurry solution of $NH_4VO_3$ (0.23 g, 1.96 mmol) suspended in 10 mL water. The resulting mixture turned brown colored and it was refluxed for around 2 days under continuous stirring until the majority of the inorganic salt was reacted. The volume of the solution was concentrated to about half under reduce pressure and left at room temperature when a yellow precipitate is formed. The resulting precipitate was filtered off and washed with at least 5 mL water, whereas the filtrate solution was kept in an open flask at room temperature when yellow needles crystalize within less than a week. (Note: Recrystallization of the yellow precipitate from methanol:water=1:1 mixture affords also suitable crystals for X-ray measurement.) Yield: 0.47 g (1.64 mmol; 84.5 %).*Anal. for* $C_{11}H_{12}N_3O_3V$ (285.17): calcd. C 46.33, H 4.24, N 14.73; found C 46.14, H 4.15, N 14.57. $^1$H NMR (400 MHz, DMSO-$d_6$): $\delta$ = 2.29 (t, 2H, C$H_2$, $^3$J=6.8 Hz), 2.78-2.82 (m, 2H, C$H_2$C=N), 3.66-3.69 (m, 2H, C$H_2$C-N-V), 6.81-6.83 (m, 2H, arom. C$H$), 7.37-7.55 (m, 2H, arom. C$H$), 8.65 (s, 1H, C$H$=N), 12.9 (br, 1H, N$H$) ppm. $^{13}$C NMR (50 MHz, DMSO-$d_6$): $\delta$ = 23.9 ($C$H$_2$), 27.7 ($C$H$_2$C=N), 57.3 ($C$H$_2$N–V), 117.6, 118.7, 119.9, 130.1, 134.3 (all arom.$C$H and $C$), 151.9 ($C$=N), 164.3 (arom.$C$O–V), 169.8 ($C$=N) ppm. $^{51}$V NMR (105 MHz, DMSO-$d_6$): $\delta$ = -577.4 ppm ($\Delta\nu_{1/2}$ = 365 Hz) and $^{51}$V NMR (105 MHz, DMF-$d_7$): $\delta$ = -574.1 ppm ($\Delta\nu_{1/2}$ = 450 Hz). ESI-MS (negative mode): m/z = 284.0 [M

- $H^+$](100%), 552.0 [$2M^-$-$O^{2-}$](20%), 591.1 [$2M^-$ + Na](5%). Selected IR data ($cm^{-1}$): $\nu$= 3435 (br, NH), 1622 and 1613 (s, -C=N-N=C-), 936 and 902 (s, $VO_2$). UV/Vis (DMF solution, $\lambda_{max}$ in nm ($\varepsilon$ in $10^3$ $M^{-1}$ $cm^{-1}$)): 332 (5.8), 418 (7.4).

**Synthesis of complex [$VO_2$(salhyah)] (15)**

To a solution of Schiff base ligand-$H_2$Salhyah×HCl (1.00 g, 3.50 mmol) in methanol (50 mL) was added $NH_4VO_3$ (0.41 g, 3.50 mmol). The resulting mixture was refluxed for 3 hours when a yellow precipitate was formed. This precipitate was filtered off and dried in vacuo. Additional material can be obtain by reduction of the solution volume under reduce pressure to about half of the initial volume. There were totally obtained 0.85 g (2.56 mmol; 73 %). *Anal. for* $C_{13}H_{18}N_3O_4V$ (331.24) (**15a)**: calcd. C 47.14, H 5.48, N 12.69; found C 47.06, H 5.25, N 12.35 and $C_{13}H_{19}N_3O_{4.5}V$ (340.25) (**15b)**: calcd. C 45.89, H 5.63, N 12.34; found C 45.90, H 5.48, N 12.48. $^1$H NMR (400 MHz, DMSO-$d_6$): $\delta$ = 1.333-1.38 (m, 2H, C$H_2$), 1.51-1.61 (m, 4H, C$H_2$), 2.27 (t, 2H, C$H_2$CO, $^3$J= 6.77 Hz), 2.77 (t, 2H, C$H_2$$NH_3^+$, $^3$J= 7.13 Hz), 6.72-6.74 (m, 2H, arom. C$H$), 7.27-7.30 (m, 1H, arom. C$H$), 7.45-7.47 (m, 1H, arom. C$H$), 7.59 (br, 3H, $NH_3^+$), 8.72 (s, 1H, C$H$=N) ppm. $^{13}$C NMR (100 MHz, DMSO-$d_6$): $\delta$ = 25.1 ($C$$H_2$), 25.5 ($C$$H_2$), 26.6 ($C$$H_2$), 31.5 ($C$$H_2$CO), 38.7 (**C**$H_2$$NH_3^+$), 116.6, 119.3, 119.7 (arom.$C$H and $C$), 132.3, 132.8 (arom.$C$H), 154.2 ($C$H=N), 164.3 (arom.$C$–OV), 175.9 ($C$–OV) ppm. $^{51}$V NMR (105 MHz, DMSO-$d_6$): $\delta$ = -532.4 ppm ($\Delta\nu_{1/2}$ = 600 Hz). ESI-MS (negative mode): m/z = 330.3 [M - $H^+$](100%), 683.2 [2M + Na](20%). Selected IR data ($cm^{-1}$): $\nu$= 3435 (s, $NH_3^+$), 1610 (br, -C=N-N=C-), 931 and 907 (s, $VO_2$). UV/Vis ($H_2O$ solution, $\lambda_{max}$ in nm ($\varepsilon$ in $10^3$ $M^{-1}$ $cm^{-1}$)): 214 (21.03), 282 (9.93), 370 (3.30) and UV/Vis ($CH_3OH$ solution, $\lambda_{max}$ in nm ($\varepsilon$ in $10^3$ $M^{-1}$ $cm^{-1}$)): 235 (12.59), 278 (8.19), 288 (7.90), 315 (shoulder), 381 (2.66).

### 4.6.4 Synthesis of *cis*-dioxomolybdenum(VI) complexes

**Synthesis of complex [$MoO_2$(salhycab)($CH_3OH$)] (16)**

To a solution of Schiff base ligand-$H_2$Salhyab×HCl (0.80 g, 3.10 mmol) in methanol (60 mL) was added NaOH (0.12 g, 3.10 mmol), followed by addition of $MoO_2(acac)_2$

(1.00 g, 3.10 mmol). The resulting red solution was refluxed for one hour when under continuous stirring. The volume of the solution was concentrated to about half under reduce pressure and left at room temperature when a orange-reddish precipitate is formed. The resulting precipitate was filtered off and the filtrate kept in an open flask at room temperature. After slow evaporation of the solvent suitable crystals for X-ray measurement were isolated. Yield: 0.72 g (1.99 mmol; 64 %).*Anal. for* $C_{12}H_{15}N_3O_4Mo$ (361.20): calcd. C 39.90, H 4.19, N 11.63; found C 40.20, H 4.16, N 11.55. $^1$H NMR (400 MHz, DMSO-$d_6$): $\delta$ = 2.06-2.14 (m, 2H, C$H_2$), 2.48-2.50 (m, C$H_2$C=N, overlap with the solvent signal), 3.15-3.16 (d, 3H, C$H_3$OH, $^2$J= 5.16 Hz)), 3.82-3.86 (t, 2H, C$H_2$C-N-Mo, $^3$J=6.86 Hz), 4.06-4.10 (quartet, 1H, $CH_3OH$, J=5.25 Hz), 6.79-6.98 (m, 2H, arom. C$H$), 7.36-7.40 (m, 1H, arom. C$H$), 7.53-7.55 (m, 1H, arom. C$H$), 8.47 (s, 1H, C$H$=N. $^{13}$C NMR (100 MHz, DMSO-$d_6$): $\delta$ = 25.4 ($CH_2$), 26.3 ($CH_2$C=N), 48.6 ($CH_3$OH), 58.3 ($CH_2$N–Mo), 118.1, 120.3, 120.8, 133.3, 133.6 (all arom.$C$H and $C$), 151.5 ($C$H=N), 160.2 (arom.$C$O–Mo), 176.5 ($C$=N) ppm. Selected IR data (cm$^{-1}$): $\nu$= 3436 (br, OH (MeOH)), 1606 (s, -C=N-N=C-), 930 and 909 (s, $MoO_2$).

**Synthesis of complex [$MoO_2$(salhyah)($CH_3OH$)] (17)**

To a solution of Schiff base ligand-$H_2$Salhyah×HCl (0.40 g, 1.40 mmol) in methanol (40 mL) was added one equivalent of NaOH (0.06 g, 1.40 mmol), followed by addition of $MoO_2(acac)_2$ (0.45 g, 1.40 mmol). The resulting clear orange solution was refluxed for 4 hours under continuous stirring. The hot solution was cooled down at room temperature and the solvent removed under strong vacuum. Initially an orange oil was formed which was slowly solidified to a yellow-orange powder. Yield: 0.12 g (0.29 mmol; 20 %). $^1$H NMR (400 MHz, DMSO-$d_6$): $\delta$ = 1.30-1.37 (m, 2H, C$H_2$), 1.51-1.63 (m, 4H, C$H_2$), 2.35 (t, 2H, C$H_2$CO, $^3$J= 7.60 Hz), 2.75 (t, 2H, C$H_2NH_3^+$, $^3$J= 7.60 Hz), 3.15, 3.16 (d, 3H, C$H_3$OH, $^2$J= 5.20 Hz), 4.05-4.09 (quartet, 1H, $CH_3OH$, J=5.60 Hz), 6.89-6.91 (m, 1H, arom. C$H$), 7.02-7.06 (m, 1H, arom. C$H$), 7.47-7.51 (m, 1H, arom. C$H$), 7.58 (br, 2H, N$H_2$) 7.65-7.67 (m, 1H, arom. C$H$), 8.72 (s, 1H, C$H$=N) ppm. $^{13}$C NMR (100 MHz, DMSO-$d_6$): $\delta$ = 25.1 ($CH_2$), 25.3 ($CH_2$), 26.6 ($CH_2$), 30.6 ($CH_2$CO), 38.7 ($CH_2NH_3^+$), 48.5 ($CH_3OH$), 118.5, 120.0, 121.5 (arom.$C$H and $C$), 134.1, 134.7 (arom.$C$H), 155.1 ($C$H=N), 159.3 (arom.$C$–OMo), 174.8 ($C$–OMo) ppm.

### 4.6.5 Reactivity of the *cis*-dioxovanadium(V) complexes

#### Spectrophotometric titration of complex 14 with $HClO_4$

1.05 mM stock solution of the vanadium complex was prepared by dissolving the complex ($VO_2$(Halhycab)(15.00 mg, 0.05 mmol) in DMF (50 mL). 200 $\mu$L were ulteriorly diluted with 2.8 mL DMF in the cuvette and used for measurements. The $HClO_4$ 9.2 M solution was diluted with DMF to a final concentration of 0.09 M and added in aliquots of 0.5 equivalents at 18 °C with continuous stirring. The spectra were collected from two to two minutes using as reference DMF (3mL). UV/Vis in DMF of complex + 2 equiv. $HClO_4$ ($\lambda_{max}$ in nm ($\varepsilon$ in $10^3$ $M^{-1}$ $cm^{-1}$)): 310 (8.5), 389 (5.0).

#### Spectrophotometric titration of complex 15 with HCl

1 mM stock solution of the vanadium complex was prepared by dissolving the complex ($VO_2$Salhyah)(33.0 mg, 0.1 mmol) in water (100 mL). 100 $\mu$L were ulteriorly diluted with 2.1 mL water in the cuvette and used for measurements. The aliquots of HCl (as is described in Protonation reaction section) were added from to 2 to 2 minutes under continuous stirring at 18 °C. Fitting of the experimental data have been performed on the titration with 5 and 10 equivalents of HCl, when the reaction was monitored by stepwise addition of 0.25 equivalents acid. UV/Vis of the aqueous mixture of complex + 10 equiv. HCl ($\lambda_{max}$ in nm ($\varepsilon$ in $10^3$ $M^{-1}$ $cm^{-1}$)): 212 (19.43), 287 (11.03), 370 (2.79).

#### Spectrophotometric titration of complex 15 with $H_2O_2$

1.2 mM stock solution of the vanadium complex was prepared by dissolving the complex ($VO_2$Salhyah)(10.0 mg, 0.03 mmol) in methanol (25 mL). 100 $\mu$L were ulteriorly diluted with 2.9 mL methanol in the cuvette and used for measurements. The $H_2O_2$ 30% solution was diluted with methanol to a final concentration of 25 mM and added in aliquots of 0.5 equivalents at 20 °C with continuous stirring. The spectra were collected from 2 to 2 minutes using as reference a mixture of $H_2O$ (50$\mu$l) and methanol (3mL). UV/Vis in $CH_3OH$ of complex + 10 equiv. $H_2O_2$ ($\lambda_{max}$ in nm ($\varepsilon$ in $10^3$ $M^{-1}$ $cm^{-1}$)): 278 (11.77), 288 (11.54), 315 (15), 392 (2.93).

### 4.6.6 Catalytic oxidative bromination of TMB

TMB (25 mg, 0.15 mmol) was dissolved in 10 mL DMF. 10 mL of stock solution of tetrabutylammonium bromide (48.3g/L) (1.5 mmol, 10 equiv.) was added, followed by addition of 1 mL of *cis*-dioxovanadium(v) complex and/or *cis*-dioxomolybdenum complex 0.15 mol% in DMF (0.015 mmol), $HClO_4$ (0.15 mmol) and $H_2O_2$ (0.15 mmol) in this order. Aliquots of the reaction (250 $\mu$L) were quenched in 2 mL of NaOH 0.002 M aqueous solution and extracted with 3 mL ethyl acetate. The reaction products were identified by gas-chromatography using the following temperature programme: 80 °C to 240 °C with a heating rate of 15 °C per minute, followed by 5 minutes holding of 240 °C temperature. The amount of formed Br-TMB was calculated by ratio with the unreacted TMB.

### 4.6.7 Catalytic oxidation of methyl phenyl sulfide

Vanadium and molybdenum complexes (0.025 mmol) were dissolved at room temperature in a mixture $CH_2Cl_2/CH_3OH$ 7:3 (25 mL) and phenyl methyl sulfide (0.29 ml, 2.5 mmol) was added. The resulting solution was cooled down on an ice-bath and $H_2O_2$ 26 % (1.2 equiv., 0.35 mL, 3 mmol) was added dropwise. The reaction solution was stirred at room temperature in a capped flask and monitored by gas-chromatography technique. After 16 and 18 hours, respectively the solvent was removed in vacuo and the products were separated by column chromatography on silica gel using diethyl ether/pentane 9:1 mixture for the unreacted sulfide and ethyl acetate for the corresponding sulfoxide.

# Chapter 5

# Vanadium(V) complexes based on N-salicylidene hydrazides that contain an guanidino-functionalized aliphatic side-chain

The guanidine functionality has a special importance from a biological and pharmacological point of view. First is a specific component of arginine, a protein amino acid hydrolyzed by arginase in the Krebs-Henseleit cycle and is responsible for detoxification of ammonia formed during the nitrogen catabolism of amino acids in organism via the formation of urea. An important role was also attributed to synthetic guanidino-amino acids, such as 3-guanidinopropionic acid which was reported to posses antidiabetic activity. The compound induces weight loss selectively from adipose tissue in obese animals with a non-insulin-dependent diabetes mellitus.[210] Moreover, N',N'-dimethylbiguanidine hydrochloride known as *metformin*, is used worldwide as hypoglycemic drugs for diabetes type 2, disease caused by a defective insulin utilization.[211,212] Vanadium complexes are also known as insulin-enhancing compounds.[9,213] In this direction a possible synergistic effect of vanadium complexes with *metformin* ligand has been studied. Although coordination of vanadium did not increase the effect of the biguanidine ligand by associative effects, the reported vanadium(IV)-metformin complex lowered the blood

glucose level similarly with previous reported bis(maltolato)-oxovanadium(IV) complex BMOV.[214] Here it is worth to mention that the BMOV complex is known as the most potent insulin-enhancing vanadium compound.[215]

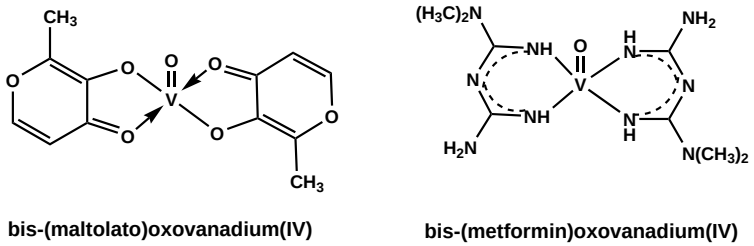


Figure 88: Vanadium complexes with insulin-like mimetic properties.

In addition, arginine is an important component of several enzymes, among these vanadium-containing haloperoxidases[38,70,128] and phosphatases.[66,97,216,217] In vanadium chloroperoxidase enzyme, two arginine residues are part of the active binding site[6] and they play an important role in catalytic reactions. The first one, Arg360 is hydrogen bonded to one of the equatorial oxygen atoms of the vanadate moiety and is supposed to compensate the negative charge of the vanadium atom through its protonated guanidinium site.[38] Mutagenesis studies performed on vanadium chloroperoxidase, by replacement of Arg360 with alanine, yielded a drastic decrease of the catalytic oxidation reaction of chloride to only 6%. Crystal structure determination of this active mutant showed a loss of hydrogen bonding rigidity around the prosthetic group which can be responsible for the loss of activity.[63,180] A vital role for the catalyzed oxidation reaction of chloride has been found for the second arginine residue, namely Arg490, which forms a salt bridge with an aspartate residue. The role of the aspartate residue is to maintain the arginine amino acid in a favorable conformation to be in hydrogen bonding interaction with the equatorial oxygen atoms of the vanadate group.[63] Alanine mutant, R490A showed no chloroperoxidase activity but still the mutant functioned as bromoperoxidase, able to catalyze the less electronegative bromide by hydrogen peroxide. To probe the role of the arginine residues in the reactivity of the prosthetic group, *cis*-dioxovanadium(V) complexes based on guanidino functionalized N-salicylidene hydrazide have also been isolated. Having into attention that a short aliphatic side-chain might increase the reactivity

of the vanadium complexes towards catalytic bromide oxidation by hydrogen peroxide, the synthesis of N-salicylidene guanidino acetic acid hydrazide has been performed. Alternatively, a direct guanilation reaction performed on a coordination compound, namely complex **15**, yielded the corresponding *cis*-dioxovanadium(V) complex which contains a 6-guanidino aliphatic side chain.

## 5.1 *cis*-Dioxovanadium(V) complex based on N-salicylidene guanidino acetic acid hydrazide hydrochloride ligand

The synthesis of the title ligand system follows the pathway described for the corresponding amino-functionalized N-salicylidene hydrazides depicted in Chapter 4, Figure 64. Starting from commercially available guanidino-acetic acid hydrochloride via intramolecular nucleophilic substitution, the corresponding guanidino-acetic methyl ester hydrochloride was isolated. This ester reacts stoichiometrically with hydrazine hydrate to form the corresponding 2-guanidino acetic acid hydrazide hydrochloride. The latter compound undergoes Schiff base condensation of the hydrazide site when reacted with salicylaldehyde, yielding the desired N-salicylidene guanidino acetic hydrazide as hydrochloride salt. Stoichiometric reaction of this new Schiff base ligand with ammonium metavanadate in refluxing methanol, yields the anionic *cis*-dioxovanadium(V) complex $[VO_2(salhyga)]$ (**18**). The compensation of the negative charge of the vanadate center is done by the positively charged guanidine functionality. This is a similar situation to one found in the *cis*-dioxovanadium(V) complex which contains an amino-functionalized side chain. Crystallization of **18** from a methanol-water mixture (1:1) afforded within less than a week suitable crystals for X-ray measurement. The molecular structure determination and numbering scheme for complex **18** is depicted in Figure 89.

The complex crystallize in the orthorhombic space group $P2_12_12_1$ with a five coordinated vanadium center in a distorted square pyramidal geometry. The angular parameter, $\tau$, has a value of 0.41 which makes the distortion to an ideal square pyramid larger and place the complex close to the edge for a trigonal bipyramidal geometry. Similar geometry

has been reported for a *cis*-dioxovanadium(V) complex derived from 2-acetyl-pyridyl-S-benzylidene-thiohydrazides, where a $VN_2SO_3$ moiety was formed.[187]

The tridentate chelate ligand coordinates in the typical dianionic form providing an ONO donor set, while the coordination sphere of the vanadium atom is completed by two oxo-groups almost symmetrical and in *cisoid* positions with the V=O bond length of around 163 pm. The vanadium to phenolate oxygen atom bond distance (V–O3), as well as the V–N1 bond length are similar with corresponding distances in previous described anionic *cis*-dioxovanadium(V) complexes with N-salicylidene hydrazide ligands. Instead the vanadium to iminole oxygen atom bond length (V–O4) is longer compared to previous described *cis*-dioxovanadium(V) to around 199.4 pm. The lengthening of this bond distance with about 4 pm is a consequence of a more conjugated system existent in complex **18**. Selected bond lengths and angles in complex **18** are given in Table 14. The enolization of the amide functionality is in agreement with observed 130 pm bond length for C8–O4 and further confirmed by partial double bond character of the C8–N2 bond of 129 pm.

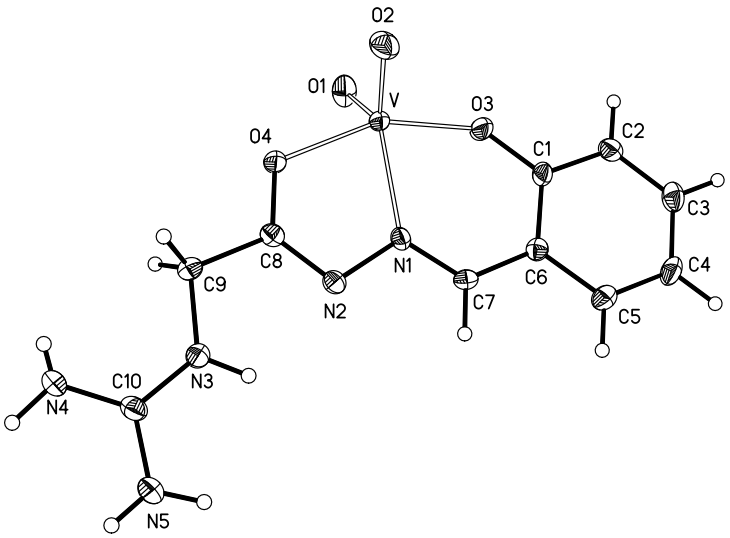


Figure 89: Molecular structure and numbering scheme of the complex $[VO_2(salhyga)]\cdot 3H_2O$ (**18**); displacement ellipsoids are drawn at 50% probability level).

Complex **18** crystalizes with three water molecules which form an extensive hydrogen bonding interaction with the double bonded oxygen atoms and guanidine group.

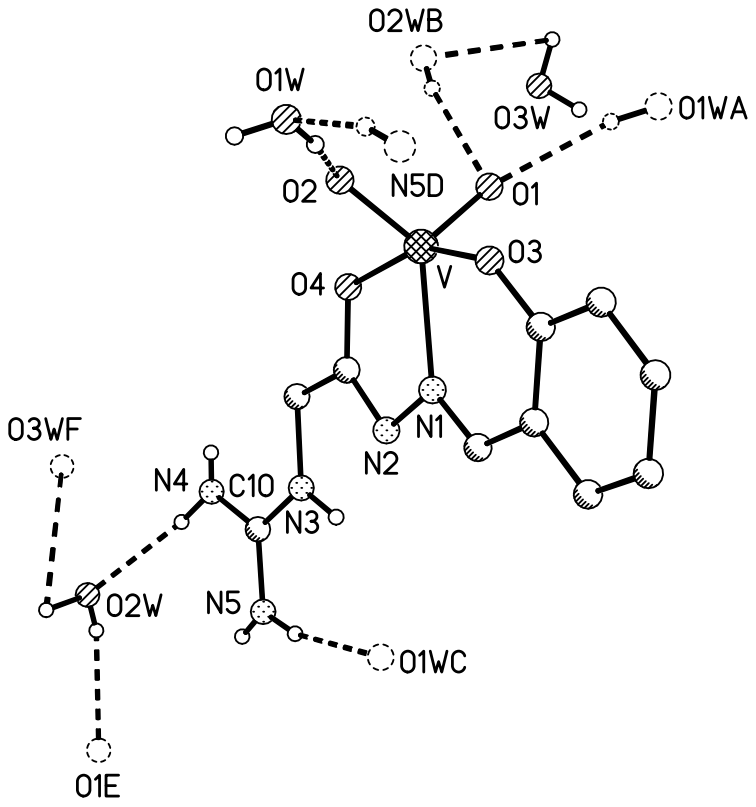


Figure 90: Schematic representation of hydrogen bonding interaction in complex $[VO_2(sahyga)]\cdot 3H_2O$ (**18**) (broken lines represent hydrogen bonds); relevant distances (in pm): O1···O1WA 279.7, O1···O2WB 278.0, O2WB···O3W 275.7, O2···O1W 278.3, O1W···N5D 293.4, O2W···N4 288.9, O1E···O2W 278.0, O3WF···O2W 275.7, N5···O1WC 293.4 (symmetry transformations: A : x-1, y, z; B: -x+2, 0.5+y, -0.5-z; C: x-0.5, -y-0.5, -z-1; D: 0.5+x, -0.5-y, -1-z; E: -x+2, y-0.5, -z-0.5, F: 1.5-x, -y, 0.5+z).

Both oxo groups are involved in intermolecular hydrogen bonding interactions with two different water of crystallization with the shortest bond length of 278 pm and the longest hydrogen bond distance of 279.7 pm (Figure 90). The observed strong hydrogen bonding interaction forms a two dimensional polymer along the [010] axis (Figure 91). The water molecules establish the intermolecular connection between the *cis*-dioxovanadate moieties through direct hydrogen bonding interaction with the doubly bonded oxygen atoms on one hand, and further by bifurcated hydrogen bonding interaction with guanidine functionality (OW···N4 288.9 and OW···N5 293.4 pm) and interstitial water molecules (OWB···OW 275.7 pm) (Figure 90).

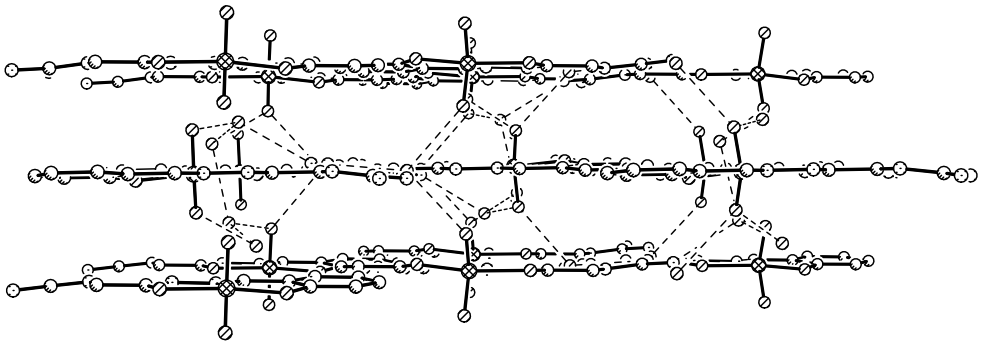

Figure 91: Representation of the hydrogen bonding network in crystals of complex $[VO_2(sahyga)]\cdot 3H_2O$ (**18**) (view along the [010] direction; broken lines represent hydrogen bonding interactions).

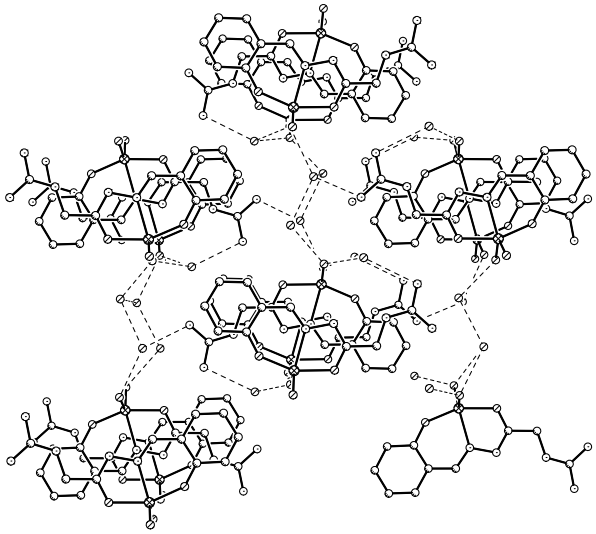

Figure 92: Representation of the hydrogen bonding network in crystals of complex $[VO_2(sahyga)]\cdot 3H_2O$ (**18**) as viewed along the [100] direction; broken lines represent hydrogen bonding interactions.

In the native form of vanadium-chloroperoxidase, interstitial water molecules were found near the Ser402 residue as well as in the vicinity of the apical oxygen atom of the vanadate moiety. The last mentioned solvent molecules form a long hydrogen bonded water channel. Thus, complex **18** presents a similar hydrogen bonding network established between water molecules, and additionally it contains a relevant side chain substitution which is also part of the hydrogen bonding network (Figure 92).

### 5.1.1 Spectroscopic studies

The determined crystal structure is also confirmed by spectroscopic characterization of the *cis*-dioxovanadium(V) complex, both in solid state as well as in solution. $^{51}$V NMR spectra recorded in DMSO-$d_6$ solution presents the resonance peak at -534 ppm ($\Delta\nu$=940 Hz) indicative of *cis*-$VO_2^+$ formation. The $^1$H NMR spectra of the free N-salicylidene 2-guanidine acetic acid hydrazide hydrochloride exhibits, as in all other previous cases, double sets of resonances at 8.32 and 8.48 ppm, respectively, associated to the azomethine protons due to the E-Z isomers in a ratio of 2.1:1. Furthermore, the methylene protons present also two sets of resonances in a shape of two dublets at 4.01-4.02 and 4.34-4.35 ppm due to the same isomerism effect manifested by the amide bound. The coordination of the vanadium atom is reflected in the down field shifts of the imine protons at 8.80 ppm as a single resonance; whereas the influence of the vanadate coordination to the $CH_2$ resonances is less drastic. A single multiplet centered at 4.05 ppm is observed in the $^1$H NMR spectrum of the complex consistent with the existence of one conformer of the amide functionality. However, the most indicative NMR isotope for a better differentiation between the free ligand and the coordinated one, is given by $^{13}$C NMR spectra. The most affected resonances are again corresponding to imine group. A deshielding effect of 14 ppm was observed in the $^{13}$C NMR spectra of the complex, whereas the phenol carbon atom and the iminol one are also shifted to around 164 ppm and 170 ppm comparing to around 157 and 168 ppm resonances in the free ligand. All the other carbon atoms are resonating in the expected region with insignificant differences. The IR spectra of the complex, performed as KBr pellets, present the specific $\nu(VO_2^+)$ stretching vibrations at 910 and 921 cm$^{-1}$ in accordance with precedent described characteristic IR vibrations. Additionally, the IR spectrum of both, the free ligand and the vanadium complex, presents rather broad bands at 3405-3390 and 3390-3211 cm$^{-1}$ attributed to the N–H stretching mode of the guanidine functionality. The IR spectra of the complex exhibits also the characteristic vibration corresponding to C=NH bands of the guanidine group, detected at 1668 and 1659 cm$^{-1}$, almost equal in intensity. The characteristic stretching vibration of the -CH=N–N=C- group, due to the enolization of the amide functionality on vanadium coordination is also seen at 1612 cm$^{-1}$ as a sharp

and strong band. Additionally, the IR spectra of the complex exhibits a broad band at 3524 $cm^{-1}$ due to the presence of water of crystallization. Selected IR data for both the free ligand and the *cis*-dioxovanadium(V) complex **18** are presented in the experimental part of the chapter. Thermogravimetric measurement, performed on the elementary analyzed complex $[VO_2(salhyag)]\cdot H_2O$, shows a 5.6% loss in weight in the temperature range 232-263 °C with no loss of weight up to this temperature. This loss corresponds to a calculated mass of 18.77 g which is around the molecular weight of a water molecule. This observation can be interpreted as a strong bonded water molecule which is present in the solid state form of complex **18** and it is based on the higher temperature required to loose its corresponding weight. Further heating up to 350 °C cause a loss of 9.13% corresponding to a calculated mass of 30.6 g. This last loss might be generated by decomposition of the guanidine functionality to the corresponding amino group.

## 5.2 *cis*-Dioxovanadium(V) complex based on N-salicylidene 6-guanidino hexanoic acid hydrazide

Stoichiometric reaction of *cis*-dioxovanadium(V) complex **15**, with 1-guanyl-3,5-dimethyl pyrazole nitrate in refluxing ethanol yields the corresponding guanidino-functionalized vanadium complex. The reaction takes place by direct guanilation of the amino functionality using a very reactive agents, such as guanyl-3,5-dimethylpyrazole. The actual reaction requires the formation of the free-base guanyl-3,5-dimethylpyrazole, by reaction of the corresponding nitrate compound with NaOH, followed by extraction with ethyl acetate. The guanilation reaction of the coordination compound **15** takes place under reflux and basic conditions.[218] The reaction leads to a yellow precipitate which represents the guanidine functionalized *cis*-dioxovanadium(V) complex, whereas the resulting pyrazole remains in solution. Attempts to use cyanamide as guanilation agent failed, while the S-methyl-isothiourea sulfate gave unsatisfactory results.

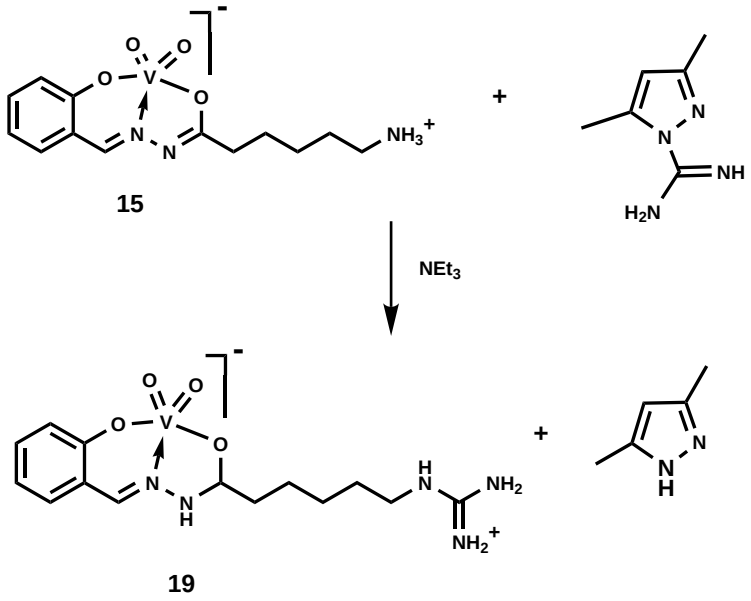


Recrystallization of the obtained *cis*-dioxovanadium(V) complex **19** from a mixture methanol-water yields yellow needle-shape crystals suitable for X-ray measurement. The molecular structure of complex **19** together with numbering scheme is depicted in Figure 93. The complex crystalizes in the monoclinic space group I2/a with the vanadium atom in a distorted square pyramidal geometry. The aromatic system and the hydrazide group lie in the one plane, whereas the vanadium atom is displaced out of this plane by 25 pm towards the apical oxygen atom. The distortion to an ideal square-pyramidal geometry is very small with a calculated $\tau$ value of 0.04. The Schiff base ligand maintains the coordination mode found in complex **15**. The vanadium to oxygen atom bond lengths and vanadium to nitrogen distance are also very similar with the corresponding distances found in the starting complex **15**. Selected bond lengths and angles in complex **19** are given in Table 14. The bond lengths N2–C8 and O4–C8 of the coordinated ligand system are consistent with the enolate form of the amide functionality and in good agreement with the bond distances found for the amino-substituted analog.

Due to the enolization of the ligand system, the resulting complex **19** has also an anionic character. Similarly to complex **18** the guanidine group is also protonated, compensating the negative charge of the *cis*-dioxovanadate moiety. Therefore, complex **19** retains very closely the characteristics of the starting compound **15**.

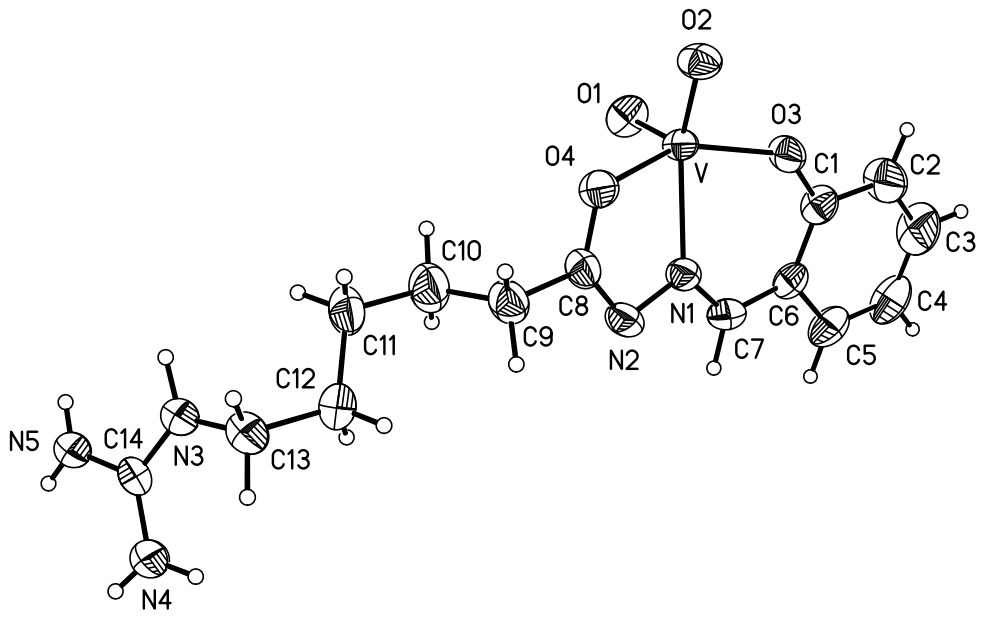


Figure 93: Molecular structure of $[VO_2(salhygh)]$ complex **19**; displacement ellipsoids are drawn at the 50% probability level.

Nevertheless, a slight different orientation of the guanidine substituted aliphatic side chain has been observed in complex **19** by comparison to the corresponding amino-substituted chain in complex **15**. This is illustrated by the torsion angle C8–C9–C10–C11 which has a value of 173° in complex **19** with the alkyl side chain orientated on the same side with the vanadate center; whereas in complex **15** the amino-substituted side chain is orientated on opposite direction with the torsion angle of 176°. This is also obvious by the overlay of the two molecular structures of complexes **15** and **19** (Figure 94) when a different orientation of the alkyl side chain of the ligand systems was observed. The overlay of the two molecular structures was done by method of least square refinement fitting the covalent parts of the two vanadium complexes, except the functionalized alkyl side-chain. This observation indicates the importance of the hydrogen bonding interactions patterns on the actual molecular structure.

However, complex **19** represents the first example of a coordination compound obtained via direct guanilation of another coordination compound. Therefore, it has been proved that functionalization of the aliphatic side chain in the N-salicylidene hydrazides is possible even, when a *cis*-dioxovanadium(V) complex is used as starting reagent.

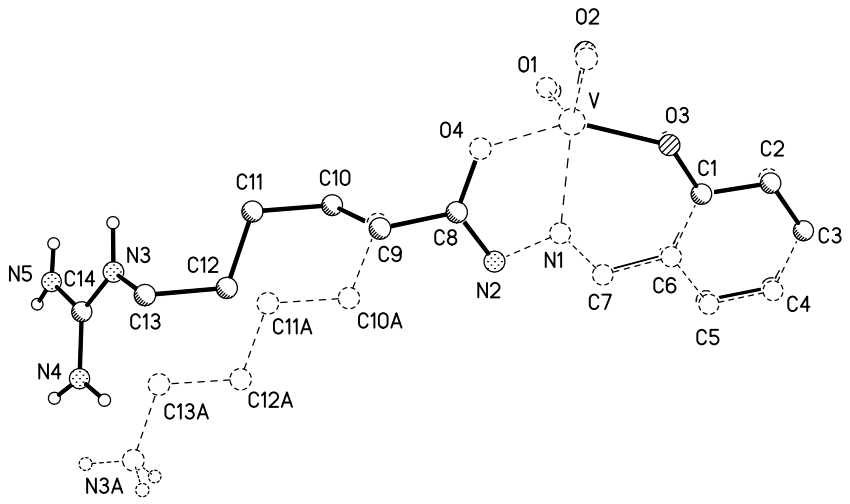


Figure 94: Overlay of the molecular structures of complex **19** (thick lines) and complex **15** (atom numbering extension A, broken lines) obtained by least-square refinement method on the coordinates of the atoms without the alkyl side-chains.

A very important role in native haloperoxidase enzymes is played by the arginine residues which compensate the negative charge on the vanadate moiety and is able to stabilize the prosthetic group by electrostatic interaction through hydrogen bonding interaction with the equatorial oxygen atoms. A similar situation has been found in complex **19** where the guanidine functionality of the aliphatic side-chain besides that compensates the negative charge of the *cis*-dioxovanadate center, it is also establishing hydrogen bonding interaction with the two oxo groups. The involvement of both oxo groups in hydrogen bonding interaction proved to be a general feature for the described anionic *cis*-dioxovanadium(V) complexes with N-salicylidene hydrazide ligands. In the case of complex **19**, the guanidine functionality establishes the hydrogen bonding contacts with the double bonded oxygen atoms. First, the equatorial oxo group O2 is in hydrogen bonding interaction with the acidic guanidine nitrogen atoms of similar chemical structure from two neighboring molecules (O2$\cdots$N5B 299.9 and O2$\cdots$N5C 282.6 pm). The apical double bonded oxygen atom O1 is hydrogen bonded to the other acidic guanidine nitrogen atom (O1$\cdots$N4A 285.6 ppm) which is further in hydrogen bonding contact with the hydrazide nitrogen atom N2 from another molecule (N4B$\cdots$N2 299.4 ppm) (Figure 95).

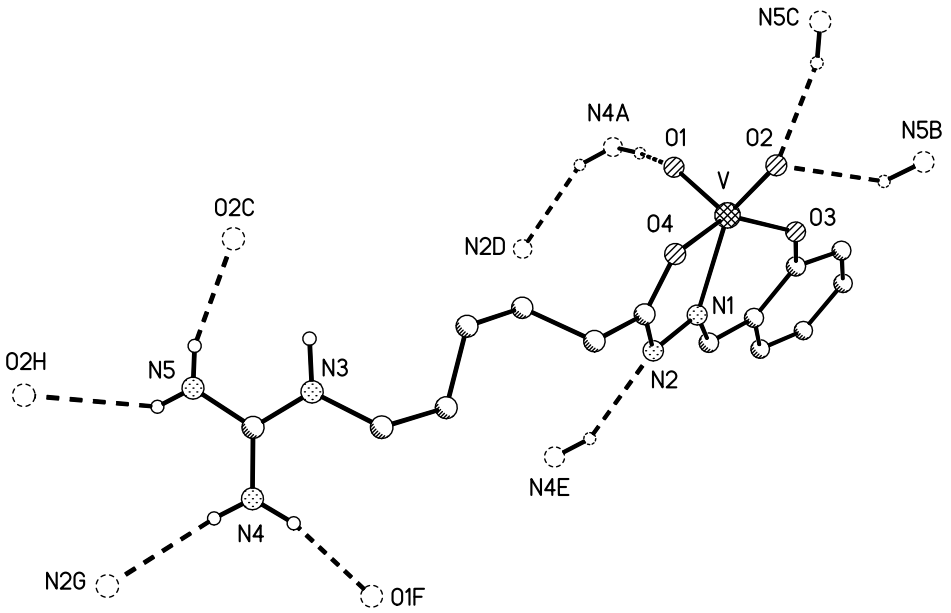


Figure 95: Schematic representation of hydrogen bonding interaction in complex $[VO_2(sahygh)]$ (**19**) (broken lines represent hydrogen bonds); relevant distances (in pm): O1···N4A 285.6, O2···N5B 299.9, O2···N5C 282.6, N4A···N2D 299.4 (symmetry transformations: A : x, -y-1.5, z+0.5; B: x-0.5, y-0.5, z+0.5; C: -x-1, -y-1, -z-1; D: -x-1, -y-1.5, -z-1; E: -x-1, y-0.5, -z-1.5, F: x, -y-1.5, z-1.5, G: -x-1, y+0.5, -z-1.5, H: x+0.5, y-0.5, z-1.5).

Table 14. Selected bond lengths (pm) and angles (°) for complexes **18** and **19**.

| | **18** | **19** | | **18** | **19** |
|---|---|---|---|---|---|
| V−O1 | 163.2(2) | 162.1(2) | V−N1 | 212.8(2) | 214.4(2) |
| V−O2 | 162.94(19) | 164.05(19) | C8−O4 | 130.1(3) | 129.4(3) |
| V−O3 | 188.34(19) | 190.00(19) | C8−N2 | 129.4(3) | 130.7(4) |
| V−O4 | 199.39(17) | 195.14(19) | N1−N2 | 1.407(3) | 140.0(3) |
| O1−V−O2 | 108.86(10) | 107.27(11) | O2−V−O3 | 97.86(12) | 95.45(9) |
| O1−V−O3 | 101.47(12) | 105.46(10) | O2−V−O4 | 92.84(12) | 92.39(9) |
| O1−V−O4 | 95.83(12) | 104.46(10) | O2−V−N1 | 130.75(11) | 147.69(10) |
| O1−V−N1 | 119.42(11) | 104.37(10) | O3−V−N1 | 82.30(8) | 82.16(8) |
| O3−V−O4 | 155.43(8) | 145.14(9) | O4−V−N1 | 74.00(7) | 73.41(8) |

### 5.2.1 Spectroscopic studies

The formation of complex **19** was also confirmed by spectroscopic characterization. Comparison of the $^{1}H$ and $^{13}C$ NMR patterns between the starting complex **15** and complex **19** confirmed the guanilation of the aliphatic side-chain. Specific guanidine resonances have been observed in both $^{1}H$ and $^{13}C$ NMR spectra, whereas the other groups resonate in similar positions with insignificant differences comparing with their resonances in complex **15**. The existence of the intact *cis*-dioxovanadate center is further established by $^{51}V$ NMR spectra which present a single resonance at -534 ppm ($\Delta\nu_{1/2}$ = 620 Hz) in deuterated DMSO solution, a resonance specific for $VO_2ONO$ entity. Furthermore, comparison of IR patterns of the two complexes sustains the proposed structure. Besides the specific IR frequencies characteristic for a *cis*-dioxovanadium moiety which appears at 937 and 893 $cm^{-1}$, there are also specific stretching vibrations of the guanidinium group. This vibrates at 3333 $cm^{-1}$ as a broad and irregular band, due to their involvement in hydrogen bonding interaction. The C=NH vibration was also detected at 1664 $cm^{-1}$, as a strong band.

## 5.3 Oxidative bromination of 1,3,5-trimethoxybenzene

The capacity of the *cis*-dioxovanadium(V) complexes based on guanidine-functionalized N-salicylidene hydrazide system to catalyze the oxidation of bromide by $H_2O_2$ has been performed following the previuos established catalytic system. The monitoring of the reaction was achieved by GC analysis of the ethyl acetate extracts which contain only TMB and bromo-TMB compounds. The results of the catalytic reaction are summarized in Table 15. From the entries, it is clear that the *cis*-dioxovanadium(V) complex based on N-salicylidene 2-guanidino acetic acid hydrazide $[VO_2(salhyga)]\cdot H_2O$, is the most potent catalyst for the oxidative bromination reaction. The complex catalyze the oxidation of bromide by $H_2O_2$ with a turnover rate of 75 mol product$\times$(mol catalyst$\times$h)$^{-1}$ when $HClO_4$ is added in stoichiometric amounts. This catalytic activity is net superior not only compared to similar complex **19**, but is also more efficient compared to all previous described *cis*-dioxovanadium(V) catalysts based on N-salicylidene hydrazides.

Table 15. Catalytic oxidation experiments using anionic *cis*-dioxovanadium(V) complexes-**18** and **19** as catalysts. The results are given in % Br-TMB obtained and as $\mu$mol Br-TMB within parenthesis.

| Complex | 2 min. | 5 min. | 10 min. | TON |
|---|---|---|---|---|
| 1. $[VO_2(salhyga)]$ (**18**) | 25.0(37.5) | 62.0(93.0) | 75.4(113.1) | 75 |
| 2. $[VO_2(salhygh)]$ (**19**) | 15.5(23.3) | 51.7(77.5) | 67.1(100.6) | 63 |

Note: The turnover number was calculated, as in all other cases, for 5 minutes reaction time.

The increase of the catalytic activity of complex **18** is indicative of an increased reactivity of the vanadate center. The Schiff base ligand behaves as a conjugated system with a high electron delocalization which will increase the reactivity on the metal center. The guanidine part of the ligand system presents strong electron withdrawing effect responsible for the electronic density decrease on the vanadate site and therefore, an increased reactivity of *cis*-dioxovanadium complex **18**. Nevertheless, it seems that the guanidine substitution of the aliphatic side chain has in general, a potent effect on the activation of vanadate moiety. The catalytic reaction proceed very fast in the first 5 minutes compared with previous described catalysts. The increased basicity of the guanidine functionality might enable the increased Lewis acid properties of the *cis*-dioxovanadium(V) center. This observation is in agreement with the observed important role of the hydrogen bonding interaction of the prosthetic group with the nearby arginine residues in vanadium chloroperoxidase enzyme.

## 5.4 Oxidation of sulfides catalyzed by *cis*-dioxovanadium(V) complexes based on guanidine functionalized N-salicylidene hydrazides

The new *cis*-dioxovanadium(V) with N-salicylidene hydrazide that contain a guanidino-functionalized side chain to function as catalyst for the oxidation of methyl phenyl sulfide when hydrogen peroxide is used as oxidant was also investigated. Following the typical

procedure described in Chapter 3, 1 mol-% catalyst have been used for the reaction with a slight excess (1.2 equivalents) of hydrogen peroxide, in a mixture $CH_2Cl_2/CH_3OH$ 7:3. The reaction was monitored qualitatively using thin layer chromatography technique comparing the $R_f$ values of the reaction mixture with standard solution of phenyl methyl sulfide and its sulfoxide. After 18 hours of reaction when the amount of sulfide decreased apparently, the reaction was assayed by GC determination. Comparison between areas of the two organic products yielded 85% sulfoxide when complex **18** was used as catalyst, whereas 82% conversion was established by the catalyst **19**. This results are similar with previous found catalytic activity of complex **15** and also similar with reported capacity of vanadium complexes to catalyze the sulfur oxidation reaction.[189–192] Therefore it can be concluded that *cis*-dioxovanadium(V) complexes with intact N-salicylidene hydrazide ligand catalyze the oxidation of organic sulfide following a common reaction pathway.

## 5.5 Conclusions

*cis*-Dioxovanadium(V) complexes with a $O_4N$-coordination environment have been synthesized and characterized. These complexes contain a guanidine functionalized aliphatic side chain and therefore, they can model the hydrogen bonding interaction of the prosthetic group of the native enzymes with the arginine residues. A different reactivity of these complexes towards catalytic bromide oxidation has been observed as a consequence of a different aliphatic chain length. Using N-salicylidene acetic acid hydrazide hydrochloride as ligand system, the resulting anionic *cis*-dioxovanadium(V) complex proved to function as the most potent catalyst of the enzymatic reaction. The increased reactivity of complex **18** might be a consequence of the electron delocalization found in the ligand system. Furthermore, the first example of a direct guanilation reaction of a coordination compound has been also described. Starting from the anionic *cis*-dioxovanadium(V) complex that contains an amino-functionalized side-chain, via reaction with 1-guanyl-3,5-dimethylpyrazole in basic medium, the corresponding guanidino-functionalized dioxovanadium(V) complex was obtained. The latter vanadium complex is also able to catalyze efficiently the oxidative bromination of 1,3,5-trimethoxybenzene. Moreover, both *cis*-dioxovanadium(V) complexes described herein catalyze the sulfoxidation reaction sim-

ilarly with the corresponding vanadium complex which contains an amino-functionalized aliphatic side chain.

## 5.6 Experimental Section

**Materials:** Methanol was dried using sodium/bezophenone system. All other reagents were used as received, without further purification. Abbreviations used throughout the text: $H_2$salhyga = 2-guanidino acetic acid (2-hydroxy-benzylidene) hydrazide hydrochloride, salhygh = 6-guanidino hexanoic acid (2-hydroxy-benzylidene) hydrazide.

### Synthesis of 2-guanidino-acetic acid methyl ester hydrochloride

A mixture of guanidino-acetic acid (4.03 g, 34.4 mmol) and $SOCl_2$ (50 mL) was stirred at room temperature for around 24 hours. The resulting solution was cooled down at -70 °C and dried methanol (150 mL) was added dropwise with a permanent control of temperature. After the addition of methanol was finished the resulting solution was stirred for an additional 15 minutes at -70 °C and then warmed slowly at room temperature. The volume of the solution was reduced under vacuum to around 1/4 and diethylether (150 mL) added for precipitation of the ester. A colorless solid is formed which is washed with diethylether and dried under strong vacuum. Yield: 1.30 g (7.75 mol; 22.5 %). $^1$H NMR (200 MHz, DMSO-$d_6$): $\delta$ = 3.65 (s, 3H, C$H_3$), 4.06-4.09 (m, 2H, C$H_2$), 7.54 (br, 2H, N$H_2$), 7.86 (t, 1H, N$H\times$HCl), 8.95 (br, 2H, N$H$) ppm. $^{13}$C NMR (50 MHz, DMSO-$d_6$): $\delta$ = 42.5 ($C$H$_2$), 48.3 ($C$H$_3$ (MeOH)), 52.2 ($C$H$_3$), 157.9, 158.9 (both $C$H-N), 169.4 ($C$=NH×HCl), 172.7 ($C$=O).

### Synthesis of 2-guanidino acetic acid hydrazide hydrochloride

To a solution of methyl 2-guanidino-acetic ester hydrochloride (1.20 g, 7.16 mmol) in absolut ethanol (40 mL), hydrazine hydroxide 100 % (0.39 g, 0.37 mL, 7.79 mmol) was added, followed by addition of other 10 mL ethanol. The resulting solution was refluxed with stirring for 24 hours. After cooling at room temperature, the solvent was removed under reduce pressure when an oily compound is formed. After extraction two times with hot absolut ethanol (10 mL) a colorless solid is formed. Yield: 1.20 g (6.70 mol; 94 %).

$^1$H NMR (400 MHz, DMSO-d$_6$): $\delta$ = 1.01 (t, 3H, C$H_3$ (EtOH)), 3.39 (q, $H_2$ (EtOH)), 3.40-4.20 (m, 4H, C$H_2$ and N$H_2$), 7.34 (br, 3H, N$H_2$ and N$H$×HCl), 7.74 (b, 1H, N$H$) ppm. $^{13}$C NMR (100 MHz, DMSO-d$_6$): $\delta$ = 18.5 (C$H_3$ (EtOH)), 42.4 and 49.1 ($C$H$_2$), 56.0 ($C$H$_2$ (EtOH)), 157.4, 157.7 (both $C$H-N), 169.7 ($C$=O). MS (EI in MeOH): m/z = 130 [M - H$^+$ - HCl](100%), 99 [(NH=C-NH (NH$_2$)-CH$_2$CO)]$^{2-}$(20%), 37 [HCl] (80%).

## Synthesis of N-salicylidene 2-guanidino-acetic acid hydrazide hydrochloride ($H_2$salhyga×HCl)

To a solution of 2-guanidino acetic acid hydrazide hydrochloride (1.10 g, 6.56 mol) in refluxing absolut ethanol (50 mL), salicylaldehyde (0.80 g, 6.56 mol, 0.70 mL) was added dropwise. The resulting yellow solution was refluxed overnight. After cooling down at room temperature a colorless solid precipitates. The solid was filtered off while the solvent of the filtrate removed under reduce pressure. Yield: 0.85 g (3.00 mol; 45 %). *Anal. for* C$_{10}$H$_{13}$N$_5$O$_2$Cl×H$_2$O (289.72): calcd. C 41.46, H 5.57, N 24.17; found C 41.40, H 5.64, N 23.76. $^1$H NMR (400 MHz, DMSO-d$_6$): $\delta$ = 3.33 ($H_2$O), 4.01-4.04 and 4.34-4.35 (d, total 2H, C$H_2$), 6.82-6.94 (m, 2H, arom. C$H$), 7.20-7.29 (m, total 2H, arom. C$H$ (1H) and N$H$ guanidine (1H)), 7.40 (br, 2H, N$H_2$), 7.50-7.52 (2H, CH=N$H$ guanidine), 7.73-7.75 (m, 1H, arom. C$H$), 8.32 and 8.48 (s, total 1H, C$H$=N, ratio 1:0.5), 10.12, 10.99, 11.62 and 12.17 (N$H$, O$H$, total 2H in ratio 1.0:0.5:1.0:0.5) ppm. $^{13}$C NMR (50 MHz, DMSO-d$_6$): $\delta$ = 42.4, 42.6 (both for $C$H$_2$CO), 116.1, 116.3, 118.6, 119.2, 119.9, 126.2, 128.9, 131.1, 131.3 (all arom. $C$H and $C$), 141.3, 147.0 (both $C$H=N), 156.4, 157.2, 157.5, 157.7, (arom. $C$-OH), 163.9 (guanidine $C$=NH), 168.5 ($C$=O) ppm. Selected IR data (cm$^{-1}$): $\nu$= 3587 (H$_2$O), 3404 (NH$_2$ guanidine), 3330 (br, NH guanidine), 3178 (br, NH), 1663 (s, C=O), 1640 (s, HC=N, guanidine), 1616 (-CH=N). ESI-MS (positive mode in MeOH): m/z = 236.1 [M + H$^+$ - HCl] (100%), 258.0 [M + Na - HCl] (10%). ESI-MS (negative mode in MeOH): m/z = 236.2 [M + H$^+$ - HCl] (90%), 293.0 [M + Na - H$^+$] (100%).

## Synthesis of *cis*-dioxovanadium(v) complex $[VO_2(salhyga)]\cdot H_2O$ (18)

To a solution of Schiff base ligand-$H_2$Salhyga×HCl (0.5 g, 1.84 mmol) in methanol (50 mL) was added $NH_4VO_3$ (0.22 g, 1.84 mmol) when a brown colored mixture was formed. The resulting mixture was refluxed for around 4 hours when a yellow precipitate was formed. The volume of the filtrate solution was concentrated to about half under reduce pressure and left at room temperature when aditional yellow precipitate is formed overnight. Recrystallization of the yellow precipitate from methanol:water mixture afforded suitable crystals for X-ray measurement. Yield: 0.32 g (0.95 mmol; 52 %).*Anal. for* $C_{10}H_{14}N_5O_5V$ (335.19): calcd. C 35.83, H 4.21, N 20.89; found C 35.89, H 4.35, N 20.43. $^1$H NMR (400 MHz, DMSO-$d_6$): $\delta$ = 3.36 (br, $H_2O$), 4.08-4.09 (m, 2H, C$H_2$), 6.75-6.76 (m, 2H, arom. C$H$), 7.18 (br, N$H_2$), 7.32 (t, 2H, $NH_2^+$), 7.51-7.53 (m, 2H, arom. C$H$), 7.59 (br, 1H, N$H$), 8.80 (s, 1H, C$H$=N) ppm. $^{13}$C NMR (50 MHz, DMSO-$d_6$): $\delta$ = 41.7 ($C$H$_2$), 116.8, 119.5, 132.7, 133.4 (all arom. $C$H and $C$), 156.1 ($C$=$NH_2^+$), 157.0 ($C$H=N), 164.5, (arom. $C$–OV), 170.7 ($C$–OV) ppm. $^{51}$V NMR (105 MHz, DMSO-$d_6$): $\delta$ = -534.3 ppm ($\Delta\nu_{1/2}$ = 940 Hz). Selected IR data ($cm^{-1}$): $\nu$= 3525 (br, $H_2O$), 3390 (br, $NH_2$ guanidine), 3281 (br, NH guanidine), 1668, 1659 (s, -CH=N guanidine), 1612 (s, -CH=N–N=C-), 910 and 921 (s, $VO_2$). ESI-MS (negative mode in MeOH): m/z = 316.0 [M + $H^+$] (100%), 633.0 [2M - $H^+$] (70%).

## Synthesis of complex $[VO_2(salhygh)]$ (19)

To 100 mL NaOH 1M aqueous solution was added 1-guanyl-3,5-dimethylpyrazole nitrate (4.90 g, 24.40 mmol). The resulting clear solution was stirred at room temperature for 15 minutes and the formed free base extracted three times with ethyl acetate (100 mL). The organic extracts were dried over $Na_2SO_4$ and the solvent removed under reduced pressure. The resulting residue was redissolved in $H_2O$ (20 mL) and complex **15** (1.65 g, 5.00 mmol) was added followed by 150 mL ethanol and triethylamine (1.40 mL, 9.80 mmol). The clear solution was refluxed under stirring for 4 hours, when a yellow precipitate was formed. This precipitate was filtered off and dried in vacuo. Yield: 1.43 g (3.83 mmol; 77.5 %). *Anal. for* $C_{14}H_{20}N_5O_4V$ (373.28): calcd. C 45.05, H 5.40, N 18.76; found C 44.99, H

5.42, N 18.62. $^{1}$H NMR (400 MHz, DMSO-$d_6$): $\delta$ = 1.30-1.33 (m, 2H, C$H_2$), 1.47-1.50 (m, 2H, C$H_2$), 1.57-1.61 (m, 2H, C$H_2$), 2.27 (t, 2H, C$H_2$CO, $^{3}$J= 6.77 Hz), 3.07-3.11 (m, 2H, C$H_2$NH), 6.72-6.74 (m, 2H, arom. C$H$), 6.91 (br, 5H, N$H$ and N$H_2$), 6.27-7.29 (m, 1H, arom. C$H$), 7.46-7.48 (m, 1H, arom. C$H$), 8.74 (s, 1H, C$H$=N) ppm. $^{13}$C NMR (50 MHz, DMSO-$d_6$): $\delta$ = 25.3 ($C$H$_2$), 25.6 ($C$H$_2$), 27.9 ($C$H$_2$), 26.6 ($C$H$_2$), 31.6 ($C$H$_2$CO), 38.2 ($C$H$_2$-guanidine), 116.5, 119.1, 119.7 (arom.$C$H and $C$), 132.2, 132.7 (arom.$C$H), 154.2 ($C$=NH$_2^+$), 156.5 ($C$H=N), 164.2 (arom.$C$–OV), 175.9 ($C$–OV) ppm. $^{51}$V NMR (105 MHz, DMSO-$d_6$): $\delta$ = -533.8 ppm ($\Delta\nu_{1/2}$ = 620 Hz). ESI-MS (positive mode in MeOH): m/z = 355.8 [**15** + Na] (35%), 395.8 [M + Na] (100%), 729.1 (20%), 768.8 [2M + Na] (80%). Selected IR data (cm$^{-1}$): $\nu$= 3334 (s, NH$_2^+$), 3164 (br, NH), 1664 (s, C=NH guanidine), 1613 (s, -CH=N-N=C-), 937 and 893 (s, $VO_2$).

## Catalytic oxidative bromination of TMB

TMB (25mg, 0.15 mmol) was dissolved in 10 mL DMF. 10 mL of stock solution of tetrabutylammonium bromide (48.3g/L) (1.5 mmol, 10 equiv.) was added, followed by addition of 1 mL of *cis*-dioxovandium(V) complex 0.15 mol% in DMF (0.015 mmol), $HClO_4$ (0.15 mmol) and $H_2O_2$ (0.15 mmol) in this order. Aliquots of the reaction (250 $\mu$L) were quenched in 2 mL of NaOH 2 mM aqueous solution and extracted with 3 mL ethyl acetate. The reaction products were identified by gas-chromatography using the following temperature programm: 80 °C to 240 °C with a heating rate of 15 °C per minute, followed by five minutes holding of 240 °C temperature.

## Catalytic oxidation of methyl phenyl sulfide

Vanadium complex (0.025 mmol) was dissolved at room temperature in a mixture $CH_2Cl_2$-$CH_3OH$ 7/3 (25 mL) and phenyl methyl sulfide (0.29 ml, 2.5 mmol) was added. The resulting solution was cooled down on an ice-bath and $H_2O_2$ 26 % (1.2 equiv., 0.35 mL, 3 mmol) was added dropwise. The reaction solution was stirred at room temperature in a capped flask and monitored by thin layer chromatography using as eluent a mixture of ethyl acetate/chloroform/methanol-5:10:3 (v/v/v)). After 18 hours 1 $\mu$L of the solution mixture was assayed by gas-chromatography technique. Temperature programm: 55 °C

hold for one minute, then increasing with a heating rate of 15 °C per minute until 200 °C followed by heating rate of 15 °C per minute until 240 °C.

# Chapter 6

# Binuclear vanadium(V) and molybdenum(VI) complexes as catalysts for sulfoxidation reaction

Transition-metal complexes are of general use as catalysts for the oxidation reactions of various organic substrates.[201] Among these reactions, the oxidation of sulfides to the corresponding sulfoxides has attracted a renewed attention. Compounds containing chiral sulfoxide moiety are useful intermediates for the synthesis of chemically and biologically significant molecules.[86] The procedures for synthesis of enantiopure sulfoxides involve either the synthesis of a sulfinylating agent which contains an electrophilic sulfur site capable to react with an organometallic compound[219–221] and/or the asymmetric oxidation of the commercially available prochiral sulfides. The last method is based on direct oxidation by use of enantiomerically pure oxidant[222–224] and more appealing possibility is the use of prochiral oxidants and a chiral catalyst. While the first approach requires expensive and unstable oxidation agents, a most efficient method to prepare sulfoxides is represented by catalytic reaction utilizing metal complexes. The reported systems able to perform the asymmetric oxidation of sulfides, involve mainly complexes of titanium,[225,226] chromium,[227,228] manganese,[229] iron[230,231] and rhenium.[232,233] More recently vanadium complexes have also been reported as competitive catalysts of sulfoxidation reaction[189,193,234–236] whereas enzymatic systems such as vanadium haloper-

oxidases are known as catalyst capable of catalyzing enatioselctively sulfide oxidation reaction.[87,89,90,175] The first report of a vanadium-catalyzed asymmetric sulfoxidation reaction date from 1986. The system was developed by Fujita and is based on a vanadium(IV) complex, whereas phenyl methyl sulfide was used as substrate.[237] The catalytic system used cumyl hydroperoxide as oxidant and dichlormethane as reaction solvent and it afforded 96% sulfoxide after 120 hours reaction time. Subsequently, Bolm reported a highly selective vanadium catalyst based on bulky chiral Schiff base ligand formed between tert-butyl salicylaldehyde derivatives and tert-leucinol.[191] In the later case the catalyst was generated in situ between vanadyl acetylacetonate and the Schiff base ligand. Using 1 mol% catalyst, 94% yield had been achieved after 16 hours.[191] Although in both cases a high enantiomeric excess has been reported, varying from 85% *ee* in the first case[237,238] to maximum 70% in Bolm's system, a very long reaction time was required in both cases for a high conversion of phenyl methyl sulfide. Bolm's catalytic procedure, based on hydrogen peroxide has the advantage of inexpensive and environmentally benign oxidant. Therefore, this catalytic system has been adopted and optimized for different substrates. For instance, Ellman et al. achieved 98% conversion with 91% e.e. in the asymmetric oxidation of tert-butyl disulfide.[239,240] Furthermore, the same catalytic conditions were also applied to iron complexes.[241] By comparison with vanadium system, the iron complex was reported as less effective catalyst and required additives for an increase of the reaction yield.[242] Later reports of vanadium complexes able to catalyze the sulfide oxidation reaction are known, but in majority of the cases the reaction time varies from 16 to 24 hours.[189,190,192] Therefore, the development of a catalyst, able to catalyze the sulfoxidation reaction more efficiently is a final goal. Based on the fact that two metal centers will be more effective than a single one, binuclear *cis*-dioxovanadium(V) and *cis*-dioxomolybdenum(VI) complexes with *bis*-N-salicylidene hydrazide ligands have been designed. The Schiff base ligands were obtained following the reported described procedure,[243] with small modification regarding the excess of hydrazine hydrate used for hydrazinolysis of the diacid esters. In the first step of the reaction the di-aliphatic esters were reacted with a slight excess (2.5 equivalents) of hydrazine hydrate solution when the *bis*-carbonic acid hydrazides were obtained quantitatively as very pure compounds. In the second step Schiff base reaction with salicylaldehyde yielded the desired

*bis*-N-salicylidene hydrazides ($H_4Ln$). The ligand system, $H_4Ln$, may be considered as two N-salicylidene hydrazides linked via a methylene chain of variable length. There are potentially four ionizable protons, two from the phenol site and two from the amide moieties, respectively. By analogy with previous described N-salicylidene hydrazides ($H_2L$), the $H_4Ln$ ligands can potentially act as hexadentate chelate system, binding two metal ions, one in each tridentate cavity. Schematic representation of the ligand system and its tautomeric form are represented in Figure 96.

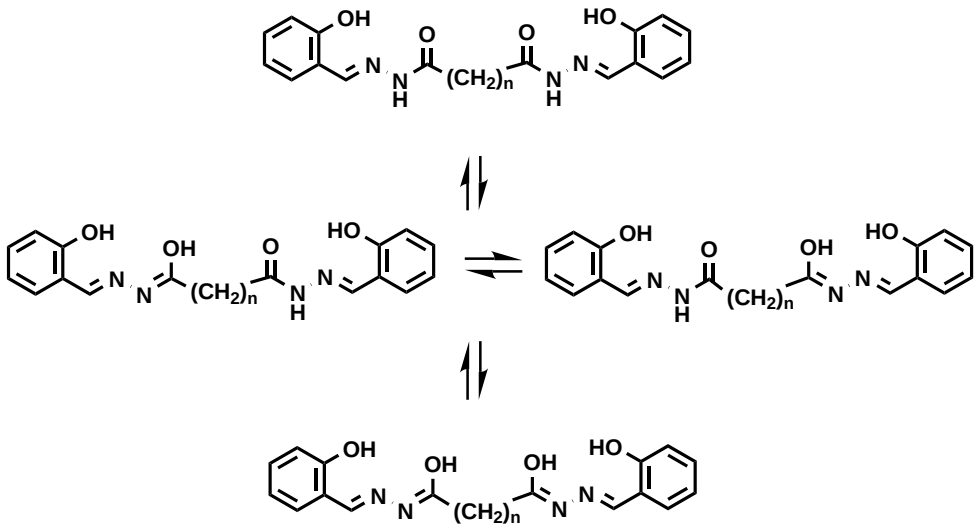

Figure 96: Schematic representation of *bis*-N-salicylidene hydrazide ligands and its tautomeric forms.

The *bis*-N-salicylidene hydrazide ligands exhibit also diverse isomerization possibilities. The first isomers, detected in NMR spectra, both in $^1H$ and $^{13}C$ NMR spectrum are the E and Z isomers of the azomethine bond. A similar isomerism is caused by the amide functionality which also permits the rotation around the partially double bound NH=C-OH. A third possible set of isomers, not NMR detectable can appear in *bis*-N-salicylidene hydrazides of succinic acid, where the methylene bridge makes possible *syn* and *anti* orientation of the two Schiff base conjugated cavities. The synthesis of vanadium and molybdenum complexes with these Schiff base ligand systems follows the previous described procedures.

## 6.1 Binuclear *cis*-dioxovanadium(V) complexes with *bis*-N-salicylidene hydrazides

Reaction of the Schiff base ligands with ammonium and/or potassium metavanadate in a 1:2 ratio, yields the anionic binuclear *cis*-dioxovanadium(V) complexes as ammonium and/or potassium salts, respectively. *bis* N-salicylidene hydrazide derived from glutaric and adipic acids were used as ligands to prepare the anionic vanadium complexes. A binuclear *cis*-dioxovanadium(V) obtained with *bis*-N-salicylidene oxalic acid dihydrazide has been crystallographically characterized.[244] In this case the two *cis*-dioxovanadium(V) moieties were reported to be in *trans* position to each other. Most likely the similar vanadium complexes obtained with *bis*-N-salicylidene hydrazide of adipic acid have a similar orientation of the two metal centers due to the zigzag conformation of the methylene chain. On the other hand, when *bis*-N-salicylidene hydrazide of glutaric acid has been used as ligand system, the two *cis*-dioxovanadate centers are, most likely, in *cis* position to each other. This is based on crystallographical characterization of a similar binuclear *cis*-dioxomolybdenum complex containing the latter ligand (Chapter 6.2).

The herein described vanadium complexes have been spectroscopically characterized. Their spectroscopic data are in good agreement with the similar reported binuclear anionic vanadium complex.[244] Therefore, the *bis*-Schiff base ligands accommodate two *cis*-$VO_2^+$ units, each in one cavity as depicted in Figures 97 and 98, respectively.

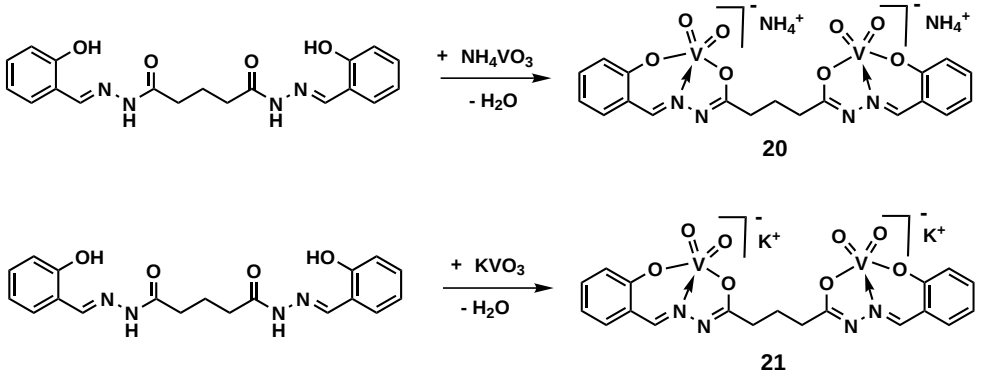


Figure 97: Schematic representation of *cis*-dioxovanadium(V) complex with *bis*-N-salicylidene hydrazide of glutaric acid.

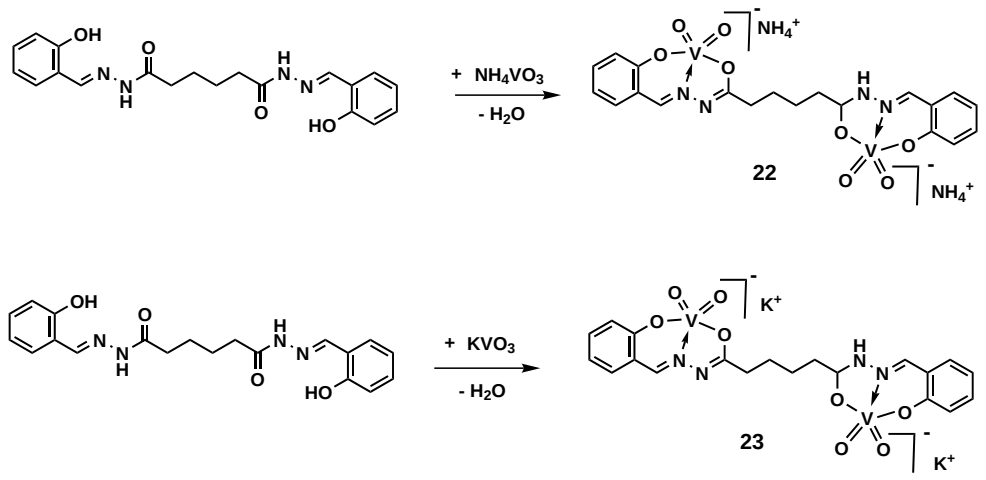


Figure 98: Schematic representation of *cis*-dioxovanadium(V) complex with *bis*-N-salicylidene hydrazide of adipic acid.

The formation of the *cis*-dioxovanadium moieties was confirmed by $^{51}$V NMR recorded in deuterated DMSO solution. The ammonium salts of the binuclear dioxovanadium complexes exhibit a single resonance at -534 ppm, whereas the potassium salts resonate at around -532 ppm. This resonances are similar with previous characterized *cis*-dioxovanadium(V) complexes with N-salicylidene aliphatic acid hydrazides. No big influence of the counter ions to the vanadium resonances has been observed. It is known that the vanadium center resonates in general according with the donor atoms which are directly involved in its coordination sphere.[11] A different width at half height of the $^{51}$V resonances (>840 Hz) has been detected comparing to previous described mononuclear *cis*-dioxovanadium complexes. This is a consequence of the interaction between the two vanadium nuclei which leads to a broadening of the signal. Therefore, a shorter methylene bridge between the two vanadium centers caused an increase of the width at half height with around 20-30 Hz. Comparison between $^{1}$H NMR patterns of the free ligand and the $^{1}$H NMR spectra of the complexes supports the formation of binuclear *cis*-dioxovanadium(V) complexes. In both, potassium and ammonium salts of the herein described *cis*-dioxovanadium(V) complexes no specific N*H* and O*H* proton resonances have been detected. This indicates that bonding of vanadium atoms occurs through the phenolate and iminole groups. A downfield shift for the azomethine (–CH=N–) protons

signal in $^{1}$H NMR spectra of the complexes relative to the corresponding free ligands supports the coordination of the azomethine nitrogen atoms. The involvement of the imine nitrogen atoms in the coordination of vanadium is also illustrated by existence of a single isomer of these double bonds with the protons resonating as singlet at around 8.77 ppm. The enolization of the amide functionality on vanadium coordination is in agreement with the upfield resonances of the methylene protons next to amide group. The aromatic protons and other methylene protons appear in the expected regions in $^{1}$H NMR spectra of the complexes with insignificant differences in the chemical shifts compared to their resonances in the $^{1}$H NMR of the free ligands. The most indicative NMR measurement that proves the ligation of the Schiff base ligands is represented by $^{13}$C NMR recording. A comparison between $^{13}$C NMR spectra of the ligand and of the corresponding anionic complexes is shown in Figure 99. Phenolate ligation is confirmed by downfield $^{13}$C resonances on going from ligand to metal complexes. Similarly, the azomethine (–CH=N–) carbon atoms have down field resonances of around 15 ppm as a consequence of their involvement in coordination. Further on, the methylene carbons adjacent to the iminole functionality have downfield resonances, although this effect is less dramatic.

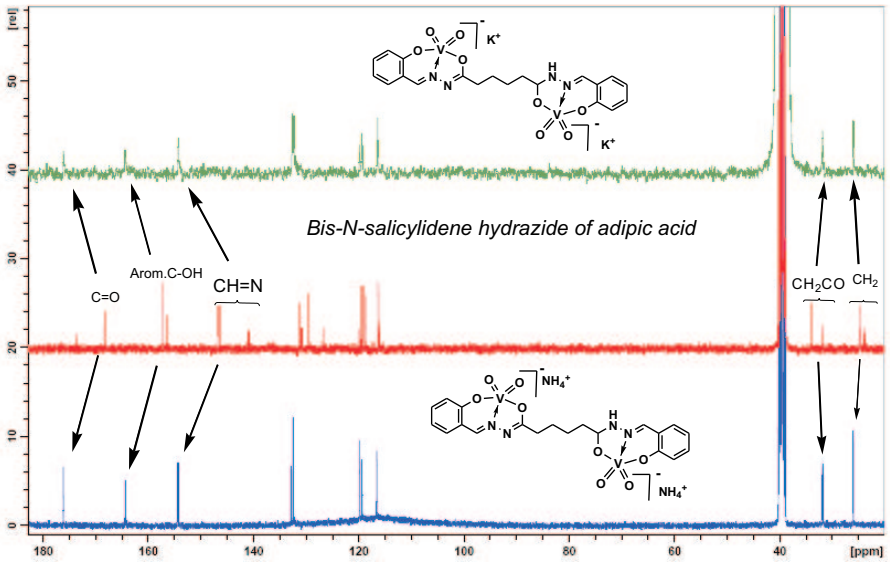


Figure 99: Comparison of $^{13}$C NMR spectrum of the *bis*-N-salicylidene adipic hydrazide ligand and the corresponding binuclear anionic *cis*-dioxovanadium complexes.

Further evidence for the coordination mode of the ligands was obtained by comparing the IR patterns of the free ligands with the IR spectra of the isolated anionic binuclear complexes. The infrared spectra of the ligands exhibit bands in the regions 1668 and 3200 $cm^{-1}$ due to $\nu$(C=O) and $\nu$(NH and OH) stretching vibrations, respectively. On vanadium complexation, these two vibrations disappeared indicating coordination through the phenolate oxygen atom as well as enolization of the amide functionality. The existence of the iminole form of the ligand in vanadium complexes is in agreement with the strong band observed at 1613 $cm^{-1}$, assigned to the stretching vibration of the conjugate –HC=N–N=C– group. This IR evidence has been registered earlier for the similar class of ligands that behave as tridentate ligands upon enolization. A broad band in the IR spectra of the ammonium salts of the binuclear *cis*-dioxovanadium complexes at approximately 3430 $cm^{-1}$ was assigned to the ammonium cations. Most important, very intense bands in the regions 881-911 and 930-933 $cm^{-1}$ in both the ammonium and the potassium salts were assigned to the stretching vibrations of the *cis*-$VO_2$ moiety. Selected IR data for both the binuclear complexes and the Schiff base ligands are presented in the Experimental Part. The IR results indicate that the Schiff base ligands exist as a mixture of keto and iminole forms in the solid state, but that on metal binding the deprotonated chelator has only iminole character.

### 6.1.1 Sulfoxidation catalytic reaction

Although a similar anionic binuclear *cis*-dioxovanadium(V) complex has been reported, there is not so far any report of similar complexes employed as catalysts in the oxidation of organic sulfides. Therefore, the herein described binuclear *cis*-dioxovanadium(V) complexes based on *bis*-N-salicylidene hydrazides were tested regarding their capacity to catalyze the oxidation of phenyl methyl sulfide. Hydrogen peroxide was used as oxidant, always in excess (1.2 equiv.) with respect to the substrate. The catalytic reactions were carried out at room temperature using a mixture of dichlormethane:methanol as reaction solvent and 1 mol% catalyst. The monitoring of the reaction was accomplished quantitatively by GC dosage of the substrate comparing to the formed sulfoxide, whereas the qualitative monitoring was done by thin-layer chromatography technique. The outcomes

of the catalytic reaction are summarized in Table 16 for both the ammonium and potassium salts of binuclear *cis*-dioxovanadium(V) complexes derived from *bis*-N-salicylidene hydrazide of glutaric and adipic acid, respectively. Fast oxidative transformation of the substrate was observed in the first 20 minutes of reaction times, when between 59 and 69% conversion was obtained. It should be mentioned that the $H_2O_2$ was added very slowly at 0 °C over a period of around 5 minutes, whereas the time of GC measurements were considered after the entire amount of oxidant was added. The stepwise addition of hydrogen peroxide was compulsory in order to avoid the overoxidation reaction. TLC monitoring of the reaction with $H_2O_2$ added at once showed large amounts of sulfone formation at the beginning of reaction. After two hours of reaction time, the GC assay of the reaction mixture showed around 78% conversion when binuclear *cis*-dioxovanadium(V) complexes based on *bis*-N-salicylidene adipic acid were used as catalysts; whereas around 84% sulfoxide was obtained when complex **20** catalyzed the oxidation reaction. A plot representing the sulfoxide conversion *vs.* time for the three catalysts is shown in Figure 100.

Table 16. Oxidation of methyl phenyl sulfide catalyzed by binuclear *cis*-dioxovanadium(V) complexes within 2 hours.

| Catalyst | Conversion % (20 min.) | Conversion % (120 min.) | TON[a] |
|---|---|---|---|
| **20** | 69.0 | 84.3 | 206 |
| **22** | 63.1 | 78.6 | 188 |
| **23** | 59.0 | 78.3 | 176 |

[a] TON: mmol substrate×(mol catalyst×h)$^{-1}$, calculated for the conversion obtained within 20 minutes.

As can be concluded from Table 16, a similar behavior of the complexes have been observed when the same length of the methylene bridge was involved in the catalyst structure, suggesting that, despite the differences in the counterparts, they exhibit the same reactivity. A slight increase of efficiency was observed for complex **20** when a shorter methylene bridge connects the two *cis*-dioxovanadium centers.

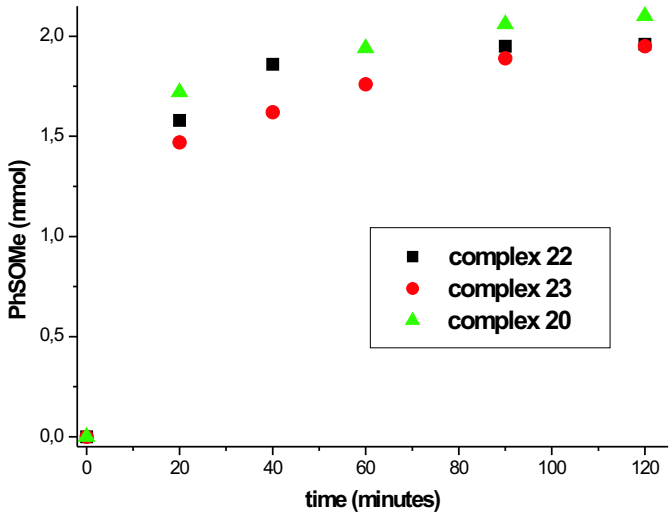


Figure 100: Profile of the progress of the oxidation of methyl phenyl sulfide catalyzed by binuclear anionic *cis*-dioxovanadium(V) complexes.

The short reaction time for 78-84% conversion of the sulfide in the corresponding sulfoxide as the sole product, is an unprecedent result for vanadium catalysts for sulfuroxidation reaction. The most efficient vanadium-based catalyst for the sulfide oxidation reaction was reported as salan-type oxovanadium(IV) complex which accomplished 91% conversion after six hours when the reaction was performed in acetonitrile, but still prolonged reaction time was reported when the catalytic reaction was performed in halogen-containing solvents.[189] The high efficient catalytic activity of the herein described binuclear anionic dioxovanadates might be related to the existence of two metal centers which accelerate the catalytic reaction. At this point the introduction of a chiral center in the vanadium catalysts seems to be a final goal for designing highly efficient, perhaps enatioselective catalysts.

## 6.2 Binuclear *cis*-dioxomolybdenum(VI) complexes based on *bis*-N-salicylidene hydrazide ligands

The *bis*-N-salicylidene hydrazide ligands were also reacted with molybdenum acetylacetonate in a 1:2 ratio, in refluxing methanol, when binuclear *cis*-dioxomolybdenum complexes have been isolated. As previous described, N-salicylidene hydrazide ligands were also able to accommodate molybdenum atoms similarly to vanadium atoms. The difference between molybdate and vanadate complexes consists in their different coordination numbers. While vanadium(V) prefers mainly five-coordination environment, molybdenum(VI) atom is commonly known as six-coordinated metal center. The hexadentate chelate system coordinates via complete deprotonation of its donor atoms, whereas the sixth coordination site on the molybdenum atoms is occupied by solvent molecules, such as methanol which was used as reaction solvent. The existence of the methanol molecules, as coordinated solvent at the molybdenum atoms, is proved by its characteristic resonances detected in both the $^{1}$H and the $^{13}$C NMR of binuclear molybdenum complexes. By comparison with precedented described binuclear *cis*-dioxovanadium(V) complexes, a shorter methylene bridge of the *bis*-N-salicylidene hydrazide, namely the derivative of the succinic acid, was also used as ligand system. Recrystallization of the binuclear *cis*-dioxomolybdenum(VI) complex (**25**) obtained with *bis*-N-salicylidene glutaric acid dihydrazide ligand, from a mixture acetonitrile:methanol afforded suitable crystals for X-ray measurement. The molecular structure determination shows two *cis*-dioxomolybdenum(VI) moieties (Figure 101). Each molybdenum atom is six-coordinated in a distorted octahedral geometry. The Schiff base ligand acts as suggested, as tetranegative chelate system, coordinating one *cis*-dioxomolybdenum moiety in each dianionic tridentate cavity. The basal plane of each polyhedra is formed by the donor atoms ONO of the ligand system together with one of the double bonded oxygen atoms (O5 and O8). The remained oxo groups (O6 and O9) of the molybdenum centers occupy the apical position. The coordination number of each molybdenum atom is completed by coordinated methanol molecules, placed *trans* to apical oxo group. Both methanol molecules are perpendicular to the near-planar system containing the molybdenum atoms and adopt *cis* orientation to each other. The ligand system forms six and five-membered chelate rings

around each *cis*-$MoO_2$ moiety. The angular distortion in the octahedral environment around molybdenum atoms comes from the bites taken by the Schiff base ligand, e.g. the angles N1–Mo1–O1 and N1–Mo1–O2 are 81 and 72° for Mo1 center and, N4–Mo2–O4 of 84° and 72° for N4–Mo2–O3, respectively, for Mo2 center. Also, indicative of the distortion to an ideal octahedral geometry are the values of the *trans* axial angles (O6–Mo1–O7 and O9–Mo2–O10) which are significantly reduced from the ideal value of 180°. Selected bond lengths and angles in complex **25** are listed in Table 17. The Mo–O and Mo–N bond distances of the two *cis*-$MoO_2$ moieties are identical within the experimental error and similar with reported corresponding bond lengths in *cis*-dioxomolybdenum(VI) complexes.[202,203,208] The Mo=O bond lengths of around 169±1 ppm are very similar with corresponding bond distances reported for similar molybdenum complexes.[245]

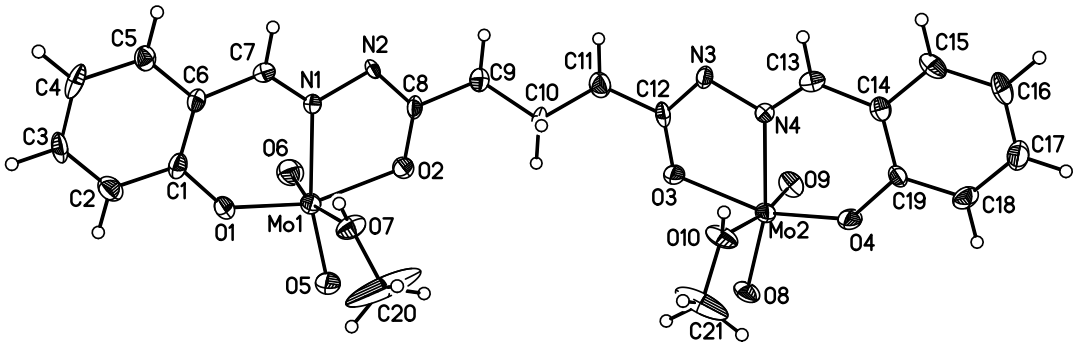


Figure 101: Molecular structure and numbering scheme of the binuclear complex $[(MoO_2)_2(salhygu)\cdot 2CH_3OH]$ (**25**); displacement ellipsoids are drawn at 50% probability level.

The binuclear *cis*-dioxomolybdenum complex exhibits hydrogen bonding interactions between the coordinated methanol molecules and the hydrazide nitrogen atom N2 and N3 of opposite enantiomeric molecules. The hydrogen bonding distances vary from 273.6 pm (N2$\cdots$O10C) to 274.5 pm (N3$\cdots$O7C), forming endless layers parallel to (010) plane (Figure 102).

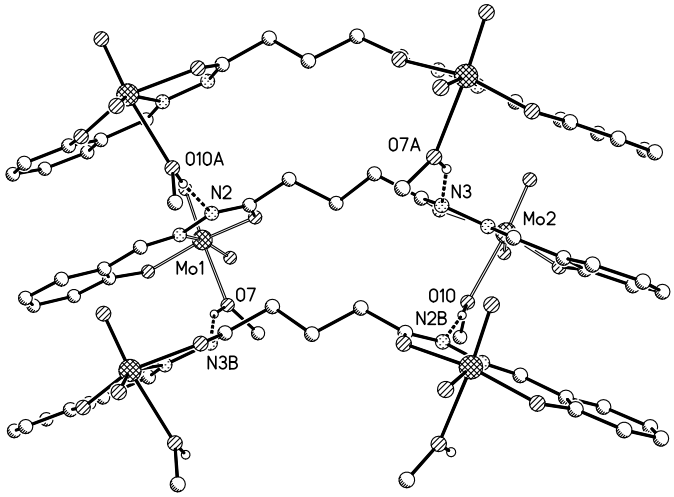


Figure 102: Representation of the hydrogen bonding network observed in crystals of $[(MoO_2)_2(salhygu)\cdot 2CH_3OH]$ (**25**) complex **25**; view along the (010) axis (broken lines represent hydrogen bonding interactions).

### 6.2.1 Spectroscopic characterization

The molybdenum complexes are soluble in DMF, DMSO and MeOH to give yellow solutions. The characteristic ligand stretching bands attributed to C=O, OH and NH were absent in the IR spectra of molybdenum complexes. As described for binuclear vanadium complexes, the Schiff base ligands also coordinates via deprotonation of all donor atoms. The molybdenum complex based on *bis*-N-salicylidene glutaric acid showed two prominent bands at 938 and 916 $cm^{-1}$ attributed to $\nu(MoO_2^{2+})$ group; whereas the binuclear molybdenum complexes formed with N-salicylidene hydrazide derived from adipic and succinic acid, respectively, exhibit such strong vibrations at 930-941 and 887-889 $cm^{-1}$. The enolization of the amide functionality on molybdenum coordination, therefore the tautomerization of the ligand during complexation is in agreement with the absence of the NH vibration and the presence of the 1609-1613 $cm^{-1}$ stretching vibration owing to the conjugated -CH=N–N=C- group. A new broad band compared to IR spectra of the free Schiff base ligands has been detected in the IR spectra of the binuclear *cis*-dioxomolybdenum complexes in the range 3308–3321 $cm^{-1}$, assigned to the vibration of the hydroxyl functionality of the coordinated methanol molecules.

The $^1H$ NMR spectra of the ligand displayed two resonances at 7.87 and 7.94 ppm attributed to azomethine, CH=N protons. However, upon chelation to $MoO_2$ moieties,

Table 17. Selected bond lengths (pm) and angles (°) for complex **25**.

| | | | |
|---|---|---|---|
| Mo1−O6 | 169.2(4) | Mo2−O8 | 169.9(4) |
| Mo1−O5 | 170.3(4) | Mo2−O9 | 169.5(4) |
| Mo1−O1 | 191.5(4) | Mo1−O4 | 192.5(4 |
| Mo1−O2 | 203.4(4) | Mo2−O3 | 203.8(4) |
| Mo1−N1 | 224.7(4) | Mo2−N4 | 224.3(4) |
| Mo1−O7 | 230.3(5) | Mo2−O10 | 231.7(4) |
| O2−C8 | 130.7(6) | O2−C12 | 130.4(6) |
| N2−C8 | 130.1(7) | N3−C12 | 129.9(7) |
| O6−Mo1−O5 | 105.8(2) | O9−Mo2−O9 | 105.36(19) |
| O6−Mo1−O1 | 100.55(19) | O9−Mo2−O4 | 99.88(18) |
| O6−Mo1−O2 | 93.13(19) | O9−Mo2−O3 | 94.65(17) |
| O6−Mo1−N1 | 94.0(2) | O9−Mo2−N4 | 94.93(19) |
| O6−Mo1−O7 | 168.03(19) | O9−Mo2−O10 | 170.94(18) |
| O5−Mo1−O1 | 102.77(19) | O8−Mo2−O4 | 102.24(18) |
| O5−Mo1−O2 | 98.51(18) | O8−Mo2−O3 | 98.57(17) |
| O5−Mo1−N1 | 158.54(19) | O8−Mo2−N4 | 158.39(19) |
| O5−Mo1−O7 | 84.07(19) | O8−Mo2−O10 | 82.61(17) |
| O1−Mo1−O2 | 150.38(17) | O4−Mo2−O3 | 150.36(16) |
| O1−Mo1−N1 | 81.12(17) | O4−Mo2−N4 | 81.09(16) |
| O1−Mo1−O7 | 83.49(17) | O4−Mo2−O10 | 82.30(16) |
| O2−Mo1−N1 | 71.75(15) | O3−Mo2−N4 | 71.98(15) |
| O2−Mo1−O7 | 78.44(17) | O3−Mo2−O10 | 79.68(16) |
| N1−Mo1−O7 | 75.35(18) | N4−Mo2−O10 | 76.65(16) |

only one singlet, deshielded at 8.77 ppm was observed. Two sets of signals, observed at 11.22 and 11.93 ppm, in $^1$H NMR spectra for the ligand were attributed N$H$ and O$H$ protons. These are distinctly absent in the spectra of the binuclear molybdenum complexes. This observation ascertains the keto-imine tautomerism to have occurred during molybdenum complexation and it confirms deprotonation and coordination of the phe-

nolic oxygen atoms. The range of chemical shifts observed for aromatic and methylene protons did not show any appreciable change upon molybdenum complexation. Therefore, the $H_4$Ln ligands coordinate the molybdenum atoms in the two tridentate binding domains as similarly described for the binuclear dioxovanadate complexes. The existence of the coordinated methanol molecules in binuclear molybdenum complexes is illustrated by the characteristic doublet resonance observed at 3.15-3.16 ppm due to the methyl protons and a quartet at 4.06-4.10 ppm owing to OH protons. Furthermore, comparison between $^{13}$C NMR spectra of *bis*-N-salicylidene hydrazides and the corresponding binuclear *cis*-dioxomolybdenum complexes sustain the proposed coordination. The differences of the $^{13}$C chemical shifts in $^{13}$C NMR of the Schiff base ligands and the $^{13}$C NMR of the binuclear molybdenum complexes are similar with discussed differences found for the binuclear *cis*-dioxovanadium complexes. $^{13}$C NMR spectra of all compounds described in this chapter are presented in the Experimental Part.

### 6.2.2 Sulfoxidation reaction

High valent *cis*-dioxomolybdenum complexes have demonstrated the ability to catalyze the oxidation of a variety of organic substrates.[195] Although numerous molybdenum(VI) complexes are reported, the molybdenum chemistry is dominated by catalytic reaction involving epoxidation of alkenes[196–199] and oxygen transfer reaction from DMSO to $PPh_3$.[202,203] At this moment very few examples of molybdenum-based catalysts for sulfoxidation reaction are known.[200] The herein described binuclear *cis*-dioxomolybdenum (VI) complexes were also used as catalysts for the oxidation of phenyl methyl sulfide by hydrogen peroxide. Compared to binuclear *cis*-dioxovanadium(V), the molybdenum complexes proved to be more efficient, with more than 95% conversion after 90 minutes. The results for the catalytic reaction are tabulated in Table 18. A small difference in reactivity within this series of complexes has been observed. Firstly, the binuclear *cis*-dioxomolybdenum complexes formed with *bis*-N-salicylidene hydrazide of succinic acid seems to be a better catalyst of the reaction, compared to glutaric and adipic acid derivatives. Nevertheless, with all three binuclear *cis*-dioxomolybdenum(VI) complexes the catalytic reaction takes place with a turnover rate higher than 200 mol sulfoxide$\times$(mol catalyst$\times$h)$^{-1}$.

Table 18. Oxidation of methyl phenyl sulfide catalyzed by binuclear *cis*-dioxomolybdenum(VI) complexes within 90 minutes.

| Catalyst | Conversion % (20 min.) | Conversion % (90 min.) | TON[a] |
|---|---|---|---|
| **24** | 75.2 | 99.2 | 225 |
| **25** | 68.0 | 95.4 | 204 |
| **26** | 73.1 | 98.9 | 218 |

[a] TON: mmol substrate×(mol catalyst×h)$^{-1}$, calculated for the conversion obtained within 20 minutes.

Due to the efficient catalytic activity of the binuclear molybdenum complexes, a chiral center was introduced in the ligand system. Starting from (+) dimethyl R-methyl succinate which is commercially available and following the described procedure, the *bis*-N-salicilidene R-methyl succinic dihydrazide has been obtained. This ligand was reacted with molybdenyl acetylacetonate in refluxing methanol, when the corresponding chiral binuclear *cis*-dioxomolybdenum(VI) complex was formed (Figure 103).

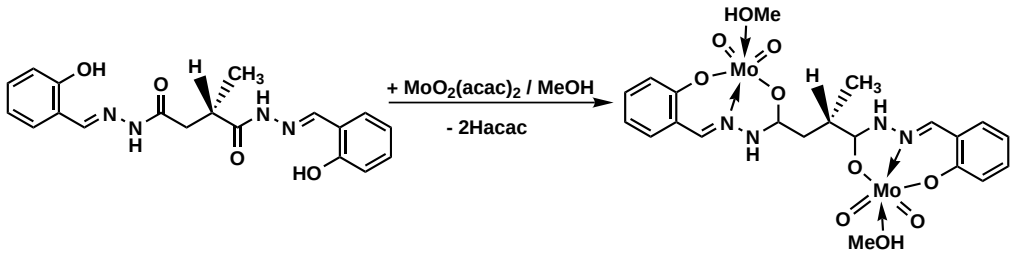


Figure 103: Schematic representation of the synthesis of chiral binuclear *cis*-dioxomolybdenum(VI) complex (**27**).

Complex **27** was also tested for catalytic sulfoxidation, following the previous conditions. The catalytic reaction took place with 96.8% conversion of phenyl methyl sulfide when the reaction was performed in dichlormethane:methanol mixture, after 90 minutes time. Unfortunately no enantiomeric excess has been obtained, the ratio between the two isomers of the sulfoxide being almost 50:50. Because the enantioselective sulfoxidation reaction had been reported as being solvent dependent,[189,240] the oxidation reaction catalyzed by complex **27** was also performed in dichlormethane with no addition of methanol. The

complex requires a longer period of time for dissolution, whereas the reaction takes place with only 34.5% conversion after one hour. Further monitoring of the reaction showed around 55% conversion within two hours and 63.6% sulfoxide formation after 150 minutes. HPLC analyze of the dichlormethane solution showed also no representative enantiomeric excess, the ratio between the two isomers of the phenyl methyl sulfoxide increasing only to 52.0 to 48 percentage, with only 4% e.e. respectively. It seems, that the methanol as cosolvent has an additive effect, contributing to the acceleration of catalytic reaction, but is decreasing the enantioselectivity of the catalyst.

Particular attention in the reported vanadium-catalyst systems[191] has been paid to the di-tert-butyl substitution of the aromatic system. Bolm explained the high enantioselective behave of the catalytic reaction as a dependence of the vanadium reactivity directly connected with the substitution groups of the ligand system. Therefore, the apparent requirement for the tert-butyl group at C-5 position of the aryl moiety might be a sterically demanding substituent. Another advantage of Bolm's catalytic system is also represented by additionally tert-butyl substituted imine framework, which was explained as capable to enable the enatioselectivity of the reaction. Schematic representation of catalytic system developed by Bolm *et al.* is shown in Figure 104. Bolm also reported that an withdrawing electron substituent on the aromatic system, has also a positive effect on vanadium activation. Therefore, at this point, at least a tert-butyl substitution on the aryl moiety in complex **27** might fulfill the required activation of molybdenum center for an enatioselective oxidation of organic sulfides.

## 6.3 Conclusions

Binuclear *cis*-dioxovanadium(V) and *cis*-dioxomolybdenum(VI) complexes have been designed as catalysts for sulfoxidation reaction. The vanadium complexes showed a lower activity compared to corresponding molybdenum complexes, but still they are rare examples of efficient vanadium-based catalysts of the oxidative reaction. Whereas the binuclear vanadium-catalysts were synthesized only as prochiral complexes, a chiral binuclear molybdenum complex was isolated. This complex showed an efficient activity towards

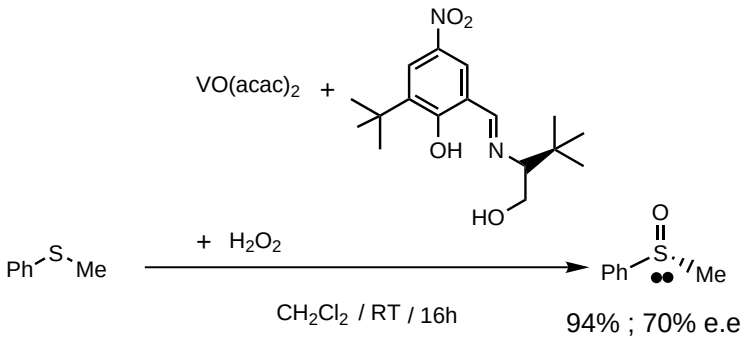


Figure 104: Schematic representation of the most efficient chiral vanadium catalyst according with reference [191].

catalytic oxidation of phenyl methyl sulfide in dichlormethane:methanol mixture, but a more slower reaction in simple dichlormethane solvent. Unfortunately, in both cases a racemic mixture of phenyl methyl sulfoxide has been obtained. An interesting features of these catalysts might be represented by replacement of salicylaldehyde with di-tert-butyl substituted aromatic aldehydes and focusing especially on vanadium-catalysts, due to their known capacity to catalyze enantioselectively the sulfoxidation reaction.

## 6.4 Experimental Part

Abbreviations used throughout the text: $H_4$salhysu = succinic acid (2-hydroxy benzylidene) dihydrazide, $H_4$salhygu = glutaric acid (2-hydroxy benzylidene) dihydrazide, $H_4$salhyad = adipic acid (2-hydroxy benzylidene) dihydrazide, salan ligand = reduced salen Schiff base ligand, salen = *bis*-N-salicylidene R-diamine derivates, where R is an alkyl rest.

### 6.4.1 Synthesis of *bis*-aliphatic acid hydrazides

#### Synthesis of glutaric acid dihydrazide

Dimethyl glutaric ester (18.4 mL, 125.0 mmol) was added stepwise under continuous stirring to hydrazine hydrate 100 % (15.2 mL, 312.5 mmol). The resulting solution was refluxed for 30 minutes when a colorless precipitate is formed. Ethanol (100 mL) was added and refluxed for one additional hour. The precipitate was filtered and washed with

ethanol. Yield: 18.7 g (117.0 mol; 93 %). $^{1}$H NMR (200 MHz, DMSO-$d_6$): $\delta$ = 1.64-1.76 (m, 2H, C$H_2$), 1.98 (t, 4H, C$H_2$CO, $^{3}$J= 8.00 Hz), 4.12 (br, 4H, N$H_2$), 8.33 (br, 2H, N$H$) ppm. $^{13}$C NMR (50 MHz, DMSO-$d_6$): $\delta$ = 21.9 ($C$H$_2$), 33.3 ($C$H$_2$CO), 171.6 ($C$=O) ppm.

**Synthesis of adipic acid dihydrazide**

Diethyl adipic ester (14.0 mL, 100.0 mmol) was added stepwise under continuous stirring to hydrazine hydrate 100 % (15.6 g, 15.2 mL, 312.0 mmol). The resulting solution was refluxed for 30 minutes when a colorless precipitate is formed. Ethanol (100 mL) was added and refluxed for one additional hour. The precipitate was filtered and washed with ethanol. Yield: 18.7 g (117.0 mol; 93 %). $^{1}$H NMR (200 MHz, DMSO-$d_6$): $\delta$ = 1.42-1.45 (m, 4H, C$H_2$), 1.98 (t, 4H, C$H_2$CO, $^{3}$J=7.80 Hz), 3.46 (br, 4H, N$H_2$), 8.93 (br, 2H, N$H$) ppm. $^{13}$C NMR (50 MHz, DMSO-$d_6$): $\delta$ = 24.9 ($C$H$_2$), 33.3 ($C$H$_2$CO), 171.5 ($C$=O) ppm.

**Synthesis of succinic acid dihydrazide**

This *bis*-hydrazide was prepared analogously to the previous similar hydrazide from diethyl succinic ester (19.2 mL, 115.0 mmol) and hydrazine hydrate (14.0 mL, 287.5 mmol) in refluxing ethanol. Yield: 15.2 g (104.0 mol; 90 %). $^{1}$H NMR (200 MHz, DMSO-$d_6$): $\delta$ = 2.19-2.23 (m, 4H, C$H_2$CO), 4.13 (br, 4H, N$H_2$), 8.98 (br, 2H, N$H$) ppm. $^{13}$C NMR (50 MHz, DMSO-$d_6$): $\delta$ = 29.3 ($C$H$_2$CO), 171.9 ($C$=O) ppm.

**Synthesis of (+) dihydrazide R-methyl succinate**

This dihydrazide was prepared analogously to the previous dihydrazides from (+) dimethyl R-succinate ester (2.5 mL, 16.7 mmol) and hydrazine hydrate (2.1 mL, 41.7 mmol) in refluxing methanol (10 mL). Yield: 2.45 g (15.30 mol; 91 %). *Anal. for* $C_5H_{12}N_4O_2$ (160.17): calcd. C 37.49, H 7.55, N 34.98; found C 37.51, H 7.24, N 35.42. $^{1}$H NMR (400 MHz, DMSO-$d_6$): $\delta$ = 0.93-0.95 (d, 3H, C$H_3$, J= 6.8 Hz), 2.00-2.06 and 2.20-2.25 (dd, 2H, C$H_2$CO, J= 8.4 and 6.3 Hz), 2.55-2.56 (m, 1H, C$H$), 4.10 and 4.12 (br, 4H, N$H_2$), 8.94 and 8.97 (br, 2H, N$H$) ppm. $^{13}$C NMR (100 MHz, DMSO-$d_6$): $\delta$ = 17.4 ($C$H$_3$), 34.4 ($C$H), 37.1 ($C$H$_2$CO), 169.9 and 174.2 ($C$=O) ppm.

### 6.4.2 Synthesis of Schiff base ligands

**Synthesis of *bis*-N-salicylidene glutaric acid hydrazide $H_4$salhygu**

To a suspension of glutaric acid dihydrazide (5.0 g, 31.2 mmol) in methanol (150 mL), salicylaldehyde (6.6 mL, 62.5 mmol) was added dropwise at 0° C. The resulting yellow solution was stirred at room temperature overnight. The formed precipitate was filtered off and dried in vacuo. Yield: 11.2 g (30.3 mmol; 97 %). $^1$H NMR (200 MHz, DMSO-$d_6$): $\delta$ = 1.85-1.96 (m, 2H, C$H_2$), 2.18-2.35 and 2.61-2.68 (m, total 4H, C$H_2$CO, ratio 1.84:0.91), 6.76-7.0 (m, 4H, arom. C$H$), 7.15-7.30 (m, 2H, arom. C$H$), 7.45-7.61 (m, 2H, arom. C$H$), 8.24, 8.26 and 8.33 (s, 2H total, C$H$=N, ratio 0.46:0.96), 10.12, 11.20-11.22 and 11.63 (N$H$, O$H$, total 4H in ratio 0.35:1.29:0.86) ppm. $^{13}$C NMR (50 MHz, DMSO-$d_6$): $\delta$ = 19.9, 20.6 ($C$H$_2$), 31.3, 31.4, 33.0 and 33.3 (all $C$H$_2$CO), 116.1, 116.3, 118.6, 119.3, 119.4, 120.0, 126.7, 129.5, 130.8, 131.2 (all arom. $C$H and $C$), 140.8, 146.5 (both $C$H=N), 156.3, 157.3, 169.0, 168.2, (arom. $C$), 173.4 and 173.6 ($C$=O) ppm. Selected IR data (cm$^{-1}$): $\nu$= 3194 (NH$_{ass}$, OH$_{ass}$), 1668 (s; C=O), 1623 and 1609 (CH=N).

**Synthesis of *bis*-N-salicylidene adipic acid hydrazide $H_4$salhyad**

To a suspension of adipic acid dihydrazide (4.0 g, 22.7 mmol) in methanol (150 mL), salicylaldehyde (4.8 mL, 45.8 mmol) was added dropwise at 0∘ C. The resulting yellow solution was stirred at room temperature overnight, when a colorless precipitate is formed. The precipitate was filtered off and dried in vacuo. Yield: 8.6 g (22.5 mmol; 99 %). $^1$H NMR (400 MHz, DMSO-$d_6$): $\delta$ = 1.53-1.62 (m, 4H, C$H_2$), 2.25 and 2.58 (t, total 4H, C$H_2$CO, $^3$J= 6.6 Hz, ratio 1.92:0.90), 6.82-6.89 (m, 4H, arom. C$H$), 7.18-7.27 (m, 2H, arom. C$H$), 7.45-7.61 (m, 2H, arom. C$H$), 8.25, 8.33 (s, 2H total, C$H$=N, ratio 0.51:0.95), 10.12, 11.18 and 11.58 (N$H$, O$H$, total 4H in ratio 0.54:1.45:0.94) ppm. $^{13}$C NMR (100 MHz, DMSO-$d_6$): $\delta$ = 23.8, 23.9, 24.6, 24.7 (all $C$H$_2$), 31.7, 33.7 (both $C$H$_2$CO), 116.1, 116.3, 118.6, 119.4, 120.0, 126.8, 129.5, 130.8, 131.1 (all arom. $C$H and $C$), 140.8, 146.5 (both $C$H=N), 156.3, 157.3, 168.3, (arom. $C$), 173.7 ($C$=O) ppm. Selected IR data (cm$^{-1}$): $\nu$= 3435, 3202 (NH, OH), 1667 (s; C=O), 1623 and 1611 (CH=N).

### Synthesis of bis-N-salicylidene succinic acid hydrazide $H_4$salhysu

This Schiff base ligand was prepared by analogs procedure from succinic acid dihydrazide (5.0 g, 34.2 mmol) and salicylaldehyde (7.2 mL, 68.50 mmol) in methanol at 0∘ C. Yield: 11.9 g (33.3 mmol; 97 %). $^1$H NMR (200 MHz, DMSO-$d_6$): $\delta$ = 2.47-2.56 (m, C$H_2$CO, overlapped with the dmso-$d_6$ signal) and 2.90-2.95 (t, C$H_2$CO, $^3$J= 6.82 Hz), 6.84-6.99 (m, 4H, arom. C$H$), 7.18-7.30 (m, 2H, arom. C$H$), 7.40-7.70 (m, 2H, arom. C$H$), 8.27, 8.33 (s, 2H total, C$H$=N, ratio 0.76:1.00), 10.14, 11.17, 11.28 and 11.70 (br, N$H$, O$H$, total 4H in ratio 0.29:0.91:0.50:0.11) ppm. $^{13}$C NMR (50 MHz, DMSO-$d_6$): $\delta$ = 24.7, 26.5 28.2, 28.7 (all $C$H$_2$CO), 116.1, 116.3, 118.6, 119.3, 119.5, 120.0, 126.8, 129.4, 130.9, 131.2 (all arom. $C$H and $C$), 141.1, 146.3, 146.4 (all $C$H=N), 156.3, 157.3, 158.6, 167.6, 167.9 (arom. $C$), 172.8 and 173.1 (both $C$=O) ppm. Selected IR data (cm$^{-1}$): $\nu$= 3200 (NH, OH), 1676 (s; C=O), 1622 and 1609 (CH=N). UV/Vis ($CH_3OH$ solution, $\lambda_{max}$ in nm ($\varepsilon$ in $10^3$ M$^{-1}$ cm$^{-1}$)): 280 (37.9), 289 (35.7), 315 (20.4).

### Synthesis of (+) *bis*-N-salicylidene R-methyl succinic acid hydrazide

To a suspension of R-methyl succinic acid dihydrazide (2.4 g, 15.0 mmol) in methanol (60 mL) was added salicylaldehyde (3.1 mL, 30.0 mmol) under continuous stirring. The resulting slurry solution was refluxed for about 15 minutes and additionally stirred at room temperature overnight, when a colorless precipitate was formed. Yield: 1.7 g (4.6 mmol; 31 %). *Anal. for* $C_{19}H_{20}N_4O_4{\cdot}H_2O$ (386.40): calc. C 59.06, H 5.74, N 14.50; found C 59.54, H 5.58, N 16.65. $^1$H NMR (400 MHz, DMSO-$d_6$): $\delta$ = 1.18-1.19 (d, 3H, C$H_3$), 2.33-2.47 and 2.68-2.73 (m, total 2H, C$H_2$CO), 2.88-3.09 (m, 1H, C$H$), 6.86-6.90 (m, 4H, arom. C$H$), 7.18-7.29 (m, 2H, arom. C$H$), 7.45-7.65 (m, 2H, arom. C$H$), 8.26, 8.29, 8.33 and 8.37 (s, 2H total, C$H$=N), 10.12, 11.14, 11.24 and 11.68 (N$H$, O$H$, total 4H) ppm. $^{13}$C NMR (50 MHz, DMSO-$d_6$): $\delta$ = 16.9, 17.8 and 18.0 ($C$H$_3$), 34.2, 34.8 and 35.7 (all $C$H), 36.8 and 37.3 (both $C$H$_2$CO), 116.1, 116.3, 118.5, 119.2, 119.4, 120.0, 126.7, 129.4, 130.9, 131.1 (all arom. $C$H and $C$), 140.9, 146.5 and 146.8 (all $C$H=N), 156.3, 157.2, 166.9 and 167.1 (arom. $C$-OH), 171.1, 171.5, 172.2 and 176.0 ($C$=O) ppm.

### 6.4.3 Synthesis of *cis*-dioxovanadium(V) complexes

## Synthesis of ammonium salts of binuclear *cis*-dioxovanadium(V) complexes

**General procedure:** To a suspension of *bis*-N-salicylidene hydrazide (1.0 g) in methanol (100 mL) was added an equimolar amount of ammonium metavanadate. The resulting brown suspension was refluxed for around three hours while became a clear solution. The hot solution was filtered and the volume reduced under reduced pressure to about half. After standing at room temperature overnight a yellow precipitate was formed. This was filtered off and washed with chloroform.

#### Synthesis of complex $(NH_4)_2[(VO_2)_2$(salhygu)] (20)

This complex was synthesized from *bis*-N-salicylidene glutaric acid hydrazide (1.00 g, 2.72 mmol) and $NH_4VO_3$ (0.64 g, 5.43 mmol) in methanol. Yield: 1.32 g (2.33 mmol; 86 %). *Anal. for* $C_{19}H_{24}N_6O_8V_2$ (566.31): calcd. C 40.30, H 4.27; found C 39.83, H 4.01. $^1$H NMR (200 MHz, DMSO-d$_6$): $\delta$ = 1.83-2.07 (m, 2H, C$H_2$), 2.33 (t, 4H, C$H_2$CO, $^3$J= 6.8 Hz), 6.74-6.76 (m, 4H, arom. C$H$), 7.12 (br, 8H, $NH_4^+$), 7.26-7.30 (m, 2H, arom. C$H$), 7.45-7.49 (m, 2H, arom. C$H$), 8.78 (s, 2H total, C$H$=N) ppm. $^{13}$C NMR (50 MHz, DMSO-d$_6$): $\delta$ = 22.9 ($C$H$_2$), 31.5 ($C$H$_2$CO), 116.5, 119.2, 119.7, 132.3, 132.8 (all arom. $C$H and $C$), 154.2 ($C$H=N), 164.2 (arom. $C$–OV), 175.9 (aliphatic $C$–OV) ppm. $^{51}$V NMR (105 MHz, DMSO-d$_6$): $\delta$ = -534.6 ppm ($\Delta\nu_{1/2}$ = 873 Hz). Selected IR data (cm$^{-1}$): $\nu$= 3430 (br, $NH_4^+$), 1612 (s, -HC=N–N=C-), 911 and 891 (s, $VO_2$). UV/Vis ($CH_3OH$ solution, $\lambda_{max}$ in nm ($\varepsilon$ in $10^3$ M$^{-1}$ cm$^{-1}$)): 278 (28.3), 290 (25.3), 312 (19.6), 389 (6.08).

#### Synthesis of complex $(NH_4)_2[(VO_2)_2$(salhyad)] (22)

This complex was synthesized from *bis*-N-salicylidene adipic acid hydrazide (1.00 g, 2.61 mmol) and $NH_4VO_3$ (0.61 g, 5.23 mmol) in methanol. Yield: 0.93 g (1.61 mmol; 62%). *Anal. for* $C_{20}H_{22}N_6O_8V_2$ (576.31): calcd. C 41.68, H 3.84, N 14.58; found C 41.45, H 4.17, N 14.54. $^1$H NMR (400 MHz, DMSO-d$_6$): $\delta$ = 1.62 (br, 4H, C$H_2$), 2.27

(t, 4H, C$H_2$CO), 6.72-6.74 (m, 4H, arom. C$H$), 7.11 (br, 8H, $NH_4^+$), 7.26-7.30 (m, 2H, arom. C$H$), 7.45-7.47 (m, 2H, arom. C$H$), 8.77 (s, 2H total, C$H$=N) ppm. $^{13}$C NMR (100 MHz, DMSO-$d_6$): $\delta$ = 25.9 ($C$H$_2$), 31.7 ($C$H$_2$CO), 116.5, 119.3, 119.8, 132.3, 132.7 (all arom. $C$H and $C$), 154.3 ($C$H=N), 164.3 (arom. $C$–OV), 176.1 (aliphatic $C$–OV) ppm. $^{51}$V NMR (105 MHz, DMSO-$d_6$): $\delta$ = -534.2 ppm ($\Delta\nu_{1/2}$ = 863 Hz). Selected IR data (cm$^{-1}$): $\nu$= 3447 (br, $NH_4$), 1610 (s, -HC=N–N=C-), 933 and 910 (s, $VO_2$). UV/Vis ($CH_3OH$ solution, $\lambda_{max}$ in nm ($\varepsilon$ in $10^3$ M$^{-1}$ cm$^{-1}$)): 278 (25.51), 290 (22.16), 312 (17.8), 389 (5.60).

## Synthesis of potassium salts of binuclear *cis*-dioxovanadium(V) complexes

**General procedure:** To a suspension of *bis*-N-salicylidene hydrazide (1.00 g) in methanol (100 mL) was added an equimolar amount of potassium metavanadate. The resulting brown suspension was refluxed for around two days when a clear yellow solution was formed. The hot solution was filtered and the volume reduced under reduced pressure to about half. After standing at room temperature overnight a yellow precipitate was formed.

### Synthesis of complex $K_2[(VO_2)_2$(salhygu)$]\cdot 4H_2O$ (21)

This complex was synthesized from *bis*-N-salicylidene glutaric acid hydrazide (1.00 g, 2.72 mmol) and $KVO_3$ (0.75 g, 5.43 mmol) in methanol. Yield: 1.63 g (2.40 mmol; 88%). *Anal. for* $C_{19}H_{16}N_4O_8K_2V_2\cdot 4H_2O$ (680.49): calcd. C 33.54, H 3.55, N 8.23; found C 33.80, H 3.43, N 8.03. Thermogravimetric measurement: 72.8-195°C loss 11.9% (80.97 g) (4.5$H_2O$). $^1$H NMR (200 MHz, DMSO-$d_6$): $\delta$ = 1.87-1.93 (m, 2H, C$H_2$), 2.29-2.33 (m, 4H, C$H_2$CO), 3.31 ($H_2O$), 6.71-6.75 (m, 4H, arom. C$H$), 7.24-7.32 (m, 2H, arom. C$H$), 7.44-7.47 (m, 2H, arom. C$H$), 8.78 (s, 2H total, C$H$=N) ppm. $^{13}$C NMR (50 MHz, DMSO-$d_6$): $\delta$ = 23.0 ($C$H$_2$), 31.7 ($C$H$_2$CO), 116.5, 119.4, 119.8, 132.3, 132.7 (all arom. $C$H and $C$), 154.4 ($C$H=N), 164.3 (arom. $C$–OV), 175.9 (aliphatic $C$–OV) ppm. $^{51}$V NMR (105 MHz, DMSO-$d_6$): $\delta$ = -531.4 ppm ($\Delta\nu_{1/2}$ = 842 Hz). Selected IR data (cm$^{-1}$): $\nu$= 3435 (br, $H_2O$), 1616 (s, -HC=N-N=C-), 930 and 910 (s, $VO_2$). UV/Vis ($CH_3OH$

solution, $\lambda_{max}$ in nm ($\varepsilon$ in $10^3$ $M^{-1}$ $cm^{-1}$)): 278 (28.12), 290 (26.25), 315 (18.87), 384 (5.90).

**Synthesis of complex $K_2[(VO_2)_2$(salhyad)] (23)**

This complex was synthesized from *bis*-N-salicylidene adipic acid hydrazide (1.00 g, 2.61 mmol) and $KVO_3$ (0.73 g, 5.23 mmol) in methanol. Yield: 1.28 g (1.94 mmol; 74%). *Anal. for* $C_{20}H_{18}N_4O_8K_2V_2$ (622.46): calcd. C 38.59, H 2.91, N 9.00; found C 38.94, H 3.06, N 9.11. $^1$H NMR (400 MHz, DMSO-$d_6$): $\delta$ = 1.61 (t, 4H, C$H_2$), 2.26 (t, 4H, C$H_2$CO), 6.69-6.73 (m, 4H, arom. C*H*), 7.25-7.29 (m, 2H, arom. C*H*), 7.44-7.46 (m, 2H, arom. C*H*), 8.76 (s, 2H total, C*H*=N) ppm. $^{13}$C NMR (50 MHz, DMSO-$d_6$): $\delta$ = 25.9 (*C*$H_2$), 31.8 (*C*$H_2$CO), 116.3, 119.3, 119.8, 132.3, 132.6 (all arom. *C*H and *C*), 154.2 (*C*H=N), 164.3 (arom. *C*–OV), 176.1 (aliphatic *C*–OV) ppm. $^{51}$V NMR (105 MHz, DMSO-$d_6$): $\delta$ = -532.6 ppm ($\Delta\nu_{1/2}$ = 842 Hz). Selected IR data ($cm^{-1}$): $\nu$= 1613 (s, -HC=N-N=C-), 930 and 909 (s, $VO_2$).

### 6.4.4 Synthesis of binuclear *cis*-dioxomolybdenum(VI) complexes

**General procedure:** To a suspension of *bis*-N-salicylidene hydrazide (around 1.0 mmol) in methanol (50 mL) was added an equimolar amount of molybdenyl acetylacetonate. The resulting yellow suspension was refluxed under continuous stirring for two hours and additionally stirred at room temperature for four hours. The resulting solution was concentrated under reduce pressure to about third of the initial volume, when a precipitate was formed. This was filtered off and washed with acetonitrile:methanol 1:1 mixture.

**Synthesis of complex $[(MoO_2)_2$(salhysu)]·$2CH_3OH$ (24)**

This complex was synthesized from *bis*-N-salicylidene succinic acid hydrazide (0.35 g, 1.00 mmol) and $MoO_2(acac)_2$ (0.65 g, 2.00 mmol) in methanol. Yield: 0.48 g (0.72 mmol; 72%). *Anal. for* $C_{20}H_{22}N_4O_10Mo_2$ (670.29): calcd. C 35.84, H 3.31, N 8.36; found C 35.76, H 3.26, N 8.24. $^1$H NMR (200 MHz, DMSO-$d_6$): $\delta$ = 2.71 (s, 4H, C$H_2$), 3.14-3.16 (d, 6H, C$H_3$OH, J=5.24 Hz), 4.08-4.12 (q, 2H, $CH_3$*OH*, J=5.25 Hz), 6.88-7.07 (m, 4H,

arom. C*H*), 7.45-7.50 (m, 2H, arom. C*H*), 7.65-7.70 (m, 2H, arom. C*H*), 8.76 (s, 2H total, C*H*=N) ppm. $^{13}$C NMR (50 MHz, DMSO-d$_6$): $\delta$ = 27.5 (*C*H$_2$), 48.6 (*C*H$_3$OH), 118.5, 120.0, 121.4, 134.2, 134.8 (all arom. *C*H and *C*), 155.4 (*C*H=N), 159.3 (arom. *C*–OMo), 173.7 (aliphatic *C*–OMo) ppm. Selected IR data (cm$^{-1}$): $\nu$= 3321 (br, OH), 1613 (s, -HC=N-N=C-), 930 and 889 (s, MoO$_2$), 820 (s) and 662 (s) and 590 (s) (Mo–O and Mo–N linkage).

**Synthesis of complex [(MoO$_2$)$_2$(salhygu)]·2CH$_3$OH (25)**

This complex was synthesized following the general procedure from *bis*-N-salicylidene glutaric acid hydrazide (0.37 g, 1.00 mmol) and MoO$_2$(acac)$_2$ (0.65 g, 2.00 mmol) in methanol. Yield: 0.59 g (0.86+mmol; 86 %). *Anal. for* C$_{21}$H$_{24}$N$_4$O$_1$0Mo$_2$ (684.31): calcd. C 36.86, H 3.53, N 8.19; found C 37.04, H 3.30, N 8.26. $^1$H NMR (400 MHz, DMSO-d$_6$): $\delta$ = 1.89-1.96 (m, 2H, C*H*$_2$), 2.42-2.48 (m, 4H, C*H*$_2$CO), 3.15-3.16 (d, 6H, C*H*$_3$OH, J=5.20 Hz), 4.06-4.10 (q, 2H, CH$_3$*OH*, J=5.21 Hz), 6.90-7.06 (m, 4H, arom. C*H*), 7.47-7.52 (m, 2H, arom. C*H*), 7.65-7.68 (m, 2H, arom. C*H*), 8.77 (s, 2H total, C*H*=N) ppm. $^{13}$C NMR (100 MHz, DMSO-d$_6$): $\delta$ = 22.5 (*C*H$_2$), 30.2 (*C*H$_2$CO), 48.6 (*C*H$_3$OH), 118.5, 120.1, 121.4, 134.2, 134.8 (all arom. *C*H and *C*), 155.3 (*C*H=N), 159.3 (arom. *C*–OMo), 174.5 (aliphatic *C*–OMo) ppm. Selected IR data (cm$^{-1}$): $\nu$= 3310 (br, OH), 1609 (s, -HC=N-N=C-), 938 and 916 (s, MoO$_2$), 821 (s) and 639 (s) and 575 (s) (Mo–O and Mo–N linkage) . UV/Vis (CH$_3$OH solution, $\lambda_{max}$ in nm ($\varepsilon$ in 10$^3$ M$^{-1}$ cm$^{-1}$)): 279 (27.8), 290 (26.5), 315 (15.8), 389 (1.62).

**Synthesis of complex [(MoO$_2$)$_2$(salhyad)]·2CH$_3$OH (26)**

This complex was synthesized following the general procedure from *bis*-N-salicylidene adipic acid hydrazide (0.36 g, 0.94 mmol) and MoO$_2$(acac)$_2$ (0.61 g, 1.88 mmol) in methanol. Yield: 0.42 g (0.60 mmol; 64 %). *Anal. for* C$_{22}$H$_{26}$N$_4$O$_1$0Mo$_2$ (698.34): calcd. C 37.85, H 3.75, N 8.02; found C 37.70, H 3.69, N 8.04. $^1$H NMR (400 MHz, DMSO-d$_6$): $\delta$ = 1.02-1.06 (m, 4H, C*H*$_2$), 2.37-2.49 (m, 4H, C*H*$_2$CO), 3.15-3.16 (d, 6H, C*H*$_3$OH, J=5.00 Hz), 4.06-4.10 (q, 2H, CH$_3$*OH*, J=5.25 Hz), 6.89-7.05 (m, 4H, arom. C*H*), 7.47-7.50 (m, 2H, arom. C*H*), 7.64-7.66 (m, 2H, arom. C*H*), 8.74 (s, 2H total, C*H*=N) ppm. $^{13}$C NMR (100 MHz, DMSO-d$_6$): $\delta$ = 25.3 (*C*H$_2$), 30.7 (*C*H$_2$CO), 48.6

($CH_3OH$), 118.5, 120.1, 121.4, 134.2, 134.6 (all arom. $CH$ and $C$), 155.3 ($CH$=N), 159.2 (arom. $C$–OMo), 174.7 (aliphatic $C$–OMo) ppm. Selected IR data ($cm^{-1}$): $\nu$= 3308 (br, OH solvent), 1613 (s, -HC=N-N=C-), 941 and 887 (s, $MoO_2$), 818 (s) and 642 (s) and 580 (s) (Mo–O and Mo–N linkage). UV/Vis ($CH_3OH$ solution, $\lambda_{max}$ in nm ($\varepsilon$ in $10^3$ $M^{-1}$ $cm^{-1}$)): 279 (22.3), 290 (20.9), 315 (12.2), 389 (1.59).

**Synthesis of chiral binuclear molybdenum complex (27)**

Complex **27** was synthesized from (+) *bis*-N-salicylidene R-methyl succinic acid hydrazide (0.37 g, 1.00 mmol) and $MoO_2(acac)_2$ (0.65 g, 2.00 mmol) in methanol (50 mL) with reflux for one hour. Yield: 0.35 g (0.51 mmol; 51 %). *Anal. for* $C_{21}H_{24}N_4O_10Mo_2$ (684.32): calcd. C 36.55, H 3.53, N 8.19; found C 36.55, H 4.40, N 7.52. $^1$H NMR (400 MHz, DMSO-$d_6$): $\delta$ = 1.20-1.22 (d, 3H, C$H_3$, J= 6.9 Hz), 2.78-2.83 (d, 2H, C$H_2$CO, J= 8.6 Hz), 2.93-3.02 (m, 1H, C$H$), 3.14-3.16 (d, C$H_3$OH), 4.01 ($CH_3OH$), 6.89-6.92 (m, 2H, arom. C$H$), 7.02-7.05 (m, 2H, arom. C$H$), 7.47-7.51 (m, 2H, arom. C$H$), 7.66-7.68 (m, 2H, arom. C$H$), 8.75 and 8.77 (s, 2H total, C$H$=N) ppm. $^{13}$C NMR (50 MHz, DMSO-$d_6$): $\delta$ = 17.6 ($CH_3$), 33.8 ($CH_2$), 35.3 ($CH$), 48.6 ($CH_3OH$), 118.5, 120.0, 121.4, 134.2, 134.7 (all arom. $CH$ and $C$), 155.4 and 155.7 (both $CH$=N), 159.2 and 159.3 (both arom. $C$–OMo), 173.0 and 176.8 (both aliphatic $C$–OMo) ppm. Selected IR data ($cm^{-1}$): $\nu$= 3198 (br, OH), 1616 (s, -HC=N-N=C-), 938 and 913 (s, $MoO_2$).

**Catalytic oxidation of methyl phenyl sulfide**

Vanadium and molybdenum complexes (0.025 mmol) was dissolved at room temperature in a mixture $CH_2Cl_2$/$CH_3OH$ 7:3 (25 mL) and phenyl methyl sulfide (0.29 ml, 2.5 mmol) was added. The resulting solution was cooled down on an ice-bath and $H_2O_2$ 26 % (1.2 equiv., 0.35 mL, 3 mmol) was added dropwise. The reaction solution was stirred at room temperature in a capped flask and monitored by thin layer chromatography using as eluent a mixture of ethyl acetate/chloroform/methanol-5:10:3 (v/v/v)). After 18 hours 1 $\mu$L of the solution was assayed by gas-chromatography technique. Temperature programm: 55 °C hold for one minute, then the temperature increased to 200 °C with a heating rate of 15 °C per minute, followed by five minutes holding of 200 °C temperature and heating up to 240 °C with 15 °C per minute. When the chiral binuclear *cis*-dioxomolybdenum(VI)

complex **27** was used as catalyst, the sulfide and the sulfoxide were separated by column chromatography on silica gel, using pentane/diethyl ether 1:1 mixture for the unreacted sulfide and ethyl acetate for the sulfoxide. The enantiomeric excess was determined by HPLC determinations using chiral stationary phase (Pirkle Covalent S,S-WHELK-01 Regis) and hexane/i-propanol 9:1 as mobile phase with a flow rate of 2 mL $min^{-1}$).

# Chapter 7

# Conclusions and Future Projects

Vanadium-containing haloperoxidases are enzymes capable to catalyze the oxidation of halides by hydrogen peroxide, resulting in hypohalous acid formation. This oxidized halide intermediate can halogenate various organic substrates[59,71,72] and/or react with a second equivalent of hydrogen peroxide to form singlet oxygen.[73–75]

$$X^- + H_2O_2 + H^+ \longrightarrow HOX + H_2O$$
$$HOX + RH \longrightarrow RX + H_2O$$
$$HOX + H_2O_2 \longrightarrow H_2O + {}^1O_2 + X^-$$

The crystal structure determination of V-BPO and V-CPO showed vanadate as the prosthetic group solely covalently bonded to a histidine residue and fixed in the protein shell through a very strong hydrogen bonding network established by the positively charged amino acid residues from its vicinity.[38,70] The geometry of the vanadium atom was proposed to be trigonal bipyramid, resembling the transition state of phosphate in phosphatase enzymes.[6,70] Moreover, vanadate was found to be vital for these class of enzyme and its replacement with molybdate or tungstate yielded an inactive enzyme.[62] Mutagenesis studies performed on V-CPO, by replacement of the amino acids involved in the hydrogen binding site with alanine, proved their important role during the catalytic turnover.[63,150,180]

Since the reaction mechanism of V-HPOs is still under debate and the number of reported vanadium model complexes with relevant hydrogen bonding interaction is

reduced,[115,116] we decided to prepare vanadium complexes based on N-salicylidene hydrazide system which exhibit strong hydrogen bonding interactions. Starting from a non substituted aliphatic side-chain, the functionalization of the aliphatic part of the ligand made possible isolation of vanadium complexes which structurally mimic the hydrogen bonding sphere of the prosthetic group in the natural system.

A monoprotonated vanadate moiety $[VO_3(OH)]^{2-}$ has been proposed as the active site in the native enzyme by analogy with phosphate chemistry although, as it has been mentioned the vanadate exists in the diprotonated form $[VO_2(OH)_2]^-$ at physiological pH. Therefore, N-salicylidene hydrazide is a versatile ligand system, being capable of accommodating both the *cis*-dioxo- and monooxovanadium(V) complexes which are regarded as structural models for the enzymatic system. Additionally, the tridentate ligand system makes possible variation of the protonation state in the obtained complexes. In instance, the N-salicylidene carbonic acid hydrazide ligand system reacts with ammonium metavanadate yielding anionic and/or neutral *cis*-dioxovanadium(V) complexes. Further, the neutral *cis*-dioxovanadium(V) complexes react stoichiometrically with 8-hydroxyquinoline to form mono-oxovanadium(V) complexes, thus proving the versatility of the chosen chelate system. The anionic *cis*-dioxovanadium(V) complexes support a protonation reaction at the basic hydrazide nitrogen atom yielding the corresponding neutral complexes, which also can be deprotonated by back-reaction with base.

In Chapter 3, vanadium(V) complexes with an hydroxyl functionalized side chain represent model systems for vanadium dependent haloperoxidases, namely regarding the serin residue. Spectrophotometric titration with aqueous hydrochloric acid of the anionic *cis*-dioxovanadium complexes in water solution, showed one protonation step which occurred at the hydrazide nitrogen atom as more basic site compared to the oxo groups of the vanadate center. Further on, the formation of the oxo-monoperoxovanadium(V) complex by reaction of dioxovanadates with $H_2O_2$ was accomplished by spectrophotometric titration in non-aqueous medium and confirmed by X-ray characterization of one of such species. The oxo-monoperoxovanadium(V) complex functioned as intermediate of the biomimetic reaction catalyzed by the corresponding *cis*-dioxovanadium(V) complex but only when one equivalent of perchloric acid was used in stoichiometric amount. Relevant hydrogen bonding interactions for the enzymatic system were observed in all

vanadium(V) complexes. A rare example of an apical hydrogen bonded oxo group in mono-oxovanadium(V) complex was also described.

In Chapter 4, the amino functionalized side chain afforded anionic *cis*-dioxovanadium complexes in which the compensation of the negative charge of the vanadate center was accomplished by the protonated amino functionality. This is a similar situation with one found in the enzymatic system, especially because the protonated amino group of the synthetic model is also in hydrogen bonding interaction with the oxo groups of the vanadate center. Therefore, these complexes represent relevant functionalized model complexes for V-HPOs regarding the lysine residue. This amino acid plays a very important role for the catalytic activity and it is believed to increase the electrophilicity on the peroxo oxygen atom through hydrogen bonding interaction in the peroxide-form of V-CPO. When a short aliphatic side chain of the Schiff base ligand was involved in vanadium complex formation, the first example of a *cis*-dioxovanadium(V) complex with *in situ* formed dihydro-pyrrole structure was obtained. The later vanadium compound was isolated both as dimeric and monomeric structures, whereas the intramolecular cyclisation reaction resulted in the formation of neutral *cis*-dioxovanadium complexes.

Further functionalization of the alkyl side chain was described in Chapter 5, where the guanidine group has been introduced both in the starting aliphatic ester and by direct guanilation reaction of a coordination compound. Therefore, the first example of functionalization of a vanadium coordination compound was presented. The two *cis*-dioxovanadium(V) complexes model the hydrogen bonding interaction of the prosthetic group of the native enzymes with the arginine residues.[6]

The described *cis*-dioxovanadium(V) complexes functioned also as catalysts of the biomimetic reaction, being capable to catalyze the oxidation of bromide by hydrogen peroxide. The reaction was monitored by gas chromatography dosage of brominated and non-brominated 1,3,5-trimethoxybenzene. Turnover rate of the catalytic reaction range from 34 to 75 mol product$\times$(mol catalyst$\times$h)$^{-1}$, with a slight increase when amino and guanidine functionalities were parts of the vanadium complex structures. Also, a shorter aliphatic side chain showed a higher catalytic activity, with the complex **18** as the best catalyst of the series of *cis*-dioxovanadium(V) complexes based on N-salicylidene hydrazides. The results of the catalytic reaction display fairly superior ability of these

complexes, compared to inorganic ammonium metavanadate which was reported to catalyze the same reaction with a turnover rate of 15 mol product×(mol catalyst×h)$^{-1}$.[117] Furthermore, the *cis*-dioxovanadium complexes shown here appeared to be slightly better than reported functional mimics of the natural system,[120,136] but still they catalyze very slow the biomimetic reaction compared to vanadium bromoperoxidase. Therefore, the design of a ligand system which provides a catalyst able to approach the enzyme in reaction rate is still a difficult task. Obviously, the structural environment of vanadate in the active-binding site plays a very important role during the catalytic cycles.

In recent years, numerous vanadium catalysts were designed for sulfide oxidation reaction.[189–192] Part of these vanadium complexes are also models of vanadium haloperoxidase which also catalyze the oxidation of organic sulfides, varying from an enantioselective behavior when vanadium bromoperoxidase mediated the reaction to a non-selective sulfide oxidation when vanadium chloroperoxidase was used as biocatalyst.[87,89,90,175] The herein described *cis*-dioxovanadium(V) complexes were also tested towards their capacity to mediate the catalytic reaction of phenyl methyl sulfide by hydrogen peroxide. The outcomes of the catalytic reaction results range from 82 to 89 % sulfide conversion within 18 hours, when *cis*-dioxovanadium(V) complexes with an intact Schiff base ligand were used as catalysts, whereas a quantitative conversion of phenyl methyl sulfide was achieved after 16 hours when the *cis*-dioxovanadium(V) complex with *in situ* formed dihydropyrrole structure catalyzed the reaction. These results are similar with reported capacity of vanadium complexes to catalyze the sulfide oxidation reaction.[237–240] Nevertheless, in the last chapter unprecedent examples of high efficient vanadium-catalysts for sulfuroxidation reaction were described. The binuclear *cis*-dioxovanadium(V) complexes catalyzed the oxidation of thioanisole with 78-84 % yields after two hours reaction time, whereas the binuclear molybdenum complexes catalyze the same reaction almost quantitatively within 90 minutes. The design of a chiral binuclear molybdenum complex showed instead a non selective reaction, yielding a mixture of R and S isomers of phenyl methyl sulfoxide.

Future research in asymmetric sulfide oxidation reaction should therefore, be focused on the development of chiral vanadium complexes. An interesting future of the chiral bis-N-salicylidene R-methyl succinic acid hydrazide is the substitution of the aromatic cycles, especially with steric hindrance electron donating groups. Another possible

ligand system, which might also lead to vanadium-catalysts that approach a high enatiomeric excess is also represented by replacement of the methyl group of the chiral center with amino functionality.

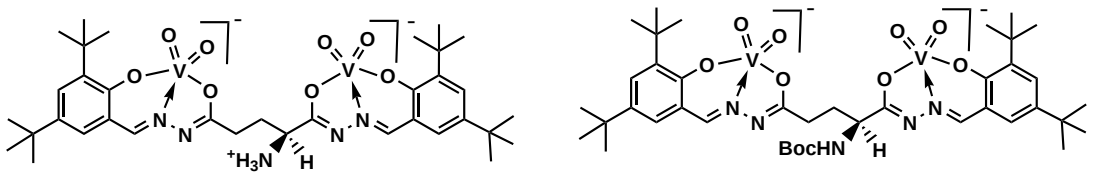


Figure 105: Schematic representation of possible chiral binuclear vanadium catalysts based on bis-N-salicylidene L-glutamic dihydrazide ligand and its Boc-protected derivative.

In this case starting from commercially available L-glutamic acid dimethyl ester and following the described procedure, the isolation of a chiral binuclear *cis*-dioxovanadium complex will be also possible. The last system has the advantage of a possible Boc-protection of the amino group which might increase the reactivity of the closer vanadate moiety.

Another interesting future prospect is regarding the reactivity of the *cis*-dioxovanadium complexes towards a possible formation of an oxo-hxdroxy-vanadate moiety $[V^{V}O(OH)]^{2+}$. In this case the spectrophotometric titration of the dioxovanadium complexes with hydrochloric acid should also be performed in non-aqueous solution; for example spectroscopically standard solution of HCl in ethanol, which is commercially available. Another possible future of the vanadium model complexes is represented by the possibility to increase the aliphatic chain length favoring therefore, the performance of the protonation reaction in unpolar solvents. The 12-dodeca amino-fucntionalized alkylic side chain might be a solution for designing a *cis*-dioxovanadium(V) complex with a moderate solubility in acetonitrile. Here should be mentioned that, Pecoraro *et al.* showed spectrophotometrically the formation of $[V^{V}O(OH)]^{2+}$ unit when *cis*-dioxovanadium complexes were reacted with HCl in acetonitrile solution.[102]

# Chapter 8

# Characterization techniques and crystallographical data

Carbon, hydrogen and nitrogen contents were determined at the "Institut für Organische und Makromolekulare Chemie", Friedrich-Schiller University, Jena using LECO CHN/932 and VARIO EL III elemental analyzers.

$^{1}$H, $^{13}$C, $^{51}$V NMR, $^{1}$H{$^{1}$H} COSY and $^{1}$H{$^{13}$C} heteronuclear correlation NMR spectra were recorded on Bruker Avance 200 and 400 MHz spectrometers.

Mass spectroscopy analysis were conducted on a MAT95XL Finnigan instrument, using electron spray ionization, negative and positive mode.

GC measurements were performed on a SRI 8610 gas chromatograph using MXT-1 Restek coloumn.

Spectrophotometric titrations and UV-Vis spectra were recorded on a Varian Cary 5000 UV/Vis/NIR spectrophotometer using solvents of high purity. The spectrophotometer was equipped with dual cell peltier accessory, which offered a continuous stirring and temperature control.

IR spectra were recorded on Bruker IFS55/Equinox spectrometer on samples prepared as KBr pellets.

Potentiometric titration were performed on a Metller Toledo DL 50 titrator, using an electrode.

HPLC measurements were carried out on Jasco-MD 1515 instrument equipped with UV-diode array multiwavelength detector. The chiral sulfoxide were assayed using a REGIS chiral column (PIRKLE COVALENT S,S-WHELK-01 10/100 FEC; 25 cm x 4.6 mm) with a mixture hexane/i-propanol:90/10 (v/v) as mobile phase.

Cyclic voltametry measurements and square wave voltametric measurements have been conducted in a three electrode technique using a home built computer controlled instrument based on the PCI 6110-E data acquisition board (National Instruments). The experiments were performed in acetonitrile solutions containing 0.25 M tetra-n-butylammonium-hexafluorophosphate under a blanket of solvent saturated with argon. The ohmic resistance that has to be compensated was determined by measuring the impedance of the system at potentials where the faradaic current was negligible. Background corrections was accomplished only for cyclic voltammograms by subtracting the current curves of the blank electrolyte containing the same concentration of the supporting electrolyte from the experimental cyclic voltammograms. Ag/AgCl was used as reference electrode in acetonitrile containing 0.25 M tetra-n-butylammonium chloride. The potential of this reference system was calibrated by measuring the potential of the couple ferrocenium/ferrocene at the end of each experiment and was found to be $0.812 \pm 0.002$ V throughout the measurements. The working electrode was drop hanging mercury ($m_{Hg-drop}$= 4 mg) produced by CGME instrument from Bioanalytical Systems Inc., West Lafayette, USA. Theoretical square wave voltammograms were simulated using DigiElch package available from www.DigiElch.de.

Electronic paramagnetic resonance measurements were performed on a Bruker ESP 300E using X-Band (9 GHz). Thermogravimetric analysis were carried out using NETZSCH STA 409PC/PG instrument. The samples were placed in a heating block with a heating rate of 5 K/minute under nitrogen atmosphere.

The crystallographic data were collected on a Nonius KappaCCD difractometer, using graphite-monochromated Mo-K$\alpha$ radiation of 71.073 pm. A summary of crystallographic data and data collection for all complexes is given in the last part of the thesis. The structures were solved by direct methods (SHELXT) and subsequent least square refinement. All non-hydrogen atoms were refined by using anisotropic displacement parameters, while the hydrogen atoms were fixed and refined including their isotropic displacement parameters. For small sized crystals a BRUKER AXS difractometer with synchrotron radiation was used for collecting the data.

**General Remarks**

N,N-Dimethylformamide (p.a.) have been purchased from Roth, stored over molecular sieves and used as received.
Hydrogen peroxide, purchased from Merck, was standardized by titration with potassium permanganate in presence of sulfuric acid.
Perchloric acid (aqueous solution) was standardized by potentiometric titration with NaOH 1M solution.
All other agents were used as received, with no further purifications, except the situations where was specified.

# Crystallographic data

Summary of crystallographic data for complex **1** $NH_4[VO_2(salhyp)]\cdot 2CH_3OH$.

| | |
|---|---|
| Formula | $C_{13}H_{22}N_3O_5V$ |
| Formula weight | 351.28 |
| Crystal size (mm) | 0.10 x 0.10 x 0.03 |
| Crystal system | triclinic |
| Space group | P-1 |
| Lattice parameters | |
| a (pm) | 751.52(4), $\alpha$ 67.902(3) |
| b(pm) | 1428.99(6)), $\beta$ 87.191(3) |
| c (pm) | 1643.68(7), $\gamma$ 79.543(3) |
| $\beta(^\circ)$ | 93.149(2) |
| Cell volume ($10^6 pm^3$) | 1607.98(13) |
| Z | 4 |
| Temperature (K) | 183(2) |
| $\Delta_{calc}$(g $cm^{-3}$) | 1.483 |
| F(000) | 736 |
| $\mu$(Mo $K_\alpha$)($mm^{-1}$) | 0.643 |
| Data collection range (°) | $2.41 \leq \Theta \leq 27.49$ |
| Index range | $-7 \leq h \leq 9$ |
| | $-18 \leq k \leq 17$ |
| | $-21 \leq l \leq 21$ |
| Reflection measured | |
| total | 7307 |
| unique | 5406 ($R_{int}$= 0.0354 ) |
| Goodness-of-fit | 1.057 |
| $R_1$ | 0.0523 |
| $wR_2$ | 0.1141 |

Summary of crystallographic data for complex **2** [$VO_2$(Hsalhyp)]

| | |
|---|---|
| Formula | $C_{12}H_{15}N_2O_4V$ |
| Formula weight | 302.20 |
| Crystal size (mm) | 0.10 x 0.10 x 0.04 |
| Crystal system | triclinic |
| Space group | P-1 |
| Lattice parameters | |
| a (pm) | 842.87(9) , $\alpha$ 66.802(6) |
| b(pm) | 1156.46(15), $\beta$ 81.107(8) |
| c (pm) | 1439.71(16), $\gamma$ 89.943(6) |
| Cell volume ($10^6$pm$^3$) | 1607.98(13) |
| Z | 4 |
| Temperature (K) | 183(2) |
| $\Delta_{calc}$(g cm$^{-3}$) | 1.579 |
| F(000) | 624 |
| $\mu$(Mo $K_\alpha$)(mm$^{-1}$) | 0.792 |
| Data collection range (°) | $2.68 \leq \Theta \leq 27.45$ |
| Index range | $-10 \leq h \leq 10$ |
| | $-13 \leq k \leq 14$ |
| | $-18 \leq l \leq 18$ |
| Reflection measured | |
| total | 5572 |
| unique | 3669 ($R_{int}$= 0.0418 ) |
| Goodness-of-fit | 1.035 |
| $R_1$ | 0.0730 |
| $wR_2$ | 0.1660 |

Summary of crystallographic data for complex **3** [VO(salhyb)(Q)]

| | |
|---|---|
| Formula | $C_{20}H_{18}N_3O_4V$ |
| Formula weight | 415.31 |
| Crystal size (mm) | 0.03 x 0.03 x 0.03 |
| Crystal system | monoclinic |
| Space group | $P2_1/n$ |
| Lattice parameters | |
| a (pm) | 981.38(3) |
| b(pm) | 1034.14(3) |
| c (pm) | 1835.78(6) |
| $\beta(^\circ)$ | 93.149(2) |
| Cell volume ($10^6$pm$^3$) | 1860.29(10) |
| Z | 4 |
| Temperature (K) | 183(2) |
| $\Delta_{calc}$(g cm$^{-3}$) | 1.483 |
| F(000) | 856 |
| $\mu$(Mo $K_\alpha$)(mm$^{-1}$) | 0.566 |
| Data collection range ($^\circ$) | $2.26 \leq \Theta \leq 27.43$ |
| Index range | $-12 \leq h \leq 12$ |
| | $-12 \leq k \leq 13$ |
| | $-23 \leq l \leq 23$ |
| Reflection measured | |
| total | 4237 |
| unique | 3187($R_{int}$= 0.0314) |
| Goodness-of-fit | 1.016 |
| $R_1$ | 0.0463 |
| $wR_2$ | 0.1153 |

Summary of crystallographic data for complex **4** [VO(salhyp)(Q)]

| | |
|---|---|
| Formula | $C_{21}H_{20}N_3O_4V$ |
| Formula weight | 429.34 |
| Crystal size (mm) | 0.03 x 0.03 x 0.02 |
| Crystal system | monoclinic |
| Space group | $P2_1/n$ |
| Lattice parameters | |
| a (pm) | 1032.82(4) |
| b(pm) | 1004.59(3) |
| c (pm) | 1918.96(7) |
| $\beta(^\circ)$ | 94.962(2) |
| Cell volume ($10^6 pm^3$) | 1983.58(12) |
| Z | 4 |
| Temperature (K) | 183(2) |
| $\Delta_{calc}$(g $cm^{-3}$) | 1.438 |
| F(000) | 888 |
| $\mu$(Mo $K_\alpha$)($mm^{-1}$) | 0.533 |
| Data collection range ($^\circ$) | $3.09 \leq \Theta \leq 27.49$ |
| Index range | $-13 \leq h \leq 13$ |
| | $-13 \leq k \leq 12$ |
| | $-24 \leq l \leq 24$ |
| Reflection measured | |
| total | 4529 |
| unique | 3079($R_{int}$= 0.0385) |
| Goodness-of-fit | 1.031(4) |
| $R_1$ | 0.0458 |
| $wR_2$ | 0.0983 |

Summary of crystallographic data for complex **5** [VO(salhyh)(Q)]

| | |
|---|---|
| Formula | $C_{22}H_{22}N_3O_4V$ |
| Formula weight | 443.37 |
| Crystal size (mm) | 0.04 x 0.03 x 0.03 |
| Crystal system | monoclinic |
| Space group | $P2_1/n$ |
| Lattice parameters | |
| a (pm) | 1031.99(3) |
| b(pm) | 1052.39(3) |
| c (pm) | 1834.62(5) |
| $\beta(^\circ)$ | 93.9260(10) |
| Cell volume ($10^6 pm^3$) | 1987.82(10) |
| Z | 4 |
| Temperature (K) | 183(2) |
| $\Delta_{calc}$(g $cm^{-3}$) | 1.481 |
| F(000) | 920 |
| $\mu$(Mo $K_\alpha$)($mm^{-1}$) | 0.534 |
| Data collection range ($^\circ$) | $2.23 \leq \Theta \leq 27.45$ |
| Index range | $-13 \leq h \leq 13$ |
| | $-13 \leq k \leq 12$ |
| | $-23 \leq l \leq 23$ |
| Reflection measured | |
| total | 4514 |
| unique | 3331($R_{int}$= 0.0322) |
| Goodness-of-fit | 1.025 |
| $R_1$ | 0.0394 |
| $wR_2$ | 0.0848 |

Summary of crystallographic data for methoxy-bis-(8-quinolinato)-oxovanadium(V) complex (**6**)

| | |
|---|---|
| Formula | $C_{19}H_{15}N_2O_4V$ |
| Formula weight | 386.27 |
| Crystal size (mm) | 0.03 x 0.03 x 0.02 |
| Crystal system | monoclinic |
| Space group | C2/c |
| Lattice parameters | |
| a (pm) | 4888.07(13) |
| b(pm) | 965.42(2) |
| c (pm) | 1427.88(4) |
| $\beta(^\circ)$ | 100.2750(10) |
| Cell volume ($10^6$pm$^3$) | 6630.2(3) |
| Z | 16 |
| Temperature (K) | 183(2) |
| $\Delta_{calc}$(g cm$^{-3}$) | 1.548 |
| F(000) | 3168 |
| $\mu$(Mo $K_\alpha$)(mm$^{-1}$) | 0.627 |
| Data collection range ($^\circ$) | $1.69 \leq \Theta \leq 27.47$ |
| Index range | $-60 \leq h \leq 63$ |
| | $-12 \leq k \leq 12$ |
| | $-16 \leq l \leq 18$ |
| Reflection measured | |
| total | 7590 |
| unique | 5537($R_{int}$= 0.0492) |
| Goodness-of-fit | 1.055 |
| $R_1$ | 0.0480 |
| $wR_2$ | 0.1042 |

Summary of crystallographic data for complex **9** $[VO(O_2)(Hsalhyhb)H_2O]\cdot H_2O$.

| | |
|---|---|
| Formula | $C_{11}H_{17}N_2O_8V$ |
| Formula weight | 356.21 |
| Crystal size (mm) | 0.04 x 0.03 x 0.03 |
| Crystal system | monoclinic |
| Space group | $P2_1/n$ |
| Lattice parameters | |
| a (pm) | 1034.3(2) |
| b(pm) | 698.86(14) |
| c (pm) | 2006.6(4) |
| $\beta(^\circ)$ | 100.74(3) |
| Cell volume ($10^6 pm^3$) | 1425.0(5) |
| Z | 4 |
| Temperature (K) | 293) |
| $\Delta_{calc}$(g $cm^{-3}$) | 1.660 |
| F(000) | 736 |
| $\mu$(Mo $K_\alpha$)($mm^{-1}$) | 0.740 |
| Data collection range (°) | $3.09 \leq \Theta \leq 29.39$ |
| Index range | $-14 \leq h \leq 14$ |
| | $-8 \leq k \leq 9$ |
| | $-27 \leq l \leq 25$ |
| Reflection measured | |
| total | 14918 |
| unique | 3887($R_{int}$= 0.1472) |
| Goodness-of-fit | 0.768 |
| $R_1$ | 0.0454 |
| $wR_2$ | 0.0807 |

Summary of crystallographic data for complex **10** [VO(salhyhb)(Q)].

| | |
|---|---|
| Formula | $C_{20}H_{18}N_3O_5V$ |
| Formula weight | 431.31 |
| Crystal size (mm) | 0.03 x 0.03 x 0.02 |
| Crystal system | triclinic |
| Space group | P-1 |
| Lattice parameters | |
| a (pm) | 1010.08(2), $\alpha$ 88.9150(10) |
| b(pm) | 1042.23(3), $\beta$ 89.170(2) |
| c (pm) | 1779.17(6) , $\gamma$ 88.790(2) |
| Cell volume ($10^6$pm$^3$) | 1872.06(9) |
| Z | 4 |
| Temperature (K) | 183(2) |
| $\Delta_{calc}$(g cm$^{-3}$) | 1.530 |
| F(000) | 888 |
| $\mu$(Mo K$_\alpha$)(mm$^{-1}$) | 0.569 |
| Data collection range (°) | $2.78 \leq \Theta \leq 27.49$ |
| Index range | $-11 \leq h \leq 13$ |
| | $-12 \leq k \leq 13$ |
| | $-23 \leq l \leq 22$ |
| Reflection measured | |
| total | 8519 |
| unique | 6635(R$_{int}$= 0.0269 ) |
| Goodness-of-fit | 1.029 |
| $R_1$ | 0.0401 |
| $wR_2$ | 0.0896 |

Summary of crystallographic data for complex **13** $[VO_2(Hsalhycab)]_2$.

| | |
|---|---|
| Formula | $C_{22}H_{24}N_6O_6V_2$ |
| Formula weight | 570.35 |
| Crystal size (mm) | 0.03 x 0.03 x 0.02 |
| Crystal system | monoclinic |
| Space group | $P2_1/c$ |
| Lattice parameters | |
| a (pm) | 695.49(9), $\alpha$ 90.00 |
| b(pm) | 1406.14(18), $\beta$ 105.190(5) |
| c (pm) | 1245.55(17) , $\gamma$ 90.00 |
| Cell volume ($10^6$pm$^3$) | 1175.5(3) |
| Z | 2 |
| Temperature (K) | 120(2) |
| $\Delta_{calc}$(g cm$^{-3}$) | 1.611 |
| F(000) | 584 |
| $\mu$(synchrotron radiation)(mm$^{-1}$) | 0.442 |
| Data collection range (°) | $2.02 \leq \Theta \leq 12.42$ |
| Index range | $-8 \leq h \leq 8$ |
| | $-17 \leq k \leq 17$ |
| | $-15 \leq l \leq 15$ |
| Reflection measured | |
| total | 2237 |
| unique | 1829($R_{int}$= 0.0664) |
| Goodness-of-fit | 1.029 |
| $R_1$ | 0.0384 |
| $wR_2$ | 0.1020 |

Summary of crystallographic data for complex **14** [$VO_2$(Hsalhycab)].

| | |
|---|---|
| Formula | $C_{11}H_{12}N_3O_3V$ |
| Formula weight | 285.18 |
| Crystal size (mm) | 0.04 x 0.04 x 0.03 |
| Crystal system | monoclinic |
| Space group | $P2_1/n$ |
| Lattice parameters | |
| a (pm) | 814.74(5), $\alpha$ 90.00 |
| b(pm) | 663.96(4), $\beta$ 91.545(3) |
| c (pm) | 2133.14(9) , $\gamma$ 90.00 |
| Cell volume ($10^6$pm$^3$) | 1153.51(11) |
| Z | 4 |
| Temperature (K) | 183(2) |
| $\Delta_{calc}$(g cm$^{-3}$) | 1.642 |
| F(000) | 584 |
| $\mu$(Mo $K_\alpha$)(mm$^{-1}$) | 0.864 |
| Data collection range (°) | $3.21 \leq \Theta \leq 27.47$ |
| Index range | $-10 \leq h \leq 8$ |
| | $-8 \leq k \leq 8$ |
| | $-27 \leq l \leq 26$ |
| Reflection measured | |
| total | 2645 |
| unique | 1796($R_{int}$= 0.0612 ) |
| Goodness-of-fit | 1.029 |
| $R_1$ | 0.0425 |
| $wR_2$ | 0.0906 |

Summary of crystallographic data for complex **15a** [$VO_2$(salhyah)].

| | |
|---|---|
| Formula | $C_{13}H_{18}N_3O_4V$ |
| Formula weight | 331.24 |
| Crystal size (mm) | 0.03 x 0.03 x 0.02 |
| Crystal system | monoclinic |
| Space group | $P2_1/n$ |
| Lattice parameters | |
| a (pm) | 762.300(10), $\alpha$ 90.00 |
| b(pm) | 2129.02(5), $\beta$ 108.1470(10) |
| c (pm) | 902.08(2) , $\gamma$ 90.00 |
| Cell volume ($10^6$pm$^3$) | 1391.21(5) |
| Z | 4 |
| Temperature (K) | 183(2) |
| $\Delta_{calc}$(g cm$^{-3}$) | 1.581 |
| F(000) | 688 |
| $\mu$(Mo $K_\alpha$)(mm$^{-1}$) | 0.733 |
| Data collection range (°) | $2.97 \leq \Theta \leq 27.50$ |
| Index range | $-9 \leq h \leq 9$ |
| | $-25 \leq k \leq 27$ |
| | $-9 \leq l \leq 11$ |
| Reflection measured | |
| total | 3180 |
| unique | 2893($R_{int}$= 0.0214) |
| Goodness-of-fit | 1.029 |
| $R_1$ | 0.0289 |
| $wR_2$ | 0.0754 |

Summary of crystallographic data for complex **15b** $[VO_2(salhyah)]\cdot 0.5H_2O$.

| | |
|---|---|
| Formula | $C_{13}H_{19}N_3O_{4.5}V$ |
| Formula weight | 340.25 |
| Crystal size (mm) | 0.04 x 0.04 x 0.03 |
| Crystal system | orthorhombic |
| Space group | Pbcn |
| Lattice parameters | |
| a (pm) | 1964.56(7), $\alpha$ 90.00 |
| b(pm) | 923.93(3), $\beta$ 90.00 |
| c (pm) | 1687.40(7) , $\gamma$ 90.00 |
| Cell volume ($10^6$pm$^3$) | 3062.83(19) |
| Z | 8 |
| Temperature (K) | 183(2) |
| $\Delta_{calc}$(g cm$^{-3}$) | 1.476 |
| F(000) | 1416 |
| $\mu$(Mo $K_\alpha$)(mm$^{-1}$) | 0.670 |
| Data collection range (°) | $2.07 \leq \Theta \leq 27.46$ |
| Index range | $-25 \leq h \leq 25$ |
| | $-11 \leq k \leq 11$ |
| | $-9 \leq l \leq 9$ |
| Reflection measured | |
| total | 3487 |
| unique | 2312($R_{int}$= 0.0709) |
| Goodness-of-fit | 1.029 |
| $R_1$ | 0.0392 |
| $wR_2$ | 0.0919 |

Summary of crystallographic data for complex **16** [$MoO_2$(salhycab)$CH_3OH$].

| | |
|---|---|
| Formula | $C_{12}H_{15}N_3O_4Mo$ |
| Formula weight | 361.21 |
| Crystal size (mm) | 0.03 x 0.02 x 0.02 |
| Crystal system | monoclinic |
| Space group | $P2_1/c$ |
| Lattice parameters | |
| a (pm) | 1021.06(3) , $\alpha$ 90.00 |
| b(pm) | 1282.03(4), $\beta$ 110.274(2) |
| c (pm) | 1091.66(2) , $\gamma$ 90.00 |
| Cell volume ($10^6 pm^3$) | 1340.48(6) |
| Z | 4 |
| Temperature (K) | 183(2) |
| $\Delta_{calc}$(g $cm^{-3}$) | 1.790 |
| F(000) | 728 |
| $\mu$(Mo $K_\alpha$)($mm^{-1}$) | 0.996 |
| Data collection range (°) | $2.55 \leq \Theta \leq 27.46$ |
| Index range | $-13 \leq h \leq 13$ |
| | $-16 \leq k \leq 16$ |
| | $-14 \leq l \leq 14$ |
| Reflection measured | |
| total | 3054 |
| unique | 2761($R_{int}$= 0.0235) |
| Goodness-of-fit | 1.064 |
| $R_1$ | 0.0283 |
| $wR_2$ | 0.0588 |

Summary of crystallographic data for complex **18** $[VO_2(salhyga)]\cdot 3H_2O$.

| | |
|---|---|
| Formula | $C_{10}H_{18}N_5O_7V$ |
| Formula weight | 371.23 |
| Crystal size (mm) | 0.03 x 0.03 x 0.03 |
| Crystal system | orthorhombic |
| Space group | $P2_12_12_1$ |
| Lattice parameters | |
| a (pm) | 674.76(2) , $\alpha$ 90.00 |
| b(pm) | 1293.61(6), $\beta$ 90.00 |
| c (pm) | 1725.39(9), $\gamma$ 90.00 |
| Cell volume ($10^6$pm$^3$) | 1506.05(11) |
| Z | 4 |
| Temperature (K) | 183(2) |
| $\Delta_{calc}$(g cm$^{-3}$) | 1.637 |
| F(000) | 768 |
| $\mu$(Mo $K_\alpha$)(mm$^{-1}$) | 0.704 |
| Data collection range (°) | $2.84 \leq \Theta \leq 27.46$ |
| Index range | $-8 \leq h \leq 8$ |
| | $-16 \leq k \leq 16$ |
| | $-21 \leq l \leq 22$ |
| Reflection measured | |
| total | 3435 |
| unique | 2777($R_{int}$= 0.0573) |
| Goodness-of-fit | 1.025 |
| $R_1$ | 0.0398 |
| $wR_2$ | 0.0807 |

Summary of crystallographic data for complex **19** [$VO_2$(salhygh)].

| | |
|---|---|
| Formula | $C_{14}H_{19}N_5O_4V$ |
| Formula weight | 372.28 |
| Crystal size (mm) | 0.04 x 0.04 x 0.03 |
| Crystal system | monoclinic |
| Space group | I2/a |
| Lattice parameters | |
| a (pm) | 1658.94(7) , $\alpha$ 90.00 |
| b(pm) | 995.55(3), $\beta$ 94.397(2) |
| c (pm) | 2076.82(9), $\gamma$ 90.00 |
| Cell volume ($10^6$pm$^3$) | 3419.9(2) |
| Z | 8 |
| Temperature (K) | 183(2) |
| $\Delta_{calc}$(g cm$^{-3}$) | 1.446 |
| F(000) | 1544 |
| $\mu$(Mo $K_\alpha$)(mm$^{-1}$) | 0.608 |
| Data collection range (°) | $2.27 \leq \Theta \leq 27.45$ |
| Index range | $-21 \leq h \leq 19$ |
| | $-12 \leq k \leq 12$ |
| | $-23 \leq l \leq 26$ |
| Reflection measured | |
| total | 3884 |
| unique | 2611($R_{int}$= 0.0577) |
| Goodness-of-fit | 1.036 |
| $R_1$ | 0.0497 |
| $wR_2$ | 0.1072 |

Summary of crystallographic data for complex **25** $[(MoO_2)_2(salhygu)\cdot 2CH_3OH]$.

| | |
|---|---|
| Formula | $C_{21}H_{24}N_4O_{10}Mo_2$ |
| Formula weight | 684.32 |
| Crystal size (mm) | 0.043 x 0.03 x 0.02 |
| Crystal system | orthorombic |
| Space group | $P2_12_12_1$ |
| Lattice parameters | |
| a (pm) | 746.59(2) , $\alpha$ 90.00 |
| b(pm) | 954.11(3), $\beta$ 90.00 |
| c (pm) | 3499.51(11), $\gamma$ 90.00 |
| Cell volume ($10^6 pm^3$) | 2492.80(13) |
| Z | 4 |
| Temperature (K) | 183(2) |
| $\Delta_{calc}$(g $cm^{-3}$) | 1.823 |
| F(000) | 1368 |
| $\mu$(Mo $K_\alpha$)($mm^{-1}$) | 1.069 |
| Data collection range (°) | $1.16 \leq \Theta \leq 27.47$ |
| Index range | $-9 \leq h \leq 9$ |
| | $-12 \leq k \leq 12$ |
| | $-28 \leq l \leq 44$ |
| Reflection measured | |
| total | 5485 |
| unique | 4056($R_{int}$= 0.0716) |
| Goodness-of-fit | 1.010 |
| $R_1$ | 0.0486 |
| $wR_2$ | 0.0799 |

# Bibliography


[1] N. D. Chasteen. In *Structure and Bonding*. Springer-Verlag, Berlin, Heidelberg **1983** 107–138.

[2] H. Vilter. *Phytochem.* **1984**. *23*, 1387–1390.

[3] N. Itoh, Y. Izumi, H. Yamata. *Biochem. Biophys. Res. Commun.* **1985**. *131*, 428–435.

[4] M. J. Mitchell, D. E. Ryan, K. Nakanishi, P. Frank, K. O. Hodgson. In H. Sigel, A. Sigel (Editors) *Metals ions in biological systems 31*. Marcel Dekker, Inc., New York **1995** 423–474.

[5] R. Meier, M. Boddin, S. Mitzenheim, K. Kanamori. In H. Sigel, A. Sigel (Editors) *Metals ions in biological systems 31*. Marcel Dekker, Inc., New York **1995** 45–83.

[6] R. Wever, W. Hemrika. In A. Messerschmidt, R. Huber, T. Poulos, K. Wieghardt (Editors) *Handbook of Metalloproteins 2*. John Wiley & Sons Ltd., Chichester **2001** 1417–1428.

[7] E. Koch, H. Kneifel, E. Bayer. *Z. Naturforsch.* **1987**. *42C*, 873–878.

[8] E. Bayer. In H. Sigel, A. Sigel (Editors) *Metals ions in biological systems 31*. Marcel Dekker, Inc., New York **1995** 407–421.

[9] K. H. Thompson, J. H. McNeill, C. Orvig. *Chem. Rev.* **1999**. *99*, 2561–2571.

[10] B. K. Köpf-Maier, H. Köpf. *Z. Naturforsch.* **1979**. *34B*, 805–807.

[11] D. Rehder, C. Weidemann, A. Duch, W. Priebsch. *Inorg. Chem.* **1988**. *27*, 584–587.

[12] C. R. Cornnman, J. Kampf, V. L. Pecoraro. *Inorg. Chem.* **1992**. *31*, 1981–1983.

[13] C. Slebodnick, B. J. Hamstra, V. L. Pecoraro. In *Structure and Bonding, Vol. 89*. Springer Verlag, Berlin, **1997** 78–94.

[14] H. Vilter, D. Rehder. *Inorganica Chimica Acta* **1987**. *136*, L7–L10.

[15] M. Henze. *Hoppe-Seylers Z. Physiol. Chem.* **1911**. *72*, 494–501.

[16] P. Frank, R. M. K. Carlson, K. O. Hodgson. *Inorg. Chem.* **1986**. *25*, 470–478.

[17] P. Frank, B. Hedman, R. M. K. Carlson, T. A. Tyson, A. L. Roe, K. O. Hodgson. *Biochemistry* **1987**. *26*, 4975–4979.

[18] P. Frank, R. M. K. Carlson, K. O. Hodgson. *Inorg. Chem.* **1988**. *27*, 118–122.

[19] E. M. Oltz, R. C. Bruening, M. J. Smith, K. Kustin, K. Nakanishi. *J. Am. Chem. Soc.* **1988**. *110*, 6162–6172.

[20] D. E. Ryan, N. D. Ghatlia, A. E. McDermott, N. J. Turro, K. Nakanishi, K. Kustin. *J. Am. Chem. Soc.* **1992**. *114*, 9659–9660.

[21] H. Michibata, N. Yamaguchi, T. Uyama, T. Ueki. *Coord. Chem. Rev.* **2003**. *237*, 41–51.

[22] T. Ueki, T. Adachi, S. Kawano, M. Aoshima, N. Yamaguchi, K. Kanamori, H. Michibata. *Biochem. Biophys. Acta* **2003**. *1626*, 43–50.

[23] R. E. Eady. In H. Sigel, A. Sigel (Editors) *Metals ions in biological systems 31*. Marcel Dekker, Inc., New York **1995** 364–405.

[24] E. Bayer, H. Kneifel. *Z. Naturforsch. B* **1972**. *27*, 207–210.

[25] R. R. Eady. *Coord. Chem. Rev.* **2003**. *237*, 23–30.

[26] J. Kim, D. C. Rees. *Biochemsitry* **1994**. *33*, 389–397.

[27] F. B. Simpson, R. H. Burris. *Science* **1984**. *224*, 1095–1097.

[28] M. K. Chan, J. Kim, D. C. Rees. *Science* **1993**. *260*, 792–794.

[29] J. Kim, D. Woo, D. C. Rees. *Biochemistry* **1993**. *32*, 7104–7115.

[30] J. A. Kovacs, R. H. Holm. *J. Am. Chem. Soc.* **1986**. *108*, 340–341.

[31] J. A. Kovacs, R. H. Holm. *Inorg. Chem.* **1987**. *26*, 711–718.

[32] H. Kneifel, E. Bayer. *J. Am. Chem. Soc.* **1986**. *108*, 3075–3077.

[33] E. M. Armstrong, R. L. Beddoes, L. J. Calviou, J. M. Charnock, D. Collison, N. Ertok, J. H. Naismith, C. D. Garner. *J. Am. Chem. Soc.* **1993**. *115*, 807–808.

[34] R. E. Berry, E. M. Armstrong, R. L. Beddoes, D. Collison, S. N. Ertok, M. Helliwell, C. D. Garner. *Angew. Chem.* **1999**. *111*, 871–873.

[35] M. F. C. G. da Silva, J. A. L. da Silva, J. J. R. F. da Silva, A. J. L. Pombeiro, C. Amatore, J. N. Verpeaux. *J. Am. Chem. Soc.* **1996**. *118*, 7568–7573.

[36] P. M. Reis, J. Armando, L. Silva, J. J. R. F. da Silva, A. J. L. Pombeiro. *Chem. Commun.* **2000**. 1845–1846.

[37] P. M. Reis, J. A. L. da Silva A. F. Palavra, J. J. R. F. da Silva, T. Kitamura, Y. Fujiwara, A. J. L. Pombeiro. *Angew. Chem., Int. Ed.* **2003**. 821–823.

[38] A. Messerschmidt, R. Wever. *Proc. Natl. Acad. Sci. U.S.A.* **1996**. *93*, 392–396.

[39] In N. D. Chasteen (Editor) *Vanadium in Biological Systems*. Kluwer Academic Publishers, Dordrecht, The Netherlands **1990** .

[40] J. J. Cruywagen, J. B. Neyns, A. N. Westra. *Inorg. Chem.* **1996**. *35*, 1556–1559.

[41] P. J. Toscano, E. J. Schermerhorn, C. Dettelbacher, D. Macherone, J. Zubieta. *Chem. Commun.* **1991**. 933–935.

[42] R. A. Henderson, D. L. Hughes, Z. Janas, R. L. Richards, P. Sobota, S. Szafert. *J. Organomet. Chem.* **1998**. *554*, 195–200.

[43] F. J. Feher, J. Walzer. *Inorg. Chem.* **1991**. *30*, 1689–1673.

[44] A. F. Nour-Eldeen, M. J. Gresser. *J. Biol. Chem.* **1985**. *260*, 6836–6842.

[45] D. G. Drueckhammer, J. R. Durrwachter, R. L. Pederson, D. C. Crans, L. Daniels, C. H. Wong. *J. Org. Chem.* **1989**. *54*, 70–77.

[46] D. C. Crans, R. W. Marshman, R. Nielsen, I. L. Felty. *J. Org. Chem.* **1993**. *58*, 2244–2252.

[47] D. C. Crans, C. M. Simone, J. S. Blanchard. *J. Am. Chem. Soc.* **1992**. *114*, 4926–4928.

[48] M. J. Gresser, A. S. Tracey. *J. Am. Chem. Soc.* **1985**. *107*, 4215–4220.

[49] K. Kustin. ACS Symposium. American Chemical Society, Washington, DC **1998** 711–735.

[50] H. Deng, R. Callender, Z. Huand, Z. Y. Zhang. *Biochemsitry* **2002**. *41*, 5865–5872.

[51] D. C. Cran. *J. Inorg. Biochem.* **2000**. *80*, 123–131.

[52] M. Zhang, M. Zhou, , R. L. van Etten, C. V. Stauffacher. *Biochemistry* **1997**. *36*, 15–23.

[53] C. L. Oppenheimer, J. E. Pessin, J. Messagué, W. Gitomer, M. P. Czech. *J. Biol. Chem.* **1983**. *258*, 4824–4830.

[54] L. J. Wardzala, I. A. Simpson, M. M. Rechler, S. W. Cushman. *J. Biol. Chem.* **1984**. *259*, 8378–8383.

[55] S. W. Cushman, L. J. Wardzala. *J. Biol. Chem.* **1980**. *255*, 4758–4762.

[56] A. Butler, J. N. Carter, M. T. Simpson. In I. Bertini, A. Sigel, H. Sigel (Editors) *Handbook of Metalloproteins 2*. Marcel Dekker, Inc., New York **2001** 154–179.

[57] O. Kirk, L. S. Conrad. *Angew. Chem.* **1999**. *111*, 1031–1033.

[58] H. Yu, J. W. Whittaker. *Biochem. Biophys. Res. Commun.* **1989**. *160*, 87–92.

[59] H. S. Soedjak, A. Butler. *Inorg. Chem.* **1990**. *29*, 5015–5017.

[60] M. G. Almeida, M. Humanes, R. Melo, J. A. Silva, J. J. R. F. da Silva, R. Wever. *Phytochemistry* **2000**. *54*, 5–11.

[61] M. G. Almeida, S. Filipe, M. Humanes, M. F. Maia, R. Melo, N. Severino, J. A. Silva, J. J. R. F. da Silva, R. Wever. *Phytochemistry* **2001**. *57*, 633–642.

[62] A. Messerschmidt, R. Wever. *Inorg. Chim. Acta* **1998**. *273*, 160–166.

[63] W. Hemrika, R. Renirie, S. Macedo-Ribeiro, A. Messerschmidt, R. Wever. *J. Biol. Chem.* **1999**. *274*, 23820–23827.

[64] R. Renirie, W. Hemrika, R. Wever. *J. Biol. Chem.* **2000**. *275*, 11650–11657.

[65] J. W. P. M. van Schijndel, L. H. Simons, E. G. M. Vollenbroek, R. Wever. *FEBS Lett.* **1993**. *336*, 239–242.

[66] K. Ishikawa, Y. Mihara, K. Gondoh, E. Suzuki, Y. Asano. *EMBO Journal* **2000**. *19*, 2412–2423.

[67] E. de Boer, R. Wever. *J. Biol. Chem.* **1988**. *263*, 12326–12332.

[68] A. Butler. *Coord. Chem. Rev.* **1999**. *187*, 17–35.

[69] A. Butler, A. H. Baldwin. In *Structure and Bonding, Vol. 89*. Springer Verlag, Berlin, Heidelberg **1997** 109–132.

[70] M. Weyand, H.-J. Hecht, M. Kiess, M.-F. Liaud, H. Vilter, D. Schomburg. *J. Mol. Biol.* **1999**. *293*, 595–611.

[71] R. Wever, H. Plat, E. de Boer. *Biochem. Biophys. Acta* **1985**. *830*, 181–186.

[72] R. R. Everett, J. R. Kanofskyen, A. Butler. *J. Biol. Chem.* **1990**. *265*, 4908–4914.

[73] R. Renirie, C. Pierlot, J. M. Aubry, A. F. Hartog, H. E. Schoemaker, P. L. Alsters, R. Wever. *Adv. Synth. Catal.* **2003**. *345*, 849–858.

[74] R. R. Everett, A. Butler. *Inorg. Chem.* **1989**. *28*, 393–395.

[75] R. R. Everett, H. S. Soedjak, A. Butler. *J. Biol. Chem.* **1990**. *265*, 15671–15679.

[76] M. G. M. Tromp, G. Olafsson, B. E. Krenn, R. Wever. *Biochem. Biophys. Acta* **1989**. *1040*, 192–198.

[77] J. A. Manthey, L. P. Hager. *J. Biol. Chem.* **1985**. *260*, 9654–9659.

[78] A. Messerschmidt, L. Prade, R. Wever. *Biol. Chem.* **1997**. *378*, 309–315.

[79] M. Çasný, D. Rehder, H. Schmidt, H. Vilter, V. Conte. *J. of Inorg. Biochem.* **2000**. *80*, 157–160.

[80] A. Butler, J. V. Walker. *Chem. Rev.* **1993**. *93*, 1937–1944.

[81] A. Butler, C. J. Carrano. *Coord. Chem. Rev.* **1991**. *109*, 61–105.

[82] A. Butler, R. A. Tschirret-Guth, M. Simpson. *Vanadium Compounds Chemistry, Biochemistry, and Therapeutic Applications*. ACS Symposium. American Chemical Society, Washington, DC **1998** 201–215.

[83] R. A. Tschirret-Guth, A. Butler. *J. Am. Chem. Soc.* **1994**. *116*, 411–412.

[84] A. Butler. In J. Reedijk, E. Bouwman (Editors) *Bioinorganic Catalysis 2nd edition*. Marcel Dekker Inc., New York **1999** 55–79.

[85] J. S. Martinez, G. L. Carroll, R. A. Tschirret-Guth, G. Altenhoff, R. D. Little, A. Butler. *J. Am. Chem. Soc.* **2001**. *123*, 3289–3294.

[86] M. C. Carreno. *Chem. Rev.* **1995**. *95*, 1717–1760.

[87] H. B. ten Brink, H. L. Holland, H. E. Schoemaker, H. van Lingen, R. Wever. *Tetrahedron Asymm.* **1999**. *10*, 4563–4572.

[88] H. B. ten Brink, A. Tuynman, H. L. Dekker, W. Hemrika, Y. Izumi, T. Oshiro, H. E. Schoemaker, R. Wever. *Inorg. Chem.* **1998**. *37*, 6780–6784.

[89] H. B. ten Brink, H. E. Schoemaker, R. Wever. *Eur. J. Biochem.* **2001**. *268*, 132–138.

[90] M. Andersson, A. Willetts, S. Allenmark. *J. Org. Chem.* **1997**. *62*, 8455–8458.

[91] M. A. Andersson, S. G. Allenmark. *Tetrahedron* **1998**. *54*, 15293–15304.

[92] R. H. Holm, P. Kennepohl, E. I. Solomon. *Chem. Rev.* **1996**. *96*, 2239–2314.

[93] H. Luecke, F. A. Quiocho. *Nature* **1990**. *347*, 402–405.

[94] O. Herzberg, P. Reddy, S. Sutrina, M. H. S. Jr., J. Reizer, G. Kapadia. *Proc. Natl. Sci. USA* **1992**. *89*, 2499–2503.

[95] R. Renirie, W. Hemrika, S. R. Piersma, R. Wever. *Biochemistry* **2000**. *39*, 1133–1141.

[96] W. Hemrika, R. Renirie, H. L. Dekker, P. Barnett, R. Wever. *Proc. Natl. Acad. Sci. U.S.A.* **1997**. *94*, 2145–2149.

[97] Y. Lindqvist, G. Schneider, P. Vihko. *Eur. J. Biochem.* **1994**. *221*, 139–142.

[98] W. Plass. *Angew. Chem.* **1999**. *111*, 960–962.

[99] J. Singh, R. C. Nordlie, R. A. Jorgenson. *Biochem. Biophys. Acta* **1981**. *678*, 477–482.

[100] N. Tanaka, V. Dumay, Q. N. Liao, A. J. Lange, R. Wever. *Eur. J. Biochem.* **2002**. *269*, 2162–2167.

[101] E. de Boer, K. Boon, R. Wever. *Biochemistry* **1988**. *27*, 1629–1635.

[102] X. Li, M. S. Lah, V. L. Pecoraro. *Inorg. Chem.* **1988**. *27*, 4657–4664.

[103] P. Noblia, E. J. Baran, L. Otero, P. Draper, H. Cerecetto, M. Gonzalez, O. E. Piro, E. E. Castellano, T. Inohara, Y. Adachi, H. Sakurai, D. Gambino. *Eur. J. Inorg. Chem.* **2004**. 322–328.

[104] M. R. Maurya, S. Agarwal, C. Bader, D. Rehder. *Eur. J. Inorg. Chem.* **2005**. 147–157.

[105] V. Vergopoulos, W. Priebsch, M. Fritzsche, D. Rehder. *Inorg. Chem.* **1993**. *32*, 1844–1849.

[106] A. G. J. Ligtenbarg, A. L. Spek, R. Hage, B. Feringa. *J. Chem. Soc., Dalton Trans.* **1999**. 659–661.

[107] N. Julien-Caitol, E. Rose, J. Vaisserman, D. Rehder. *J. Chem. Soc., Dalton Trans.* **1996**. 2111–2115.

[108] A. K. Tomov, V. C. Gibson, D. Zaher, M. R. J. Elsegood, S. H. Dale. *Chem. Commun.* **2004**. 1956–1957.

[109] W. Plass. *Z. Anorg. Allg. Chem.* **1994**. *620*, 1635–1644.

[110] A. Butler, M. J. Clague, G. E. Meister. *Chem. Rev.* **1994**. *94*, 625–638.

[111] G. J. Colpas, B. J. Hamstra, J. W. Kampf, V. L. Pecoraro. *J. Am. Chem. Soc.* **1996**. *118*, 3469–3478.

[112] K. Kanamori, K. Nishida, N. Miyata, K. Okamota, y. Miyoshi, A. Tamura, H. Sakurai. *Chem. Lett.* **1998**. 1267–1268.

[113] K. Kanamori, K. Nishida, N. Miyata, K. Okamota, y. Miyoshi, A. Tamura, H. Sakurai. *J. Inorg. Biochem.* **2001**. 649–656.

[114] G. J. Colpas, B. J. Hamstra, J. W. Kampf, V. L. Pecoraro. *Inorg. Chem.* **1994**. *33*, 4669–4675.

[115] C. Kimblin, X. Bu, A. Butler. *Inorg. Chem.* **2002**. *41*, 161–163.

[116] M. Casny, D. Rehder. *Chem. Commun.* **2001**. 921–922.

[117] R. I. de la Rosa, M. J. Clague, A. Butler. *J. Am. Chem. Soc.* **1992**. *114*, 760–761.

[118] M. J. Clague, A. Butler. *J. Am. Chem. Soc.* **1995**. *117*, 3475–3484.

[119] F. Secco. *Inorg. Chem.* **1980**. *19*, 2722–2725.

[120] M. J. Clague, N. L. Keder, A. Butler. *Inorg. Chem.* **1993**. *32*, 4754–4761.

[121] B. J. Hamstra, G. J. Colpas, V. L. Pecoraro. *Inorg. Chem.* **1998**. *37*, 949–955.

[122] C. R. Cornman, K. M. Geiser-Bush, S. P. Rowley, P. D. Boyle. *Inorg. Chem.* **1997**. *36*, 6401–6408.

[123] D. K. Johnson, T. B. Murphy, N. J. Rose, W. H. Goodwin, L. Pickart. *Inorganica Chimica Acta* **1982**. *67*, 159–165.

[124] L. Pickart, W. H. Goodwin, W. Burgua, T. B. Murphy, D. K. Johnson. *Biochem. Pharmacol.* **1983**. *32*, 3868–3871.

[125] M. L. Vitolo, J. Webb. *J. Inorg. Biochem.* **1984**. *20*, 255–262.

[126] E. Baker, M. L. Vitolo, J. Webb. *J. Biochim. Pharmacol.* **1985**. *34*, 3011–3017.

[127] P. Noblia, m. Vieites, B. S. Parajón-Costa, E. J. Baran, H. Cerecetto, P. Draper, M. González, O. O. Piro, E. E. Castellano, A. Azqueta, A. L. de Ceráin, A. Monge-Vega, D. Gambino. *Polyhedron* **2005**. *99*, 443–451.

[128] M. N. Isupov, A. R. Dalby, A. A. Brindley, Y. Izumi, T. Tanabe, G. N. Murshudov, J. A. Littlechild. *J. Mol. Biol.* **2000**. *299*, 1035–1049.

[129] C. J. Carrano, C. M. Nunn, R. Quan, J. A. Bonadier, V. L. Pecoraro. *Inorg. Chem.* **1990**. *29*, 944–951.

[130] W. Plass, A. Pohlmann, H.-P. Yozgatli. *J. Inorg. Biochem.* **2000**. *80*, 181–183.

[131] W. Plass, H.-P. Yozgatli. *Z. Anorg. Allg. Chem.* **2003**. *629*, 65–70.

[132] L. E. Sayed, M. F. Iskander. *J. Inorg. Nucl. Chem.* **1971**. *33*, 435–443.

[133] M. F. Iskander, L. E. Sayed, N. M. H. Salem, W. Haase, H. J. Linder, S. Foro. *Polyhedron* **2004**. *23*, 23–31.

[134] W. Plass. *Coord. Chem. Rev.* **2003**. *237*, 205–212.

[135] A. Pohlmann, S. Nica, T. K. K. Luong, W. Plass. *Inorg. Chem. Comm.* **2005**. *8*, 289–292.

[136] A. G. J. Ligtenbarg, R. Hage, B. L. Feringa. *Coord. Chem. Rev.* **2003**. *237*, 89–101.

[137] S.-X. Liu, S. Gao. *Polyhedron* **1998**. *17*, 81–84.

[138] S. P. Rath, K. K. Rajak, A. Chakravorty. *Inorg. Chem.* **1999**. *38*, 4376–4377.

[139] S. Gao, Z. Q. Weng, S. X. Liu. *Polyhedron* **1998**. *7*, 3595–3598.

[140] W. Chen, S. Gao, S.-X. Liu. *Acta Crystallogr., Sect. C: Cryst. Struct. Commun.* **1999**. *55*, 531–533.

[141] S. P. Rath, K. K. Rajak, S. Mondal, A. Chakravorty. *J. Chem. Soc., Dalton Trans.* **1998**. 2097–2101.

[142] J. M. Arber, E. de Boer, C. D. Garner, S. S. Hasnain, R. Wever. *Biochemistry* **1989**. *28*, 7968–7973.

[143] J. Bard, L. R. Faulkner. In *Electrochemical Methods, Fundamentals and Applications*. John Wiley & Sons Ltd., New York **2001** .

[144] A. J. Blair, D. A. Pantony, G. J. Minkoff. *J. Inorg. Nucl. Chem.* **1958**. *5*, 316–331.

[145] T. L. Riechel, D. T. Sawyer. *Inorg. Chem.* **1975**. *14*, 1869–1875.

[146] A. Giacomelli, C. Floriani, A. O. de Suaza Duarte, A. Chiesi-Villa, C. Guastini. *Inorg. Chem.* **1982**. *21*, 3310–3316.

[147] W. R. Scheidt. *Inorg. Chem.* **1973**. *12*, 1758–1761.

[148] L. W. Amos, D. T. Sawyer. *Inorg. Chem.* **1974**. *13*, 78–83.

[149] H. Dau, J. Dittmer, M. Epple, J. Hanss, E. Kiss, D. Rehder, C. Schulzke, H. Vilter. *FEBS Letters* **1999**. *457*, 237–240.

[150] N. Tanaka, Z. Hasan, R. Wever. *Inorg. Chim. Acta* **2003**. *356*, 288–296.

[151] A. Pohlmann. *Wasserstoffbrckenbindungen in bergangsmetallkomplexen*. Ph.D. thesis, Universitt Siegen, Siegen **2002**.

[152] A. Pohlmann, M. Mança, W. Plass **to be published**.

[153] M. Časný, D. Rehder. *Dalton Trans.* **2004**. 839–846.

[154] M. R. Maurya, S. Khurana, C. Schulzke, D. Rehder. *Eur. J. Inorg. Chem.* **2001**. 779–788.

[155] M. R. Maurya, S. Agarwal, C. Bader, M. Ebel, D. Rehder. *Dalton Trans.* **2005**. 537–544.

[156] B. A. Brennan, G. Alms, M. J. Nelson, L. T. Durney, R. C. Scarrow. *J. Am. Chem. Soc.* **1996**. *118*, 9194–9195.

[157] M. J. Nelson. *J. Am. Chem. Soc.* **1988**. *110*, 2985–2986.

[158] R. C. Scarrow, M. G. Trimitsis, C. P. Buck, G. N. Grove, R. A. Cowling, M. J. Nelson. *Biochemistry* **1994**. *33*, 15219–15229.

[159] E. Jabri, M. B. Carr, R. P. Hausinger, P. A. Karplus. *Science* **1995**. *268*, 998–1004.

[160] W. N. Lipscomb, N. Sträter. *Chem. Rev.* **1996**. *96*, 2375–2433.

[161] D. E. Wilcox. *Chem. Rev.* **1996**. *96*, 2435–2458.

[162] A. Orlandini, L. Sacconi. *Inorg. Chem.* **1976**. *15*, 78–85.

[163] S. E. Kucharski, B. W. Skelton, A. H. White. *Aust. J. Chem.* **1978**. *31*, 47–51.

[164] S. Hikichi, T. Ogihara, K. Fujisawa, N. Kitajima, M. Akita, Y. Moro-oko. *Inorg. Chem.* **1997**. *36*, 4539–4547.

[165] S. Ogo, S. Wada, Y. Watanabe, M. Iwase, A. Wada, M. Harata, K. Jitsukawa, H. Masuda, H. Einaga. *Angew. Chem. Int. Ed.* **1998**. *37*, 2102–2104.

[166] G. Parkin. *Chem. Commun.* **2000**. 1971–1985.

[167] E. J. Tolis, M. J. Manos, A. J. Tasiopoulos, C. P. Raptopoulou, A. Terzis, M. P. Sigalas, Y. Deligiannakis, T. A. Kabanos. *Angew. Chem.* **2002**. *114*, 2921–2925.

[168] G. D. Triantafillou, E. J. Tolis, A. Terzis, Y. Deligiannakis, C. P. R. A. M. P. Sigalas, T. A. Kabanos. *Inorg. Chem.* **2004**. *43*, 79–91.

[169] M. Kosugi, S. Hikichi, M. Akita, Y. Moro-oka. *Inorg. Chem.* **1999**. *38*, 2567–2578.

[170] K. Wieghardt, U. Bossek, K. Volckmar, W. Swirdoff, J. Weiss. *Inorg. Chem.* **1984**. *23*, 1387–1389.

[171] K. Wieghardt, M. Hahn, W. Swirdoff, J. Weiss. *Angew. Chem. Int. Ed.* **1983**. *22*, 491–492.

[172] R. Mannar, M. R. Maurya, S. Khurana, A. Azam, W. Zhang, D. Rehder. *Eur. J. Inorg. Chem.* **2003**. 1966–1973.

[173] H. Gampp, M. Maeder, C. J. Meyer, A. D. Zuberbuehler. *Talanta* **1985**. *32*, 95–101.

[174] H. Gampp, M. Maeder, C. J. Meyer, A. D. Zuberbuehler. *Talanta* **1985**. *32*, 257–264.

[175] H. B. ten Brink, A. Tuynman, H. L. Dekker, W. Hemrika, Y. Izumi, T. Oshiro, H. E. Schoemaker, R. Wever. *Inorg. Chem.* **1998**. *37*, 6780–6784.

[176] V. Conte, F. di Furia, S. Moro. *J. Mol. Catal. A* **1995**. *104*, 159–169.

[177] M. Sivak, V. Sucha, L. Kuchta, J. Marek. *Polyhedron* **1998**. *18*, 93–99.

[178] G. Zampella, J. Kravitz, C. Webster, P. Fantucci, M. Hall, H. Carlson, V. Pecoraro, L. Gioia. *Inorg. Chem.* **2004**. *43*, 4127–4136.

[179] M. Bangesh, W. Plass. *J. Mol. Struct. Theochem.* **2005**. *725*, 163–175.

[180] S. Macedo-Ribeiro, W. Hemrika, R. Renirie, R. Wever, A. Messerschmidt. *J. Biol. Inorg. Chem.* **1999**. *4*, 209–219.

[181] S. Ohta, M. Okamoto. *Chem. Pharm. Bull.* **1980**. *28*, 1917–1919.

[182] D. R. Shridhar, M. Jogibhukta, P. P. Joshi. *Indian J. Chem., Sect. B: Org. Chem. Incl. Med. Chem.* **1981**. *20*, 132–4.

[183] M. Sivák, M. Mad'arová, J. Tatiersky, J. Marek. *Eur. J. Inorg. Chem.* **2003**. 2078–2081.

[184] A. G. J. Ligtenbarg. *Vanadium and Iron Complexes for Catalytic Oxidation*. Ph.D. thesis, Rijksuniversiteit Groningen, Groningen **2001**.

[185] A. C. Gonzalez-Baró, E. E. Castellano, O. E. Piro, B. S. Parajón-Costa. *Polyhedron* **2005**. *24*, 49–55.

[186] A. S. Tracey, J. S. Jaswal. *J. Am. Chem. Soc.* **1992**. *114*, 3835–3840.

[187] M. R. Maurya, S. Khurana, W. Zhang, D. Rehder. *J. Chem. Soc., Dalton Trans.* **2002**. 3015–2023.

[188] X. Wang, X. M. Zhang, H. X. Liu. *Inorg. Chim. Acta* **1994**. *223*, 193–197.

[189] J. Sun, C. Zhu, Z. Dai, M. Yang, Y. Pan, H. Hu. *J. Org. Chem.* **2004**. *69*, 8500–8503.

[190] N. N. Karpyshev, O. D. Yakovleva, E. P. Talsi, K. P. Bryliakov, O. V. Tolstikova, A. G. Tolstikov. *J. Mol. Cat. A: Chem.* **2000**. *157*, 91–95.

[191] C. Bolm, F. Bienewald. *Angew. Chem.* **1995**. *107*, 2883–2385.

[192] C. Bolm, T. K. K. Luong, K. Harms. *Chem. Ber.* **1997**. *130*, 887–890.

[193] T. S. Smith, V. L. Pecoraro. *Inorg. Chem.* **2002**. *41*, 6754–6760.

[194] R. Hille. *Chem. Rev.* **1996**. *96*, 2757–2816.

[195] R. H. Holm. *Coord. Chem. Rev.* **1990**. *100*, 183–221.

[196] J.-M. Bregeault. *Dalton Trans.* **2003**. 3289.

[197] K. A. Jorgensen. *Chem. Rev.* **1989**. *89*, 431–458.

[198] S. N. Rao, K. N. Munshi, N. N. Rao. *J. Mol. Cat. A: Chem.* **2000**. *156*, 205–211.

[199] J. A. Brito, M. Gomez, G. Muller, H. Teruel, J.-C. Clinet, E. Dunach, M. A. Maestro. *Eur. J. Inorg. Chem.* **2004**. 4278–4285.

[200] S. Campestrini, V. Conte, F. D. Furia, G. Modena. *J. Org. Chem.* **1988**. *53*, 5721–5724.

[201] B. Meunier. *Metal-Oxo and Metal-Peroxo Species in Catalytic Oxidations*. Springer, Berlin **2000**.

[202] L. Stelzig, S. Ktte, B. Krebs. *Dalton Trans.* **1998**. 2921–2926.

[203] R. Dinda, P. Sengupta, H. Mayer-Figge, W. S. Sheldrick. *J. Chem. Soc., Dalton Trans.* **2002**. 4434–4439.

[204] C. L. Copper, E. Koubek. *Inorg. Chim. Acta* **1999**. *288*, 229–232.

[205] G. E. Meister, A. Butler. *Inorg. Chem.* **1994**. *33*, 3269–3275.

[206] M. S. Reynolds, K. J. Babinski, M. C. Bouteneff, J. L. Brown, R. E. Campbell, M. A. Cowan, M. R. Durwin, T. Foss, P. O'Brien, H. R. Penn. *Inorg. Chim. Acta* **1997**. *263*, 225–230.

[207] C. P. Rao, A. Sreedhara, P. V. Rao, M. B. Verghese, K. Rissanen, E. Kolehmainen, N. K. Lokanath, M. A. Sridhar, J. S. Prasad. *J. Chem. Soc., Dalton Trans.* **1998**. 2383–2393.

[208] M. Cindrić, N. Strukan, V. Vrdoljak, B. Kamenar. *Z. Anorg. Allg. Chem. Chem.* **2004**. *630*, 585–590.

[209] R. V. Parish (Editor) *NMR, NQR, EPR, and Mssbauer Spectroscopy in Inorganic Chemistry*. Ellis Horwood Lim., Chichester, New York, London, Toronto, Sydney, Tokyo, Singapore **1990**.

[210] M. D. Meglasson, J. M. Wilson, J. H. Yu, D. D. Robinson, M. M. Wyse, C. J. de Souza. *J. Pharmacol. Exp. Ther.* **1993**. *266*, 1454–1462.

[211] A. Klip, L. A. Leiter. *Diabetes Care* **1990**. *13*, 696–704.

[212] C. R. Sirtori, C. Pasik. *Pharmacol. Res.* **1994**. *30*, 187–228.

[213] M. Melchior, K. H. Thompson, J. M. Jong, S. J. Rettig, E. Shuter, V. G. Yuen, Y. Zhou, J. H. McNeill, C. Orvig. *Inorg. Chem.* **1999**. *38*, 2288–2293.

[214] L. C. Y. Woo, V. G. Yuen, K. H. Thompson, J. H. McNeill, C. Orvig. *J. Inorg. Biochem.* **1990**. *76*, 251–257.

[215] P. Caravan, L. Gelmini, N. Glover, F. G. Herring, H. Li, J. H. McNeil, S. J. Rettig, I. A. Setyawati, E. Shuter, Y. Sun, A. S. Tracey, V. G. Yuen, C. Orvig. *J. Am. Chem. Soc.* **1995**. *117*, 12759–12770.

[216] M. Zhang, M. Zhou, R. L. V. Etten, C. V. Stauffacher. *Biochemistry* **1997**. *36*, 15–23.

[217] Q. X. Zhang, C. S. Pilquil, J. Dewald, L. G. Berthiaume, D. N. Brindley. *Biochem. J.* **2000**. *345*, 181–184.

[218] R. L. Barton, S. L. Briggs, G. A. Koppel. *US Patent* **1985**. *4,501,703*, Feb. 26.

[219] Z. Han, D. Krishnamurthy, P. Grover, Q. K. Fang, C. H. Senanayake. *J. Am. Chem. Soc.* **2002**. *124*, 7880–7881.

[220] J. K. Whitessel, M. S. Wong. *J. Org. Chem.* **1994**. *59*, 597–601.

[221] N. Khiar, S. C. Araujo, F. Alcudia, I. Fernandez. *J. Org. Chem.* **2002**. *67*, 345–356.

[222] F. A. Davis, R. T. reddy, W. Han, P. J. Carroll. *J. Am. Chem. Soc.* **1992**. *114*, 1428–1437.

[223] W. Adam, M. N. Korb, K. J. Roschmann, C. R. Saha-Moller. *J. Org. Chem.* **1998**. *63*, 3423–3428.

[224] F. A. Davis, H. C. Weiamiller. *J. Am. Chem. Soc.* **1989**. *111*, 5964–5965.

[225] P. Pitchen, E. D. nach, M. N. Deshmukh, H. B. Kagan. *J. Am. Chem. Soc.* **1989**. *106*, 8188–8193.

[226] S. H. Zhao, O. Samuel, H. B. Kagan. *Tetrahedron* **1987**. *43*, 5135–5144.

[227] C. R. J. Lepage, L. Mihichuk, D. G. Lee. *Can. J. Chem.* **2003**. *81*, 75–80.

[228] S. S. Kim, G. Rajagopal. *Synthesis* **2003**. *16*, 2461–2463.

[229] S. Schoumacker, O. Hamelin, J. Pecaut, M. Fontecave. *Inorg. Chem.* **2003**. *42*, 8110–8116.

[230] V. L. S. M. Ganesan, S. Rajagopal, R. Ramaraj. *J. Org. Chem.* **2002**. *67*, 1506–1514.

[231] Y. Mekmouche, H. Hummel, R. Y. N. Ho, J. L. Que, V. Schünemann, F. Thomas, A. X. Trautwein, C. Lebrun, K. Gorgy, J. C. Leprêtre, M. N. Collomb, A. Deronzier, M. Fontecave, S. Ménage. *Chem. Eur. J.* **2002**. *8*, 1196–1204.

[232] K. A. Vassell, J. H. Espenson. *Inorg. Chem.* **1994**. *33*, 5491–5498.

[233] J. Arias, C. R. Newlands, M. M. Abu-Omar. *Inorg. Chem.* **2001**. *40*, 2185–2192.

[234] G. Santoni, G. Licini, D. Rehder. *Chem. Eur. J.* **2003**. 4700–4708.

[235] E. Kwiatkowski, G. Romanowski, W. Nowicki, M. Kwiatkowski, K. Suwińska. *Polyhedron* **2003**. *22*, 1509–1018.

[236] A. Barbarini, R. Maggi, M. Muratori, G. Sartori, R. Sartorio. *Tetrahedron Asymm.* **2004**. *15*, 2467–2473.

[237] K. Nakajima, K. Kojima, T. Aoyama, J. Fujita. *Chem. Lett.* **1986**. 1483–1486.

[238] K. Nakajima, K. Kojima, T. Aoyama, J. Fujita. *Bull. Chem. Soc. Jpn.* **1990**. *623*, 2620–2630.

[239] D. A. Cogan, G. Liu, K. Kim, B. J. Backes, J. A. Ellman. *J. Am. Chem. Soc.* **1998**. *120*, 8011–8019.

[240] S. A. Blum, R. G. Bergman, J. A. Ellman. *J. Org. Chem.* **2003**. *68*, 150–155.

[241] J. Legros, C. Bolm. *Angew. Chem.* **2004**. *116*, 4321–4324.

[242] J. Legros, C. Bolm. *Chem. Eur. J.* **2005**. *11*, 1086–1092.

[243] J. Ranford, J. J. Vittal, Y. M. Wang. *Inorg. Chem.* **1998**. *37*, 1226–1231.

[244] X.-M. Zhang, X.-Z. You, X. Wang. *Polyhedron* **1996**. *15*, 1793–1796.

[245] C. Zhang, G. Rheinwald, V. Lozan, B. Wu, P. G. Lassahn, H. Lang, C. Janiak. *Z. Anorg. Allg. Chem.* **2002**. *628*, 1259–1268.

**Selbständigkeitserklärung**

Ich erkläre, dass ich die vorliegende Arbeit selbständig und unter Verwendung der angegebenen Hilfsmittel, persönlichen Mitteilungen und Quellen angefertigt habe.

Ort, Datum Unterschrift des Verfassers/der Verfasserin

# Curriculum Vitae

## Personal Details


| | |
|---|---|
| Name | Simona Filofteia Nica |
| Address | Am Herrenberge 11, App. 417, Jena, 07745, Germany |
| Sex | Female |
| Marital status | Single |
| Nationality | Romanian |
| Telephone | |
| mobile | 01795457171 |
| office | 03641948138 |
| Date of birth | December $19^{th}$ 1976 |
| e-mail | simona.nica@uni-jena.de |


## Academic Career and Education

| | |
|---|---|
| 1995 - 1999 | **Chemistry studies** at Faculty of Chemistry from University of Bucharest, Romania |
| 1999 | **Bachelor of Science in organic chemistry** with the topic *Synthesis and reactivity of 4-hydroxycoumarin* under the supervision of Prof. Dr. Ovidiu Maior |
| 1999 - 2001 | **Master of Science studies** in Organic Chemistry at Faculty of Chemistry from University of Bucharest, Romania |
| 2001 | **Master of Science in organic chemistry** with the topic *Synthesis and biochemical properties of N-benzoyl-N'-aryl thioureas* under the supervision of Prof. Dr. O. Maior |
| Dec. 2001 - present | **Ph. D. student** in Bioinorganic chemistry at Siegen University and Friedrich-Schiller University, Jena, Germany under the supervision of Prof. Dr. Winfried Plass<br>**Title of Doctoral thesis:** Bioinspired model complexes for vanadium haloperoxidases |

## Professional Experience

| | |
|---|---|
| 2000-2001 | **Analytical Chemist** at Research and Development Departament of the pharmacological company BIOFARM S.A. Bucharest, Romania |
| **Research topics** | Qualitative and quantitative characterization of the ingredients of natural extracts.<br>Development of new methods for dosage of the active ingredients and excipients for different formats of drugs.<br>Studies on compatibilities between the ingredients of the new pharmaceutical drugs.<br>Studies on stability of the active ingredients of the present and new pharmaceutical drugs in order to establish the validity period of the drugs.<br>Preparation of the new series of drugs in micropilot scale. |

## List of publications

1. A. Pohlmann, S. Nica, W. Plass
   *Dioxovanadium(*V*) complexes with side chain substituted* N*-salicylidenehydrazides: modelling supramolecular interactions in vanadium haloperoxidases*, Inorg. Chem. Commun. 2005, *8*, 289-292.
2. S. Nica, A. Pohlmann, W. Plass
   *Vanadium(*V*) oxoperoxo complexes with side chain substituted* N*-salicylidenehydrazides: modelling supramolecular interactions in vanadium haloperoxidases*, Eur. J. Inorg. Chem. 2005, 2032-2036.
3. S. Nica, M. Rudolph, W. Plass
   *cis-Dioxovanadium complexes - structural and functional models for Vanadium Haloperoxidase*, Eur. J. Inorg. Chem. in preparation
4. S. Nica, M. Rudolph, W. Plass
   *Synthesis and structural characterization of new* $VO^{3+}$ *complexes*

*based on N-salicylidene hydrazide and 8-quinolinol*, Z. Anorg. Allg. Chem. in preparation

5. S. Nica, M. Rudolph, W. Plass
*Structural characterization and electrochemical behavior of new oxovanadium*(V) *complexes*, Inorganica Chimica Acta in preparation

## Conferences

*Synthesis and structural characterization of vanadium complexes: model systems for vanadium-containing haloperoxidase*: Mitteldeutsches Anorganiker Nachwunchssymposium (MANS); Chemnitz 2003-oral presentation

*cis-Dioxovanadium complexes and their speciation in solution*; The $4^{th}$ international symposium on chemistry and biological chemistry of vanadium; Szeged 2004-poster

*New aspects of vanadium-containing oxidation catalyst*; Young scientists conference on chemistry (JCF), Berlin 2005 poster

## Other skills

**Languages** Romanian:mother language
English: fluent (spoken and written)
French: good (spoken and written)
German: beginner

**Computers** Good knowledge and easy handling of the Microsoft Office package and other programme such as: Origin, CorelDraw, ChemDraw, LaTeX, etc.

## Hobbies

Interwar literature, music, tennis and mountaineering.

Place, Date Signature